Synthetic, Structural, and Mechanistic Studies of Interactions of Carbon, Nitrogen, and Oxygen Nucleophiles with Bis-Pentamethylcyclopentadienyl Zirconium and Hafnium Derivatives

Thesis by

Eric Jan Moore

In Partial Fulfillment of the Requirements

for the degree of

Doctor of Philosophy

California Institute of Technology

Pasadena, California

1984

(Submitted June 30, 1983)

ACKNOWLEDGMENTS

My stay at Caltech has been an odd mixture of elation and frustration. Always, however, I have been exposed to exceptional science. My advisor, John Bercaw, has provided me with an atmosphere of freedom and creativity for which I am extremely grateful. Ever on the run (even from my softball pitching), John still managed to follow my ever changing projects and make valuable contributions toward my understanding of them. Several discussions (both chemistry related and hiking and climbing related) with Professors Terry Collins, Dave Evans, and Bobb Grubbs are also greatly appreciated.

The members of the Bercaw group, past and present, are thanked for their numerous contributions. In particular, Paul Barger, Steve Cohen, and Rich Threlkel helped me to get my feet wet and my line pumped down. Greg Hillhouse (the Hoosier) and Chris McDade ran many of my FT NMR samples for which I am grateful. Greg also contributed several ideas concerning the diazoalkane project.

Bernie Santarsiero deserves special mention. Although not officially a Bercaw group member (he possesses no synthetic skills) Bernie is still considered one of the "boys". Aside from proofreading the initial drafts of this thesis, Bernie performed much of the crystallographic work and even taught me something about X-ray crystallography. I now know the difference between B's and U's and I can even take a radiograph of my hand. Thanks again, Beenard, for your help and friendship (and the keys to your condo).

Several people at Caltech made my stay more enjoyable. They

are: Jay Audett, Ken Doxsee, Steve Hentges, Dan and Karen Nocera, Mark Paffett, John Stille, and Terry Smith. My cohorts at Stanford, Keith Woo and Scott Raybuck (who are still grinding away), are thanked for providing me with a place to stay when I visited the Bay Area and inviting me on numerous Collman Group ski trips.

Henriette Wymar deserves special thanks for typing this thesis and not complaining too much about my small print.

Karen Klages (die Blondine von P.C.C.) made this last year truly worthwhile. Danke viel Mal, Karen.

Lastly, I thank my family for their patience and support and especially my mother, for her cakes and pies.

ABSTRACT

The reactivity of permethylzirconocene and permethylhafnocene complexes with various nucleophiles has been investigated. Permethylzirconocene reacts with sterically hindered ketenes and allenes to afford metallacycle products. Reaction of these cummulenes with permethylzirconocene hydride complexes affords enolate and σ-allyl species, respectively. Reactions which afford enolate products are nonstereospecific, whereas reactions which afford allyl products initially give a cis-σ-allyl complex which rearranges to its trans isomer. The mechanism of these reactions is proposed to occur either by a Lewis Acid-Lewis Base interaction (ketenes) or by formation of a π-olefin intermediate (allenes).

Permethylzirconocene haloacyl complexes react with strong bases such as lithium diisopropylamide or methylene trimethylphosphorane to afford ketene compounds. Depending on the size of the alkyl ketene substituent, the hydrogenation of these compounds affords enolate-hydride products with varying degrees of stereoselectivity. The larger the substituent, the greater is the selectivity for cis hydrogenation products.

The reaction of permethylzirconocene dihydride and permethylhafnocene dihydride with methylene trimethylphosphorane affords methyl-hydride and dimethyl derivatives. Under appropriate conditions, the metallated-ylide complex 1, $(\eta^5\text{-}C_5(CH_3)_5)_2\overline{Zr(H)CH_2PMe_2CH_2}$, is also obtained and has been structurally characterized by X-ray diffraction techniques. Reaction of 1 with CO affords

$(\eta^5\text{-}C_5(CH_3)_5)_2Zr(C,O\text{-}\eta^2\text{-}(PMe_3)HC{=}CO)H$ which exists in solution as an equilibrium mixture of isomers. In one isomer (2), the η^2-acyl oxygen atom occupies a lateral equatorial coordination position about zirconium, whereas in the other isomer (3), the η^2-acyl oxygen atom occupies the central equatorial position. The equilibrium kinetics of the 2 → 3 isomerization have been studied and the structures of both complexes confirmed by X-ray diffraction methods. These studies suggest a mechanism for CO insertion into metal-carbon bonds of the early transition metals.

Permethylhafnocene dihydride and permethylzirconocene hydride complexes react with diazoalkanes to afford η^2-N,N′-hydrazonido species in which the terminal nitrogen atom of the diazoalkane molecule has inserted into a metal-hydride or metal-carbon bond. The structure of one of these compounds, $Cp^*_2Zr(NMeNCTol_2)OH$, has been determined by X-ray diffraction techniques. Under appropriate conditions, the hydrazonido-hydride complexes react with a second equivalent of diazoalkene to afford η'-N-hydrazonido-η^2-N,N′-hydrazonido species.

TABLE OF CONTENTS

LIST OF TABLES

LIST OF TABLES

LIST OF FIGURES

LIST OF SCHEMES

ABBREVIATIONS

acac	acetylacetonate anion
Anal	elemental analysis
atm	atmosphere
B	temperature factor
bp	boiling point
bkgrd	background
br	broad
Bu	butyl, C_4H_{10}
c	central
calcd	calculated
CH_2Ph	benzyl
Cp	cyclopentadienyl anion, η^5-C_5H_5
Cp^{EJ}	(2-methyl-5-t-butyl)phenyltetramethylcyclopentadienyl anion
CPK	Corey-Pauling-Koltun molecular models
Cp′	methylcyclopentadienyl anion, η^5-$C_5H_4CH_3$
Cp*	pentamethylcyclopentadienyl anion, η^5-$C_5(CH_3)_5$
d	doublet
DMP	2,2-dimethoxypropane
dmpe	1,2-bis(dimethylphosphino)ethane
Et	ethyl, $-CH_2CH_3$
Et_2O	diethyl ether
F_o	structure factor
H^+	mineral acid
hr	hour

IR	infrared spectroscopy
J	spin-spin coupling constant
k	rate constant
K_{eq}	equilibrium constant
ℓ	lateral
L	ligand
lit	literature
LUMO	lowest unoccupied molecular orbital
m	multiplet
M	metal atom
Me	methyl, $-CH_3$
MeOH	methanol
min	minutes
mp	melting point (uncorrected)
MW	molecular weight
n	normal
NMR	nuclear magnetic resonance
NOE	nuclear Overhauser enhancement
pet. ether	40-60°C petroleum ether
Ph	phenyl, $-C_6H_5$
ppm	parts-per-million
Pr	propyl, $-C_3H_5$
psi	pounds-per-square-inch
p-tol	para-tolyl, p-$CH_3C_6H_4$
pyr	pyridine
R	alkyl or aryl ligand

s	singlet
t	triplet, time
t	tertiary
T	temperature
THF	tetrahydrofuran
TMS	tetramethylsilane
Tol	para-tolyl
TsOH	p-toluenesulfonic acid
$t_{\frac{1}{2}}$	half life
U	temperature factor
ν	IR stretching frequency
δ	NMR chemical shift
ρ	density

CHAPTER 1

The Reaction of Ketenes and Allenes with Permethylzirconocene Derivatives

1.1 Introduction

1.1.1 General Introduction

Current interest in carbon monoxide reduction to synfuel products has prompted a closer investigation into the mechanism by which these reduction processes operate. As an example, metal-bound ketene complexes have been prepared as early as 1970,[1] but only recently have such complexes been proposed as possible intermediates in the Fischer-Tropsch reduction and coupling of CO to alcohols.[2,5] Conceivably, the carbonylation of metal-bound carbene moieties to ketene intermediates may be a general phenomenon.

Our interest in this area has grown from mechanistic considerations into the reduction of CO, both free and coordinated, with $(\eta^5\text{-}C_5(CH_3)_5)_2ZrH_2$ ($Cp^*_2ZrH_2$) (1). It was found that treatment of 1 with CO afforded, among other products, the trans-enediolate dimer 3 (eq. 1),[3] while treatment with $Cp^*_2Zr(CO)_2$ gave the cis-enediolate dimer 8 (eq. 2).[4] Each reaction is 100% stereoselective and the

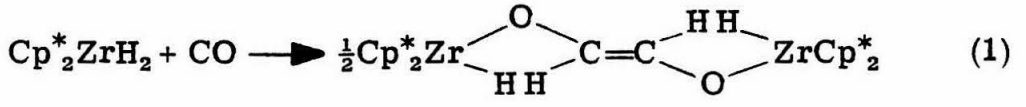

(1)

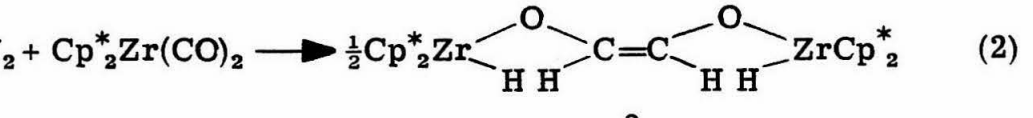

(2)

isomeric enolate products cannot be interconverted. A mechanism proposed for the formation of the trans-enediolate dimer (Scheme 1.1)[5]

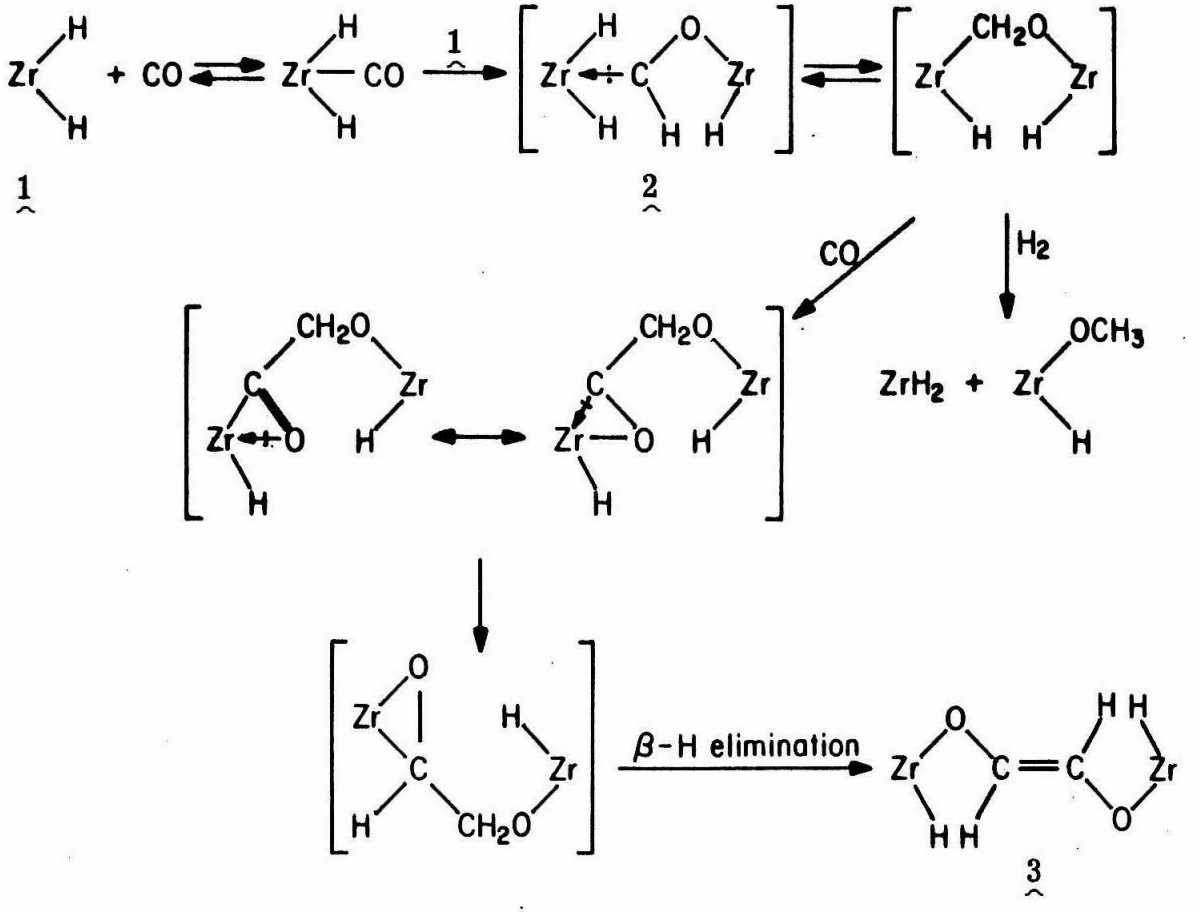

SCHEME 1.1. Mechanism for the Formation of trans-$(Cp^*_2ZrH)_2(OCHCHO)$ (3).

involves initial CO coordination to 1 followed by attack of a second molecule of 1 to give the zirconoxycarbene intermediate 2. Insertion of the carbene into a metal-hydride bond followed again by CO coordination, insertion, hydride transfer, and lastly by β-hydride elimination gives the trans-enediolate dimer 3. The β-hydride elimination step dictates the stereoselective formation of the trans-enediolate product.

The proposed mechanism for the formation of the cis-enediolate dimer (Scheme 1.2)[5] involves initial attack of 1 on a carbonyl ligand of $Cp^*_2Zr(CO)_2$ to give the zirconoxycarbene intermediate 4. Carbonylation of the metal-bound carbene would then give a zirconium-ketene intermediate 5 in which the ketene is coordinated through the olefinic double bond. π-Overlap between the olefinic bond and the available zirconium orbitals necessarily forces the ketene substituents into the pentamethylcyclopentadienyl ligands. Rearrangement of 5 to the intermediate 6 in which the carbonyl double bond of the ketene is coordinated to the metal, rotates the ketene 90° so that the substituents are now forced in and out of the equatorial "wedge" formed by the pentamethylcyclopentadienyl ligands. Rearrangements of this type have precedent in the fluxional behavior of coordinated allenes.[6] The isomerization of 5 to 6 should be especially favorable because of the high oxophilicity of of zirconium[3,4] and because the $-OZrCp^*_2$ moiety is placed in the least sterically hindered position. The $-OZrCp^*_2$ moiety would necessarily point out of the "wedge" to reduce steric interactions between the bulky pentamethylcyclopentadienyl ligands to a minimum. Oxidative addition of H_2 to 6 to give 7 followed by reductive elimination of a C-H bond would afford the cis-enediolate dimer 8. The configuration of the

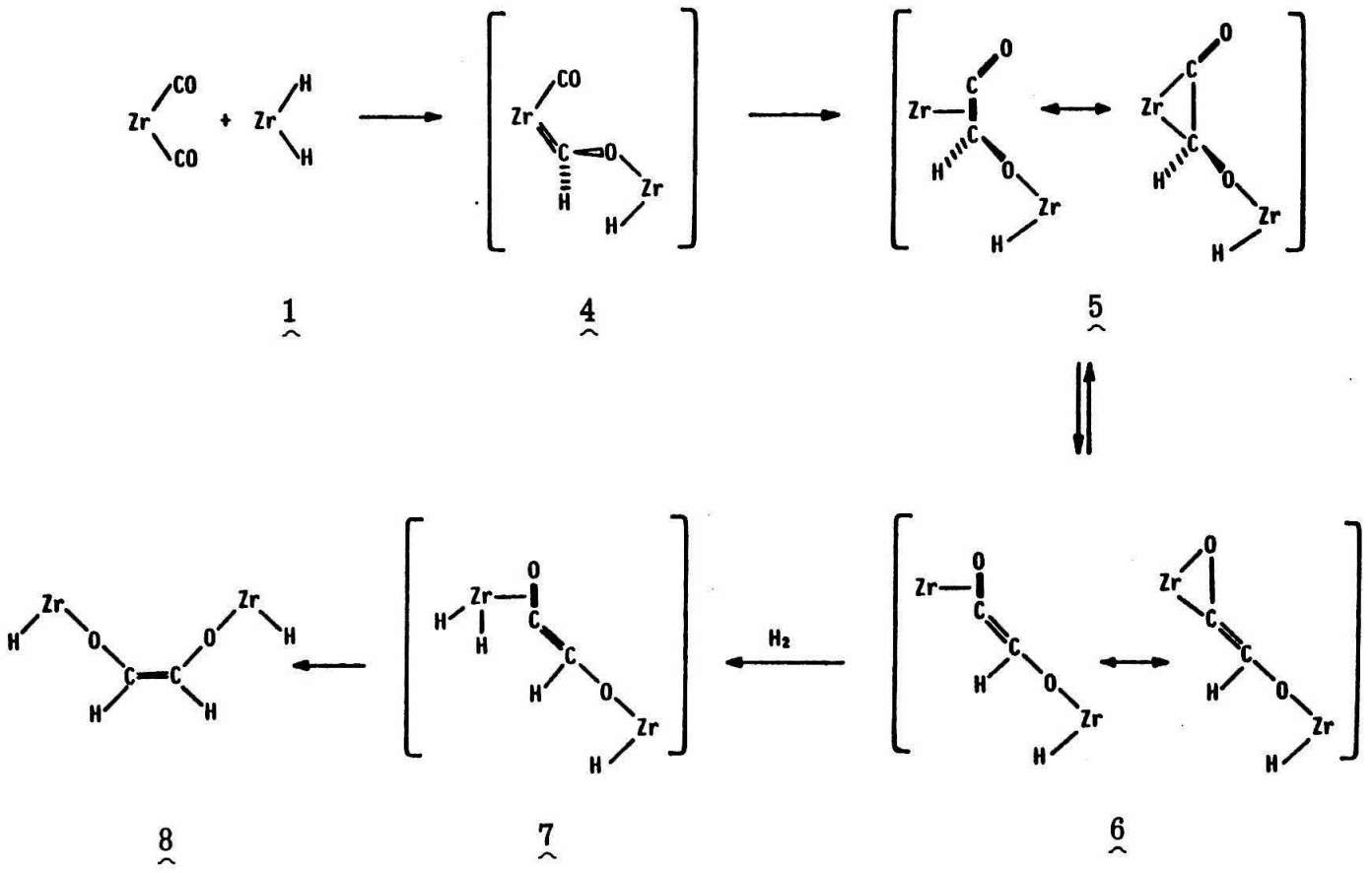

SCHEME 1.2. Mechansim for the Formation of cis-$(Cp^*_2ZrH)_2(OCHCHO)$ (8).

ketene intermediate 6, in which the -OZrCp*$_2$, moiety points out of the equatorial wedge, dictates the stereoselective formation of a cis-enediolate product.

It was our hope to model some of the intermediates proposed in the cis-enediolate mechanism (Scheme 1.2) by treating a form of "permethylzirconocene" ("Cp*$_2$Zr") with sterically hindered monosubstituted ketenes. In this way, a ketene intermediate could be isolated or observed and then treated with H_2 to generate a cis-enolate complex (Scheme 1.3). The substituent on the ketene should be quite large to successfully model the -OZrCp*$_2$ moiety. Only one zirconium-ketene complex had been reported in the literature.[7] Further investigation of the synthesis and reactivity of zirconium-ketene complexes appeared warranted.

1.1.2 Metal-Ketene Complexes

Metal-ketene complexes have been porposed as intermediates in a number of organic reaction pathways.[2a,8] Early attempts to model these intermediates were frustrated because the treatment of ketenes with metal compounds generally decarbonylated the ketene affording either a metal carbonyl complex and carbene-coupled products[9] or a metal-carbene complex and CO.[10] The first reported transition metal ketene complexes were prepared by treatment of silver,[1] copper,[11] or gold[12] salts with ketene in a polar solvent. Although originally formulated as σ-bound bimetallic adducts (Figure 1.1), the low solubility properties suggested a polymeric structure. Indeed, the X-ray structural analysis indicated a sheet-like structure consisting

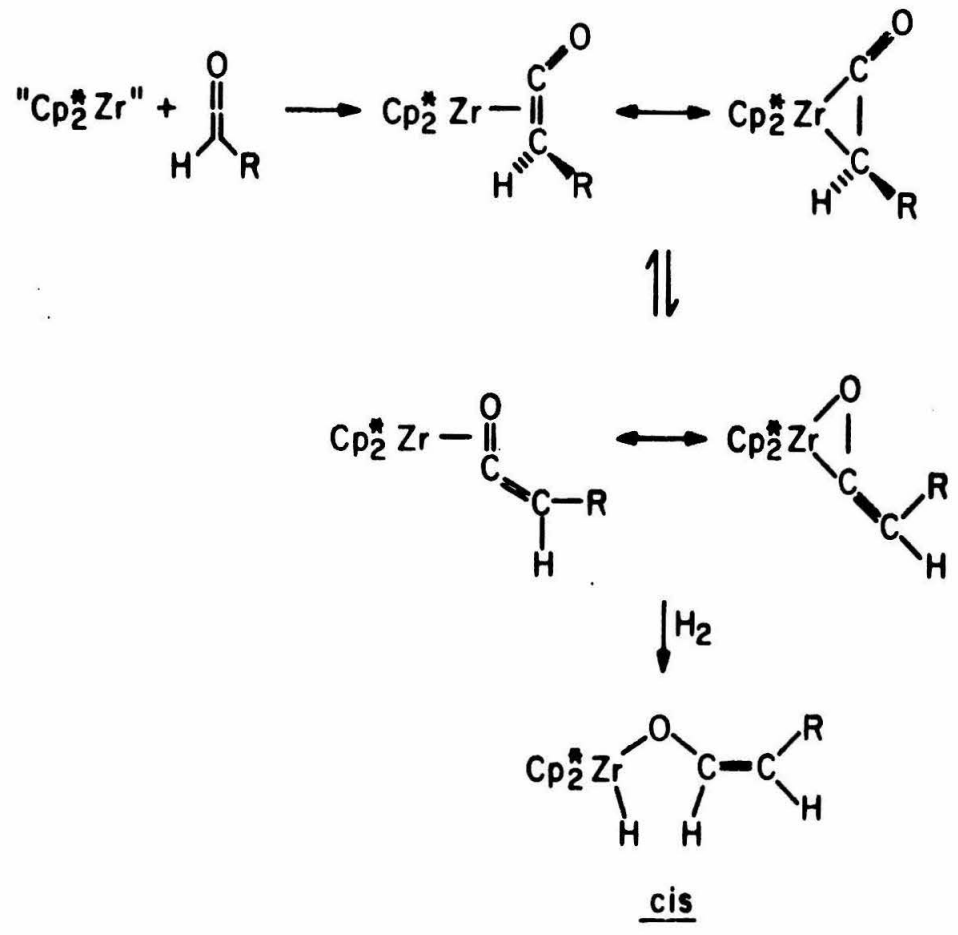

SCHEME 1.3. Mechanism for the Reaction of Permethylzirconocene with Monosubstituted Ketenes.

of metal atoms arrayed in a square network with C=C=O groups separating the layers.[13]

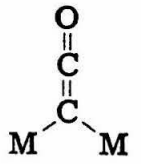

M = Ag, Cu, Au

FIGURE 1.1. Proposed Structure of Group I-b Metal-Ketene Complexes.

A π-bound metal-ketene complex (9) was first prepared by irradiating $CpMn(CO)_3$ and treating the unsaturated intermediate with diphenylketene (eq. 3).[14] ^1H NMR studies of the product revealed

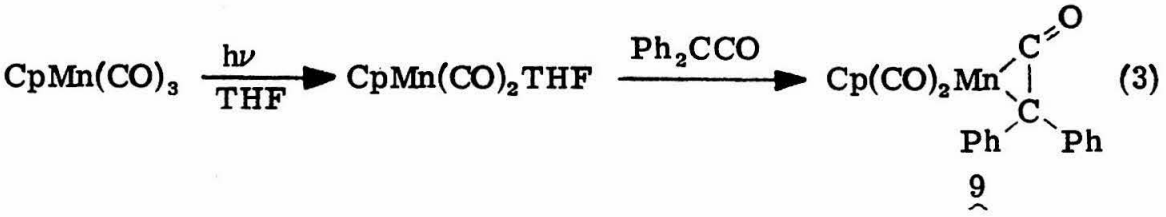

(3)

9

that the Cp resonance had shifted 0.43 ppm upfield, suggesting that the ketene was bound through the electron-rich olefinic bond (hence a ketene → metal charge transfer) and not the somewhat electron withdrawing carbonyl bond; X-ray structural analysis confirmed this reasoning.[15] Floriani has found that treatment of $Cp_2Ti(CO)_2$ with one equivalent of diphenylketene gives the carbonyl-bound ketene complex 10, which upon further reaction with the ketene gave the unsymmetrical metallocycle 11 (eq. 4).[16]

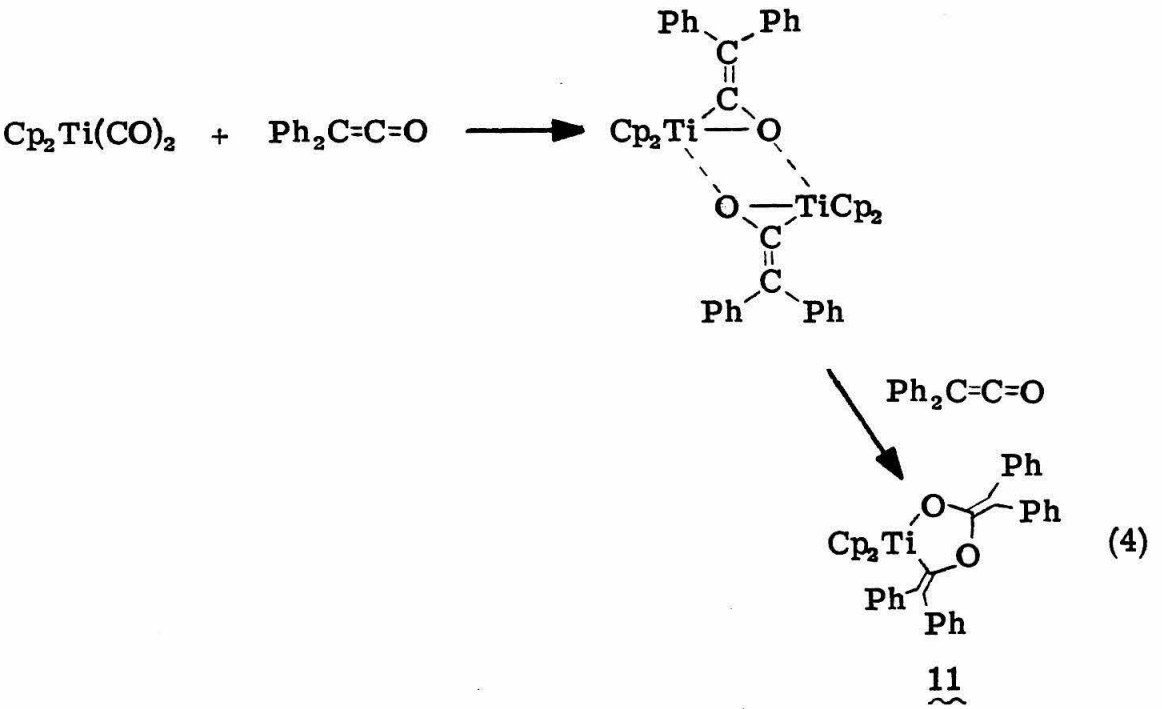

(4)

Perhaps the most interesting syntheses of metal-ketene complexes are those involving metal-carbene and carbyne precursors. Herrmann was able to prepare the π-bound diphenylketene manganese compound 9 mentioned earlier by treating a manganese alkylidene species with CO (eq. 5).[17] Subsequent treatment of 9 with H_2 afforded

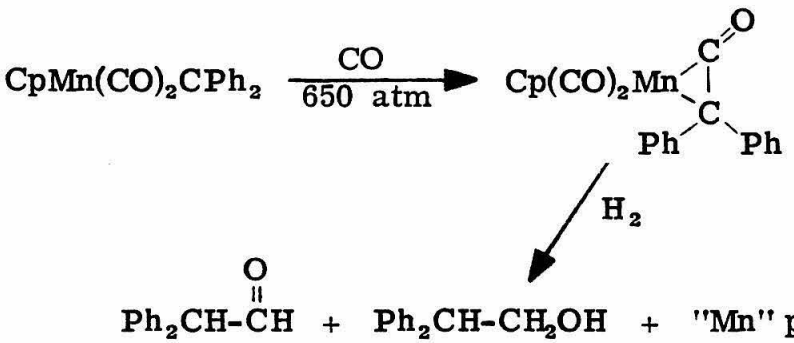

(5)

aldehydes and alcohols, providing a working model for the Fischer-Tropsch reaction. Although the reaction of metal carbonyl complexes with diazoalkanes usually affords N-substituted products, Herrmann was able to prepare the η^2-anthronylketene complex 10 by treating 9-diazoanthrone with a mixture of $CpMn(CO)_3$ and $CpMn(CO)_2THF$.[18] Labeling experiments suggest that 10 is formed by an intermolecular carbene-carbonyl coupling mechanism (eq. 6). In contrast, recent

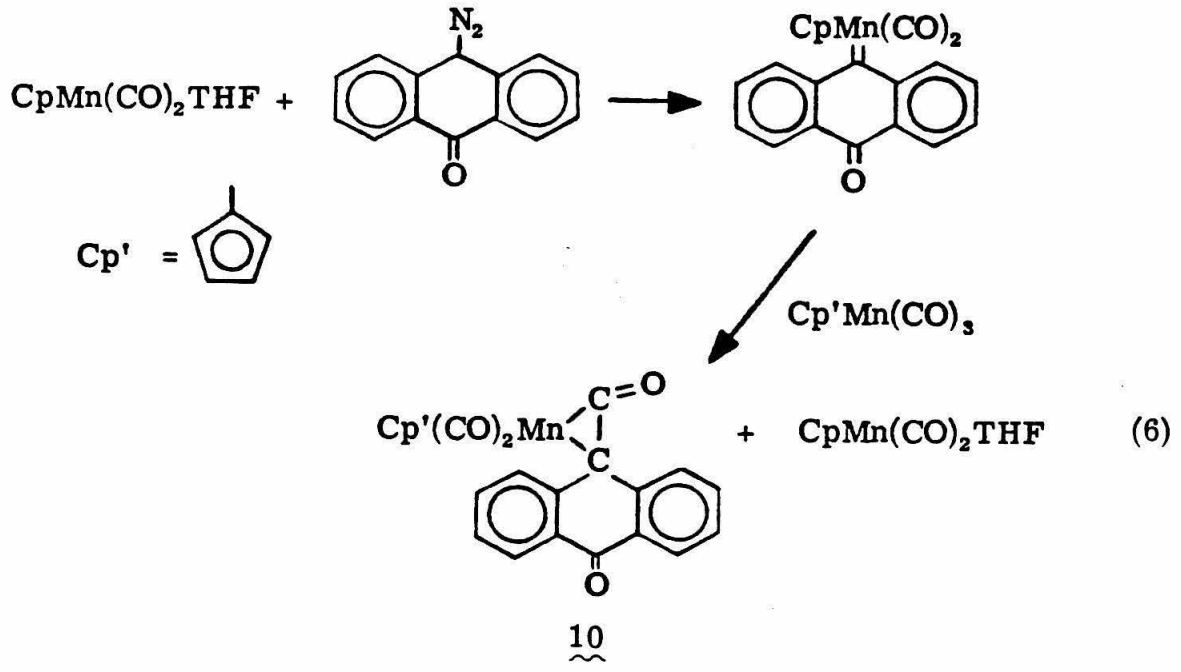

work in our laboratories suggests that the zirconium ketene complex 11 is formed by an intramolecular carbene-carbonyl coupling mechanism (eq. 7).[19] Kreissl has found that treatment of a tungsten

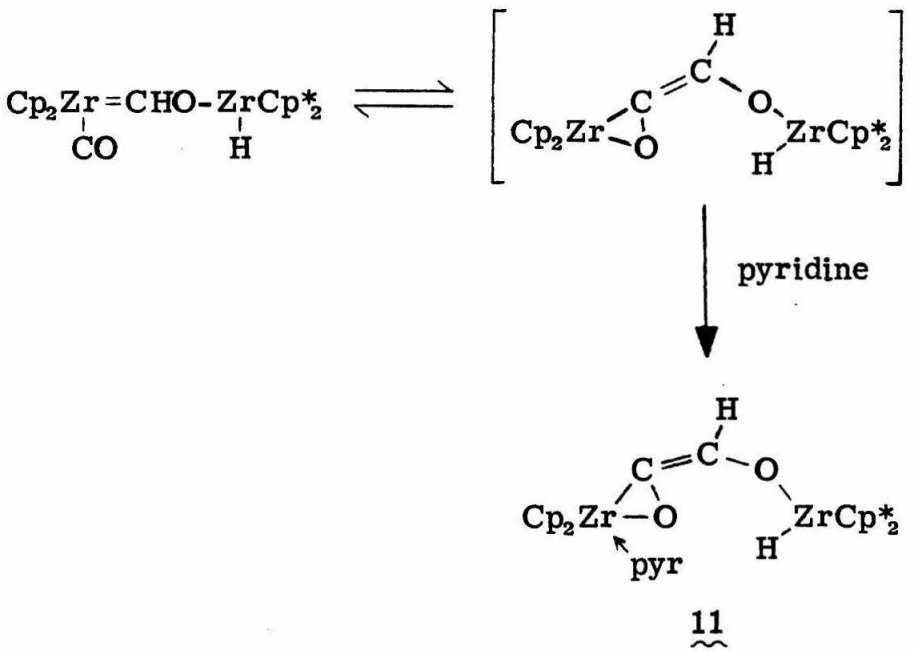

(7)

11

alkylidyne compound with PMe_3 affords a σ-bound ketene complex which rearranges to a π-complex upon warming (eq. 8).[20] Finally,

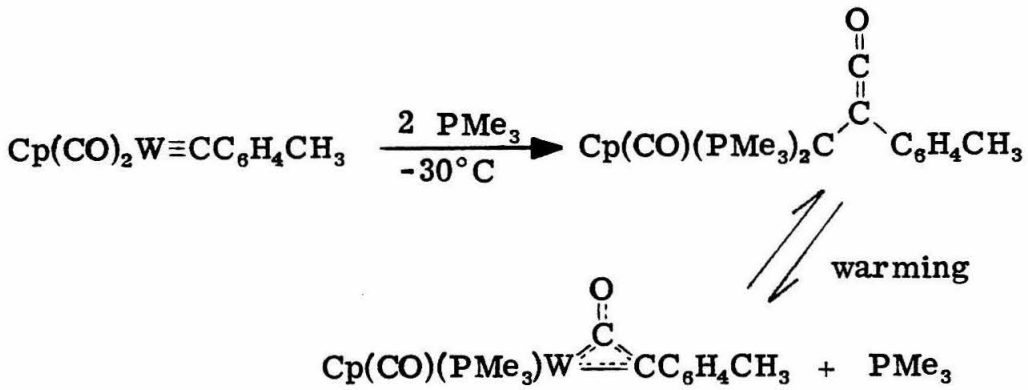

(8)

the reaction of CO with $Cp_2Ta(CHCMe_3)Cl$ or $Ta(CHPh)Cl_3(PMe_3)_2$ gives the corresponding ketene compounds, although no structural assignments were made from the spectroscopic data.[21]

The only reported zirconium-ketene complex has been prepared by Lappert.[7] Treatment of the zirconocene dialkyl complexes $Cp_2Zr(CHPh_2)R$ ($R = CH_3$, $CH_2Si(Me_3)_3$) with CO affords the dimeric diphenylketene complex $[Cp_2Zr(OCCPh_2)]_2$ and the acyl derivative $Cp_2Zr(COR)(CHPh_2)$. The mechanism of this reaction is not well understood.

1.2 Results and Discussion

1.2.1 Reaction of Permethylzirconocene with Trimethylsilylketene (13)

To establish whether zirconium-ketene intermediates are plausible in the cis-enediolate mechanism requires an unsymmetrical ketene possessing a bulky substituent to successfuly model the zirconium-ketene intermediate 6 (Scheme 1.2). Trimethylsilylketene (13) was chosen for this study because it is one of the few

monosubstituted ketenes which is relatively stable at room temperature.[22] Because $[Cp^*_2ZrN_2]_2N_2$ (12) is a ready source of "permethylzirconocene,"[23] it was thought that treatment of 12 with trimethylsilylketene might give a zirconium-ketene complex (Scheme 1.3). Treatment of 12 with 13 affords complete reaction, however, only when two equivalents of ketene per zirconium are used. This stoichiometry is maintained even at -50° C as evidenced by low temperature ^{1}H NMR spectroscopy, preventing isolation of a mono-ketene adduct. Thus, when 12 is treated with four equivalents of 13, three equivalents of N_2 are liberated[24] and the bis-ketene adduct 14 is formed in quantitative yield by ^{1}H NMR spectroscopy (eq. 9).

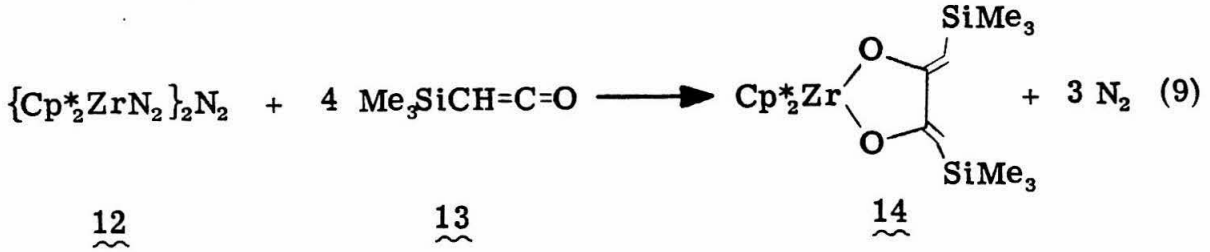

Compound 14 may be isolated as a yellow-brown crystalline solid in 59% yield by recrystallization from petroleum ether. The ^{1}H NMR spectrum of 14 consists of single resonances for the η^5-$C_5(CH_3)_5$ (δ 1.87), $Si(CH_3)_3$ (δ 0.40), and olefinic (δ 4.95) protons. The absence of additional proton resonances and the high oxophilicity of Zr(IV),[3,4] leads to the formulation of 14 as the symmetrical endo-substituted[25] dioxometallacyclopentane. Although an exo-substituted metallacycle would give similar ^{1}H NMR spectral data, steric interactions between the trimethylsilyl groups would be highly unfavorable. The ^{13}C NMR spectrum of 14 supports this configuration with two resonances for

the two different olefinic carbons at δ 178 and δ 92. The absence of any resonance downfield of δ 200 in the ^{13}C NMR spectrum strongly suggests a dioxometacyclic product.[26] This configuration is in contrast with the structure reported by Floriani for the unsymmetrical titanium metallacycle 11 (eq. 4). Apparently, unfavorable pentamethylcyclopentadienyl-trimethylsilyl ligand steric interactions as well as the greater oxophilicity of zirconium as compared with titanium dictate the formation of a dioxometallacycle in the zirconium system.

The zirconium metallacycle 14 can also be prepared by heating a solution of $Cp^*_2Zr(CO)_2$ and trimethylsilylketene in benzene for 12 hours. Whereas the formation of 14 from 12 is quantitative by ^1H NMR spectroscopy, the formation from $Cp^*_2Zr(CO)_2$ never exceeded 78%.

Since a mono-ketene adduct of zirconium could not be isolated or observed by low temperature ^1H NMR spectroscopy, it was hoped that treatment of a solution of $[Cp^*_2ZrN_2]_2N_2$ and trimethylsilylketene with H_2 at low temperature might effectively trap a mono-ketene adduct, affording an enolate-hydride product as per Scheme 1.2. Thus, although a mono-ketene adduct of zirconium would not be observed, its presence could be inferred by formation of an enolate-hydride product. Treatment of 12 with two equivalents of 13 at -78° C followed by reaction with H_2 and warming of the solution to room temperature afforded 14 as the single product. If H_2 is added to a -78° C solution of 12 followed by two equivalents of 13, varying amounts of 14 and Cp^*ZrH_2 (1) are formed upon warming the solution to room temperature; 1 undoubtedly being formed by reaction of 12 with H_2.[27] If

mono-ketene adducts analogous to 2 in Scheme 1.2 are formed in these reactions, further reaction with a second equivalent of ketene must be more rapid than reaction with H_2. Since free ketenes are presumably never present in reactions of $Cp^*Zr(CO)_2$ with $Cp^*_2ZrH_2$, the use of free ketenes to model intermediate 6 was deemed impractical.

1.2.2 Reaction of $Cp^*_2ZrH_2$ (1) with Ketenes

Due to our inability to obscure or detect a mono-ketene adduct of permethylzirconocene, we felt that the cis-enediolate mechanism might be entered through a complex analogous to 7 (Scheme 1.2) by treating $Cp^*_2ZrH_2$ (1) with ketenes (Scheme 1.4). Hopefully, a ketene

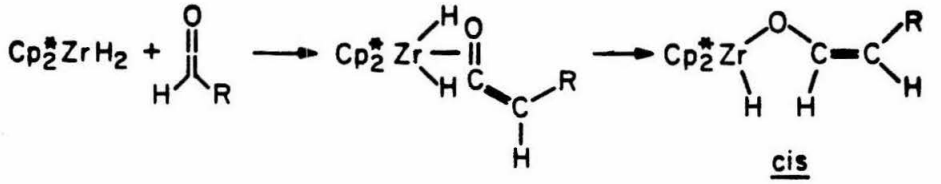

SCHEME 1.4. Mechanism for the Reaction of Permethylzirconocene Dihydride with Monosubstituted Ketenes.

π-adduct of 1 would be formed which, by hydride migration, would afford a cis-enolate product. That enolate complexes are a product in the reaction of zirconium hydride compounds with ketenes was demonstrated by the following reaction. Treatment of 1 with one equivalent of diphenylketene gave a yellow oil formulated as $Cp^*_2Zr(H)OCH{=}CPh_2$ (15) (eq. 10). The ^1H NMR spectrum of 15

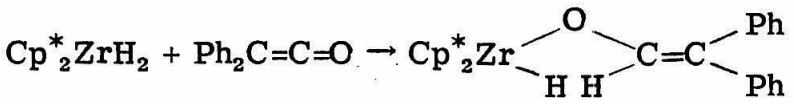

(10)

consists of singlet resonances for the η^5-$C_5(CH_3)_5$ (δ 1.82) and Zr-H (δ 6.29) protons as well as phenyl proton resonances. Although the hydride complex could not be crystallized, treatment of 15 with excess CH_3I afforded the yellow crystalline solid $Cp^*_2Zr(I)OCH{=}CPh_2$ (16) (52% isolated yield based on 1) and methane (0.9 mole CH_4/mole 15)[24] (eq. 11). Elemental analysis, molecular weight, ^1H NMR spectros-

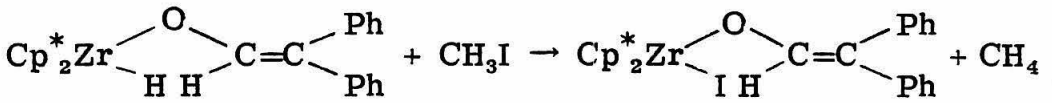

(11)

15 16

copy, and IR spectroscopy are all consistent with the formulation of 16 as an enolate complex.

Due to the equivalence of the substituents on the ketene, no stereochemical information was obtained from the reaction of diphenylketene with 1. To obtain this information, trimethylsilylketene (13) was used. Treatment of 1 with 13 in toluene solution affords a yellow oil consisting of two products formulated as cis- and trans-$Cp^*_2Zr(H)OCH{=}CHSiMe_3$ (17c and 17t, respectively) in a ratio of cis/trans = 3/1 (eq. 12). The ^1H NMR spectrum of the 17c-17t

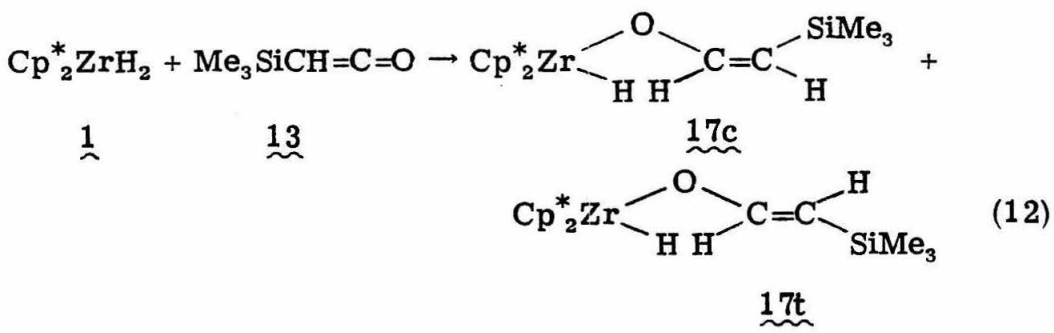

1 13 17c 17t (12)

mixture consists of two η^5-$C_5(CH_3)_5$ proton resonances, one at δ 1.85 for the cis isomer, the other at δ 1.80 for the trans isomer. Two hydride ligand resonances are observed at δ 6.20 (cis) and δ 5.44 (trans), consistent with those found for cis- and trans-$\{Cp^*Zr(H)\}_2$-(OCH=CHO).[28] The trimethyl silyl protons are also inequivalent with resonances at δ 0.29 (cis) and δ 0.23 (trans). The somewhat larger, downfield shift of the trimethylsilyl proton resonance of the cis isomer is expected because of the greater interaction and resulting deshielding effect with the pentamethylcyclopentadienyl ligands. The stereochemical assignments are based on the $^3J_{HH}$ coupling constants of the vinylic doublets. Two doublets ($^3J_{HH}$ = 9 Hz) are observed for the cis isomer at δ 7.05 and δ 3.89, while doublets ($^3J_{HH}$ = 14 Hz) for the trans isomer are found at δ 7.06 and δ 4.45;[28] typical coupling constants for trans and cis vinylic hydrogens are 13-18 Hz and 6-11 Hz, respectively.[29] Examples are given in Table 1.1. It can be seen that increasing the electron withdrawing ability of the olefinic substituents results in a decrease in the value of the vinylic coupling constants. Thus, while the observed values for 17c and 17t are not as large as that for cis- and trans-$Me_3SiCH{=}CHPh$, they are greater than those for

TABLE 1.1. $^{3}J_{HH}$ Vinylic Proton Coupling Constants of Some Representative Olefinic Compounds.

Compound	cis (Hz)	trans (Hz)
$Me_3SiCH{=}CHPh$	15	19
$Me_3SiCH{=}CHMe_3$	14.4	18.6
$Me_3SiCH{=}CHOZr(H)Cp^*_2$	9	14
$Me_3CH{=}CHOEt$	7	13
$\{Cp^*_2ZrH\}_2(OCH{=}CHO)$	3.5	10

cis- and trans-$\{Cp^*_2ZrH\}_2(OCH{=}CHO)$. The stereochemical assignments of the other ^1H NMR resonances were based on integrations relative to these vinylic doublets. Treatment of the 17c-17t mixture with excess CH_3I gave another yellow oil formulated as cis- and trans-$Cp^*_2Zr(I)OCH{=}CHSiMe_3$ and CH_4 (0.9 mol CH_4/mol 1).[24] The ^1H NMR spectrum of the iodo derivatives is virtually identical to that of the 17c-17t mixture, except for the expected absence of the hydride ligand resonances. Unfortunately, no separation of the isomers or crystallization of the oil could be achieved.

The question arises as to why both isomers are observed in the reaction of 1 with 13 instead of the single cis isomer as expected from Schemes 1.2 and 1.4. A thermodynamic rearrangement of the cis isomer can be invoked to explain the formation of the trans complex. Attempts to convert the cis-trans mixture into the thermodynamically favored all trans geometry failed, however. Neither moderate heating

(< 100° C) nor exposure to short-term UV radiation (254 nm) had discernable effect; more forcing conditions simply decomposed the mixture. Low temperature ^{1}H NMR studies confirm that the isomer ratio is established at temperatures as low as -50° C and remains unchanged when the reaction is performed at higher temperatures.

1.2.3 Reaction of $Cp^*_2Zr(H)X$ (X = Cl, F) with Trimethylsilylketene (13)

A second pathway in competition with that proposed in Schemes 1.2 and 1.4 might also account for the formation of the trans isomer. One could envision the ketene coordinating to the zirconium center in an acyl fashion with hydride transfer to the β-carbon resulting in the formation of the acyl-hydride intermediate 18 (Scheme 1.5). A second

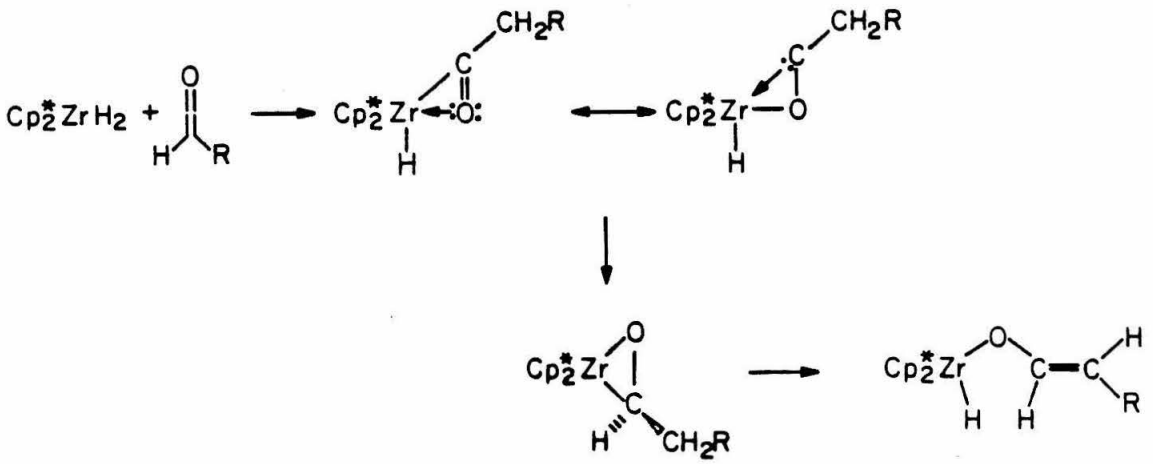

SCHEME 1.5. Mechanism for the Formation of trans-$Cp^*_2Zr(H)OCH{=}CHSiMe_3$ (17t) in the Reaction of $Cp^*_2ZrH_2$ (1) with Trimethylsilylketene (13).

hydride transfer to the α-carbon followed by β-hydride elimination affords the trans-enolate complex as per Scheme 1.1. Precedent for the acyl-hydride intermediate and subsequent steps comes from work

in our laboratories with permethylzirconocene alkyl-hydride complexes. Compounds such as 19 react with CO at -50° C to afford the η^2-acyl intermediate 20 which, upon warming, undergo α-hydride transfer and trapping by CO to give the aldehyde-carbonyl complex 21 (eq. 13).[30]

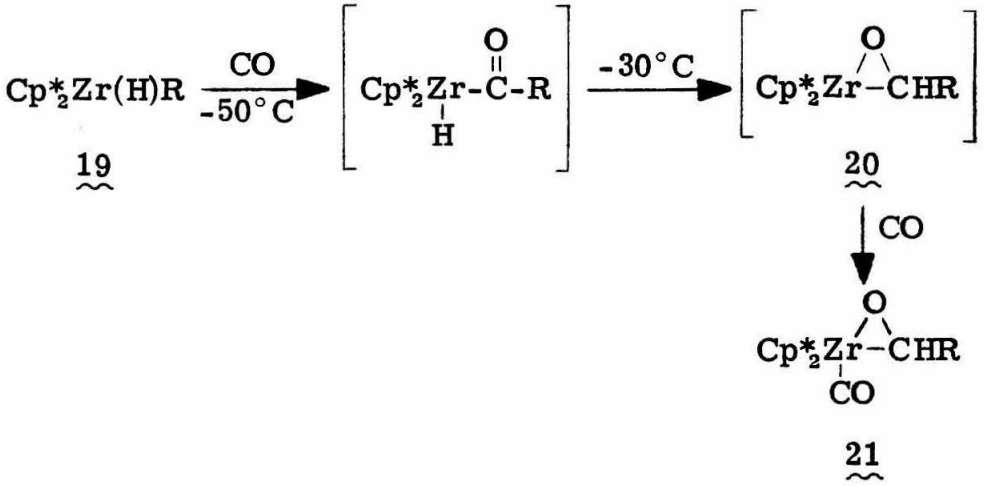

(13)

To test this hypothesis, a monohydrido-permethylzirconocene complex was used so that transfer of the second hydride would be precluded. None of the trans-enolate complex should then be observed. Treatment of $Cp^*_2Zr(H)X$ (X = Cl, F) with one equivalent of 13 affords a yellow oil consisting of two products formulated as cis- and trans-$Cp^*_2Zr(X)OCH{=}CHSiMe_3$. The ^1H NMR spectrum of this mixture is identical to that observed for the iodo derivatives of 17c and 17t. The isomer ratio, however, is dependent both on X and on the reaction solvent (Table 1.2), but in all cases the concentration of the trans isomer was equal to or exceeded that of the cis isomer. Scheme 1.5 is, therefore, not the only possible mechanism for the formation of the trans isomer in this system.

TABLE 1.2. Isomer Ratios Obtained from the Reaction of $Cp^*_2Zr(H)X$ (X = H, Cl, F) with Trimethylsilylketene (13) in Varying Solvents.

Starting Material	Solvent	Isomer Ratio (trans/cis)
$Cp^*_2Zr(H)F$	toluene	9/1
$Cp^*_2Zr(H)F$	pet. ether	2/1
$Cp^*_2Zr(H)Cl$	toluene	3/1
$Cp^*_2Zr(H)Cl$	pet. ether	1/1
$Cp^*_2Zr(H)Cl$	THF	2/1
$Cp^*_2ZrH_2$	pet. ether	1/3
$Cp^*_2ZrH_2$	toluene	1/3
$Cp^*_2ZrH_2$	THF	1/2

1.2.4 Reaction of Cp^*ZrH_2 (1) with t-Butylallene (22).

The foregoing results are consistent with a mechanism involving nucleophilic attack of an oxygen lone pair of the ketene on the highly oxophilic zirconium(IV) center in $Cp^*_2Zr(H)X$ (X = H, Cl, F) (Scheme 1.6).

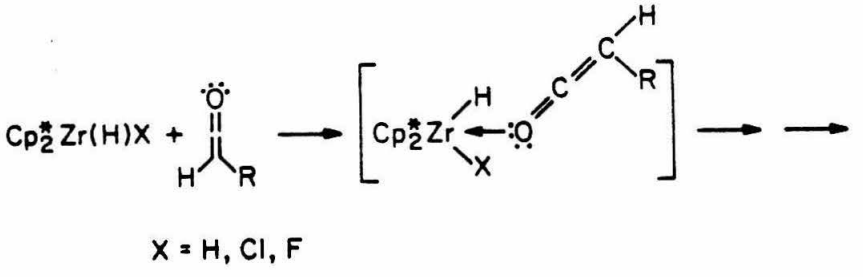

SCHEME 1.6. Interaction of Ketenes with Monohydride Derivatives of Permethylzirconocene.

The isomer ratio might then depend on electronic effects associated with each substituent X as well as on solvent. This contrasts with a mechanism involving initial π-coordination to either the carbonyl or olefinic bond of the ketene. Because a ketene π-adduct similar to intermediate 7 in Scheme 1.2 is not formed, the reaction of free ketenes with $Cp^*_2Zr(H)X$ need not be stereoselective. Thus, a mixture of isomeric products is obtained. To preclude this "lone pair" attack, a sterically hindered monosubstituted allene (t-butylallene (22)) was used. Reaction of 1 with 22 would be expected to give the unstable π-allyl intermediate 23 which would rearrange to the more stable cis-σ-allyl zirconium hydride complex 24 (Scheme 1.7). Although reaction

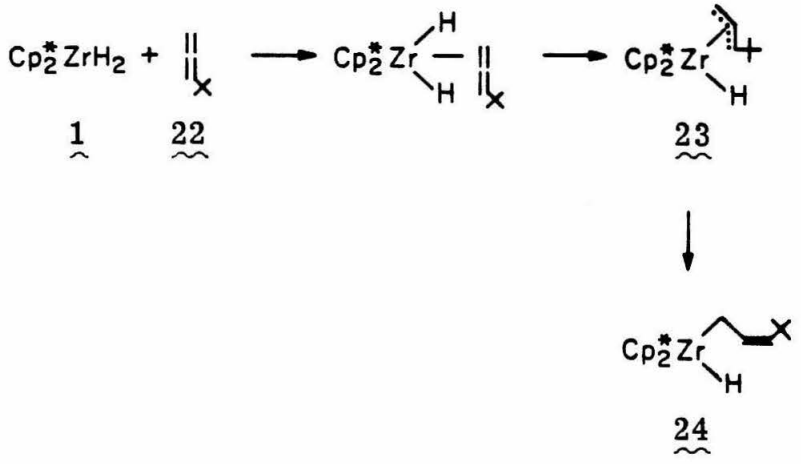

SCHEME 1.7. Proposed Mechansim for the Reaction of $Cp^*_2ZrH_2$ (1) with t-Butylallene (22).

of 1 with allene gives only the stable π-allyl complex 25 (eq. 14),[31] unfavorable steric interactions between the t-butyl group and the

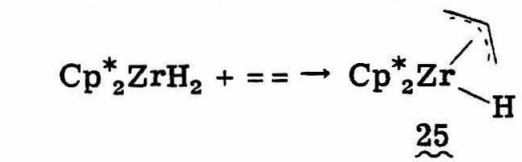

(14)

25

pentamethylcyclopentadienyl ligands should give the more stable σ-allyl complex with the substituted allene.

Treatment of 1 with one equivalent of 22 affords an orange solution containing unreacted 1 and two products identified as $Cp^*_2Zr(H)CH_2CH_2C(CH_3)_3$ (27) and $Cp^*_2ZrC{=}CHC(CH_3)_3CH_2C{=}CCHC(CH_3)_3CH_2$ (26) (eq. 15). No σ-allyl or π-allyl complexes were observed. Although neither product could be isolated from the reaction mixture, their presence was verified by ^1H NMR spectroscopy following their successful isolation (vide infra). When 1.5 equivalents of 22 are used, no unreacted 1 is observed and both 26 and 27 are formed in equimolar amounts (eq. 16). If excess 22 is employed (> 1.5 equivalents), 23 and a new product, identified as $CH_2{=}CHCH_2C(CH_3)_3$ (28), are the only products observed in addition to unreacted allene (eq. 17).

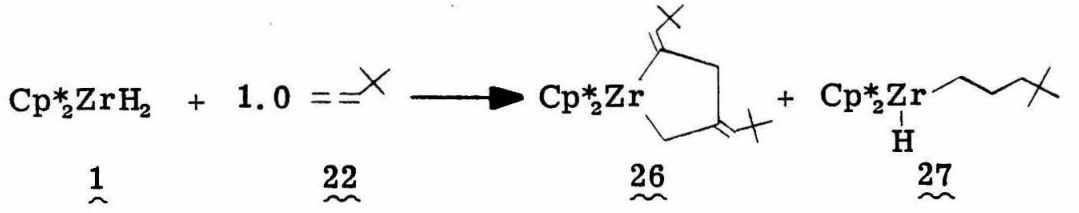

1 22 26 27

+ unreacted 1 (15)

(16)

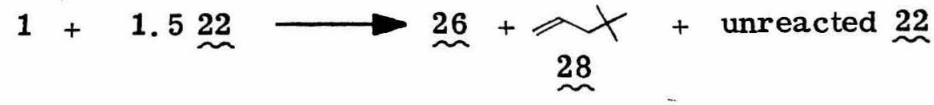

28 (17)

A mechanism which accounts for these observations is outlined in Scheme 1.8. $Cp^*_2ZrH_2$ reacts with t-butylallene to give a π-allyl intermediate 23 which rearranges by an equilibrium step to the π-olefin complex 29, analogous to the equilibrium that has been *invoked to*

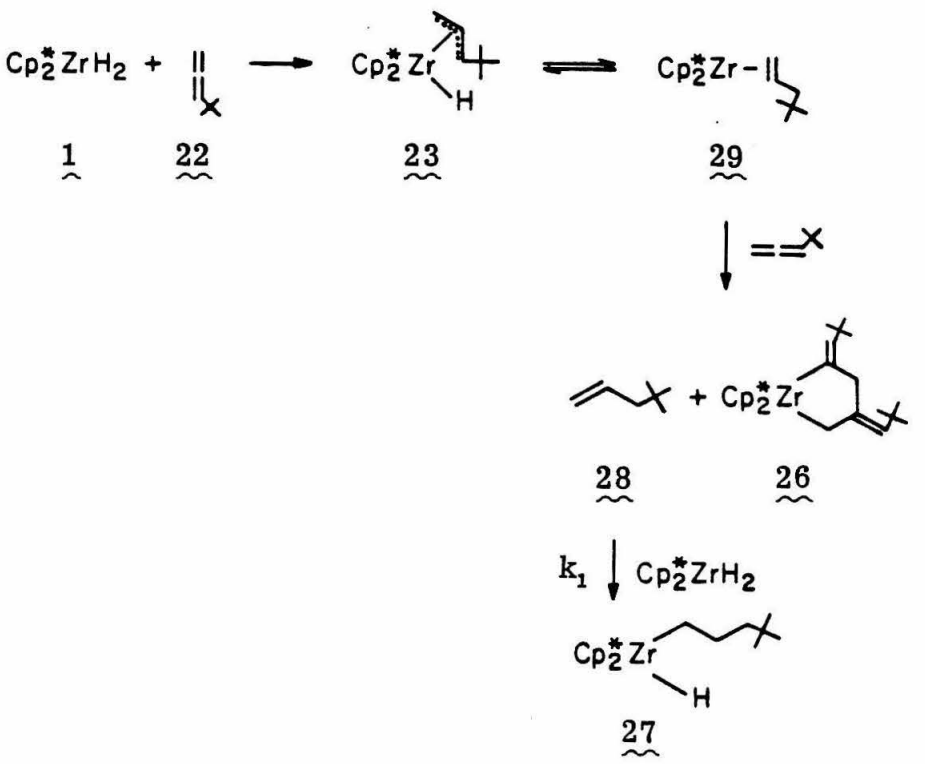

SCHEME 1.8. Mechanism for the Reaction of $Cp^*_2ZrH_2$ (1) with t-Butylallene (22).

explain the equivalence of the methylene hydrogen resonance and the hydride ligand resonance in the ^{1}H NMR spectrum of $Cp^*_2Zr(H)(\eta^3\text{-}C_3H_5)$.[32] Unreacted allene then competes with the olefin for the permethylzirconocene fragment giving the metallacycle 22 and 1-neoheptene. Reaction of 1 with 1-neoheptene in the rate-determining step k_1 affords the alkyl-hydride complex 27. Because the previous steps are rapid compared with the final rate-determining step k_1, the supply of either 1 or 22 is exhausted before the final step can occur. Thus, 27 is formed only when the supply of allene is exhausted and excess 1 remains. The relative rate between k_1 and the steps leading to formation of 26 was demonstrated by means of a competition experiment in which a homogeneous mixture of two equivalents of t-butylallene and one equivalent of 1-neoheptene was added to a solution of $Cp^*_2ZrH_2$ at -78° C. Upon warming to room temperature, the ^{1}H NMR spectrum of the solution indicated 26 had formed in greater than 95% yield. One may conclude that k_1 is at least twenty times slower than the next slowest step in Scheme 1.7. Thus, when less than 1.5 equivalents of 22 are used, the allene is depleted to form 26 and 28. Unreacted 1 then reacts with 28 to give 27. When 1.5 equivalents are used, equal amounts of 26 and 27 are formed and no unreacted 1 remains. However, when excess 22 is used (>1.5 equivalents) 1 is depleted before any 27 can be formed and only 26 and 28 are observed as products.

The permethylzirconocene alkyl-hydride complex 27 was identified by comparison of its ^{1}H NMR spectrum with an authentic sample

prepared by treating 1 with 1-neoheptene (eq. 18). The ^{1}H NMR

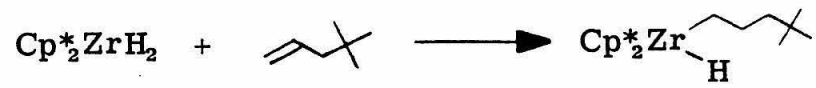

(18)

spectrum of 27 consists of singlet resonances for the η^5-$C_5(CH_3)_5$ (δ 1.90) and $C(CH_3)_3$ (δ 0.97) protons and a broad singlet at δ 5.43 for the hydride ligand resonance. A high field triplet ($^3J_{HH}$ = 6 Hz) observed at δ 0.23 is assigned to the zirconium-methylene resonance.[33] The remaining methylene proton resonances were not observed, presumably because they are buried under the η^5-$C_5(CH_3)_5$ resonance. The 1-neoheptene (28) produced in equation 17 was also identified by comparison of its ^{1}H NMR spectrum with that of an authentic sample.

The exo-unsaturated metallacyclopentane 26 was identified by comparison of its ^{1}H NMR spectrum with that of the product obtained by treating $[Cp^*_2ZrN_2]_2N_2$ (12) with four equivalents of t-butylallene (eq. 19). The product is very similar to one of two isomers obtained

(19)

by Duggan in the reaction of 12 with methylallene (eq. 20),[34] and

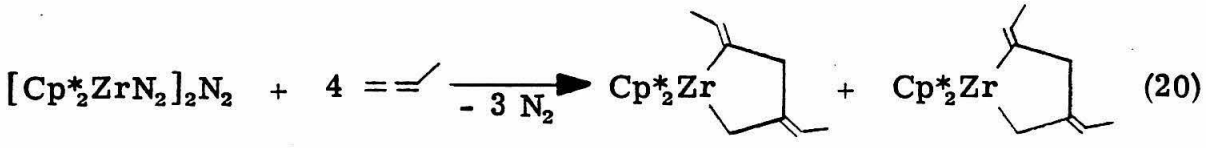

(20)

assignment was made on that basis. Reaction of allene with transition metal complexes has been shown to give any of three different isomers (Figure 1.2). Reaction of allene with 12 has been shown to give com-

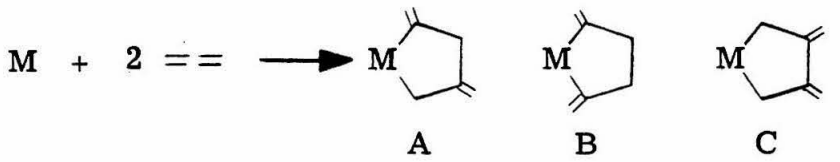

FIGURE 1.2. Observed Isomeric Metallacycles in the Reaction of Allene with Transition Metal Complexes.

plexes of type A and B exclusively.[34] However, when methylallene is used, only type A is observed. The ^1H NMR spectrum of 26 is in accord with this type. One η^5-$C_5(CH_3)_5$ proton resonance at δ 1.90 and two t-butyl proton resonances at δ 1.43 and δ 1.26 are consistent with a single isomer consisting of two inequivalent t-butyl groups. Broad multiplets at δ 4.97, δ 3.79, and δ 3.43 are assigned to the H(6), H(7), and H(3) proton resonances respectively, in accord with the assignments made by Duggan (Table 1.3). The chemical shift of the H(6) proton resonance is indicative of an exo-substituted t-butyl group at C(6) and no resonance suggestive of endo-substitution (located at δ 6.06 in 30) is observed. This seems reasonable due to unfavorable t-butyl-pentamethylcyclopentadienyl ligand interactions which would occur in the C(6) endo-substituted isomer. Unfortunately, resolution of the multiplets could not be achieved using a 90 MHz spectrometer. The $^{13}C\{^1H\}$ NMR spectrum was also consistent with the proposed

TABLE 1.3. Comparison of ^{1}H and ^{13}C NMR Spectral Data for Two Permethylzirconocene Metallacyclopentanes.

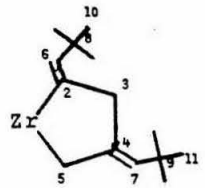

26

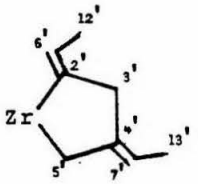

31

	^{1}H NMR (δ)		
H(7)	4.97	H(7')	5.05
H(6)	3.79	H(6')	4.24
H(3)	3.43	H(3')	3.04
η^5-$C_5(CH_3)_5$	1.90	η^5-$C_5(CH_3)_5$	1.81
		H(13')	under rings
		H(12')	1.66
H(11)	1.43		
H(10)	1.26		
H(5)	under t-butyl	H(5')	1.18
	^{13}C NMR (δ)		
C(2)	196	C(2')	196.8
C(4)	142	C(4')	144.6
C(6)	136	C(6')	120.0
C(7)	135.6	C(7')	109.5
η^5-$\underline{C}_5(CH_3)_5$	119	η^5-$\underline{C}_5(CH_3)_5$	119.3
C(3)	52.8	C(3')	49.1
C(5)	48.3	C(5')	48.5
C(8)	34.6		
C(9)	34.2		
C(10)	32.4		
C(11)	31.6		
		C(12')	15.62
		C(13')	15.46
η^5-$C_5(\underline{C}H_3)_5$	11.9	η^5-$C_5(\underline{C}H_3)_5$	11.9

configuration. The η^5-$C_5(CH_3)_5$ carbon resonances at δ 119 (η^5-$\underline{C}_5(CH_3)_5$) and δ 11.9 (η^5-$C_5(\underline{C}H_3)_5$) and t-butyl carbon resonances at δ 34.6 (C(8)), δ 32.4 (C(9)), and δ 34.2 (C(10)), δ 31.6 (C(11)) are in accord with a single isomer consisting of two inequivalent t-butyl groups. The one low field resonance at δ 196 is characteristic of a single sp^2-hybridized carbon adjacent to zirconium (C(2)) and the high field resonance at δ 48.3 is assigned to an sp^3-hybridized carbon adjacent to zirconium (C(5)). The remaining carbon assignments were made by comparison with the $^{13}C\{^1H\}$ NMR spectrum of 31 and by carbon-hydrogen coupling constants in the coupled spectrum of 26. Although the stereochemistry of C(7) is somewhat uncertain, the reaction of 12 with methylallene never affords an isomer with endo-stereochemistry at C(7'). By analogy, we believe 26 is also exo-substituted at C(7).

1.2.5 Reaction of $Cp^*_2Zr(H)Cl$ with t-Butylallene (22)

The reaction of $Cp^*_2ZrH_2$ with t-butylallene was not successful in generating a σ-allyl complex because of the second hydride migration to afford the π-olefin intermediate 29. To preclude the transfer of a second hydride ligand, the mono-hydride complex $Cp^*_2Zr(H)Cl$ (32) was used. Treatment of 32 with one equivalent of 22 affords cis-$Cp^*_2Zr(Cl)CH_2CH{=}CHCMe_3$ (33c) quantitatively by ^1H NMR spectroscopy (eq. 21). The $^3J_{HH}$ vinylic coupling constant of 13 Hz observed in the

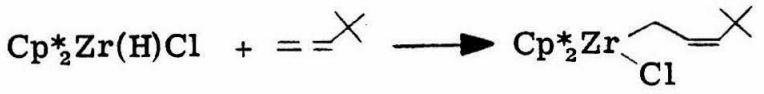

(21)

32 22 33c

^{1}H NMR spectrum of 33c is consistent with the proposed cis-stereochemistry.[35] Although only one isomeric product is initially observed in the reaction of 32 with 22 (evident by single η^5-$C_5(CH_3)_5$ and $C(CH_3)_3$ proton resonances), solutions of 33c do isomerize completely after 24 hours at room temperature to give the corresponding trans isomer 33t (eq. 22). trans-$Cp^*_2Zr(Cl)CH_2CH{=}CHCMe_3$ can be isolated as an

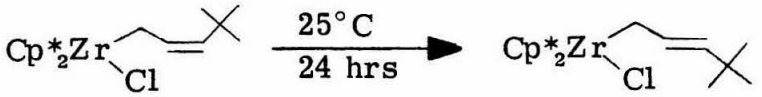

33c 33t (22)

orange crystalline solid in 57% yield by recrystallization from petroleum ether. The ^{1}H NMR spectrum of 33t is similar to that of 33c, except for the expected resonance shifts and the larger $^3J_{HH}$ vinylic coupling constant of 15 Hz, consistent with the proposed trans stereochemistry.[35] The C=C stretch observed at 1630 cm^{-1} in the IR spectrum of 33t is also consistent with the formulation of 33t (and most likely 33c) as a σ-allyl complex.[36] The results of equation 23 support the initial postulate of Scheme 1.2 that if a π-cummulene-permethylzirconocene derivative can be formed, steric interactions dictate the stereoselective formation of a cis product.

A proposed mechanism for the isomerization of 33c to 33t is depicted in Scheme 1.9 and involves formation of a π-allyl species which rearranges to the σ-allyl intermediate 34. Rotation about the C-C single bond affords the σ-allyl intermediate 35. Intermediate 35 rearranges to a second π-allyl species which affords the trans σ-allyl complex 33t. Such a pathway would not be available to an enolate

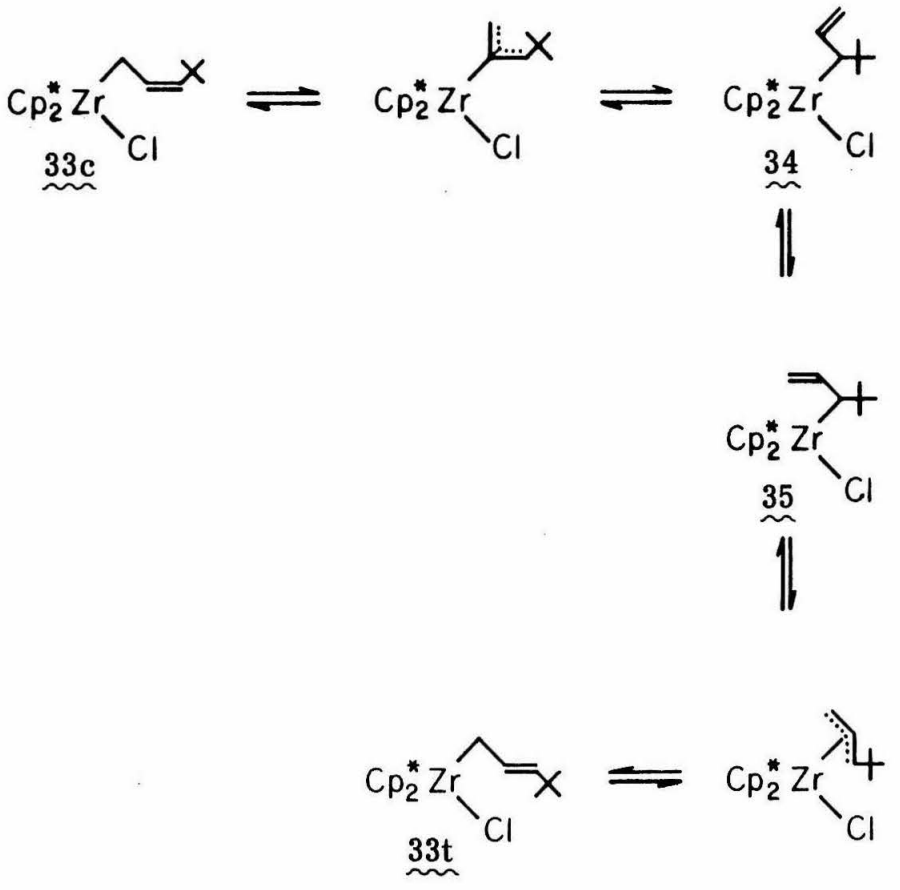

SCHEME 1.9. Mechanism for the Isomerization of cis-$Cp^*_2Zr(Cl)CH_2CH{=}CHCMe_3$ (33c) to trans-$Cp^*_2Zr(Cl)CH_2CH{=}CHCMe_3$ (33t).

complex, thereby explaining the absence of any trans-enediolate compound formed from rearrangement of the corresponding cis isomer in the reaction of $Cp^*_2Zr(CO)_2$ with $Cp^*_2ZrH_2$.

1.3 Conclusion

The results of this study confirm that, under appropriate conditions, the hydrogenation of cummulenes by permethylzirconocene hydride complexes is stereoselective for cis-substituted products, and lends credence to the mechanism outlined in Scheme 1.2. It is unfortunate that the use of free ketenes has not allowed us to successfully model this mechanism. The symmetric coupling of two ketenes to a single zirconium center is not surprising, however, considering the high oxophilicity of zirconium in these compounds and the steric constraints imposed by the two permethylcyclopentadienyl ligands. This oxophilicity is further demonstrated by the apparent attack of the zirconium center in $Cp^*_2Zr(H)X$ (X = H, Cl, F) not at the olefinic or carbonyl bond of the ketene, but rather at an oxygen lone pair. Such an attack need not follow the steric requirements imposed by Scheme 1.2. Thus, both cis and trans isomers are observed as reaction products. The reaction of t-butylallene with $Cp^*_2Zr(H)Cl$ to afford exclusively that cis-substituted σ-allyl complex 33c, suggests that if π-coordination of a cummulene to a permethylzirconocene center can occur, steric interactions dictate the stereoselective formation of a cis product. In the absence of free ketenes, Scheme 1.2 is a viable mechanism for the formation of the cis-enediolate complex 8 formed in the reaction of $Cp^*Zr(CO)_2$ with $Cp^*_2ZrH_2$.

1.4 Experimental Section

1.4.1 General Methods

All manipulations were performed in an inert atmosphere using high vacuum line, Schlenk-type, or glove box techniques. Argon, hydrogen, and nitrogen were passed through MnO on vermiculite[37] and 4 Å molecular sieves.

1.4.2. Physical and Spectroscopic Methods

Proton magnetic resonance spectra were recorded using either a Varian EM390 or Bruker WM500 spectrometer. Chemical shifts are reported in ppm (δ) relative to Me_4Si (δ 0.0). Carbon magnetic resonance spectra were recorded using a JEOL FX 90Q spectrometer. Chemical shffts are reported in ppm (δ) relative to Me_4Si (δ 0.0). Infrared spectra were recorded using NaCl plates on a Beckman 4240 spectrometer.

Molecular weight determinations (by osmometry) and elemental analyses were performed by the Alfred Bernhardt Analytical Laboratory.

1.4.3 Solvents and Reagents

Solvents were purified by vacuum transfer first from $LiAlH_4$ and then from "titanocene."[38] The NMR solvents benzene-d_6 and toluene-d_8 (Stohler, Inc.) were vacuum transferred from titanocene. THF-d_8 (Stohler, Inc.) was distilled from sodium benzophenone ketyl. Methyl iodide was vacuum transferred from CaH_2. 1-Neoheptene (Pfaltz and Bauer) was used without further purification.

The following compounds were prepared by the reported procedures: $[Cp^*_2ZrN_2]_2N_2$,[39] $Cp^*_2ZrH_2$,[27] $Cp^*_2Zr(H)Cl$,[40] $Cp^*_2Zr(H)F$,[40]

$Cp^*_2Zr(CO)_2$,[3] $Ph_2C{=}C{=}O$,[41] $Me_3SiCH{=}C{=}O$,[42] $Me_3CCH{=}C{=}CH_2$.[43]

1.4.4 $Cp^*_2\overline{ZrOC{=}CHSiMe_3C{=}CHSiMe_3O}$ (14)

$[Cp^*_2ZrN_2]_2N_2$ (12) (265 mg, 0.33 mmol) was dissolved in toluene (30 ml) and the solution cooled to -78°C. A solution of $Me_3SiCH{=}C{=}O$ (13) (180 μL, 1.3 mmol) in toluene (0.15 mL) was added with stirring and the mixture warmed to room temperature. Upon warming, the color of the solution turned from deep purple to dark red. Toepler pump analysis of the gas product indicated 2.9 mol N_2/mol 12. The volume of the solution was reduced to 15 mL in vacuo and the solution cooled to -78° C. A brown solid precipitated which was isolated by filtration to afford 14 as a yellow-brown crystalline solid (130 mg). A second crop was obtained from petroleum ether (15 mL) at -78° C (70 mg). Combined yield was 59%. Anal. Calcd for $C_{30}H_{50}O_2Si_2Zr$: C, 61.06; H, 8.54; Zr, 15.46 Found: C, 61.06; H, 8.64; Zr, 15.28. ^1H NMR (benzene-d_6): δ 4.95 (s, 2H, CH); 1.87 (s, 30H, $C_5(CH_3)_5$); 0.40 (s, 18H, $Si(CH_2)_3$). ^{13}C NMR (benzene-d_6): δ 178 (s, OC), 123 (s, $\underline{C}_5(CH_3)_5$), 92.0 (d, $^1J_{CH}$ = 133 Hz, $\underline{C}HSiMe_3$); 10.9 (q, $^1J_{CH}$ = 127 Hz, $C_5(\underline{C}H_3)_5$; 1.23 (q, $^1J_{CH}$ = 118 Hz, $Si(\underline{C}H_3)_3$). IR (nujol): ν(C=C) 1560 cm^{-1}, ν(C-O) 1280, ν(C-O) 1130.

1.4.5 Reaction of $Cp^*_2Zr(CO)_2$ with $Me_3SiC{=}C{=}O$ (13) to give 14

$Cp^*_2Zr(CO)_2$ (25 mg, 0.06 mmol) was dissolved in C_6D_6 (0.15 mL) in an NMR tube. The solution was frozen at -196° C and $Me_3SiC{=}C{=}O$ (13) (0.12 mmol) added. The tube was sealed with a torch and heated at 80° C for 12 hours. The ^1H NMR spectrum of this solution indicated 14 had formed in 78% yield. Increasing the ketene concentration did not significantly increase the product yield.

1.4.6 $Cp^*_2Zr(H)OCH{=}CPh_2$ (15)

The procedure described in Section 1.4.4 was followed using 250 mg (0.69) $Cp^*_2ZrH_2$ (1) in 12 mL toluene and adding a solution of 123 μL (0.69 mmol) $Ph_2C{=}C{=}O$ in 12 mL toluene. The color of the solution turned from blue to amber upon warming. Removal of solvent in vacuo afforded 15 as an amber oil. ^{1}H NMR (benzene-d_6): δ 7.68-7.00 (m, 10H, Ph); 6.29 (S, 1H, ZrH); 1.82 (S, 30H, $C_5(CH_3)_5$). The olefinic proton resonance is obscured by phenyl resonances. IR (nujol): ν(C=C) 1590 cm^{-1}, ν(C-O) 1250, ν(C-O) 1125.

1.4.7 $Cp^*_2Zr(I)OCH{=}CPh_2$ (16)

$Cp^*_2Zr(H)OCH{=}CPh_2$ (15) (0.69 mmol) (formed in situ following the procedure of section 1.4.6) was dissolved in toluene (25 mL) and the solution cooled to -78° C. CH_3I (1.4 mmol) was added with stirring and the mixture allowed to warm to room temperature and stir for 12 hours. Toepler pump analysis of the gas product indicated 0.9 mol CH_4/mol 1. The volume of the solution was reduced to 15 mL in vacuo and the solution cooled to -78° C. A yellow solid precipitated which was isolated by filtration to afford 16 as a yellow crystalline solid (138 mg). A second crop was obtained from toluene (10 mL) at -78° C (115 mg). Combined yield was 52%. Anal. Calcd for $C_{34}H_{41}IOZr$: C, 59.72; H, 6.04; I, 18.56; Zr, 13.34; MW, 675. Found: C, 59.84; H, 6.29; I, 18.76; Zr, 13.23; MW, 684. ^{1}H NMR (benzene-d_6): 7.60-7.07 (m, 10H, Ph); 2.82 (s, 30H, $C_5(CH_3)_5$). The olefinic proton resonance is obscured by phenyl resonances. IR (nujol): ν(C=C) 1592 cm^{-1}, ν(C-O) 1238; ν(C-O) 1120.

1.4.8 cis- and trans-$Cp^*_2Zr(H)OCH{=}CHSiMe_3$ (17c, 17t)

The procedure described in section 1.4.4 was followed using 250 mg (0.69 mmol) $Cp^*_2ZrH_2$ (1) in 50 mL toluene and adding a solution of 92.5 μL (0.69 mmol) $Me_3SiCH{=}C{=}O$ (13) in 15 mL toluene. Removal of solvent in vacuo afforded the 17c-17t mixture as a yellow oil. The ^1H NMR spectrum of this oil indicated an isomer ratio of cis/trans = 2/1.

17c. ^1H NMR (benzene-d_6): δ 7.05 (d, $^3J_{HH}$ = 9 Hz. 1H, $CHSiMe_3$), 1.85 (s, 30H, $C_5(CH_3)_5$), 0.23 (s, 9H, $Si(CH_3)_3$).

17t. ^1H NMR (benzene-d_6): δ 7.06 (d, $^3J_{HH}$ = 14 Hz, 1H, $CHSiMe_3$); 1.80 (s, 30H, $C_5(CH_3)_5$); 0.23 (s, 9H, $Si(CH_3)_3$).

1.4.9 cis- and trans-$Cp^*_2Zr(I)OCH{=}CHSiMe_3$

The cis-, trans-$Cp^*_2Zr(H)OCH{=}CHSiMe_3$ (17c, 17t) mixture (0.69 mmol) (formed in situ following the procedure of section 1.4.8) was dissolved in pet. ether (30 mL) and the solution cooled to -78° C. CH_3I (1.4 mmol) was added with stirring and the mixture allowed to warm to room temperature and stir for 3 hours. Toepler pump analysis of the gas product indicated 0.9 mol CH_4/mol 1. Removal of solvent afforded a yellow oil.

cis Isomer. ^1H NMR (benzene-d_6): 7.01 (d, $^3J_{HH}$ = 9Hz, 1H, OCH); 4.07 (d, $^3J_{HH}$ = 9Hz, 1H, $CHSiMe_3$), 1.85 (s, 30H, $C_5(CH_3)_5$); 0.31 (s, 9H, $Si(CH_3)_3$).

trans Isomer. ^1H NMR (benzene-d_6): 7.12 (d, $^3J_{HH}$ = 14 Hz, 1H, OCH); 4.55 (d, $^3J_{HH}$ = 14 Hz, 1H, $CHSiMe_3$); 1.80 (s, 30H, $C_5(CH_3)_5$), 0.27 (s, 9H, $Si(CH_3)_3$).

1.4.10 cis- and trans-$Cp^*_2Zr(Cl)OCH{=}CHSiMe_3$

$Cp^*_2Zr(H)Cl$ (32) (50 mg, 0.13 mmol) was dissolved in toluene (15 mL) and the solution frozen at -196° C. $Me_3SiCH{=}C{=}O$ (13) (0.13 mmol) was added by vacuum transfer and the solution warmed to room temperature with stirring. Removal of solvent in vacuo afforded a yellow oil. The ^1H NMR spectrum of this oil indicated an isomer ratio cis/trans = 1/3.

cis Isomer. ^1H NMR (benzene-d_6): δ 4.11 (d, $^3J_{HH}$ = 9Hz, 1H, CHSiMe3); 1.87 (s, 30H, $C_5(CH_3)_5$); 0.32 (s, 9H, $Si(CH_3)_3$). The remaining vinylic doublet was obscured by solvent.

trans Isomer. ^1H NMR (benzene-d_6): δ 6.89 (d, $^3J_{HH}$ = 14Hz, 1H, OCH); 4.59 (d, $^3J_{HH}$ = 14 Hz, 1H, $CHSiMe_3$); 1.87 (s, 30H, $C_5(CH_3)_5$); 0.20 (s, 9H, $Si(CH_3)_3$).

1.4.11 cis- and trans-$Cp^*_2Zr(F)OCH{=}CHSiMe_3$

The procedure described in section 1.4.10 was followed using 250 mg (0.65 mmol) $Cp^*_2Zr(H)F$ in 25 mL toluene and adding 0.65 mmol $Me_3SiCH{=}C{=}O$ (13). Removal of solvent in vacuo afforded a light yellow oil. The ^1H NMR spectrum of this oil indicated an isomer ratio of cis/trans = 1/9.

cis Isomer. ^1H NMR (benzene-d_6): δ 4.12 (d, $^3J_{HH}$ = 9Hz, 1H, $CHSiMe_3$); 1.81 (s, 30H, $C_5(CH_3)_5$), 0.35 (s, 9H, $Si(CH_3)_3$). The remaining vinylic doublet was obscured by solvent.

trans Isomer. ^1H NMR (benzene-d_6): δ 6.99 (d, $^3J_{HH}$ = 14Hz, 1H, OCH); 4.54 (d, $^3J_{HH}$ = 14Hz, 1H, $CHSiMe_3$); 1.87 (s, 30H, $C_5(CH_3)_5$); 0.20 (s, 9H, $Si(CH_3)_3$).

1.4.12 Reaction of $Cp^*_2ZrH_2$ (1) With 1.0 Equivalents of $Me_3CCH=C=CH_2$ (22)

$Cp^*_2ZrH_2$ (1) (25 mg, 0.068 mmol) was placed in an NMR tube and dissolved in 0.3 mL toluene-d_8. The solution was frozen at -196° C, the tube evacuated, and $Me_3CH=C=CH_2$ (0.068 mmol) added by vacuum transfer. The tube was sealed with a torch, warmed to -78° C, shaken, and then warmed to room temperature. The color of the solution changed from blue to orange upon warming. The ^1H NMR spectrum of this solution indicates the presence of unreacted 1, 26, and 27 based on comparison with the ^1H NMR spectra of authentic samples (vide infra).

1.4.13 Reaction of $Cp^*_2ZrH_2$ (1) with 1.5 Equivalents of $Me_2SiCH=C=CH_2$ (22)

The procedure described in section 1.4.12 was followed using 25 mg (0.068 mmol) $Cp^*_2ZrH_2$ (1) in 0.3 mL toluene-d_8 and adding 0.102 mmol $Me_2CH=C=CH_2$ (22). The ^1H NMR spectrum of this solution indicates the presence of 26 and 27 in approximately equal concentrations based on comparison with the ^1H NMR spectra of authentic samples (vide infra).

1.4.14 Reaction of $Cp^*_2ZrH_2$ (1) with 3.0 Equivalents of $Me_3CCH=C=CH_2$ (22)

The procedure described in section 1.4.12 was followed using 25 mg (0.068 mmol) $Cp^*_2ZrH_2$ (1) in 0.3 mL toluene-d_8 and adding 0.20 mmol $Me_3CH=C=CH_2$ (22). The ^1H NMR spectrum of this solution indicates the presence of unreacted 22, 1-neoheptene (28) and 26 based on comparison with the ^1H NMR spectra of authentic samples (vide infra).

1.4.15 Reaction of $Cp^*_2ZrH_2$ (1) with $Me_3CCH=C=CH_2$ (22) and 1-neoheptene (28) - Competition Experiment

$Cp^*_2ZrH_2$ (1) (10 mg, 2.8 mmol) was placed in an NMR tube and dissolved in toluene-d_8 (0.4 mL). The solution was cooled to -78° C and a homogeneous mixture of $Me_3CCH=CH_2$ (22) (10 μL, 1.0 mmol) and 1-neoheptene (28) (4.0 μL, 4.0 mmol) added *via* syringe. The tube was capped with a rubber septum, shaken, and slowly warmed to room temperature with constant sloshing of the solution. The ^1H NMR spectrum of this solution indicated 26 in greater than 95% yield.

1.4.16 $Cp^*_2\overline{ZrCH_2C=CHCMe_3CH_2C=CCH}CMe_3$ (26)

$[Cp^*_2ZrN_2]_2N_2$ (12) (150 mg, 0.19 mmol) was dissolved in toluene (12 mL) and the solution cooled to -78° C. $Me_3CCH=C=CH_2$ (22) (26 μL, 0.076 mmol) was added *via* syringe and the solution slowly warmed to room temperature with stirring. The color of the solution changed from purple to orange upon warming. Toepler pump analysis of the gas product indicated 2.9 mol N_2/mol 12. The solvent was removed *in vacuo* and the residue triterated with pet ether (5 mL). The mixture was cooled to -78° C and then filtered at this temperature to afford 26 as an orange crystalline solid (80 mg, 78%). Anal. Calcd for $C_{34}H_{54}Zr$: C, 73.69; H, 9.83; Zr, 16.48. Found: C, 73.60; H, 9.61; Zr, 16.66. ^1H NMR (benzene-d_6) - see Table 1.3: δ 4.97 (m, 1H, H(6)); 3.79 (m, 1H, H(6)); 3.43 (m, 2H, H(2)); 1.90 (s, 30H, $C_5(CH_3)_5$); 1.43 (s, 9H, H(9)); 1.26 (s, 9H, H(10)). The C(4)H_2 resonances were presumably buried under the t-butyl resonances. ^{13}C NMR (benzene-d_6) see Table 1.3: δ 196 (s, C(1)); 142 (s, C(3)); 136 (d, $^1J_{CH}$ = 167 Hz, C(5));

135.6 (d, $^1J_{CH}$ = 167 Hz, C(6)); 119 (s, $\underline{C}_5(CH_3)_5$); 52.8 (m, C(2)); 48.3 (m, C(4)); 34.6 (s, C(7)); 34.2 (s, C(8)); 32.4 (q, $^1J_{CH}$ = 127 Hz, $C_5(\underline{C}H_3)_5$).

1.4.17 $Cp^*_2Zr(H)CH_2CH_2C(CH_3)_3$ (27)

$Cp^*_2ZrH_2$ (1) (200 mg, 0.055 mmol) was dissolved in toluene (10 mL) and the solution cooled to -78° C. 1-Neoheptene (28) (75 mg, 0.076 mmol) was added via syringe and the solution warmed to room temperature with stirring. The color of the solution turned from blue to yellow-green upon warming. Removal of solvent in vacuo afforded 27 as a yellow-green waxy solid (90 mg, 35%). Anal. Calcd for $C_{27}H_{46}Zr$: C, 70.21; H, 10.04. Found: C, 69.97; H, 9.80. ^{1}H NMR (benzene-d_6): δ 5.43 (s, 1H, ZrH); 1.90 (s, 30H, $C_5(CH_3)_5$); 0.97 (s, 9H, $C(CH_3)_3$); 0.23 (t, $^3J_{HH}$ = 6 Hz, 2H, $ZrCH_2$). The remaining methylene resonances were not located.

1.4.18 cis-$Cp^*_2Zr(Cl)CH_2CH{=}CHCMe_3$ (33c)

$Cp^*_2Zr(H)Cl$ (32) (30 mg, 0.098 mmol) was placed in an NMR tube and dissolved in C_6D_6 (0.3 mL). $Me_3CCH{=}C{=}CH_2$ (22) (10 mg, 0.10 mmol) was added to the solution via syringe and the tube capped and rapidly shaken. The color of the solution turned from colorless to bright orange upon addition at the allene. The ^{1}H NMR spectrum of this solution indicated 33c had formed quantitatively and the spectrum was taken immediately as 33c isomerizes to 33t over a period of hours. ^{1}H NMR (benzene-d_6): δ 5.40 (dt, $^3J_{HH}$ = 13 Hz, $^3J_{HH}$ = 8 Hz, 1H, $CH_2C\underline{H}$); 4.87 (d, $^3J_{HH}$ = 13 Hz, $C\underline{H}CMe_3$); 1.83 (s, 30H, $C_5(CH_3)_5$); 1.42 (dd, $^4J_{HH}$ = 8 Hz, $^3J_{HH}$ = 2 Hz, $ZrCH_2$); 1.30 (s, 9H, $C(CH_3)_3$).

1.4.19 trans-$Cp^*_2Zr(Cl)CH_2CH{=}CHCMe_3$ (33t)

$Cp^*_2Zr(H)Cl$ (32) (120 mg, 0.30 mmol) was dissolved in toluene (8 mL) and the solution cooled to -78° C. $Me_3CCH{=}C{=}CH_2$ (42 μL, 0.44 mmol) was added and the solution warmed to room temperature and stirred for 24 hours. The color of the solution turned from colorless to bright orange upon warming. The solvent was removed in vacuo and the residue triturated with pet. ether (5 mL). The mixture was cooled to -78° C and filtered at this temperature to afford 33t as an orange crystalline solid (85 mg, 57%). Anal. Calcd for $C_{27}H_{43}ClZr$: C, 65.61; H. 8.77. Found: C, 65.28; H, 8.58. ^{1}H NMR (benzene-d_6): δ 5.73 (dt, $^3J_{HH}$ = 15 Hz, $^3J_{HH}$ = 1.5 Hz, 1H, CH_2CH); 5.15 (d, $^3J_{HH}$ = 15 Hz, 1H, $CHCMe_3$); 1.83 (s, 30H, $C_5(CH_3)_5$); 1.50 (dd, $^4J_{HH}$ = 8.0 Hz, $^3J_{HH}$ = 1.5 Hz, $ZrCH_2$); 1.13 (s, 9H, $C(CH_3)_3$). IR (nujol): ν(C=C) 1630 cm^{-1}.

1.5 References and Notes

1. E. T. Blues and D. Bryce-Smith, J. Chem. Soc., Chem. Commun., 699 (1970).
2. a) W. A. Herrmann and J. Plank, Angew. Chem. Int. Ed. Engl., 15, 615 (1976);
   b) G. H. Olive and S. Olive, ibid., 15, 136 (1976);
   c) G. Blyholder and P. H. Emmett, J. Phys. Chem., 64, 470 (1960);
   d) G. Blyholder and P. H. Emmett, ibid., 63, 962 (1959).
3. J. M. Manriquez, D. R. McAlister, R. D. Sanner, and J. E. Bercaw, J. Amer. Chem. Soc., 98, 6733 (1976).
4. P. T. Wolczanski, R. S. Threlkel, and J. E. Bercaw, ibid., 101, 218 (1979).
5. The mechanisms proposed in Schemes 1.1 and 1.2 have recently been reviewed. P. T. Wolczanski and J. E. Bercaw, Accounts Chem. Res., 13, 121 (1980).
6. a) R. Ben-Shosan and R. Pettit, J. Amer. Chem. Soc., 89, 2231 (1967);
   b) B. Foxman, D. Martin, A. Rosan, S. Raghu, and M. Rosenblum, ibid., 99, 2160 (1977).
7. G. S. Bristow, P. B. Hitchcock, and M. F. Lappert, J. Chem. Soc., Chem. Commun., 636 (1975).
8. a) R. Aumann and H. Wormann, Chem. Ber., 112, 1233 (1979);
   b) A. E. Stevens and J. L. Beauchamp, J. Amer. Chem. Soc., 100, 2584 (1978);
   c) B. Dorrer and E. O. Fischer, Chem. Ber., 107, 2683 (1974).

9. H. Hoberg and J. Korff, J. Organomet. Chem., 152, 255 (1978).

10. a) D. A. Young, Inorg. Chem., 12, 482 (1973);
b) D. S. Mills and A. D. Redhouse, J. Chem. Soc., Chem. Commun., 44 (1966);
c) P. Hong, N. Niskii, K. Sonogashira, and N. Hagihara, ibid., 993 (1972).

11. E. T. Blues, D. Bryce-Smith, B. Kettlewell, and M. Roy, ibid., 921 (1973).

12. E. T. Blues, D. Bryce-Smith, I. W. Lawston, and G. D. Wall, ibid., 513 (1974).

13. D. Bryce-Smith, Chem. Ind., 154 (1975).

14. W. Herrmann, Angew. Chem. Int. Ed. Engl., 13, 335 (1974).

15. A. D. Redhouse and W. A. Herrmann, ibid., 15, 615 (1976).

16. G. Fachinetti, C. Biran, C. Floriani, A. Chiesi-Villa, and C. Guastini, Inorg. Chem., 17, 2995 (1978).

17. W. A. Herrmann and J. Plank, Angew. Chem. Int. Ed. Engl., 17, 525 (1978).

18. W. A. Herrmann, J. Plank, M. L. Ziegler, and K. Weidenhammer, J. Amer. Chem. Soc., 101, 3133 (1979).

19. P. T. Barger, J. Armantrout, B. D. Santarsiero, and J. E. Bercaw, manuscript in preparation.

20. a) F. R. Kreissl, K. Eberl, and W. Vedelhoven, J. Amer. Chem. Soc., 17, 525 (1978);
b) F. R. Kreissl, P. Friedrich, and G. Hultner, ibid., 16, 102 (1977).

21. L. Messerle, Ph.D. Dissertation, Massachuetts Institute of Technology, Cambridge, MA, 1979.

22. Ketenes normally dimerize, especially when heated.

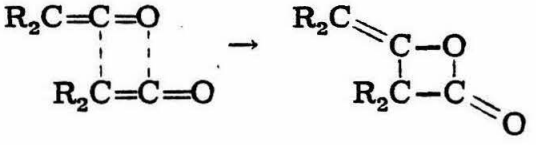

23. In solution the nitrogen ligands of $[Cp^*_2ZrN_2]_2N_2$ are labile, providing a source of "Cp^*_2Zr." J. M. Manriquez and J. E. Bercaw, J. Amer. Chem. Soc., 96, 6229 (1974).

24. Verified by Toepler pump analysis.

25. Endo-Exo refers to substitution on the ethylidene unit with respect to the zirconium.

26. An sp^2-hybridized carbon bound to zirconium is normally found near δ 200 in the ^{13}C NMR (see ref. 34). An oxygen adjacent to this carbon would most certainly shift the resonance to lower field.

27. J. E. Bercaw, Adv. Chem. Ser., No. 167, 136 (1978).

28. For example, the hydride ligand resonance of $\{Cp^*Zr(H)\}_2$-(OCH=CHO) is observed at δ 6.06 for the cis isomer and at δ 5.73 for the trans isomer. The olefinic proton resonance is observed at δ 5.43 for the cis isomer and at δ 6.55 for the trans isomer. J. M. Manriquez, D. R. McAlister, R. D. Sanner, and J. E. Bercaw, J. Amer. Chem. Soc., 100, 2716 (1978). See also ref. 4.

29. a) A. G. Brook, J. M. Duff, and W. F. Reynolds, J. Organomet. Chem., 121, 293 (1976);

b) D. Seyferth and L. G. Vaughan, ibid., 1, 138 (1963);

c) R. R. Schrock, J. Amer. Chem. Soc., 98, 5399 (1976).

30. D. M. Roddick and J. E. Bercaw, manuscript in preparation.

31. D. K. Erwin and J. E. Bercaw, unpublished results.

32. D. K. Erwin, Ph.D. Dissertation, California Institute of Technology, Pasadena, CA, 1979.

33. Protons bound to an sp^3-hybridized carbon adjacent to zirconium resonate in the δ 0.5- -1.5 region of the ^1H NMR spectrum. See ref. 30.

34. D. M. Duggan and J. R. Schmidt, Inorg. Chem., 20, 1164 (1981).

35. For example, in the ^1H NMR spectrum of cis-$CH_3CH_2CH_a{=}CH_bCMe_3$, $^3J_{H_aH_b}$ = 12.01 Hz. For the corresponding trans isomer, $^3J_{H_aH_b}$ = 15.56 Hz. F. H. A. Rummens and J. W. DeHaan, Org. Mag. Rev., 2, 351 (1970).

The ^1H NMR spectral data do not distinguish between a σ-allyl complex and one which is in equilibrium with its π-allyl isomer.

36. The C=C stretch of σ-allyl complexes is observed above 1590 cm^{-1} in the IR spectrum. That of π-allyl complexes is observed below 1590 cm^{-1}. E. G. Hoffman, R. Kallweit, G. Schroth, K. Seevogel, W. Stempfle, and G. Wilke, J. Organomet. Chem., 97, 183 (1975).

37. T. L. Brown, D. W. Dickerhoof, D. A. Bafus, and G. L. Morgan, Rev. Sci. Instrum., 33, 491 (1962).

38. R. H. Marvich and H. H. Brintzinger, J. Amer. Chem. Soc., 93, 2046 (1971).

39. J. M. Manriquez, R. D. Sanner, R. E. Marsh, and J. E. Bercaw, ibid., 98, 3042 (1976).

40. R. Threlkel, Ph.D. Dissertation, California Institute of Technology, Pasadena, CA, 1980.

41. H. Stoudinger, Ber. Deut. Chem. Ges., 44, 1619 (1911).

42. R. A. Ruden, J. Org. Chem., 39, 3607 (1974).

43. G. Zweifel, A. Horng, and J. T. Snow, J. Amer. Chem. Soc., 92, 1427 (1970).

CHAPTER 2

Synthesis and Reactivity of Ketene Complexes of Permethylzirconocene

2.1 Introduction

The results presented in Chapter 1 indirectly suggest that ketene adducts of permethylzirconocene may be viable models for intermediates in the reaction of $Cp^*_2Zr(CO)_2$ with $Cp^*_2ZrH_2$. Although free ketenes were shown to model this system poorly, the reaction of $Cp^*_2Zr(H)Cl$ with t-butylallene confirmed that if π-coordination of a cummulene to a permethylzirconocene center can occur, steric requirements dictate the stereoselective formation of a cis product upon hydride migration. The results using t-butylallene are encouraging and instructive, but to properly model the ketene intermediates proposed in Scheme 1.2, mononuclear monoketene adducts of permethylzirconocene were required.

Two reports indicate that zirconocene-ketene complexes can be prepared by the base-induced dehydrohalogenation of zirconocene haloacyl compounds. Messerle has found that treatment of $Cp^*_2Zr(COCH_2CMe_3)Cl$ with CH_2PMe_3 affords two isomeric ketene complexes, as evidenced by ^1H and ^{13}C NMR spectroscopy (eq. 1).[1] Molecular weight analysis of this mixture indicated that the ketene compounds were best formulated as dimers. Similarly, Straus and Grubbs have found that treatment of $Cp_2Zr(COCH_2CH_2CMe_3)Cl$ with $NaN(SiMe_3)_2$ afforded the dimeric ketene complex $\underset{\sim}{1}$ (eq. 2).[2] Attempts to hydrogenate $\underset{\sim}{1}$ or trap a mononuclear species were unsuccessful.

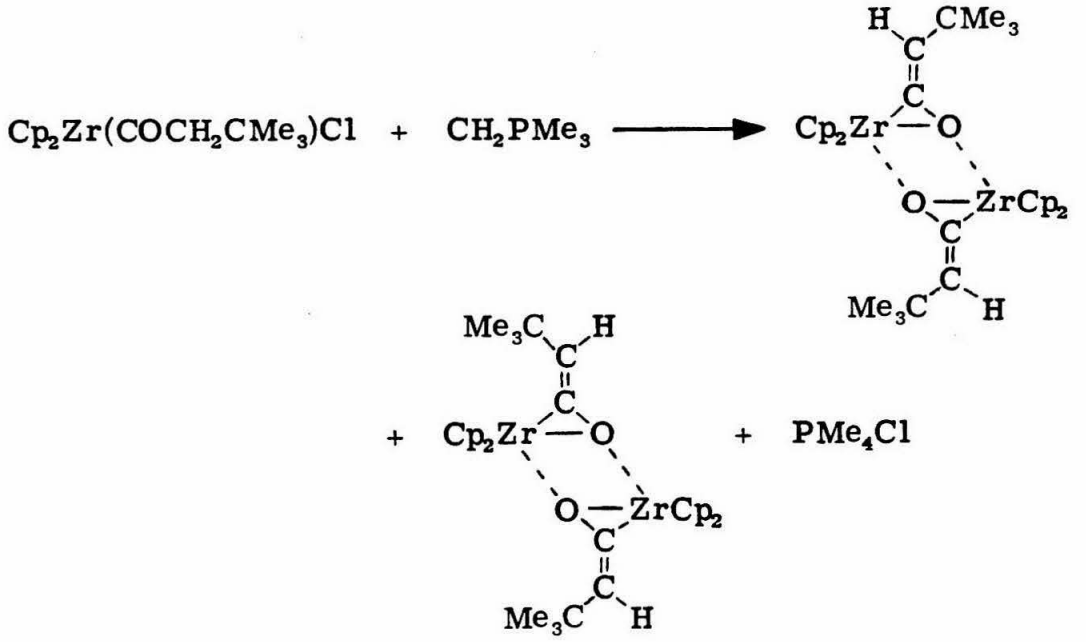

$$Cp_2Zr(COCH_2CMe_3)Cl + CH_2PMe_3 \longrightarrow \text{(1)}$$

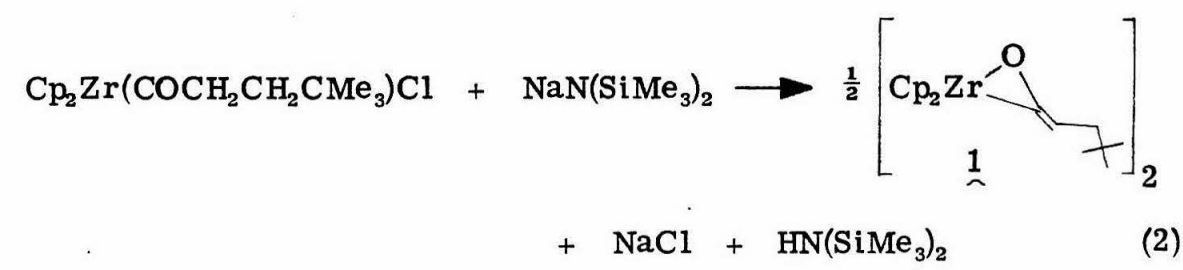

$$Cp_2Zr(COCH_2CH_2CMe_3)Cl + NaN(SiMe_3)_2 \longrightarrow \tfrac{1}{2}\,[\,\underset{\underset{\text{1}}{\frown}}{Cp_2Zr(O)}\,]_2 + NaCl + HN(SiMe_3)_2 \quad (2)$$

In an effort to prepare a monomeric zirconium-ketene complex, Straus and Grubbs began investigations into a permethylzirconocene system. Treatment of $Cp^*_2Zr(COCH_3)Br$ with $NaN(SiMe_3)_2$ affords the anionic ketene complex $\underset{\frown}{2}$ which contains a molecule of coordinated base (Scheme 2.1).[3a, b] Although $\underset{\frown}{2}$ decomposed in vacuo and could not be isolated, treatment with pyridine afforded the neutral pyridine-coordinated ketene complex $\underset{\frown}{3}$. ^1H and ^{13}C NMR spectroscopy were

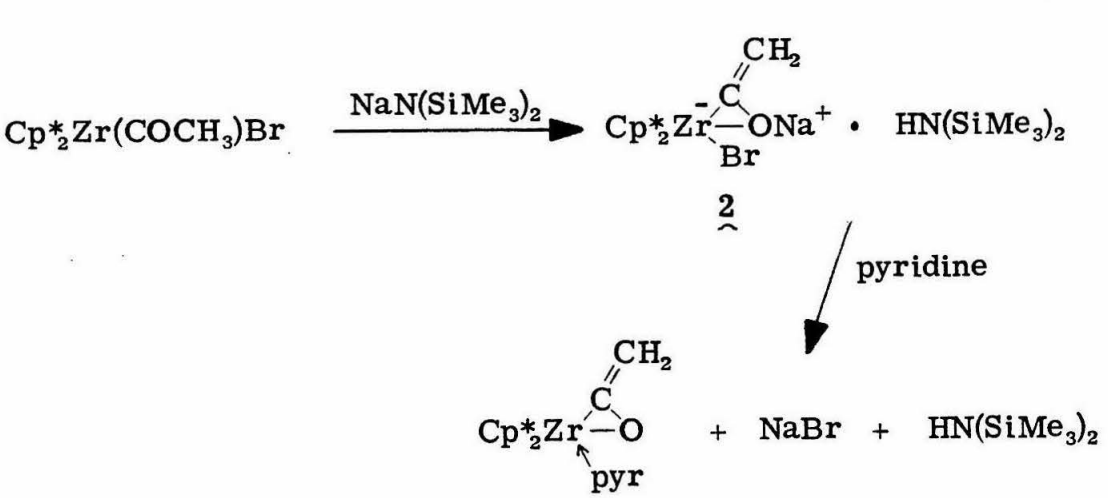

SCHEME 2.1. Synthesis of Anionic and Neutral Permethylzirconocene Ketene Complexes.

consistent with a ketene formulation. A single crystal X-ray diffraction study of 3 indicates a monomeric structure in which the ketene is bound to the zirconium in an η^2-(C,O) fashion.[3b] Of particular interest is the reaction of 3 with H_2. Unlike the dimeric zirconocene-ketene complexes discussed earlier, the monomeric permethylzirconocene-ketene complexes 2 and 3 react rapidly with H_2 to afford the enolate-hydride compound 4 (Scheme 2.2). Thus, it appears that hydrogenation of a permethylzirconocene-ketene species does afford an enolate complex as suggested by the mechanism for the formation of the cis-enediolate complex (Scheme 1.2).

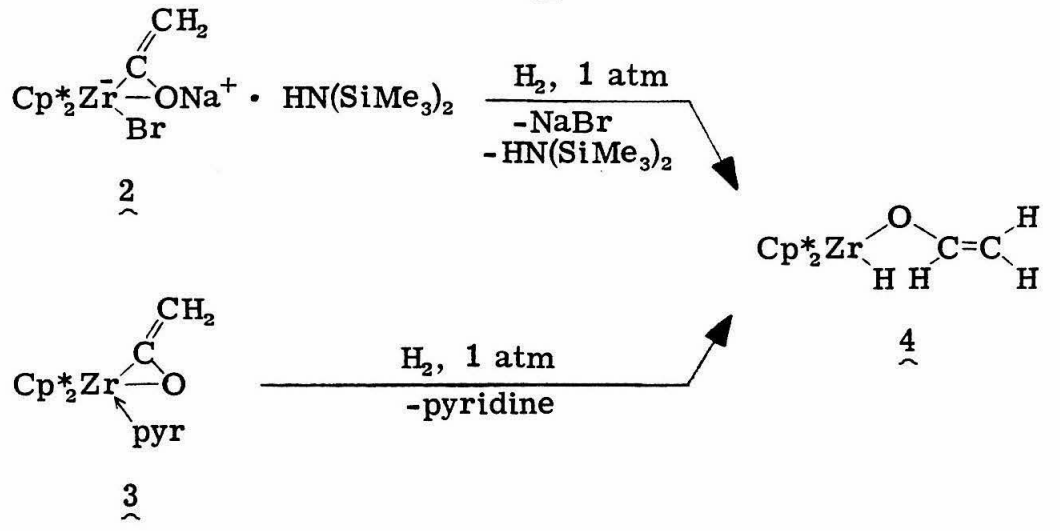

SCHEME 2.2. Hydrogenation of Anionic and Neutral Permethylzirconocene Ketene Complexes.

To investigate the stereochemistry of the permethylzirconocene-ketene hydrogenation, a ketene complex was required in which R was an alkyl group.[4] Because R = H in compounds 2 and 3, no stereochemical information is obtained in the hydrogenation of these compounds. This chapter discusses the synthesis and reactivity of permethylzirconocene-ketene complexes in which R = Me and t-butyl and the viability of these complexes as models for intermediates in the cis-enediolate mechanism (Scheme 1.2).

2.2 Results and Discussion

2.2.1 Synthesis and Reactivity of Permethylzirconocene Haloacyl Complexes

The synthesis of a series of permethylzirconocene haloalkyl complexes was achieved by reaction of the corresponding dihalide species with one equivalent of the appropriate Grignard or lithio reagent. The ethyl-bromide (4) and neopentyl-chloride (5) derivatives

were prepared in this manner (eqs. 3, 4). Treatment of the haloalkyl

$$Cp^*_2ZrBr_2 + EtMgBr \xrightarrow[12\ hrs]{toluene} Cp^*_2Zr(Et)Br + MgBr_2 \qquad (3)$$

$$\underset{\sim}{4}$$

$$Cp^*_2ZrCl_2 + LiCH_2CMe_3 \xrightarrow[12\ hrs]{toluene} Cp^*_2Zr(CH_2CMe_3)Cl + LiCl \qquad (4)$$

$$\underset{\sim}{5}$$

compounds with 1 atm CO affords the haloalkyl complexes in good yield. The propionyl compound $\underset{\sim}{6}$ is isolated as a white powder and both ^1H and ^{13}C NMR spectroscopy indicate only a single isomer in solution. The configuration of $\underset{\sim}{6}$ is shown in equation 5 in which the

$$Cp^*_2Zr(Et)Br \xrightarrow[1\ atm]{CO} Cp^*_2Zr\langle \overset{Et}{\underset{Br}{C=O}} \qquad (5)$$

$$\underset{\sim}{4} \qquad\qquad \underset{\sim}{6}$$

η^2-acyl oxygen occupies the central equatorial bonding site. Structural studies of related zirconocene acyl derivatives all demonstrate this type of oxygen coordination.[5] Treatment of the neopentyl chloride complex $\underset{\sim}{5}$ with CO, however, gives a mixture of products identified by ^1H and ^{13}C NMR spectroscopy as kinetic ($\underset{\sim}{7}$) and thermodynamic ($\underset{\sim}{8}$) acyl isomers with $K_{eq26°C} = 0.98$ (eq. 6). In the kinetic form ($\underset{\sim}{7}$), the η^2-acyl oxygen occupies a lateral or "outer" site in the equatorial bonding plane while in the thermodynamically more favored form $\underset{\sim}{8}$, the oxygen occupies the central or "inner" site. Although only a single η^5-$C_5(CH_3)_5$ resonance at δ 1.27 is observed in the ^1H NMR spectrum of

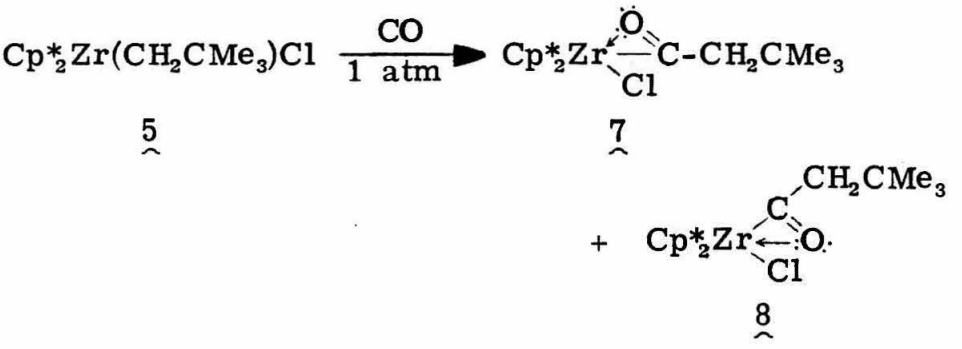

$Cp^*_2Zr(CH_2CMe_3)Cl$ (5) $\xrightarrow[1\ atm]{CO}$ $Cp^*_2Zr(Cl)(O{=}C\text{-}CH_2CMe_3)$ (7) + $Cp^*_2Zr(Cl)(O{=}C(CH_2CMe_3))$ (8) (6)

$$K_{eq\,26^\circ C} = [8]/[7] = 0.98$$

the 7, 8 mixture, distinct t-butyl (δ 1.27 (7), δ 1.07 (8)) and methylene (δ 2.37 (7), δ 3.09 (8)) proton resonances are observed as well as distinct acyl carbon resonances (δ 329.4 (7), δ 316.1 (8)) in the ^{13}C NMR spectrum. Isomerizations of this type have been observed in related systems[6] and, recently, the crystal structures of both kinetic and thermodynamic isomeric forms of permethylzirconocene acyl-ylide complexes have been obtained (see Chapter 3). Presumably, steric interactions between the neopentyl and pentamethylcyclopentadienyl ligands result in a substantial relative concentration of 7 at equilibrium, a condition which does not occur to any great extent in solutions of 6.

Upon heating the acyl mixture (7, 8) at 80°C for several days, two new products formed in equal concentration were observed (whereas an increase in the concentration of the thermodynamic isomer 8 would have been expected). The ^{1}H and ^{13}C NMR spectra of this mixture suggest that the new products are the cis (9c) and trans (9t) enolate chlorides formed by tautomerization of the acyl chlorides (eq. 7). The vinylic proton coupling constants of 8.2 Hz for the cis isomer and

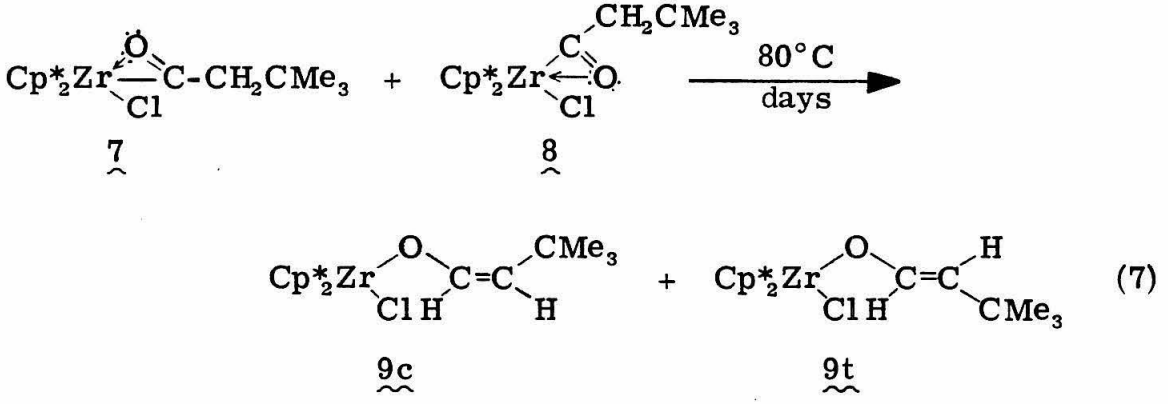

(7)

14.3 Hz for the trans isomer confirm this formulation. A similar tautomerization was observed by Marks et al. when solutions of a thorium acyl compound were heated.[7] If the acyl species 7 and 8 are, at least in part, represented by an oxy-carbene formulation[8] (Scheme 2.3), the tautomerization depicted in equation 7 corresponds to a formal

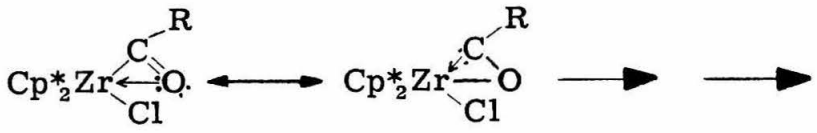

SCHEME 2.3. Representation of Oxy-Carbene Formulation.

1,2-hydrogen shift from an sp^3-hybridized carbon to the carbene. However, heating a mixture of the monodeuterated acyls 10 and 11 at 80°C (eq. 8) affords the corresponding enolate products $12c_H$, $12c_D$, $12t_H$, and $12t_D$ with $k_H/k_{D80°C} = 1.75$ (implying that C-H bond breakage is not the only factor involved in formation of the transition state).[9] It is also interesting to note that the acyl tautomerization does not occur until $7/8 \cong 1$.[10] The formation of the enolate products then proceeds with $9c/9t \cong 1$ over the course of the 80°C reaction, the ratio of the starting acyl species also remaining constant during this time. This tautomerization could conceivably follow one of three pathways: (1) each acyl isomer affords a single enolate isomer at relatively the same rate (e.g., $7 \xrightarrow{k_1} 9c$ and $8 \xrightarrow{k_2} 9c$ where $k_1 \cong k_2$);

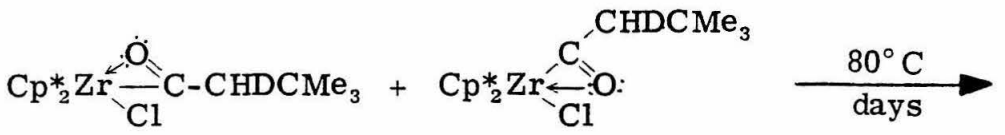

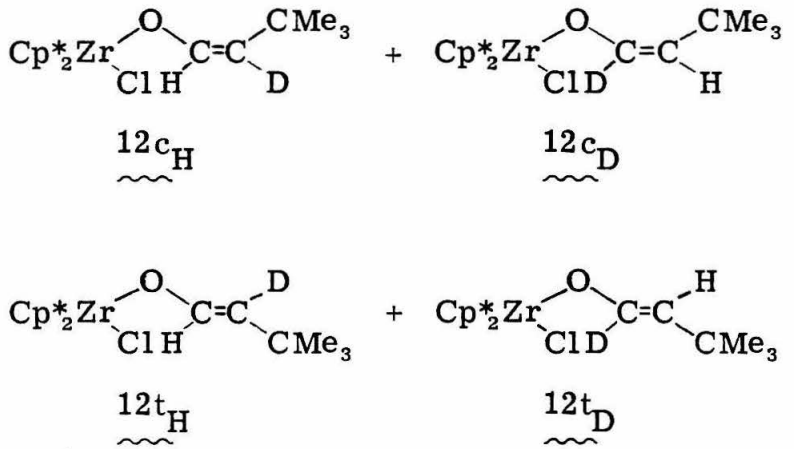

(8)

(2) only one acyl complex (in rapid equilibrium with its other isomer) tautomerizes to a 1:1 mixture of the enolate products (e.g., $\underset{\sim}{7} \rightleftharpoons \underset{\sim}{8} \rightarrow \underset{\sim}{9c} + \underset{\sim}{9t}$); or (3) only one acyl complex (again in relatively rapid equilibrium with its other isomer) tautomerizes to a single enolate product which in turn is in relatively rapid equilibrium with its other isomer (e.g., $\underset{\sim}{7} \rightarrow \underset{\sim}{9c} \rightleftharpoons \underset{\sim}{9t}$). Differentiation between these three possibilities has not proved possible.

2.2.2 Synthesis and Reactivity of Permethylzirconocene Ketene Complexes

Extension of the methodology used by Straus and Grubbs in the preparation of ketene complexes from $Cp^*_2Zr(COMe)Br$[3] was attempted with $Cp^*_2Zr(COEt)Br$ ($\underset{\sim}{6}$). Treatment of $\underset{\sim}{6}$ with $LiN(CHMe_2)_2$, however, did not lead to clean dehydrohalogenation. Treatment of $\underset{\sim}{6}$ with two

equivalents of CH_2PMe_3 did afford a clean mixture of two products identified by ^1H, ^{13}C, and ^{31}P NMR spectroscopy as E- and Z-$Cp^*_2Zr(OCCHMe) \cdot CH_2PMe_3$ (13E, 13Z)[11] in a ratio of 13E/13Z = 1/1.6 (eq. 9). The 13E, 13Z mixture can be isolated as a white-yellow

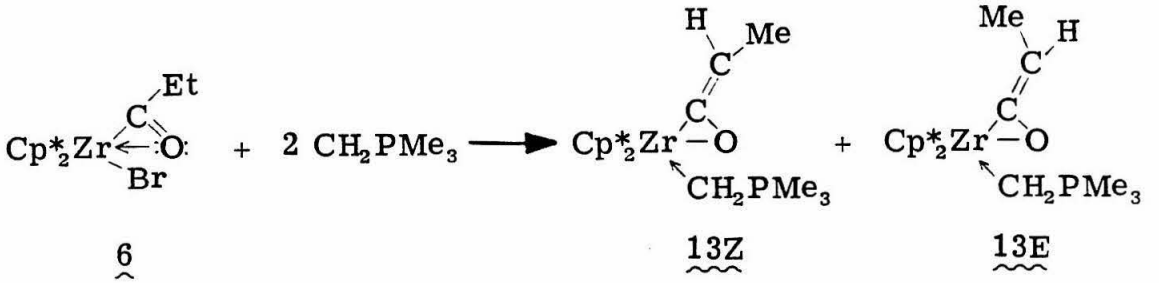

6 13Z 13E

$$+ \quad PMe_4Br \qquad (9)$$

solid in 71% yield. Elemental analysis as well as spectral data are consistent with formulation of 13E and 13Z as ketene-ylide species. Both isomers are similar to the neutral pyridine complex $Cp^*_2Zr(OCCH_2) \cdot$ pyr (3), where a base (in this case CH_2PMe_3) is coordinated to the zirconium center. The ketenic proton resonances observed at δ 5.80 (13E) and δ 4.50 (13Z) in the ^1H NMR spectrum of the mixture are in the same general region as the ketenic proton resonances of 3 (δ 4.57, 3.51).[3,12] Both 13E and 13Z are formulated as the oxygen "in" isomers, since it is unlikely that an oxygen "in"-oxygen "out" rearrangement would occur upon dehydrohalogenation of the starting acyl complex. The higher relative concentration of the Z isomer is expected because of the minimal steric repulsions between the Cp* ligands and the ketenic proton in 13Z as compared with a greater steric interaction between the Cp* ligands and the methyl group

in 13E. The 13E, 13Z mixture does not appear to be an equilibrium condition; heating the mixture at 80°C results in decomposition, and not the isomerization from one isomer to the other. However, it may be the case that a shift in equilibrium is simply not detected with the temperature range employed.

Treatment of the $Cp^*_2Zr(COCH_2CMe_3)Cl$ mixture (7, 8) with two equivalents of CH_2PMe_3 affords a single ketene-ylide complex, formulated as Z-$Cp^*_2Zr(OCCHCMe_3) \cdot CH_2PMe_3$ (14), in 43% isolated yield (eq. 10). Molecular weight analysis of 14 indicates a monomeric

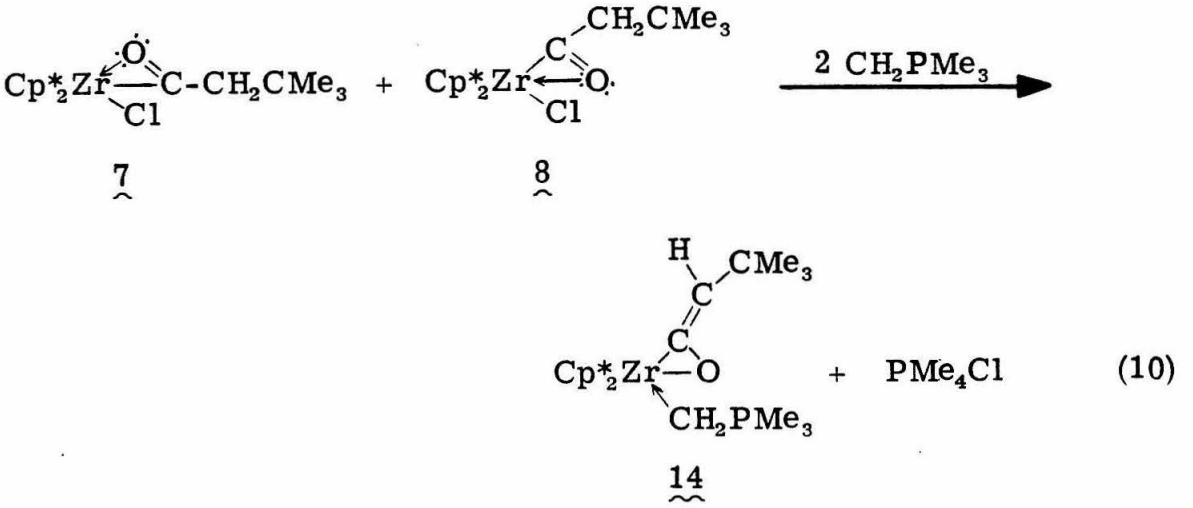

(10)

structure. The ketenic proton resonance observed at δ 4.22 in the ^1H NMR spectrum of 14 is very similar in chemical shift to that observed for complex 13Z (δ 4.44). In addition, structural studies of the related kinetic and thermodynamic acyl-hydride complexes 15 and 16 (Figure 2.1) indicate that these species are represented in part by a ketene formulation (see Chapter 3). In both cases, the PMe_3 group is Z to the $-OZrCp^*_2$ moiety. Thus, the configuration of 14 is also

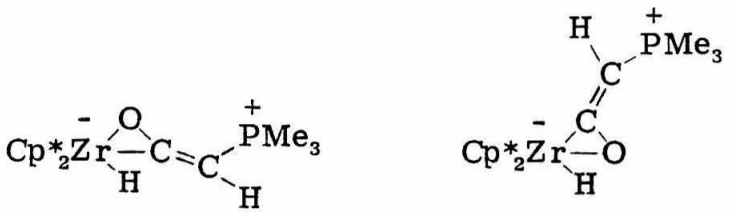

15

16

FIGURE 2.1. Permethylzirconocene Acyl-Ylide Complexes.

assigned the Z geometry. Apparently, steric interactions between the Cp^* ligands and the t-butyl group are important so that formation of the E isomer is inhibited. As proposed in Scheme 1.2, only a single Z ketene isomer should be observed if the ketene substituent is sufficiently large. Thus, 14 seems to be a good model for the ketene intermediate 2 proposed in Scheme 1.2.

The addition of one equivalent of $LiN(CHMe_2)_2$ to a solution of the acyl mixture 8, 9 results in the formation of the anionic ketene-amine complex 17 (eq. 11). Unlike its analogue, $[Cp^*_2Zr(OCCH_2)Cl]^-Li^+ \cdot HN(SiMe_3)_2$, 17 is stable in vacuo and can be isolated as an orange-white solid in 72% yield. Molecular weight analysis indicates that 17 exists as a monomer in solution. The ^1H NMR spectrum of 17 indicates the presence of coordinated $HN(CHMe_2)_2$ and a ketenic proton resonance is observed at δ 4.19. The position of this ketenic proton resonance is quite close to that found for 13Z (δ 4.44) and 14 (4.24) and indicates that 17 is also best formulated as the Z isomer. In analogy with 14,

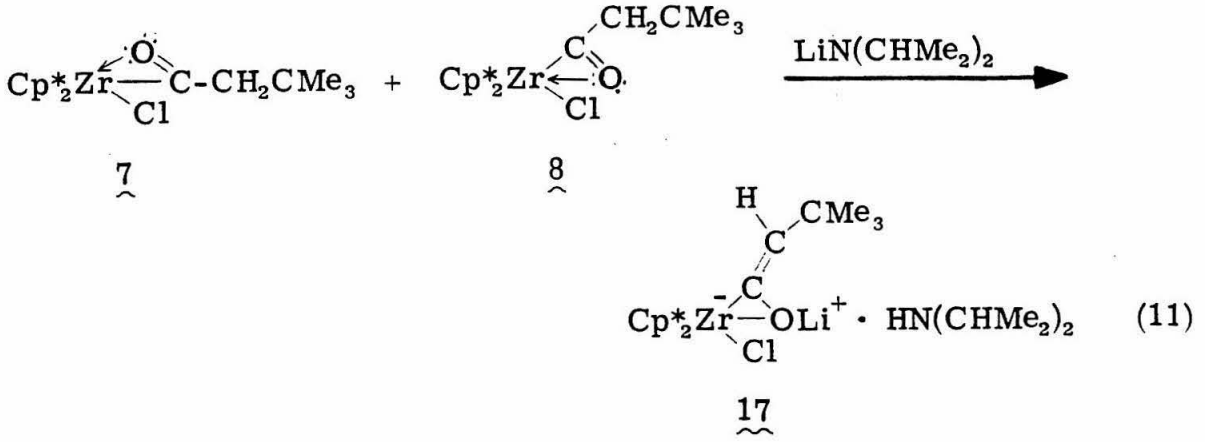

7 8 17 (11)

steric repulsions inhibit the formation of the E isomer.

Analogous to the reactivity of 2, 17 reacts with bases to form neutral, base-coordinated ketene complexes. The reaction of 17 with CH_2PMe_3 in benzene solution results in precipitation of LiCl and formation of the ketene-ylide complex 14 (eq. 12). Treatment of 17 with 1 atm CO affords the novel ketene-carbonyl complex 18 (eq. 13).

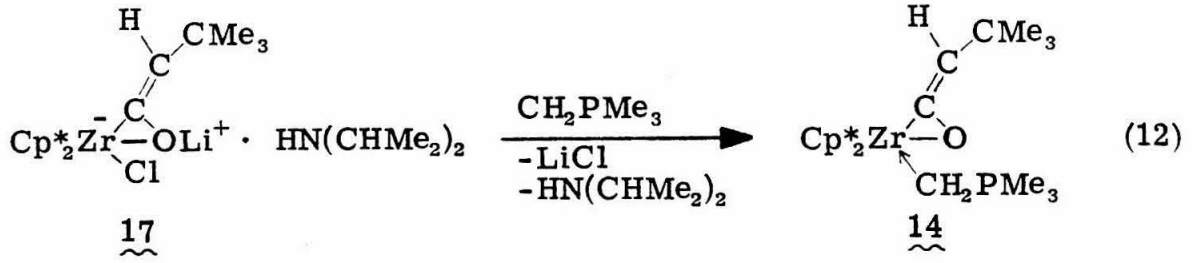

17 14 (12)

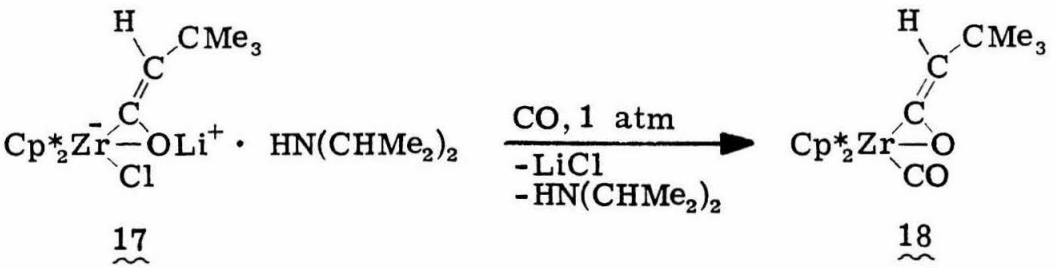

17 18 (13)

Although 16 can only be isolated as a green oil, spectral data confirm a ketene-carbonyl formulation; a ketenic proton resonance at δ 4.49 and a carbonyl carbon resonance at δ 228.0 are observed in the ^{1}H and ^{13}C NMR spectra, respectively. The IR spectrum of a benzene solution of 16 displays a single band in the terminal carbonyl region at 1987 cm^{-1}. This frequency is somewhat lower than that found in a Zr(IV) species ($Cp^{*}_{2}ZrH_{2}(CO)$, $\nu(CO)$ = 2046 cm^{-1})[13] yet higher than that of a Zr(II) species ($Cp^{*}_{2}Zr(CO)_{2}$, $\nu(CO)$ = 1942 cm^{-1}).[14] Thus 16, and undoubtedly some of the other permethylzirconocene-ketene complexes, can be formulated to some extent as π-bound ketene adducts (Figure 2.2), again establishing the viability of these species as models for intermediate 2 in Scheme 1.2.

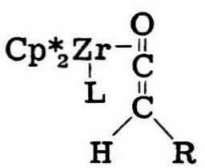

FIGURE 2.2. π-Bound Ketene Adduct of Permethylzirconocene.

2.2.1 Reaction of Permethylzirconocene-Ketene Complexes with Hydrogen

The proposed stereoselective hydrogenation of the permethylzirconocene-ketene intermediate 2 is the last step in the formation of the cis-enediolate complex (Scheme 1.2). As mentioned earlier, the hydrogenation of $[Cp^*_2Zr(OCCH_2)Cl]Na \cdot HN(SiMe_3)_2$ (2) or $Cp^*_2Zr(OCCH_2) \cdot$ pyr (3) does afford the enolate hydride complex 4, although no stereochemical information is obtained because of the equivalence of the ketene substituents. Treatment of the 13E, 13Z mixture (13Z/13E = 1.6) with 1 atm H_2, however, affords both cis (19c) and trans (19t) enolate hydride complexes in a ratio of 19c/19t = 1.6 (eq. 14). $^3J_{HH}$ vinylic proton coupling constants of 13.3 Hz and 7.0 Hz

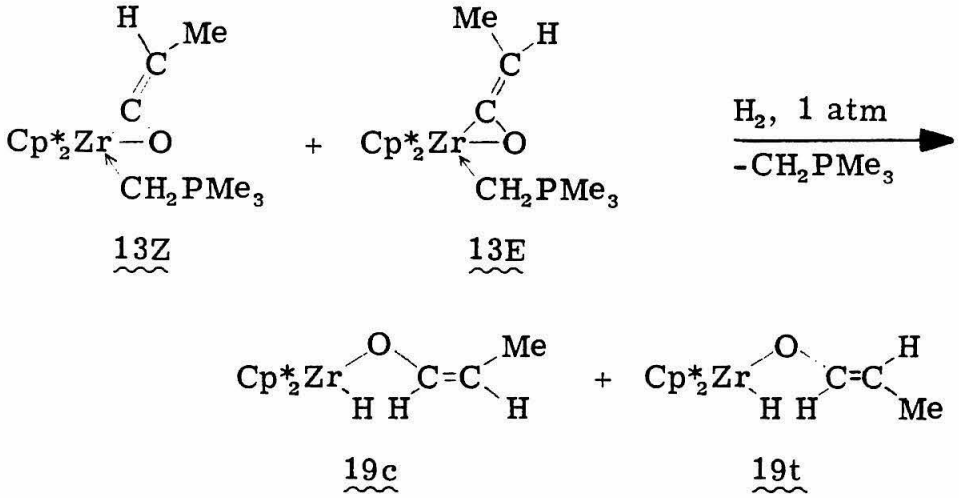

(14)

for the trans and cis isomers, respectively, are observed in the ^1H NMR spectrum of the 17c/17t mixture and confirm this formulation. Distinct hydride ligand resonances at δ 6.80 (19t) and δ 6.10 (19c) as well as distinct Cp* and t-butyl proton resonances are also observed.

Analogous to the hydrogenation of 3, that of the 13E, 13Z mixture also proceeds with dissociation of the complexed base, leaving the enolate-hydride mixture ylide free. Comparison of the ketene mixture ratio (13Z/13E = 1.6) with the enolate hydride mixture ratio (19c/19t = 1.6) suggests that the ketene hydrogenation occurs with retention of stereochemistry.

Finally, the original premise that a sterically-hindered permethylzirconocene-ketene species should undergo hydrogenation stereoselectively to a cis-enolate product is supported by the hydrogenation of the t-butyl ketene derivatives. Treatment of 14, 17, or 18 with 1 atm H_2 affords the cis-enolate hydride complex 20 (>96% cis) (Scheme 2.4). The ^1H NMR spectrum of 20 indicates a single hydride

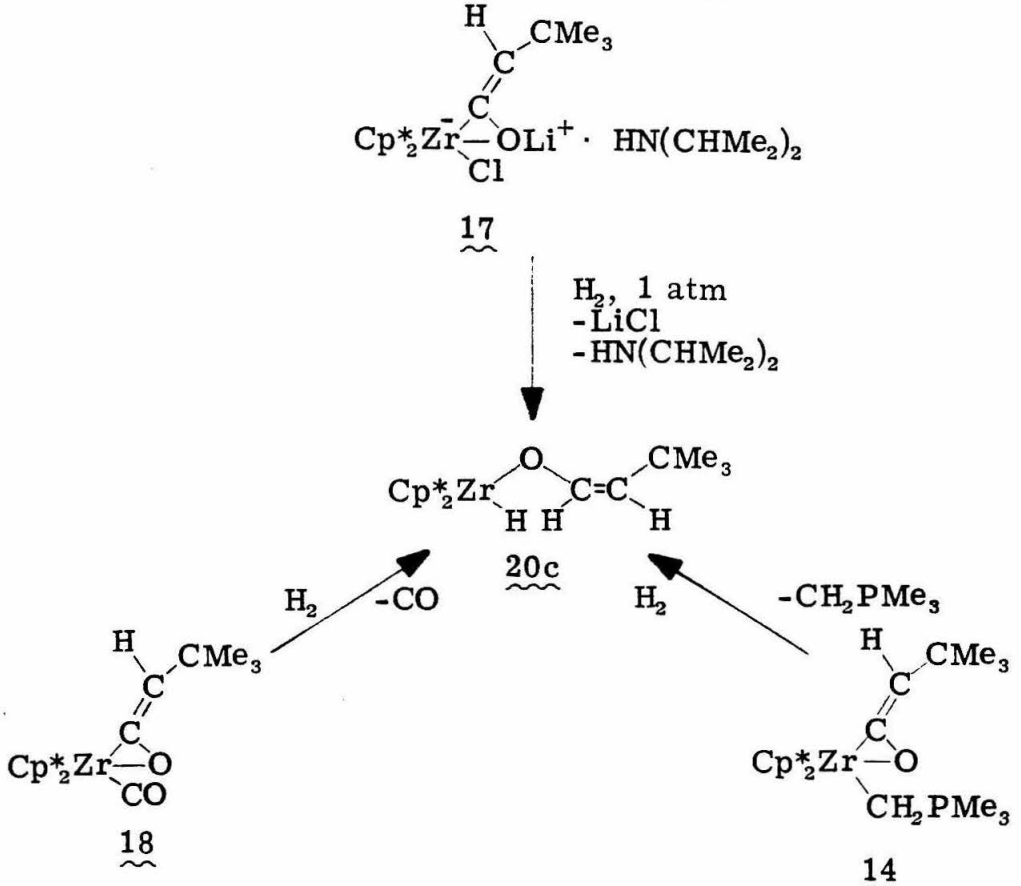

SCHEME 2.4. Hydrogenation of Sterically-Hindered Ketene Complexes of Permethylzirconocene.

ligand resonance at δ 6.23 and two vinylic proton resonances at δ 6.26 and δ 3.49 ($^3J_{HH}$ = 7.9 Hz). Complex 20 can be isolated as an extremely hydrocarbon-soluble white solid in 43% yield by treating 17 with H_2. Unfortunately, attempts to convert the cis isomer into the trans geometry, which is expected to be thermodynamically favored, were unsuccessful. Similar to the thermal stability observed with other permethylzirconocene enolate-hydride species (see Chapter 1), complex 20 is stable at modest temperatures (80°C). Treatment of 20 with excess CH_3I affords the cis iodo derivative 21c ($^3J_{HH}$ = 7.9 Hz) and methane (0.92 mol CH_4/mol 18) (eq. 15). Heating a solution of 21c at 80°C for several days, however, does completely convert 21c to the trans-enolate-iodide 21t ($^3J_{HH}$ = 13.2 Hz) (eq. 16), establishing that the trans isomer is thermodynamically favored. The reason for the lower thermal stability of the enolate-iodide 21c as compared with the enolate-hydride 20 is not known.

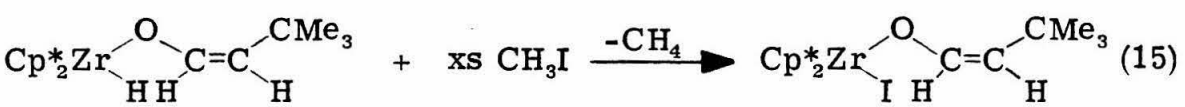

20c 21c (15)

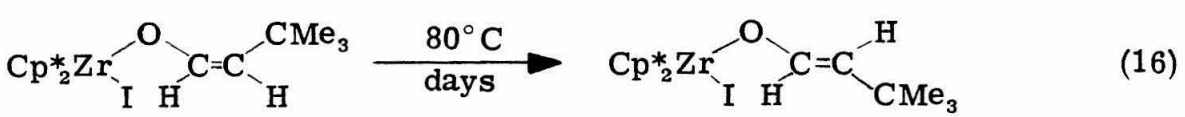

21c 21t (16)

2.3 Conclusion

The results presented in this chapter support the postulate presented in Scheme 1.2 that hydrogenation of mononuclear sterically-hindered ketene complexes of permethylzirconocene afford stereoselectively cis-substituted enolate-hydride products. Recently, the carbene-carbonyl coupling step has also been verified in our laboratories. $Cp_2Zr(CO)=CHOZr(H)Cp^*_2$ was found to rearrange in the presence of pyridine to the ketene complex $Cp_2Zr(pyr)OC=CHOZr(H)Cp^*_2$.[15] Unfortunately, the hydrogenation of this compound does not proceed cleanly to an enolate product. Nevertheless, these results provide an insight into the mechanism by which $Cp^*_2Zr(CO)_2$ and $Cp^*_2ZrH_2$ react to form cis-$[Cp^*_2Zr(H)]_2(OCHCHO)$.

2.4 Experimental Section

2.4.1 General Methods

All manipulations were performed in an inert atmosphere using high vacuum line or glove box techniques. Argon and hydrogen were passed through MnO on vermiculite[15] and 4 Å molecular sieves.

2.4.2 Physical and Spectroscopic Methods

Proton magnetic resonance spectra were recorded using either a Varian EM390 or JEOL FX90Q spectrometer. Chemical shifts are reported in ppm (δ) relative to Me_4Si (δ 0.0). Carbon magnetic resonance were recorded using a JEOL FX90Q spectrometer. Chemical shifts are relative to Me_4Si (δ 0.0). Phosphorous magnetic resonance spectra were recorded using a JEOL FX90Q spectrometer.

Chemical shifts are relative to external H_3PO_4 (δ 0.0). Infrared spectra were recorded using NaCl plates on a Beckman 4240 spectrometer.

Elemental analyses were performed by the Dornis and Kolbe Microanalytical laboratories. Molecular weight analyses were performed using isothermal distillation following the Signer method.[17]

2.4.3 Solvents and Reagents

Solvents were purified by vacuum transfer first from $LiAlH_4$ and then from "titanocene".[18] NMR solvents benzene-d_6 and toluene-d_8 were vacuum transferred from titanocene. CH_3I was vacuum transferred from CaH_2. Carbon monoxide (Matheson) was used without further purification.

The following compounds were prepared by the reported procedures: $Cp^*_2ZrCl_2$,[19] $Cp^*_2ZrBr_2$,[3b] CH_2PMe_3,[20] $LiCH_2CMe_3$,[21a] $LiCHDCMe_3$.[21a, b]

2.4.4 $Cp^*_2Zr(Et)Br$ (4)

Ethylmagnesium bromide (2.8 M in Et_2O, 180 μL, 0.50 mmol) was added via syringe to a stirred suspension of $Cp^*_2ZrBr_2$ (250 mg, 0.48 mmol) in toluene (8 mL) at -78° C. The suspension was warmed to room temperature and stirred for 12 hours. White $MgBr_2$ began to precipitate from the yellow solution after several hours. The solvent was removed in vacuo, the residue triturated with pet ether (10 mL), and the suspension then filtered to remove the $MgBr_2$. The volume of the solution was reduced to 2 mL in vacuo. Cooling of the solution to -78° C for 1 hour afforded 4 as a yellow crystalline solid which was

isolated by filtration (170 mg, 75%). Anal. Calcd for $C_{22}H_{35}BrZr$: C, 56.14; H, 7.50; Br, 16.98. Found: C, 56.29; H, 7.45; Br, 17.20. ^1H NMR (benzene-d_6): δ 1.88 (s, 30H, $C_5(CH_3)_5$); 1.40 (t, $^3J_{HH}$ = 8.6 Hz, 3H, $CH_2C\underline{H}_3$); 0.58 (q, $^3J_{HH}$ = 8.6 Hz, 2H, $ZrCH_2$).

2.4.5 $Cp^*_2Zr(CH_2CMe_3)Cl$ (5)

$Cp^*_2ZrCl_2$ (750 mg, 1.7 mmol) and $LiCH_2CMe_3$ (170 mg, 2.2 mmol) were dissolved in toluene (20 mL) and the solution stirred for 12 hours at room temperature. The suspension was filtered to remove the white LiCl and the yellow filtrate evaporated to dryness <u>in vacuo</u>. The residue was triturated with pet. ether (8 mL), the suspension cooled to -78° C for 1 hour, and then filtered at this temperature to afford 5 as a yellow powder (624 mg, 77%). Anal. Calcd for $C_{25}H_{41}ClZr$: C, 64.12; H, 8.82, Zr, 19.48. Found: C, 64.07; H, 8.64; Zr, 19.71. ^1H NMR (benzene-d_6): δ 1.80 (s, 30H, $C_5(CH_3)_5$); 1.23 (s, 9H, $C(CH_3)_3$); 0.53 (s, 2H, $ZrCH_2$).

2.4.6 $Cp^*_2Zr(COEt)Br$ (6)

$Cp^*_2Zr(Et)Br$ 4 (150 mg, 0.32 mmol) was dissolved in toluene (8 mL) and the solution stirred under 1 atm CO for 2 hours. The solvent was removed <u>in vacuo</u> and the yellow-white residue triturated with pet. ether (4 mL). The suspension was cooled to -78° C for 1 hour and then filtered at this temperature to afford 6 as a white powder (130 mg, 82%). Anal. Calcd for $C_{23}H_{35}BrOZr$: C, 55.40; H, 7.08; Zr, 18.29. Found: C, 55.29; H, 6.96; Zr, 18.17. ^1H NMR (benzene-d_6): δ 2.82 (q, $^3J_{HH}$ = 7.6 Hz, 2H, $ZrCH_2$); 1.77 (s, 30H, $C_5(CH_3)_5$); 1.06 (t, $^3J_{HH}$ = 7.6 Hz, 3H, $CH_2C\underline{H}_3$). $^{13}C\{^1H\}$ NMR *(benzene-d_6)*:

δ 323.6 (s, CO); 117.4 (s, $\underline{C}_5(CH_3)_5$); 38.21 (s, $ZrCH_2$); 12.03 (s, $C_5(\underline{C}H_3)_5$); 11.77 (s, $CH_2\underline{C}H_3$). IR (nujol): ν(CO) 1537 cm^{-1}.

2.4.7 $Cp^*_2Zr(COCH_2CMe_3)Cl$ (7, 8)

The procedure described in section 2.4.6 was followed using 0.50 g (1.1 mmol) $Cp^*_2Zr(COCH_2CMe_2)Cl$ (5) in 8 mL toluene and stirring under 1 atm CO for 2 hours. The solvent was removed in vacuo and the residue triturated with pet. ether (5 mL). Cooling of this suspension at -78° C followed by filtration at this temperature afforded the 7, 8 mixture as a light-yellow powder (350 mg, 66%). Anal. Calcd for $C_{26}H_{41}ClOZr$: C, 62.92; H, 8.33; Zr, 18.38. Found: C, 62.85; H, 8.20; Zr, 18.54. The ^1H NMR spectrum of this solid indicates 8/7 = 3.1.

7. ^1H NMR (benzene-d_6): δ 2.37 (s, 2H, CH_2); 1.73 (s, 30H, $C_5(CH_3)_5$); 1.27 (s, 9H, $C(CH_3)_3$). $^{13}C\{^1H\}$ NMR (benzene-d_6): δ 329.4 (s, CO); 118.6 (s, $\underline{C}_5(CH_3)_5$); 59.4 (s, CH_2); 31.0 (s, $\underline{C}(CH_3)_3$); 30.5 (s, $C(\underline{C}H_3)_3$); 11.8 (s, $C_5(\underline{C}H_3)_5$).

8. ^1H NMR (benzene-d_6): δ 3.09 (s, 2H, CH_2); 1.73 (s, 30H, $C_5(CH_3)_5$); 1.07 (s, 9H, $C(CH_3)_2$). $^{13}C\{^1H\}$ NMR (benzene-d_6): 316.1 (s, CO); 117.3 (s, $\underline{C}_5(CH_3)_5$); 51.8 (s, CH_2); 31.0 (s, $\underline{C}(CH_3)_3$); 30.2 (s, $C(\underline{C}H_3)_3$); 11.8 (s, $C_5(\underline{C}H_3)_5$).

2.4.8 Thermolysis of $Cp^*_2Zr(COCH_2CMe_3)Cl$ (7, 8) to form cis- and trans-$Cp^*_2Zr(Cl)OCHCHCMe_3$ (9c, 9t)

$Cp^*_2Zr(COCH_2CMe_3)Cl$ (7, 8) (60 mg, 0.13 mmol) and C_6D_6 (0.9 mL) were placed in an NMR tube which was then sealed under vacuum with a torch. The solution was heated at 80° C for 6 days.

The ^{1}H NMR spectrum of this solution indicates 9c/9t = 1/1.

9c. ^{1}H NMR (benzene-d_6): δ 6.22 (d, $^3J_{HH}$ = 8.2 Hz, 1H, CHO); 4.01 (d, $^3J_{HH}$ = 8.2 Hz, 1H, C$\underline{H}$CMe$_3$); 1.86 (s, 30H, $C_5(CH_3)_5$); 1.28 (s, 9H, $C(CH_3)_3$). $^{13}C\{^1H\}$ NMR (benzene-d_6): δ 144.7 (s, CHO); 121.8 (s, $\underline{C}_5(CH_3)_5$); 114.4 (s, $\underline{C}$HCMe$_3$); 31.46 (s, C($\underline{C}$H$_3$)$_3$); 30.86 (s, $\underline{C}(CH_3)_3$); 11.61 (s, $C_5(\underline{C}H_3)_5$).

9t. ^{1}H NMR (benzene-d_6): δ 6.63 (d, $^3J_{HH}$ = 14.3 Hz, 1H, CHO); 4.82 (d, $^3J_{HH}$ = 14.3 Hz, 1H, $\underline{C}$HCMe$_3$); 1.85 (s, 30H, $C_5(CH_3)_5$); 1.08 (s, 9H, $C(CH_3)_3$). $^{13}C\{^1H\}$ NMR (benzene-d_6): δ 146.8 (s, CHO); 121.8 (s, $\underline{C}_5(CH_3)_5$); 118.0 (s, $\underline{C}$HCMe$_3$); 31.11 (s, C($\underline{C}$H$_3$)$_3$); 30.51 (s, $\underline{C}(CH_3)_3$); 11.61 (s, $C_5(\underline{C}H_3)_5$).

2.4.9 $Cp^*_2Zr(CHDCMe_3)Cl$

The procedure described in Section 2.4.5 was followed using 250 mg (0.58 mmol) Cp^*ZrCl_2 and 50 mg (0.64 mmol) $LiCHDCMe_3$ in 8 mL toluene. After filtration and removal of solvent, the residue was triturated with 6 mL pet. ether and the suspension cooled to -78° C for 2 hours. Filtration of this suspension at -78° C afforded the product as a yellow crystalline solid (150 mg, 55%).

2.4.10 Reaction of $Cp^*_2Zr(CHDCMe_3)Cl$ with CO and Thermolysis to Form cis-, trans-$Cp^*_2Zr(Cl)OCHCDCMe_3$ (12c$_H$, 12t$_H$) and cis-, trans-$Cp^*_2Zr(Cl)OCDCHCMe_3$ (12c$_D$, 12t$_D$)

$Cp^*_2Zr(CHDCMe_3)Cl$ (120 mg, 0.26 mmol) was dissolved in toluene (15 mL) and the solution stirred under 1 atm CO for 12 hours. The solvent was removed in vacuo and the residue redissolved in 0.4 mL C_6D_6. The solution was transferred to a NMR tube which was

then sealed with a torch. The solution was heated at 80° C for 72 hours. to give a mixture of $\underset{\sim}{12c}_H$, $\underset{\sim}{12t}_H$, $\underset{\sim}{12c}_D$, and $\underset{\sim}{12t}_D$ as evidenced by ^1H NMR spectroscopy ($\underset{\sim}{12c}_H/\underset{\sim}{12t}_H = \underset{\sim}{12c}_D/\underset{\sim}{12t}_D = 1$, $\underset{\sim}{12c}_H/\underset{\sim}{12c}_D = 1.74$, $\underset{\sim}{12t}_H/\underset{\sim}{12t}_D = 1.75$).

$\underset{\sim}{12c}_H$ ^1H NMR (benzene-d_6): δ 6.23 (t, $^3J_{DH}$ = 3.3 Hz, 1H, CHO); 1.86 (s, 30H, $C_5(CH_3)_5$); 1.28 (s, 9H, $C(CH_3)_3$).

$\underset{\sim}{12c}_D$ ^1H NMR (benzene-d_6): δ 4.01 (t, $^3J_{DH}$ = 3.3 Hz, 1H, $CHCMe_3$); 1.86 (s, 30H, $C_5(CH_3)_5$); 1.28 (s, 9H, $C(CH_3)_3$).

$\underset{\sim}{12t}_H$ ^1H NMR (benzene-d_6): δ 6.63 (t, $^3J_{DH}$ = 6.6 Hz, 1H, CHO); 1.85 (s, 30H, $C_5(CH_3)_5$); 1.07 (s, 9H, $C(CH_3)_3$).

$\underset{\sim}{12t}_D$ ^1H NMR (benzene-d_6): δ 4.80 (t, $^3J_{DH}$ = 6.6 Hz, 1H, $CHCMe_3$); 1.85 (s, 30H, $C_5(CH_3)_5$); 1.07 (s, 9H, $C(CH_3)_3$).

2.4.11 E-, Z- $Cp^*_2Zr(OCCH_3) \cdot CH_2PMe_3$ ($\underset{\sim}{13E}$, $\underset{\sim}{13Z}$)

$Cp^*_2Zr(COMe)Br$ ($\underset{\sim}{6}$) (180 mg, 0.36 mmol) was dissolved in toluene (8 mL) and the solution cooled to -78° C. With rapid stirring, CH_2PMe_3 (180 μL, 1.3 mmol) was added to the solution via syringe and the mixture allowed to warm to room temperature and stir for 12 hours. The yellow suspension was filtered to remove the white PMe_4Br and the solvent removed in vacuo. The yellow residue was triturated with pet. ether (3 mL), the suspension cooled to -78° C for 1 hour and then filtered at this temperature to afford $\underset{\sim}{13E}$, $\underset{\sim}{13Z}$ as a white-yellow crystalline solid (130 mg, 71%). The ^1H NMR spectrum of this solid indicates $\underset{\sim}{13Z}/\underset{\sim}{13E}$ = 1.6/1. Anal. Calcd for $C_{27}H_{45}OPZr$: C, 63.86; H, 8.93; Zr, 17.96. Found: C, 63.56; H, 8.99; Zr, 18.11.

$\underset{\sim}{13E}$. ^1H NMR (benzene-d_6): δ 5.80 (q, $^3J_{HH}$ = 6.6 Hz, 1H, $C\underline{H}(CH_3)$;

2.38 (d, $^3J_{HH}$ = 6.6 Hz, 3H, CH(C$\underline{H}_3$)); 1.97 (s, 30H, $C_5(CH_3)_5$), 0.99 (d, $^2J_{PH}$ = 14.6 Hz, 9H, $P(CH_3)_3$); -0.43 (d, $^2J_{PH}$ = 18.1 Hz, 2H, CH_2P). $^{31}P\{^1H\}$ NMR (benzene-d_6): δ 26.65 (s, P). $^{13}C\{^1H\}$ NMR (benzene-d_6): δ 190.8 (s, CO); 112.9 (s, $\underline{C}_5(CH_3)_5$); 81.02 (s, $\underline{C}H(CH_3)$); 30.14 (s, CH($\underline{C}H_3$)); 16.40 (d, $^2J_{PC}$ = 53 Hz, $P(CH_3)_3$); 12.28 (s, $C_5(\underline{C}H_2)_5$); 5.57 (d, $^2J_{PC}$ = 25 Hz, CH_2P).

13Z. ^1H NMR (benzene-d_6): δ 4.50 (q, $^3J_{HH}$ = 6.6 Hz, 1H, C$\underline{H}$(CH_3)); 2.38 (d, $^3J_{HH}$ = 6.6 Hz, 3H, CH(C$\underline{H}_3$)); 1.03 (d, $^2J_{PH}$ = 14.6 Hz, 9H, $P(CH_3)_3$); -0.43 (d, $^2J_{PH}$ = 18.1 Hz, 2H, CH_2P). $^{31}P\{^1H\}$ NMR (benzene-d_6): δ 26.45 (s, P); $^{13}C\{^1H\}$ NMR (benzene-d_6): δ 190.4 (s, CO); 113.4 (s, $\underline{C}_5(CH_3)_5$); 81.63 (s, $\underline{C}H(CH_3)$); 30.14 (s, CH($\underline{C}H_3$)); 16.71 (d, $^2J_{PC}$ = 74 Hz, $P(CH_3)_3$); 12.46 (s, $C_5(\underline{C}H_3)_5$); 5.57 (d, $^2J_{PC}$ = 25 Hz, CH_2P).

2.4.12 Z-$Cp^*_2Zr(OCCHCMe_3) \cdot CH_2PMe_3$ (14)

The procedure described in section 2.4.11 was followed using 200 mg (0.43 mmol) $Cp^*_2Zr(COCH_2CMe_3)Cl$ (7, 8) in 8 mL toluene and adding 90 μL (1.0 mmol) CH_2PMe_3. After filtration and removal of solvent, the residue was triturated with pet. ether (4 mL), the suspension cooled to -78° C and then filtered at this temperature to afford 14 as an off-white powder (102 mg, 43%). Anal. Calcd for $C_{30}H_{51}OPZr$: C, 65.52; H, 9.35; P, 5.63; Zr, 16.59; mol. wt. 550. Found: C, 65.45; H, 9.18; P, 5.40; Zr, 16.75; mol. wt. 582 (see ref. 17). ^1H NMR (benzene-d_6): δ 4.22 (s, 1H, CH); 1.87 (s, 30H, $C_5(CH_3)_5$); 1.64 (s, 9H, $C(CH_3)_3$); 0.97 (d, $^2J_{PH}$ = 14.0 Hz, 9H, $P(CH_3)_3$); -0.43 (d, $^2J_{PH}$ = 13.2 Hz, 2H, CH_2P). $^{31}P\{^1H\}$ NMR

(benzene-d_6): δ 26.59 (s, P); $^{13}C\{^1H\}$ NMR (benzene-d_6): δ 186.8 (s, C)); 112.7 (s, $\underline{C}_5(CH_3)_5$); 97.32 (s, $\underline{C}HC(CH_3)_3$); 34.30 (s, $\underline{C}(CH_3)_3$); 33.26 (s, $C(\underline{C}H_3)_3$); 13.97 (d, $^1J_{PC}$ = 49 Hz, $P(CH_3)_3$); 12.37 (s, $C_5(\underline{C}H_3)_5$); 5.53 (d, $^1J_{PC}$ = 23 Hz, CH_2P).

2.4.13 $\underline{Z}$-$[Cp^*_2Zr(OCCHCMe_3)Cl]^-Li^+ \cdot HN(CHMe_2)_2$ (17)

$Cp^*_2Zr(COCH_2CMe_3)Cl$ (7, 8) (450 mg, 0.91 mmol) and $LiN(CHMe_2)_2$ (110 mg, 1.0 mmol) were dissolved in toluene (8 mL) and the suspension stirred for 12 hours at room temperature. The cloudy orange solution was then filtered and the solvent removed in vacuo. The residue was triturated with pet. ether (6 mL), the suspension cooled to -78° C for 1 hour and then filtered at this temperature to afford 17 as an orange-white powder (364 mg, 72%). Anal. Calcd for $C_{32}H_{55}ClLiNOZr$: C, 64.00; H, 9.19; Zr, 15.12; mol. wt. 561. Found: C, 64.52; H, 9.22; Zr, 15.37; mol. wt. 430 (see refs. 17 and 22). ^1H NMR (benzene-d_6): δ 4.19 (s, 1H, CH); 2.43 (m, 1H, NCH); 1.90 (s, 30H, $C_5(CH_3)_5$); 1.40 (s, 9H, $CHC(C\underline{H}_3)_3$); 0.83 (d, $^3J_{HH}$ = 6.6 Hz, 12H, $N(CHC(C\underline{H}_3)_2)_2$). The amine proton resonance was not located. $^{13}C\{^1H\}$ NMR (benzene-d_6): δ 189.3 (s, CO); 115.3 (s, $\underline{C}_5(CH_3)_5$); 102.8 (s, $\underline{C}HC(CH_3)_3$); 45.68 (s, $\underline{C}H(CH_3)_2$); 32.71 (s, $\underline{C}(CH_3)_3$); 32.59 (s, $C(\underline{C}H_3)_3$); 22.88 (s, $CH(\underline{C}H_3)_2$, 12.13 (s, $C_5(\underline{C}H_3)_5$).

2.4.14 Reaction of $\underline{Z}$-$[Cp^*_2Zr(OCCHCMe_3)Cl]^-Li^+ \cdot HN(CHMe_2)_2$ (17) with CH_2PMe_3 to give $\underline{Z}$-$Cp^*_2Zr(OCCHCMe_3) \cdot CH_2PMe_3$ (14)

$\underline{Z}$-$[Cp^*_2Zr(OCCHCMe_3)Cl]^-Li^+ \cdot HN(CHCMe_2)_2$ (17) (20 mg, 0.04 mmol) was dissolved in C_6D_6 (0.4 mL) in an NMR tube and CH_2PMe_3 (5 μL, 0.06 mmol) added to the solution via syringe. The ^1H

NMR spectrum of the solution indicates 14 and $HN(CHMe_2)_2$ as the only products by comparison with the ^1H NMR spectra of authentic samples (vide supra).

2.4.15 Z-$Cp^*_2Zr(OCCHCMe_3)CO$ (18)

Z-$[Cp^*_2Zr(OCCHCMe_3)Cl]^-Li^+ \cdot HN(CHMe_2)_2$ (17) (30 mg, 0.06 mmol) was dissolved in toluene (5 mL) and the solution stirred under 1 atm CO for 2 hours. Upon addition of the CO, the color of the solution turned from yellow to green. Removal of solvent in vacuo afforded 18 as a dark green oil (80% by ^1H NMR spectroscopy). ^1H NMR (benzene-d_6): δ 4.49 (s, 1H, CH); 1.67 (s, 30H, $C_5(CH_3)_5$); 1.53 (s, 9H, $C(CH_3)_3$). $^{13}C\{^1H\}$ NMR (benzene-d_6): δ 228.0 (s, CO); 176.2 (s, COZr); 113.5 (s, $\underline{C}_5(CH_3)_5$; 91.10 (s, CH); 33.1 (s, $\underline{C}(CH_3)_3$); 32.3 (s, $C(\underline{C}H_3)_3$); 10.6 (s, $C_5(\underline{C}H_3)_5$). IR (benzene solution): ν(CO) 1987 cm^{-1}.

2.4.16 Reaction of E-, Z-$Cp^*_2Zr(OCCHMe) \cdot CH_2PMe_3$ (13E, 13Z) with H_2 to give cis- and trans-$Cp^*_2Zr(OCHCHMe)H$ (19c, 19t).

E-, Z-$Cp^*_2Zr(OCCHMe) \cdot CH_2PMe_3$ (13E, 13Z) (100 mg, 0.20 mmol) was dissolved in toluene (5mL) and the solution stirred for 1 hour under 1 atm H_2. Removal of solvent in vacuo afforded an extremely soluble white residue, the ^1H NMR spectrum of which indicates 19c and 19t (19c/19t = 1.6/1).

19c. ^1H NMR (benzene-d_6): δ 6.64 (dq, $^3J_{HH}$ = 7.0 Hz, $^4J_{HH}$ = 1.9 Hz, 1H, CHO); 6.10 (s, 1H, ZrH); 4.20 (dq, $^3J_{HH}$ = 7.0 Hz, $^3J_{HH}$ = 6.7 Hz, 1H, $C\underline{H}CH_3$); 1.90 (s, 30H, $C_5(CH_3)_5$); 1.63 (dd, $^3J_{HH}$ = 6.7 Hz, $^4J_{HH}$ = 1.9 Hz, 3H, $CHC\underline{H}_3$). $^{13}C\{^1H\}$ NMR (benzene-d_6): δ 147.4 (s, CHO); 117.9 (s, $\underline{C}_5(CH_3)_5$); 97.13 (s, $\underline{C}HCH_3$); 12.26 (s, $CH\underline{C}H_3$);

11.54 (s, $C_5(\underline{C}H_3)_5$).

19t. ^{1}H NMR (benzene-d_6): δ 6.80 (s, 1H, ZrH); 6.68 (dq, $^3J_{HH}$ = 13.3 Hz, $^4J_{HH}$ = 1.7 Hz, 1H, CHO); 4.65 (dq, $^3J_{HH}$ = 13.3 Hz, $^3J_{HH}$ = 6.7 Hz, 1H, C$\underline{H}$CH$_3$); 1.94 (s, 30H, $C_5(CH_3)_5$); 1.56 (dd, $^3J_{HH}$ = 6.7 Hz, $^4J_{HH}$ = 1.7 Hz, 3H, CHC$\underline{H}_3$). ^{13}C{^{1}H} NMR (benzene-d_6): δ 149.1 (s, CHO); 118.1 (s, $\underline{C}_5(CH_3)_5$); 99.99 (s, $\underline{C}$HCH$_3$); 11.74 (s, $C_5(\underline{C}H_3)_5$); 9.66 (s, CH$\underline{C}$H$_3$).

2.4.17 cis-$Cp^*_2Zr(OCHCHCMe_3)H$ (20)

Z-$[Cp^*_2Zr(OCCHCMe_3)Cl]^-Li^+ \cdot HN(CHCMe_2)$ (17) (300 mg, 0.54 mmol) was dissolved in toluene (8 mL) and stirred for 30 minutes under 1 atm H_2. Upon addition of H_2, the solution turned from yellow to light purple in color and became cloudy as LiCl precipitated. The solvent was removed in vacuo and the purple-white residue redissolved in pet. ether (3 mL) and the suspension filtered. Cooling of the filtrate at -78°C afforded little solid and so the solvent was removed in vacuo and 20 isolated by scraping the reaction flask with a spatula (106 mg, 43%). Anal. Calcd for $C_{26}H_{42}OZr$: C, 67.70; H, 9.17; Zr, 19.75. Found: C, 67.20; H, 8.78; Zr, 19.23. ^{1}H NMR (benzene-d_6): δ 6.26 (d, $^3J_{HH}$ = 7.9 Hz, 1H, CHO); 6.23 (s, 1H, ZrH); 3.94 (d, $^3J_{HH}$ = 7.9 Hz, 1H, C$\underline{H}(CH_3)_3$); 1.97 (s, 30H, $C_5(CH_3)_5$); 1.32 (s, 9H, $C(CH_3)_3$). ^{13}C NMR (benzene-d_6): δ 144.3 (dd, $^1J_{CH}$ = 172 Hz, $^3J_{CH}$ = 6.6 Hz, CHO); 118.1 (s, $\underline{C}_5(CH_3)_5$); 113.5 (dd, $^1J_{CH}$ = 149.0 Hz, $^3J_{CH}$ = 8 Hz, $\underline{C}HC(CH_3)_3$); 32.36 (s, $\underline{C}(CH_3)_3$); 31.91 ($^1J_{CH}$ = 126 Hz, $C(\underline{C}H_3)_3$); 11.70 (q, $^1J_{CH}$ = 126 Hz, $C_5(\underline{C}H_3)_5$). IR (nujol): ν(ZrH) 1537 cm^{-1}.

2.4.18 Reaction of Z-$Cp^*_2Zr(OCCHCMe_3)CO$ (18) with H_2 to give cis-$Cp^*_2Zr(OCHCHCMe_3)H$ (20).

Z-$Cp^*_2Zr(OCCHCMe_3)CO$ (18) (~ 10 mg) was dissolved in C_6D_6 (0.4 mL) in an NMR tube. H_2 (600 torr) was added at room temperature and the tube sealed with a torch. After 5 minutes of shaking, the solution had turned from green to yellow as 20 was formed as confirmed by comparison of the ^1H NMR spectrum of this solution with that of an authentic sample (vide supra).

2.4.19 Reaction of Z-$Cp^*_2Zr(OCCHCMe_3) \cdot CH_2PMe_3$ (14) with H_2 to give cis-$Cp^*_2Zr(OCHCHCMe_3)H$ (20).

The procedure described in Section 2.4.18 was followed using 30 mg (0.55 mmol) Z-$Cp^*_2Zr(OCCHCMe_3) \cdot CH_2PMe_3$ (14) in 0.4 mL C_6D_6 and sealing the NMR tube under 600 torr H_2. After 5 minutes of shaking, the solution lightened in color as 20 was formed as evidenced by comparison of the ^1H NMR spectrum of this solution with that of an authentic sample (vide supra).

2.4.20 cis-$Cp^*_2Zr(OCHCHCMe_3)I$ (21c)

cis-$Cp^*_2Zr(OCHCHCMe_3)H$ (20) (0.71 mmol), generated in situ following the procedure described in section 2.4.17, was dissolved in toluene (8 mL) and the solution frozen at -196° C. CH_3I (1.4 mmol) was added by vacuum transfer and the solution warmed to room temperature and stirred for 1 hour. The color of the solution turned from light purple to yellow upon warming. The solvent was removed in vacuo and the yellow residue triturated with pet. ether (4 mL), the suspension cooled to -78° C and then filtered at this temperature to

afford 21c as a yellow microcrystalline solid (100 mg, 24%). ^{1}H NMR (benzene-d_6): δ 6.07 (d, $^3J_{HH}$ = 7.9 Hz, 1H, CHO); 4.03 (d, $^3J_{HH}$ = 7.9 Hz, 1H, C<u>H</u>C(CH$_3$)$_3$); 1.88 (s, 30H, C$_5$(CH$_3$)$_5$); 1.29 (s, 9H, C(CH$_3$)$_3$. ^{13}C{^{1}H} NMR (benzene-d_6): δ 145.2 (s, CHO); 129.0 (s, <u>C</u>$_5$(CH$_3$)$_5$); 127.9 (s, <u>C</u>HC(CH$_3$)$_3$); 31.69 (s, C(<u>C</u>H$_3$)$_3$); 31.37 (s, <u>C</u>(CH$_3$)$_3$); 12.84 (s, C$_5$(<u>C</u>H$_3$)$_5$).

2.4.21 Toepler Pump Analysis of the Reaction of <u>cis</u>-Cp*$_2$Zr(OCHCHCMe$_3$)H (21c) with CH$_3$I

<u>cis</u>-Cp*$_2$Zr(OCHCHCMe$_3$)H (21c) (20 mg, 0.043 mmol) was dissolved in toluene (4 mL) and the solution frozen at -196° C. CH$_3$I (0.10 mmol) was added by vacuum transfer and the solution warmed to room temperature and stirred for 1 hour. Analysis of the gas product revealed 0.040 mmol CH$_4$ (0.92 mol CH$_4$/mol 21c).

2.4.22 Thermolysis of <u>cis</u>-Cp*$_2$Zr(OCHCHCMe$_3$)I (21c) to give <u>trans</u>-Cp*$_2$Zr(OCHCHCMe$_3$)I (21t)

<u>cis</u>-Cp*$_2$Zr(OCHCHCMe$_3$)I (21c) (<u>ca</u>. 20 mg) was dissolved in C$_6$D$_6$ (0.4 mL) in an NMR tube and the solution heated at 80°C for 9 days. The ^{1}H NMR spectrum of this solution indicated 21t had formed quantitatively. ^{1}H NMR (benzene-d_6): δ 6.37 (d, $^3J_{HH}$ = 13.2 Hz. 1H, CHO); 4.85 (d, $^3J_{HH}$ = 13.2 Hz, 1H, C<u>H</u>C(CH$_3$)$_3$); 1.93 (s, 30H, C$_5$(CH$_3$)$_5$); 1.08 (s, 9H, C(CH$_3$)$_3$).

2.5 References and Notes

1. L. Messerle, Ph.D. Thesis, Massachusetts Institute of Technology, Cambridge, MA, 1979.
2. D. A. Straus and R. H. Grubbs, J. Amer. Chem. Soc., 104, 5499 (1982).
3. a) D. A. Straus, Ph.D. Thesis, California Institute of Technology, Pasadena, CA, 1982;
   b) E. J. Moore, D. A. Straus, J. Armantrout, B. D. Santarsiero, R. H. Grubbs, and J. E. Bercaw, J. Amer. Chem. Soc., 105, 2068 (1983).
4. R refers to the substituent on the β carbon of the ketene moiety.
5. a) G. Fachinetti, G. Fochi, and C. Floriani, J. Chem. Soc., 2297 (1977);
   b) G. Fachinetti, G. Fochi, and C. Floriani, ibid., 1946 (1977).
6. a) G. Erker and F. Rosenfeldt, Angew. Chem. Int. Ed. Engl. 17, 605 (1978);
   b) G. Erker and F. Rosenfeldt, J. Organomet. Chem., 188, C1 (1980).
7. a) T. J. Marks, J. M. Manriquez, P. J. Fagan, V. W. Day, C. S. Day, and S. H. Vollmer, "Lanthanide and Actinide Chemistry and Spectroscopy," p. 3, N. M. Edelstein, Ed., (ACS Symposium Series 131), American Chemical Society, Washington, D.C., 1980;
   b) D. A. Katahira, K. G. Moloy, and T. J. Marks, Organometallics, 1, 1723 (1982).

8. a) J. M. Manriquez, D. R. McAlister, R. D. Sanner, and J. E. Bercaw, J. Amer. Chem. Soc., 100, 2716 (1978);
b) P. T. Wolczanski, R. S. Threlkel, and J. E. Bercaw, ibid., 101, 218 (1979);
c) R. S. Threlkel and J. E. Bercaw, ibid., 103, 2650 (1981).

9. Determined by the ratios $\underset{\sim}{12c}_H/\underset{\sim}{12c}_D = 1.74$ and $\underset{\sim}{12t}_H/\underset{\sim}{12t}_D = 1.75$ obtained from the ^1H NMR spectrum of the mixture. See experimental section. The observed isotope effect is smaller than a primary isotope effect ($k_H/k_D \cong 3$), yet greater than 1, implying some contribution from C-H bond breakage in formation of the transition state. See C. McDade, J. C. Green, and J. E. Bercaw, Organometallics, 1, 1629 (1982).

10. Determined by ^1H NMR spectroscopy.

11. The E, Z nomenclature refers to olefinic substitution relative to the $-OZrCp^*_2$ moiety.

12. It should be noted that the ^1H NMR spectrum of 3 was taken in THF-d_8, while that of the 13E, 13Z mixture was taken in benzene-d_6.

13. J. R. Marsella, C. J. Curtis, J. E. Bercaw, and K. G. Coulton, J. Amer. Chem. Soc., 102, 7244 (1980).

14. J. M. Manriquez, D. R. McAlister, R. D. Sanner, and J. E. Bercaw, ibid., 98, 6733 (1976).

15. a) P. T. Barger, Ph.D. Thesis, California Institute of Technology, Pasadena, Ca, 1983;
b) P. T. Barger, J. Armantrout, B. D. Santarsiero, and J. E. Bercaw, manuscript in preparation.

16. T. L. Brown, D. W. Dickerhoof, D. A. Batus, and G. L. Morgan, Rev. Sci. Instrum., 33, 491 (1962).

17. a) R. Signer, Justus Liebigs Ann. Chem., 478, 246 (1930); b) E. P. Clark, Ind. Eng. Chem. Anal. Ed., 13, 820 (1941).

18. R. H. Marvich and H. H. Brintzinger, J. Amer. Chem. Soc., 93, 2046 (1971).

19. J. M. Manriquez and J. E. Bercaw, ibid., 96, 6229 (1974).

20. a) R. Koster, D. Simic, and M. A. Grassberger, Justus Liebigs Ann. Chem., 739, 211 (1970);
b) J. March, "Advanced Organic Chemistry: Reactions, Mechanisms, and Structure," McGraw Hill, New York, 1977, pp. 864-872.

21. a) R. R. Schrock and J. D. Fellman, ibid., 100, 3359 (1978); b) B. Stevenson, G. Solladic, and H. S. Mosher, ibid., 94, 4184 (1972).

22. The molecular weight of 17 is anomalously low and is probably due to a small amount of amine dissociation.

CHAPTER 3

The Reaction of Permethylzirconocene and Permethylhafnocene Hydride Complexes with Phosphorous Ylides

3.1 Introduction

The use of phosporous ylides as reagents in organic synthesis is ubiquitous.[1] Only recently, however, have these phosphoranes found application as reagents in the synthesis of organometallic compounds. Early work in this area focused on the use of phosphorous ylides in chelating or nucleophilic reactions.[2] Little use was made of the phosphorane as a carbene transfer reagent (Wittig reagent) or as a strong base; properties which were exploited in synthetic organic chemistry.

The basicity of phosphorous ylides was used by Schrock in the preparation of several zirconium and tantalum complexes. The preparation of $Cp_2TaMeCH_2$ from Cp_2TaMe_2 and methylenetrimethylphosphorane (eq. 1) results not <u>via</u> methylene transfer from the ylide, but rather by proton abstraction from one of the two methyl ligands.[3] Other compounds were prepared using the ylide first as a nucleophile and second as a dehydrohalogenating agent (eq. 2).[4] Phosphorous

$$[Cp_2TaMe_2]BF_4 + CH_2PMe_3 \rightarrow Cp_2TaMeCH_2 + PMe_3 \qquad (1)$$

$$Cp_2Zr(Me)Cl + 2\ CH_2PMe_3 \rightarrow Cp_2ZrMe(CH{=}PMe_3) \qquad (2)$$

ylides have also been successfully employed in the synthesis of several zirconium-ketene complexes by the dehydrohalogenation of zirconium haloacyl compounds.[5]

Similar to their use as carbene transfer reagents in organic synthesis, phosphorous ylides have been used to prepare several early transition metal carbene species by the direct transfer of a carbene fragment from an ylide to an organometallic compound. Schrock has

reported the preparation of tantalum alkylidene complexes by the reaction of phosphine compounds with the appropriate phosphorane (eq. 3).[6] A similar result was later reported by Schwartz in a zirconium system, offering spectroscopic evidence for the first reported example of a zirconium methylene species (eq. 4).[7]

$$Cp_2Ta(Me)L + CHR'PR_3 \rightarrow Cp_2Ta(CHR')Me + L + PR_3 \qquad (3)$$

L = PMe_3, PMe_2Ph

R = Me, Et, Ph

R′ = H, Me, Ph

$$Cp_2Zr(PPh_2Me)_2 \xrightarrow{CH_2PMe_3} Cp_2Zr(CH_2)PPh_2Me \qquad (4)$$

To further investigate the possibility of CH_2-transfer from phosphorous ylides, their reactions with permethylzirconocene and permethylhafnocene dihydride ($Cp^*_2ZrH_2$, $Cp^*_2HfH_2$) has been explored. These hydride complexes are known to act as powerful hydride transfer reagents[8] and it was thought that hydride migration to the ylide nucleophilic carbon might be achieved to give a series of alkyl-hydride compounds. The insertion of methylene into a metal-hydride bond to afford a methyl-hydride derivative is known for some of the Group VI and VII transition metals using diazomethane as the carbene source, although the yields are typically low.[9] The insertion of methylene into a metal-hydride bond using a phosphorous ylide had not been previously reported. This chapter describes the use of methylenetrimethylphosphorane as a reagent in the synthesis of permethylzirconocene and permethylhafnocene methyl hydride as well as a permethylzirconocene

metallated-ylide complex. The reactivity of this metallated-ylide complex with CO is also discussed.

3.2 Results and Discussion

3.2.1 Synthetic Advantages of Using Methylenetrimethylphosphorane

Methylenetrimethylphosphorane (CH_2PMe_3) was chosen for this study for several reasons. First, it is one of the most nuecleophilic of all phosphorous ylides.[1] Coordination of the ylide to the highly electrophilic metal center in $Cp^*_2MH_2$ (M = Hf, Zr) should proceed quite readily. Second, it is the least serically demanding of all phosphorous ylides. Because the pentamethylcyclopentadienyl ligands are themselves quite large, the incoming ylide must be small to successfully enter the coordination sphere of the $Cp^*_2MH_2$ complex. Third and last, once the ylide has transferred the methylene fragment to a metal complex, the resulting PMe_3 can either be used as a ligand to stabilize the complex if necessary, or simply removed from the reaction mixture by evacuation.

3.2.2 Synthesis and Characterization of $Cp^*_2Hf(H)Me$ (4)

Bis(pentamethylcyclopentadienyl)hafnium dihydride ($Cp^*_2HfH_2$ (1)) reacts with one equivalent of CH_2PMe_3 at 80°C after 1.5 hours to afford PMe_3 and $Cp^*_2Hf(H)Me$ (4) in greater than 95% yield as evidenced by ^1H NMR spectroscopy (eq. 5).[10] Although the colorless methyl-

$$\underset{1}{Cp^*_2HfH_2} + CH_2PMe_3 \rightarrow \underset{4}{Cp^*_2Hf(H)Me} + PMe_3 \qquad (5)$$

hydride complex is extremely soluble in hydrocarbon solvents, it may

be recrystallized from petroleum ether at -78°C in 30° yield. The ^1H NMR spectrum of $\underset{\sim}{4}$ consists of a single resonance for the Cp^* protons (δ1.90) and a high field singlet at δ -0.65 consistent with a methyl group bound to hafnium.[11] The hydride ligand resonance is observed as a broad singlet at δ 12.97, upfield of the starting complex $\underset{\sim}{1}$ (δ 15.6). A Hf-H stretch is also observed in the IR spectrum at 1600 cm^{-1}.

The formation of $Cp^*_2Hf(H)Me$ from $Cp^*_2HfH_2$ and CH_2PMe_3 is unique in that it is the first example of methylene insertion into a metal-hydride bond using a phosphorous ylide as the carbene source. Hydrides of the later transition metals are, apparently, not sufficiently hydridic to effect this transformation;[12] the protonic nature of later transition metal hydrides probably results in their deprotonation when treated with phosphorous ylides. Complex $\underset{\sim}{4}$ is also unique in that it is the first example of a monomeric group IV methyl-hydride complex.[13] Although $Cp_2Zr(H)Me$ has been reported, it is undoubtedly polymeric and has not been well characterized.[14] The general instability of methyl-hydride complexes has been suggested to account for the rarity of these species.[15,16] $Cp^*_2Hf(H)Me$ is, however, remarkably stable; solutions of $\underset{\sim}{4}$ remain unchanged even after several weeks at 80° C.

3.2.3 Mechanism of the Formation of $Cp^*_2Hf(H)Me$ ($\underset{\sim}{4}$)

The mechanism of this insertion reaction could follow one of two pathways. In the first (Scheme 3.1), the ylide coordinates to the highly electrophilic hafnium(IV) center through the nucleophilic carbon giving the 18-electron ylide-dihydride intermediate $\underset{\sim}{2}$. Loss of PMe_3 from $\underset{\sim}{2}$ affords a dihydrido-methylene intermediate which then

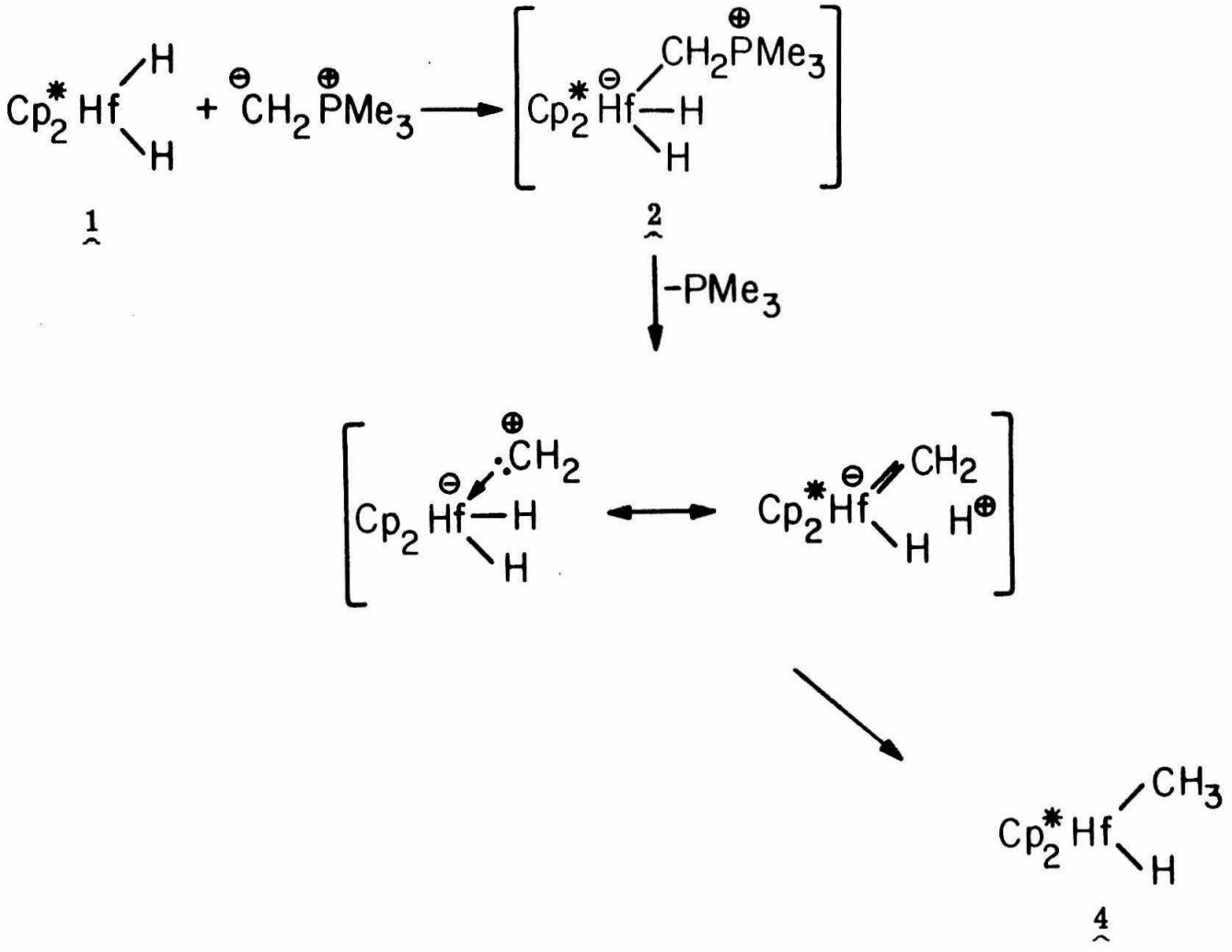

SCHEME 3.1. Carbene Mechanism for the Formation of $Cp^*_2Hf(H)Me$ (4).

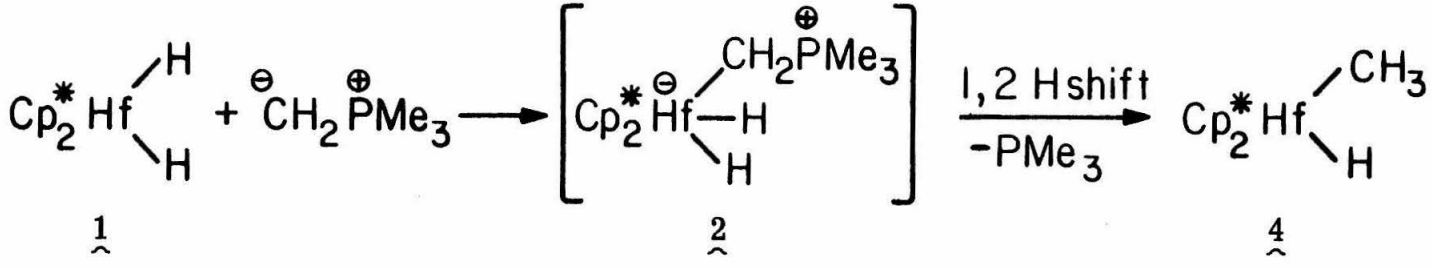

1 2 4

SCHEME 3. 2. 1, 2-Hydrogen Shift Mechanism for the Formation of $Cp^*_2Hf(H)Me$ (4).

undergoes methylene insertion into a hafnium-hydride bond affording the product 4. In the second mechanism (Scheme 3.2), the ylide-hydride intermediate 2 is again formed and by a concerted 1,2-hydrogen shift with loss of PMe_3, affords the methyl-hydride complex 4 directly.

Intermediates such as 2 have been proposed in other reactions involving ylides and zirconium complexes[7,17] and Green has isolated a tungsten ylide-hydride species in the reaction of a tungsten-ethylene complex with PMe_2Ph.[18] Although several tantalum carbene compounds have been prepared,[3,6] few are known for zirconium. Schwartz has obtained spectroscopic evidence for a zirconium methylidene species[7] and recent work in our laboratories has afforded the crystal structure of the zirconocene carbene complex $Cp_2Zr(CO)(CHOZr(H)Cp^*_2)$.[19] The 1,2-hydrogen shift mechanism (Scheme 3.2) is similar to that involving hydride migration to an alkyl ligand with resultant loss of PMe_3. If one views the ylide-hydride intermediate 2 as a stabilized carbene complex, the difference between the two mechanistic pathways is small. At present, it is uncertain which pathway is operative.

3.2.4 Reaction of $Cp^*_2Hf(H)Me$ (4) with CH_3I

Treatment of 4 with excess methyl iodide affords the yellow iodo derivative $Cp^*_2Hf(I)Me$ (5) and methane (0.90 mol CH_4/mol 4)[21] (eq. 6), verifying that 4 is a monohydride species.[22] ^1H NMR and IR spectral data indicate a formulation analogous to that of 4.

$$\underset{4}{Cp^*_2Hf(H)Me} + CH_3I \rightarrow \underset{5}{Cp^*_2Hf(Me)I} + CH_4 \qquad (6)$$

3.2.5 Reaction of $Cp^*_2ZrH_2$ (6) with CH_2PMe_3

The zirconium analogue of 1, $Cp^*_2ZrH_2$ (6), also reacts with a three-fold excess of CH_2PMe_3 at room temperature but affords two products identified by ^1H NMR spectroscopy (vide infra) as $Cp^*_2Zr(H)Me$ (7) (71%) and $Cp^*_2\overline{Zr(H)CH_2PMe_2CH_2}$ (11) (29%) (eq. 7). Toepler pump

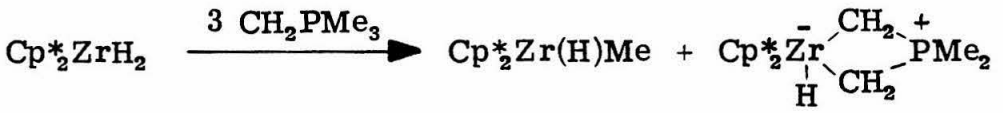

6 7 (71%) 11 (29%)

$$+ CH_4 + PMe_3 \qquad (7)$$

analysis of the gas product confirmed that for each equivalent of 11 formed, one equivalent of CH_4 was also produced. Although neither 7 nor 11 could be isolated cleanly from the conditions of equation 7, 7 could be obtained in greater than 90% yield (^1H NMR spectroscopy) by treating an 80° C toluene solution of 6 with excess CH_2PMe_3 and heating for 30 minutes (eq. 8). Recrystallization from petroleum ether at

$$Cp^*_2ZrH_2 + \text{xs } CH_2PMe_3 \xrightarrow[30\ min]{80°C} Cp^*_2Zr(H)Me + PMe_3 \qquad (8)$$

6 7

-78°C afforded 7 in 31% isolated yield.[20] The spectral data of 7 are similar to that of 4 except for the expected higher field shift of the hydride ligand resonance in the ^1H NMR spectrum (δ 6.15). Analogous to 4, 7 reacts with excess methyl iodide to afford methane (0.9 mol CH_4/mol 7)[21] and a yellow compound formulated as $Cp^*_2Zr(I)Me$ (14).

Further heating of the zirconium methyl-hydride complex 7 with

CH_2PMe_3 at 80°C for 24 hours affords the dimethyl compound $Cp^*_2ZrMe_2$ (13) (eq. 9) identified by comparison of its ^1H NMR spectrum with that

$$Cp^*_2Zr(H)Me + xs\ CH_2PMe_3 \xrightarrow[24\ hrs]{80^\circ C} Cp^*_2ZrMe_2 + PMe_3 \quad (9)$$

7 13

of an authentic sample.[23] No resonances characteristic of 11 were observed. Although $Cp^*_2ZrMe_2$ is readily formed when $Cp^*_2Zr(H)Me$ is treated with CH_2PMe_3, no such product is obtained when $Cp^*_2Hf(H)Me$ is treated with CH_2PMe_3, even after several weeks at 80° C. Typically, the hydride complexes of zirconium are found to be more reactive than those of hanium.[24]

3.2.6 Synthesis and Characterization of $Cp^*_2\overline{Zr(H)CH_2PMe_2CH_2}$ (11)

The metallated-ylide complex 11 is prepared by treating $Cp^*_2Zr(H)Cl$ (8) with two equivalents of CH_2PMe_3 at room temperature for 12 hours (eq. 10). PMe_4Cl is removed from the toluene solution by

$$Cp^*_2Zr(H)Cl + 2\ CH_2PMe_3 \longrightarrow Cp^*_2Zr\begin{matrix} {}^{-}CH_2 \\ H \\ CH_2 \end{matrix}{}^{+}PMe_2 + PMe_4Cl \quad (10)$$

8 11

filtration and 11 can be isolated from the filtrate as an orange crystalline solid in 73% yield. The ^1H NMR spectrum of 11 consists of a single resonance due to the Cp* protons (δ 1.93) and a doublet ($^3J_{PH}$ = 45.6 Hz) for the hydride ligand resonance at relatively high field (δ 4.40). Although the two methyl groups on phosphorous are equivalent

(δ 1.03, $^2J_{PH}$ = 12.5 Hz), the two methylene moieties (δ -0.68 and δ -0.90) are not. Selective decoupling experiments establish that the lower field methylene ligand is coupled to the hydride ligand ($^3J_{HH}$ = 2.6 Hz). The ^{13}C NMR spectrum confirms the inequivalence of the methylene moieties with high-field resonances at δ -4.17 ($^1J_{PC}$ = 39.56 Hz) and δ -5.70 ($^1J_{PC}$ = 41.03 Hz). Schwartz has prepared the Cp analogue of 11, $Cp_2\overline{Zr(H)CH_2PMe_2CH_2}$, by a different method (vide infra).[17] The spectral data of these two compounds are nearly identical.

3.2.7 Crystal Structure of $Cp^*_2\overline{Zr(H)CH_2PMe_2CH_2}$ (11)

The structure of $Cp^*_2\overline{Zr(H)CH_2PMe_2CH_2}$ (11) was confirmed by X-ray diffraction. Orange crystals of 11 grown from toluene are monoclinic, crystallizing in the space group $P2_1/c$ with four molecules per unit cell. The pertinent crystal data are summarized in Table 3.1. 5540 independent measurements were taken with $4° < 2\theta < 55°$ ($+h, \pm k, \pm \ell$). Using anisotropic Gaussian amplitudes for all nonhydrogen atoms, the least-squares refinement gave R = 0.052 (with 3456 $F_o^2 > 3\sigma_{F^2}$) and a goodness-of-fit of 2.16.

The molecular structure of $Cp^*_2\overline{Zr(H)CH_2PMe_2CH_2}$ (11) is presented in Figure 3.1 and a skeletal view of the immediate ligation about zirconium with relevant bond distances and bond angles is given in Figure 3.2. The η^5-$C_5(CH_3)_5$ ligands are disordered and attempts to model this disorder resulted in a 60:40 ratio of electron density for rings A and B. No unusual nonbonding contacts between hydrogen atoms of the pentamethylcyclopentadienyl ligands and atoms of the

TABLE 3.1. Crystal Data for $Cp^*_2\overline{Zr(H)CH_2PMe_2CH_2}$ (11).

Formula	$C_{21}H_{41}PZr$
Formula Weight	451.78
Space Group	$P2_1/c$
a	13.7765(14) Å
b	10.9262(12) Å
c	15.9459(19) Å
β	93.358(9)°
V	2396.1(8) $Å^3$
Z	4

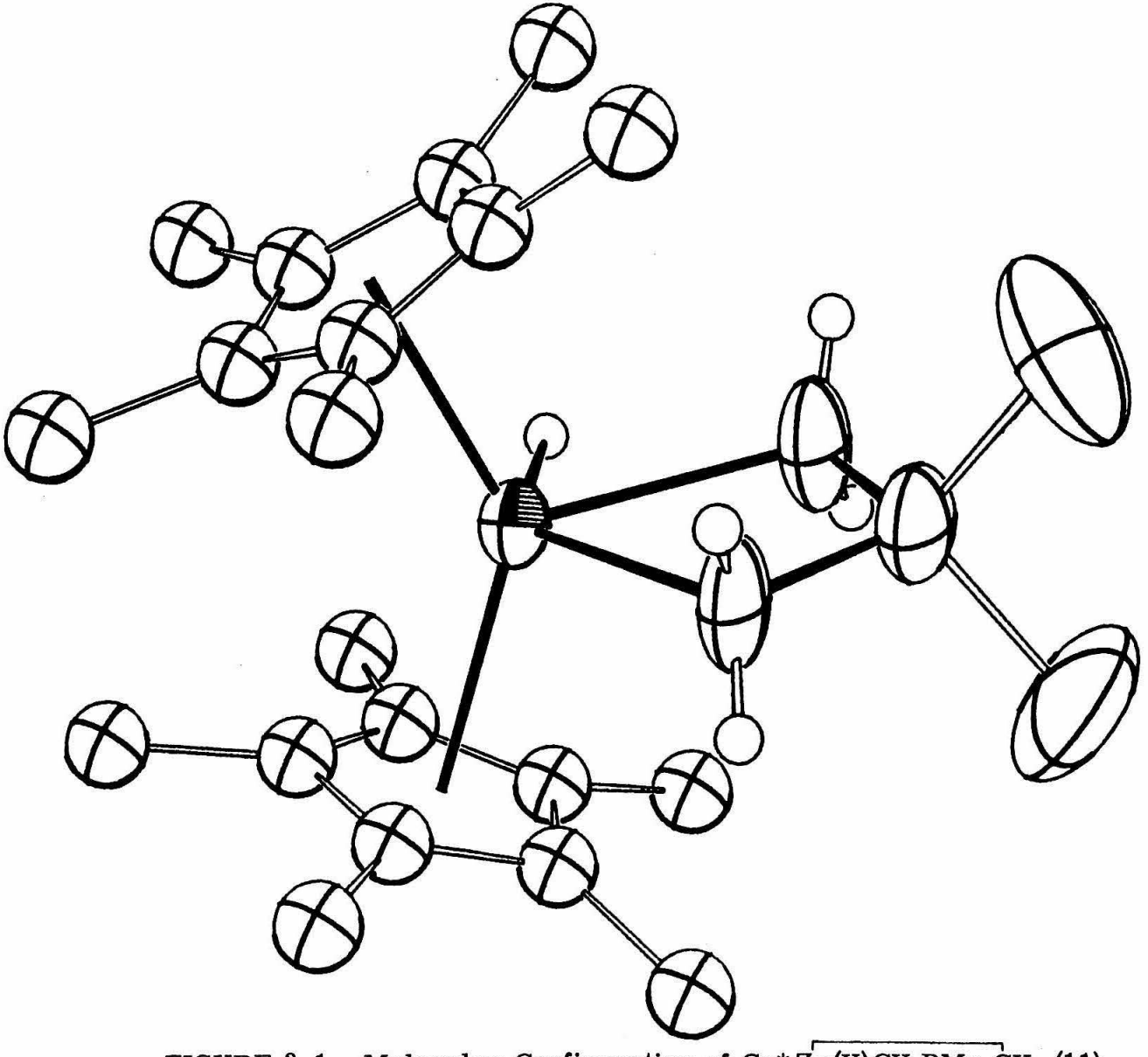

FIGURE 3.1. Molecular Configuration of $Cp^*_2\overline{Zr(H)CH_2PMe_2CH_2}$ (11).

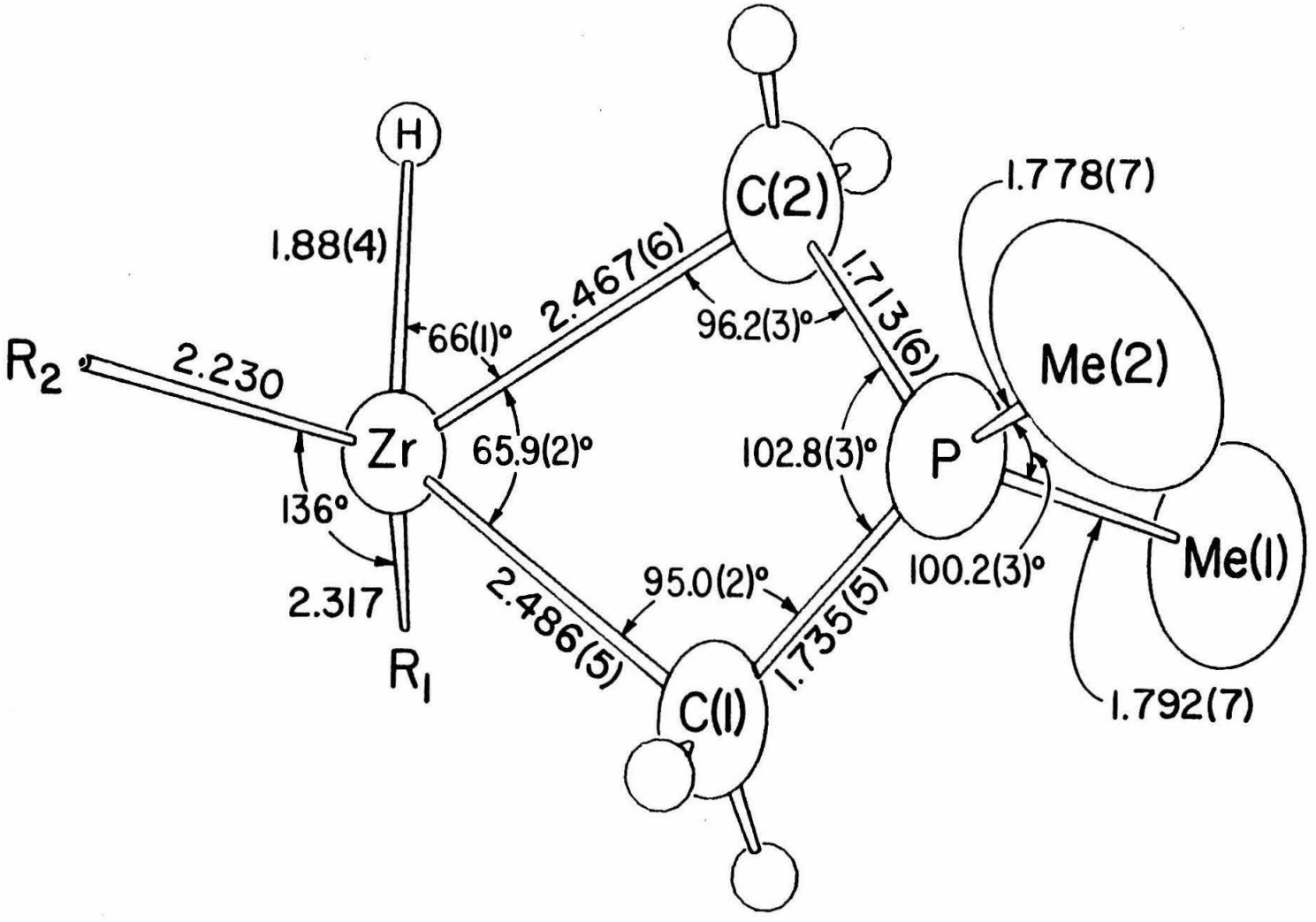

FIGURE 3. 2. Skeletal View of $Cp^*_2Zr(H)CH_2PMe_2CH_2$ (11). [a]

[a]Bond distances are in Å.

metallacycle ring are observed. The atoms of the metallocycle ring are nearly coplanar, with the phosphorous atom displaced from this plane by 0.05 Å.

The Zr-C(1) (2.486(5) Å), Zr-C(2) (2.467(6) Å), P-C(1) (1.735(5) Å), and P-C(2) (1.713(6) Å) bond distances as well as the C(1)-Zr-C(2) angle (65.9(2)°) are similar to that of $Zr_2[(CH_2)_2PMe_2]_4$-$(\mu$-$CPMe_3)_2$, cf., the average Zr-C(2.534(5) Å) and P-C (1.738(5) Å) bond distances and C-Zr-C bond angle (65.9(2) Å).[25] The Zr-C bond distances are unusually long compared to those observed for zirconocene alkyl complexes, e.g., $Cp_2Zr(CH_2SiMe_3)_2$ (2.28 Å)[26] or $Cp_2Zr(CH_2CMe_3)_2$ (2.29 Å),[26] and a zirconocene acyl complex, e.g., $Cp_2Zr(COCH_3)CH_3$ (2.336(7) Å).[27] However, the sterically encumbered molecule, $Cp_2Zr(CHPh_2)_2$, displays an average Zr-C bond distance of 2.513(15) Å.[28] Thus, the long Zr-C bond distances observed in 11 may be a result of steric crowding in the coordination group around the zirconium atom. The P-C(1) and P-C(2) bond distances are somewhat shorter tham might be expected for a single P-C bond (1.84 Å),[29] implying additional electron delocalization into the P-C bonds of the CH_2-P-CH_2 moiety. The Zr-H bond distance of 1.88(4) Å compares to that of other zirconium complexes containing terminal hydride ligands, e.g., $[(C_5H_4CH_3)_2ZrH(\mu$-$H)]$ (1.78(2) Å)[30] and $HZr(C_8H_{11})(dmpe)_2$ (1.67 Å),[31] and the Hf-H bond distance in $Cp^*_2Hf(\eta^3$-$C_3H_5)H$ (1.86(7) Å).[32]

The metallated-ylide complex 11 is one of the few structurally characterized Cp_2ZrL_3-type compounds. Similar compounds whose structures have been established by X-ray diffraction are $Cp_2Zr(COMe)Me$,[27] $Cp_2\overline{Zr(Cl)SNMe_2S}$,[33] and $Cp^*_2Zr(OCCH_2)pyr$.[5b]

In addition, the structure of 11 is also the first example of a mononuclear zirconium-hydride complex in which the hydride ligand was located by difference Fourier techniques and refined.

3.2.8 Thermal Decomposition of $Cp^*_2\overline{Zr(H)CH_2PMe_2CH_2}$ (11)

In contrast to the limited thermal stability of $Cp_2\overline{Zr(H)CH_2PMe_2CH_2}$ as observed by Schwartz,[17] the Cp* derivative 11 is moderately stable. Solutions of 11 do decompose after several weeks at room temperature and within hours at 80°C, but the decomposition is remarkably clean for the dimethylphosphinomethyl-methyl complex 12 (eq. 11). Complex

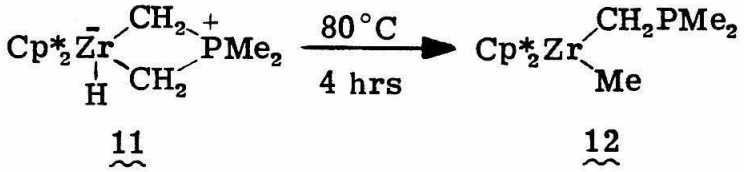

11 12 (11)

12 can only be isolated as an amber oil, but high field doublets in the ^1H NMR spectrum at δ 0.0 ($^2J_{PH}$ = 6.1 Hz) and δ -0.43 ($^4J_{PH}$ = 0.24 Hz) suggest a formulation in which two alkyl ligands are coordinated to zirconium. The η^5-$C_5(CH_3)_5$ proton resonance at δ 1.83 displays no splitting by phosphorous and is observed as a sharp singlet. Formation of 12 most probably proceeds by methylene insertion into the Zr-H bond followed by elimination of the neutral phosphino ligand. This insertion is similar to that observed in the formation of $Cp^*_2M(H)Me$ (M = Zr, Hf), except that the leaving $-PMe_2$ ligand remains bonded to the zirconium through one of the original methylene bridges of the metallated-ylide complex 11. A similar compound, $Cp_2Zr(Cl)CH_2PPh_2$, has been

prepared by Schore in the reaction of Cp_2ZrCl_2 with $LiCH_2PPh_2$.[34] X-ray crystal structure analysis of this compound indicates that the phosphorous atom is not coordinated to zirconium and that the Zr-C-P angle is 130°. The structure of 12 is probably quite similar to that observed for $Cp_2Zr(Cl)CH_2PPh_2$. Any limited stability gained by coordinating the phosphorous atom to the zirconium would be negated by unfavorable bond distortions in forming a metallacycle-like product.

3.2.9 Mechanism of the Formation of $Cp^*_2\overline{Zr(H)CH_2PMe_2CH_2}$ (11)

A possible mechanism of the formation of 11 from $Cp^*_2Zr(H)Cl$ (8) and CH_2PMe_3 is outlined in Scheme 3.3. The first step involves formation of an ylide-hydridochloride intermediate 9 analogous to intermediate 2 in Schemes 3.1 and 3.2. A second equivalent of ylide then deprotonates the coordinated $-CH_2PMe_3$ ligand and by loss of Cl^- forms PMe_4Cl and the metallated-ylide-hydride complex 10 which rearranges to the product 11.

The mechanism of the formation of 11 from $Cp^*_2ZrH_2$ (6) and CH_2PMe_3 is more complicated, however. It is clear from Toepler pump measurements, that for each equivalent of 11 formed, one equivalent of methane is also produced. One could envision that CH_2PMe_3 promotes the reductive elimination of CH_4 from $Cp^*_2Zr(H)CH_3$ and that the resulting Zr(II) species then inserts into a C-H bond of a methyl group on phosphorous. Schwartz has prepared the Cp analogue of 11 by this method. $Cp_2Zr(H)CH_2\overline{CH(CH_2)_4CH_2}$ reacts with CH_2PMe_3 to afford $Cp_2\overline{Zr(H)CH_2PMe_2CH_2}$ and methylcyclohexane (eq. 12).[17] The reaction of the corresponding dideuterated compound,

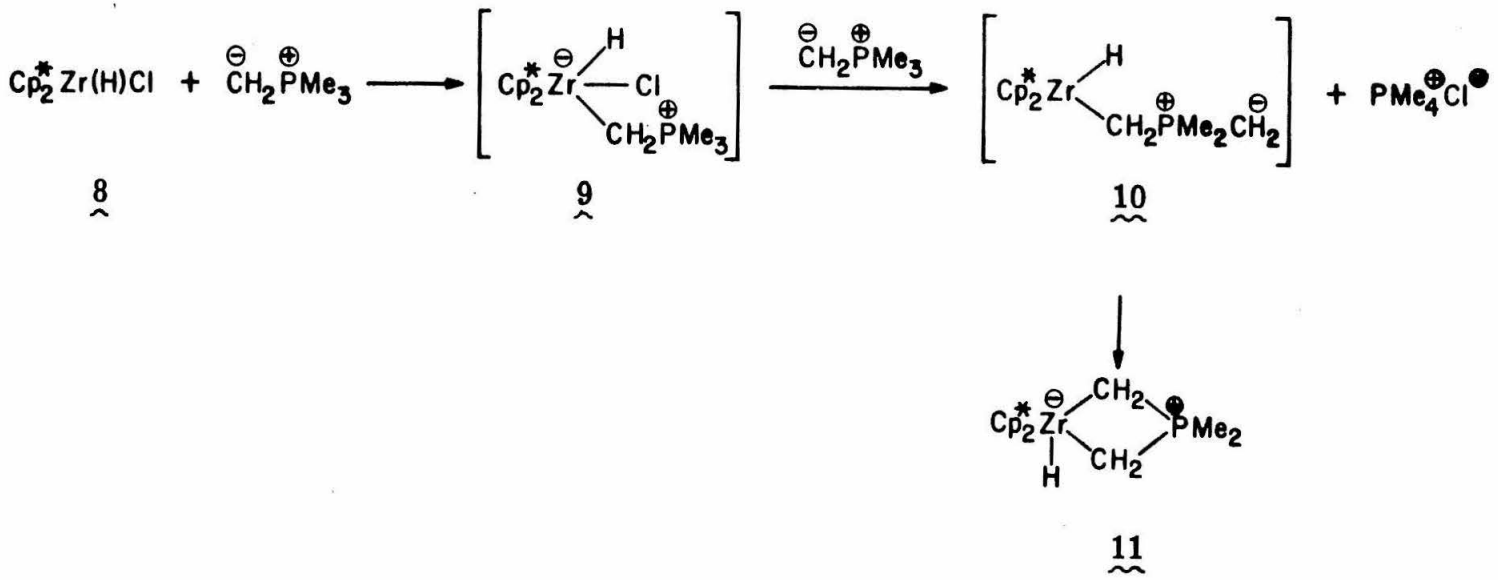

8 9 10 11

SCHEME 3.3. Mechanism for the Formation of $Cp^*_2\overline{Zr(H)CH_2PMe_2CH_2}$ (11) from $Cp^*_2Zr(H)Cl$ (8) and CH_2PMe_3.

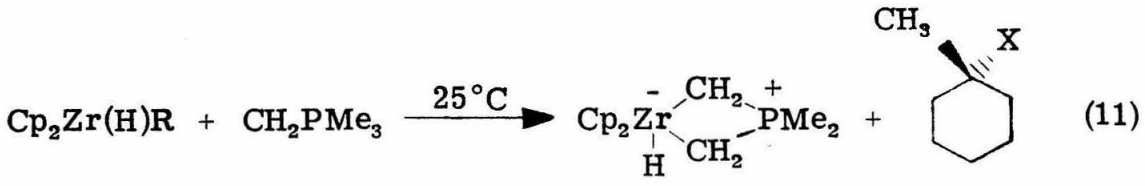

(11)

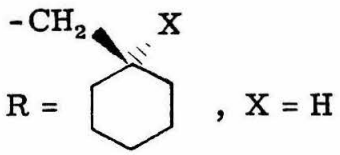

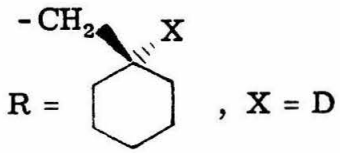

$CpZr(D)CH_2\overline{CD(CH_2)_4CH_2}$, with CH_2PMe_3 gave labeled methylcyclohexane and $Cp_2\overline{Zr(H)CH_2PMe_2CH_2}$ which was unlabeled (eq. 12). The specific deuterium incorporation observed in this reaction suggests that reductive elimination of alkane from the Zr(IV) starting material is a step in the mechanistic pathway. Such a process cannot be operative in the Cp* system, however. Treatment of $Cp^*_2Zr(H)Me$ (7) with CH_2PMe_3 does not afford 11, but rather gives the bis-inserted product $Cp^*_2ZrMe_2$ (13) (vide supra). A possible mechanism for the formation

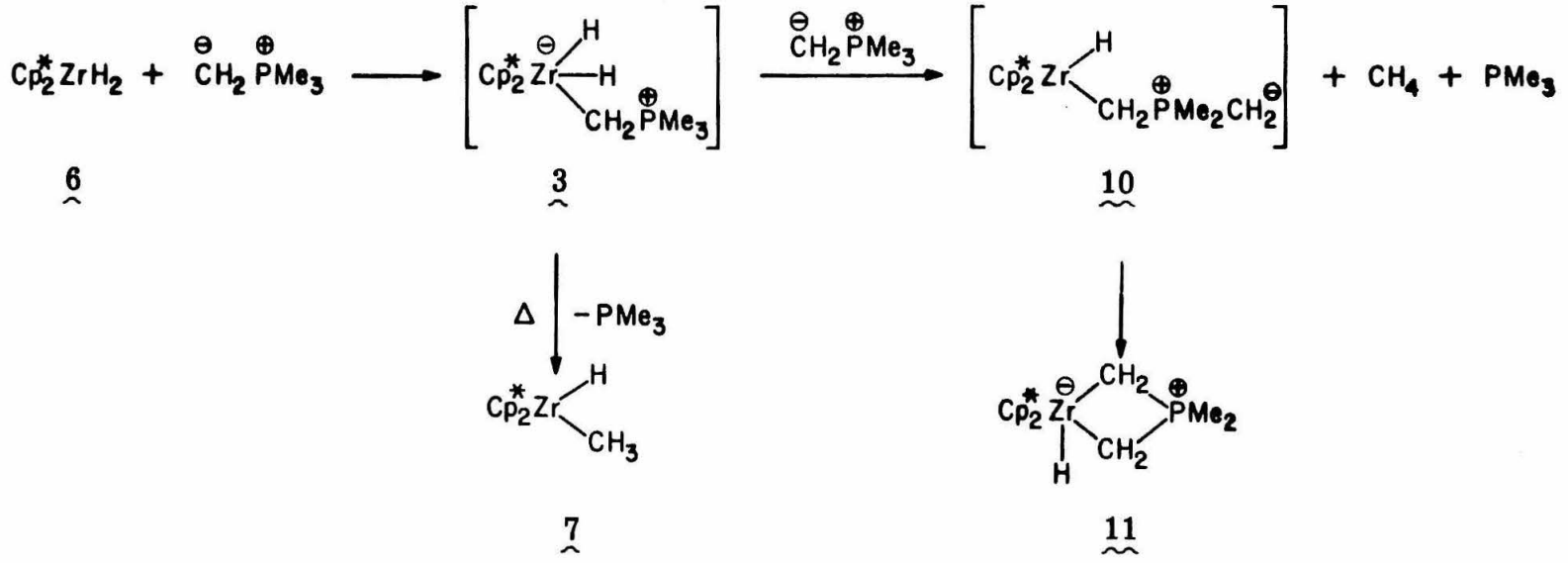

SCHEME 3.4. Mechanism for the Formation of $Cp^*_2\overline{Zr(H)CH_2PMe_2CH_2}$ (11) from $Cp^*_2ZrH_2$ (6) and CH_2PMe_3.

of 11 from $Cp^*_2ZrH_2$ (6) and CH_2PMe_3, analogous to that starting with $Cp^*_2Zr(H)Cl$ (8), is shown in Scheme 3.4. The ylide-dihydride intermediate 3 is the first intermediate formed and can proceed along either of two mechanistic pathways to afford two different products. Upon heating, 3 decomposes by a mechanism outlined in Scheme 1.1 or 1.2 to give the methyl-hydride complex, $Cp^*_2Zr(H)Me$ (7), and PMe_3. As was mentioned earlier, solutions of $Cp^*_2ZrH_2$ (6) and CH_2PMe_3 heated at 80°C afford a greater relative concentration of 7 (as compared to 11) than do solutions maintained at room temperature. If the ylide-dihydride intermediate 3 proceeds along the second mechanistic pathway, a second molecule of ylide deprotonates the coordinated $-CH_2PMe_3$ ligand to afford the ylide-hydride intermediate 10 and tetramethylphosphonium hydride. Complex 10 rearranges to the product 11 and PMe_4H immediately disproportionates to give CH_4 and PMe_3. Although a literature search failed to provide an example of hydride reduction of the tetramethylphosphonium cation (PMe_4^+) to give CH_4 and PMe_3, this does appear to be a viable reaction. Treatment of PMe_4Cl with one equivalent of $Cp^*_2ZrH_2$ (6) affords $Cp^*_2\overline{Zr(H)CH_2PMe_2CH_2}$ (11) (36%) and $Cp^*_2Zr(H)Cl$ (8) (64%) as the only zirconium containing products[36] and H_2 (38%) and CH_4 (62%) as the only noncondensable (-196° C) gas products.[21] The ^1H NMR spectrum of this mixture also indicates the presence of free PMe_3 and, presumably, HCl is also present. Thus, permethylzirconocene hydride complexes are capable of reducing the tetramethylphosphonium cation to methane and trimethylphosphine. The mechanism presented in Scheme 3.4 is still more complicated,

however. Treatment of $(\eta^5\text{-}C_5(CD_3)_5)_2ZrD_2$ with CH_2PMe_3 affords as gas products, CH_4, CH_3D, and CH_2D_2 in approximately equal concentrations.[37] Although the formation of CH_4 and CH_3D can be accounted for by the mechanism outlined in Scheme 3.4, the formation of CH_2D_2 cannot. The mechanism by which deuterium atoms scramble in this reaction is not known.

3.2.10 Synthesis and Characterization of (O-ℓ)-$Cp^*_2Zr(COCHPMe_3)H$ (15)[39]

Although the metallated-ylide complex 11 is unreactive towards H_2 and ethylene, 11 does react with CO at 0° C to afford the η^2-acyl-hydride complex 15 quantitatively by ^1H NMR spectroscopy (eq. 13).

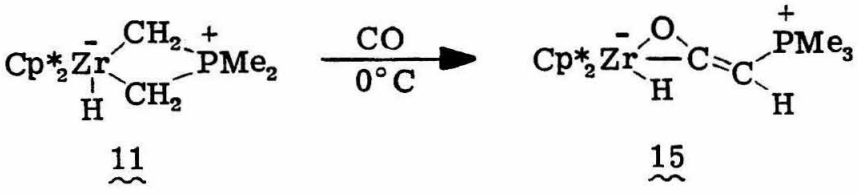

11 15 (13)

Complex 15 may be isolated as a purple-white solid in 61% yield be recrystallization from petroleum ether. The ^1H NMR spectrum of 15 displays a broad singlet at δ 3.50 assigned to the hydride ligand resonance and a doublet ($^2J_{PH}$ = 43 Hz) at δ 3.90 assigned to the olefinic proton resonance. The presence of the acyl ligand is verified by a low field carbon resonance observed as a doublet ($^2J_{PC}$ = 17.1 Hz) at δ 250.32 in the $^{13}C\{^1H\}$ NMR spectrum and by a CO stretching frequency of 1427 cm^{-1} ($\nu(^{13}CO)$ 1390 cm^{-1}, calcd 1397) observed in

the IR spectrum. The CO stretching frequency observed for 15 is the lowest yet reported for an early transition metal η^2-acyl complex. Typical values range from 1470-1625 cm^{-1}.[38] Because of this unusually low CO stretching frequency and because of the ambiguity in coordination around the zirconium, the crystal structure of 15 was undertaken.

3.2.11 Crystal Structure of (O-ℓ)-$Cp^*_2Zr(COCHPMe_3)H \cdot \frac{1}{2}C_7H_8$ (15)[39]

The structure of (O-ℓ)-$Cp^*_2Zr(COCHPMe_3)H$ (15)[39] was confirmed by X-ray diffraction methods. Blue-white crystals of 15 grown from toluene are monoclinic, crystallizing in the space group $P2_1/n$ with four molecules per unit cell. The pertinent crystal data are presented in Table 3.2. Crystals of 15 were found to decompose over a period of several days upon exposure to X-rays, and so the data were collected rapidly. 2838 independent measurements were taken with $3 < 2\theta < 30°$ (+h, ±k, ±ℓ). Using anisotropic Gaussian amplitudes for all nonhydrogen atoms, the least squares refinement gave R = 0.086 (with 847 $F_o^2 > 3\sigma_{F^2}$) and a goodness-of-fit of 4.25.

The molecular structure of (O-ℓ)-$Cp^*_2Zr(COCHPMe_3)H$ (15) is presented in Figure 3.3, and a skeletal view of the immediate ligation about zirconium with relevant bond distances and bond angles is given in Figure 3.4. Although the hydride ligand was not located, the lateral displacement of the Zr-C(1)-C(2)-P moiety from the R_1-Zr-R_2 plane (~1.7 Å) indicates that the oxygen atom occupies the central equatorial coordination position. The PMe_3 group is Z relative to the -$OZrCp^*_2$ moiety and the Zr, O, C(1), C(2), and P atoms are coplanar.

TABLE 3.2. Crystal Data for (O-ℓ)-$Cp^*_2Zr(COCHPMe_3)H \cdot \frac{1}{2}C_7H_8$ (15).

Formula	$C_{25}H_{41}OPZr \cdot \frac{1}{2}C_7H_8$
Formula Weight	527.89
Space Group	$P2_1/n$
a	15.125(3) Å
b	10.646(4) Å
c	18.306(4) Å
β	90.168(25)°
V	2948(1) $Å^3$
Z	4
ρ_{calcd}	1.19 g/cm^3
Crystal Size	0.25 × 0.30 × 0.60 mm

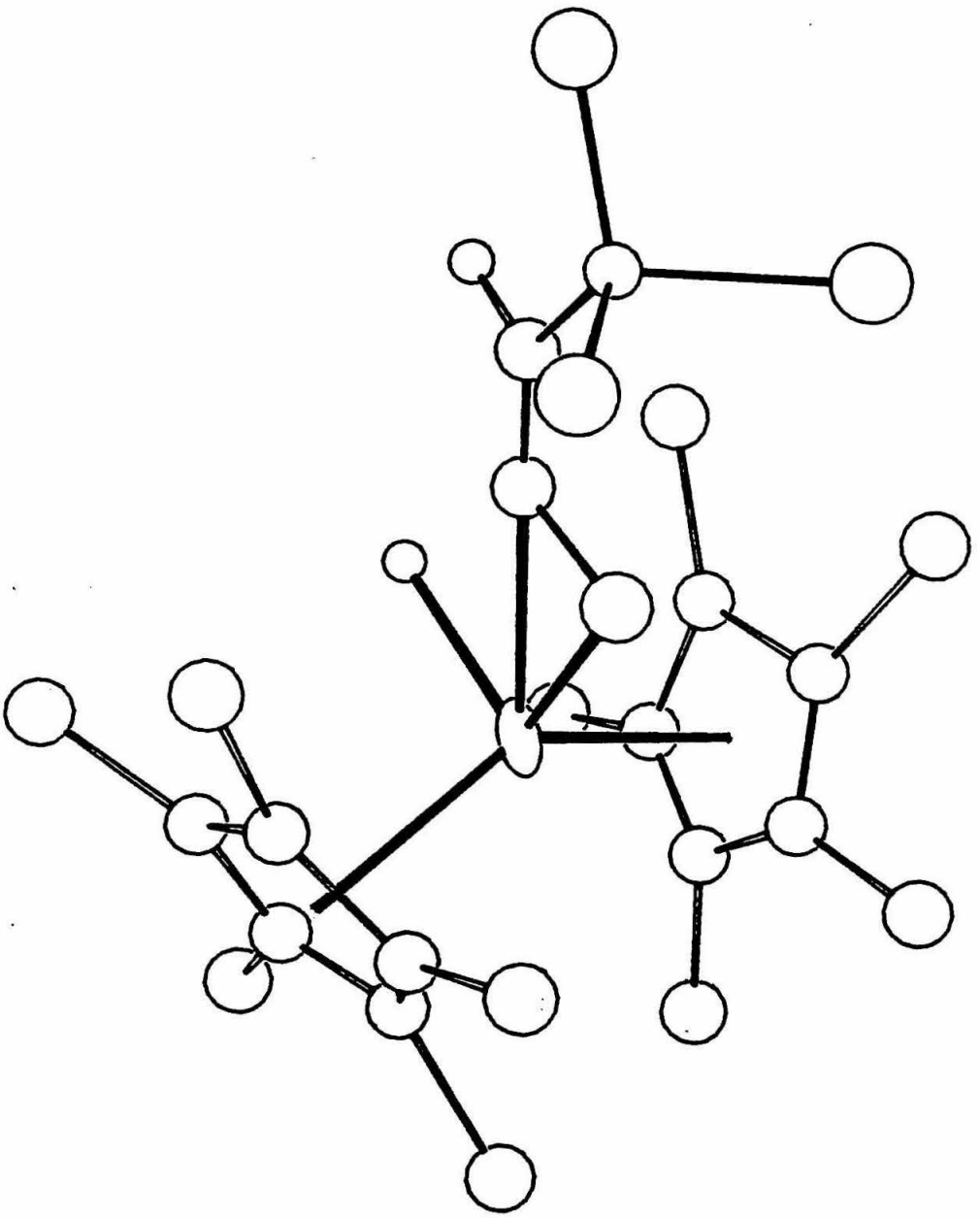

FIGURE 3.3. Molecular Configuration of (O-ℓ)-$Cp^*_2Zr(COCHPMe_3)H$ (15).

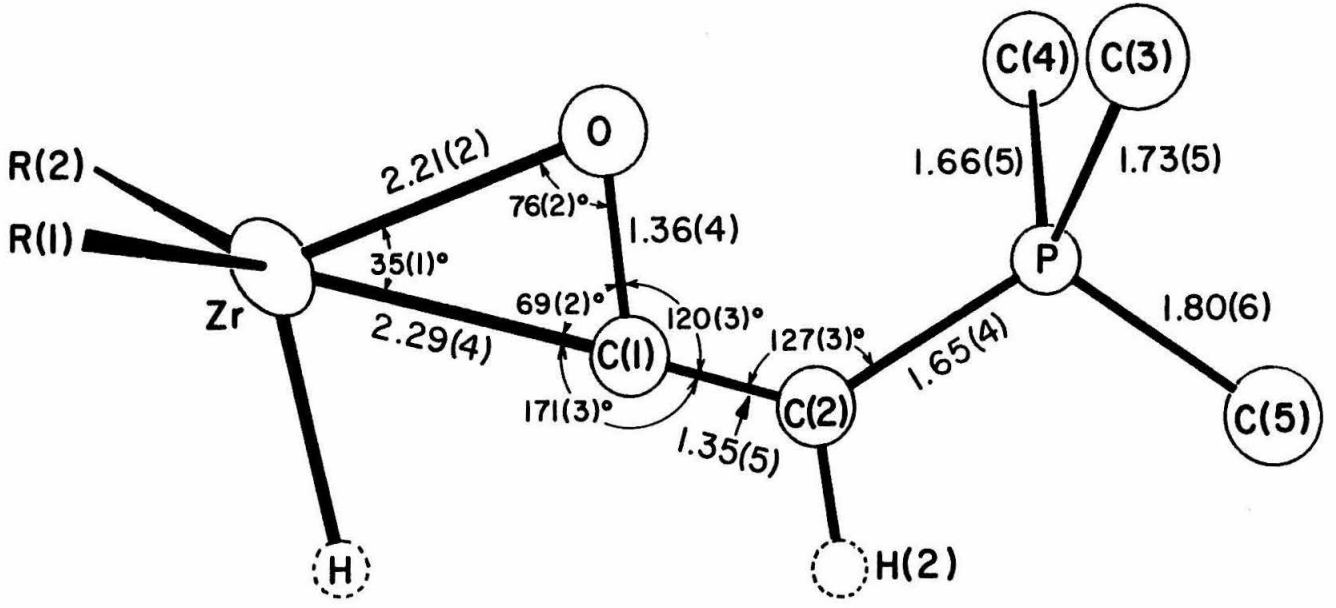

FIGURE 3.4. Skeletal View of (O-ℓ)-$Cp^*_2Zr(COCHPMe_3)H$ (15). [a]

[a]Bond distances are in Å. The H and H(2) hydrogens were not located.

It is unfortunate that because of crystal decomposition, the data obtained from the crystal structure of 15 are not precise enough to make valid comparisons with the structural data reported for other η^2-acyl complexes. However, the structural data are sufficient to confirm that the oxygen atom of the η^2-acyl ligand occupies the central equatorial coordination site of the zirconium between the hydride ligand and carbon atom, unlike that observed for other η^2-acyl compounds in which the oxygen atom occupies a lateral equatorial coordination position.[5b, 27] The crystal structure of the thorium η^2-acyl complex $Cp^*_2Th(COCHCMe_3)Cl$ is the only example which exhibits the same type of atom arrangement around the metal center.[40]

3.2.12 Synthesis and characterization of (O-c)-$Cp^*_2Zr(COCHPMe_3)H$ (16)

If solutions of 15 are allowed to warm to room temperature, a second η^2-acyl complex (16) is formed which is found to be in equilibrium with 15 ($K_{eq25°C}$ = 1.58) (eq. 14). Complex 16 may be obtained

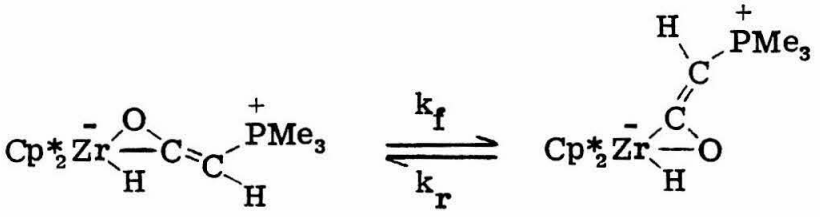

15 $\rightleftharpoons$ 16 (14)

$K_{eq25°C} = k_f/k_r = 1.58$

by heating solutions of 15 at 80°C for 24 hours. The spectral data of 16 are similar to that of 15 except for the lower field shift of the

hydride ligand resonance in the ^1H NMR spectrum (δ 4.30) and a slightly higher field shift of the acyl doublet in the $^{13}C\{^1H\}$ spectrum (δ 247.08, $^2J_{PC}$ = 13.67 Hz). Analogous to 15, complex 16 also exhibits a very low CO stretching frequency of 1417 cm^{-1} (ν (^{13}CO) 1380 cm^{-1}, calcd 1370) in the IR spectrum.

3.2.13 Crystal Structure of (O-c)-$Cp^*_2Zr(COCHPMe_3)H$ (16).[39]

The structure of (O-c)-$Cp^*_2Zr(COCHPMe_3)H$ (16)[39] was confirmed by X-ray diffraction methods. Colorless crystals of 16 grown from toluene are monoclinic, crystallizing in the space group $P2_1/c$ with four molecules per unit cell. The pertinent crystal data are presented in Table 3.3. 4800 independent measurements were taken with $3° < 2\theta < 51°$ ($\pm h, \pm k, -\ell$). Using anisotropic Gaussian amplitudes for all nonhydrogen atoms, the least squares refinment gave R = 0.029 (3486 $F_o^2 > \sigma_{F^2}$) with a goodness-of-fit of 1.48.

The molecular structure of (O-c)-$Cp^*_2Zr(COCHPMe_3)H$ (16)[39] is presented in Figure 3.5 and a skeletal view of the immediate ligation about ziconium with relevant bond distances and bond angles is given in Figure 3.6. In contrast to the structure of 15, the η^2-acyl oxygen atom of 16 occupies the central equatorial position. Similar to the structure of 15, the PMe_3 group is Z relative to the -$OZrCp^*_2$ fragment about the olefinic bond and the H, Zr, O, C(1), C(2), H and P atoms are essentially coplanar.

The structure of 16 is very similar to that reported for the uranium η^2-acyl complex $Cp_3U(COCHPMePh_2)$ (17).[42] The C-O bond distances observed for 16 (1.303(3) Å) and 17 (1.27(3) Å) are shorter

TABLE 3.3. Crystal Data for (O-c)-$Cp^*_2Zr(COCHPMe_3)H$ (16).

Formula	$C_{25}H_{41}OPZr$
Formula Weight	479.79
Space Group	$P2_1/c$
a	9.9362(12) Å
b	10.0229(12) Å
c	25.9367(29) Å
β	96.292(10)°
V	2567.5(9) $Å^3$
Z	4

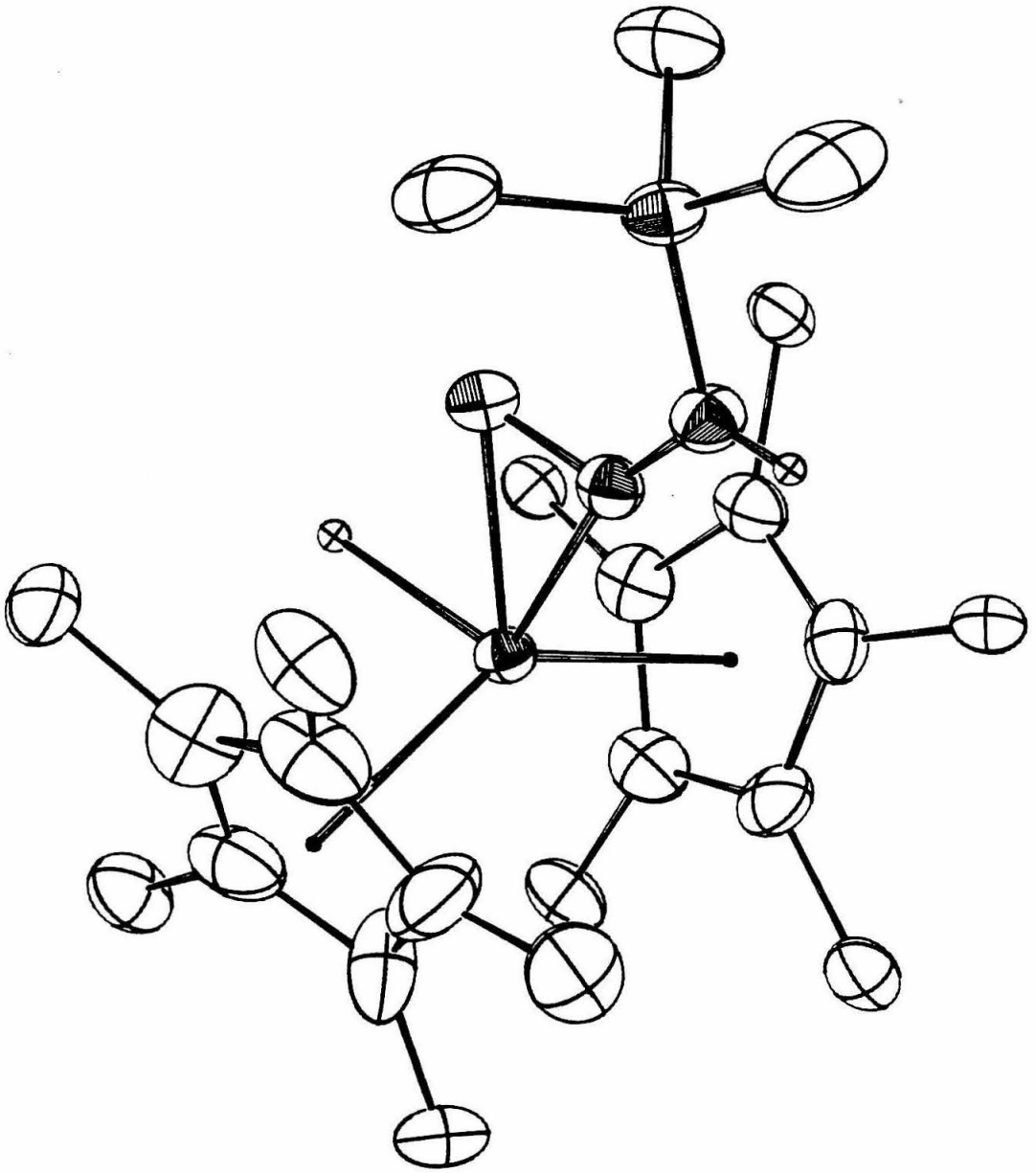

FIGURE 3.5. Molecular Configuration of (O-c)-$Cp^*_2Zr(COCHPMe_3)H$ (16).

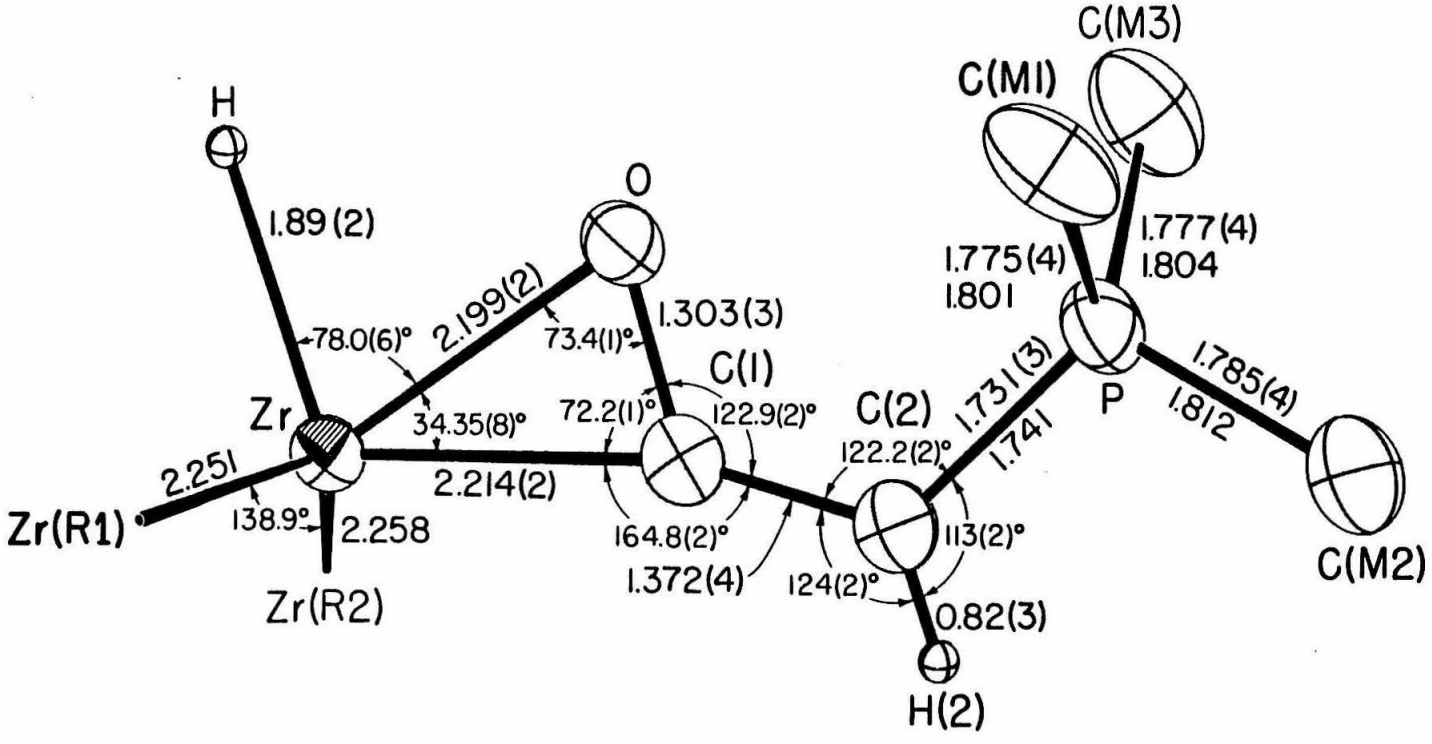

FIGURE 3. 6. Skeletal View of (O-c)-$Cp^*_2Zr(COCHPMe_3)H$ (16). [a]

[a]Bond distances are in Å.

than that expected for a C-O single bond (1.43),[29] yet longer than that reported for the zirconium η^2-acyl compound $Cp_2Zr(COMe)Me$ (1.211(8) Å), explaining why the CO stretching frequency of this compound (1540 cm^{-1}) is much higher than that of 16 (1417 cm^{-1}). The C(1)-C(2) bond distance of 1.372(4) Å observed for 16 is identical to the C(1)-C(2) bond distance of 1.37(3) observed for 17 and is typical of a C=C double bond. Although the P-C(2) bond distance in 17 (1.77(2)) is typical for a P-C single bond, the P-C(2) bond distance in 16 is considerably shorter (1.731(3) Å), implying some P=C double bond character. Thus, the structure of 16 is best represented as a composite of the canonical forms A, B, and C (Figure 3.7) in which electron density is distributed along the O-C(1)-C(2)-P backbone.

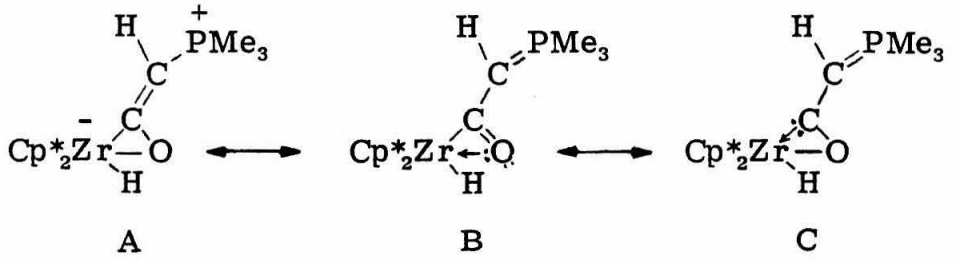

FIGURE 3.7. (O-c)-$Cp^*_2Zr(COCHPMe_3)H$ (16) Resonance Structures.

The structure of the zirconium η^2-C,O ketene complex $Cp^*_2Zr(COCH_2) \cdot pyr$ (18) is also quite similar to that of 16.[5b] The C(1)-C(2) bond distance in 18 (1.333(3) Å) is somewhat shorter than that in 16, but the C-O distance (1.338(2) Å) is longer. This implies little electron delocalization from the C=C double bond into the C-O

single bond, in contrast to the electron delocalization observed for 16. The Zr-H bond distance of 1.89(2) Å compares with that observed for $Cp^*_2\overline{Zr(H)CH_2PMe_2CH_2}$ (11) (1.88(4) Å) and also that observed for $Cp^*_2Hf(\eta^3\text{-}C_3H_5)H$ (1.86(7) Å).[32]

3.2.14 Kinetic-Thermodynamic η^2-Acyl Isomerization

The spatial arrangement of the coordination group about zirconium in 16 (vide supra) contrasts with that of 15 in that the η^2-acyl oxygen atom in 16 occupies the central equatorial coordination site. The reaction of 11 with CO proceeds by the stereoselective formation of the kinetic η^2-acyl isomer 15 (oxygen-lateral), which then isomerizes to the thermodynamic η^2-acyl isomer 16 (oxygen-central). Isomerizations of this type have been observed spectroscopically by Erker in the reaction of Cp_2ZrR_2 (R = Me, Ph) with CO (eqs. 15 and 16).[38c,41] Erker proposed that CO insertion into metal-carbon bonds of the early transition metals affords an intermediate η^2-acyl

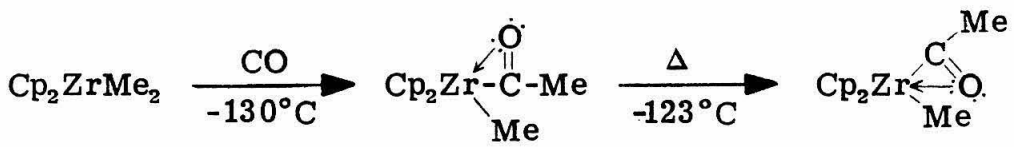

(15)

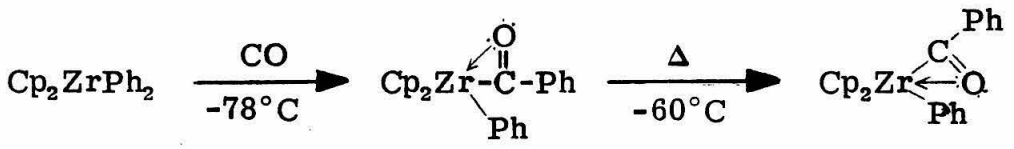

(16)

species in which the oxygen atom occupies a lateral coordination position. This intermediate then isomerizes rapidly at higher temperatures to afford the η^2-acyl product in which the oxygen atom occupies the central coordination position. The thermodynamic stability of other oxygen-central η^2-acyl complexes is evident by the fact that nearly all crystal structures of η^2-acyl complexes exhibit this type of oxygen-central coordination.[5b, 27] As mentioned previously, the one exception is the crystal structure of the oxygen-lateral thorium η^2-acyl complex $Cp^*_2Th(COCH_2CMe_3)Cl$.[40] However, this complex does not isomerize to the oxygen-central isomer when heated, but rather affords a cis-enolate-chloride compound (eq. 17). The isomerization of 15 to 16 is the first example of a system in which both kinetic and thermodynamic η^2-acyl isomers have been isolated and structurally characterized.

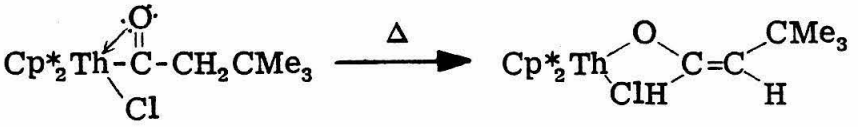

(17)

A proposed mechanism for the formation of the η^2-acyl complexes 15 and 16 from 11 and CO is depicted in Scheme 3.5. Carbon monoxide promotes the reductive elimination of an alkyl ligand from 11 to give a carbonyl intermediate which is represented as a methylenetrimethylphosphorane adduct of Zr(II). The coordinated CO then

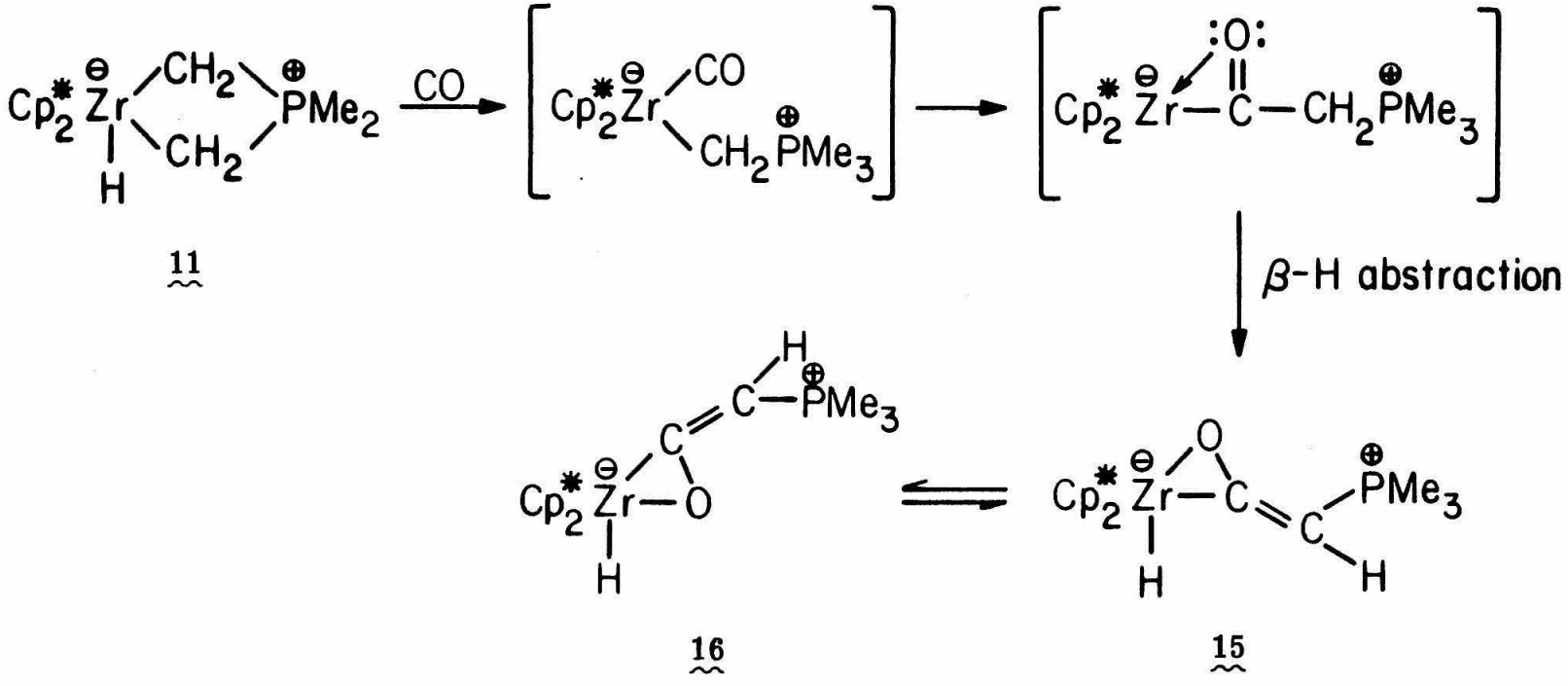

11

16

15

SCHEME 3.5. Mechanism for the Formation of (O-ℓ)-$Cp^*_2Zr(COCHPMe_3)H$ (15) and (O-c)-$Cp^*_2Zr(COCHPMe_3)H$ (16).

inserts into the Zr-C bond to afford an η^1-acyl intermediate. β-H abstraction affords the kinetic (oxygen-lateral) η^2-acyl complex 15 which above 0° C is in equilibrium with its thermodynamic (oxygen-central) η^2-acyl isomer 16.

3.2.15 Kinetics of the (O-ℓ)-$Cp^*_2Zr(COCHPMe_3)H$ (15) ⇌ (O-c)-$Cp^*_2Zr(COCHPMe_3)H$ (16) Isomerization

The equilibrium isomerization of 15 to 16 occurs relatively slowly at room temperature over the course of several hours. Thus, the kinetics of the approach of 15 to its equilibrium with 16 can be studied conveniently by monitoring the relative integrations of the PMe_3 proton resonance by ^1H NMR spectroscopy. First order rates for k_f were measured at five temperatures (Table 3.4) and the equilibrium rate expression plotted in Figure 3.8.[43] An Arrhenius plot

TABLE 3.4. Rate Constants for (O-ℓ)-$Cp^*_2Zr(COCHPMe_3)H$ (15) (O-c)-$Cp^*_2Zr(COCCHPMe_3)H$ (16) Isomerization.

Temperature (°C)	k_f ($\times 10^{-4}$ sec^{-1})	k_r ($\times 10^{-4}$ sec^{-1})
24	0.16(1)	0.10(1)
41	1.6(1)	0.93(7)
48	3.4(3)	2.3(2)
56	8.1(6)	5.8(5)
63	14(1)	10(1)

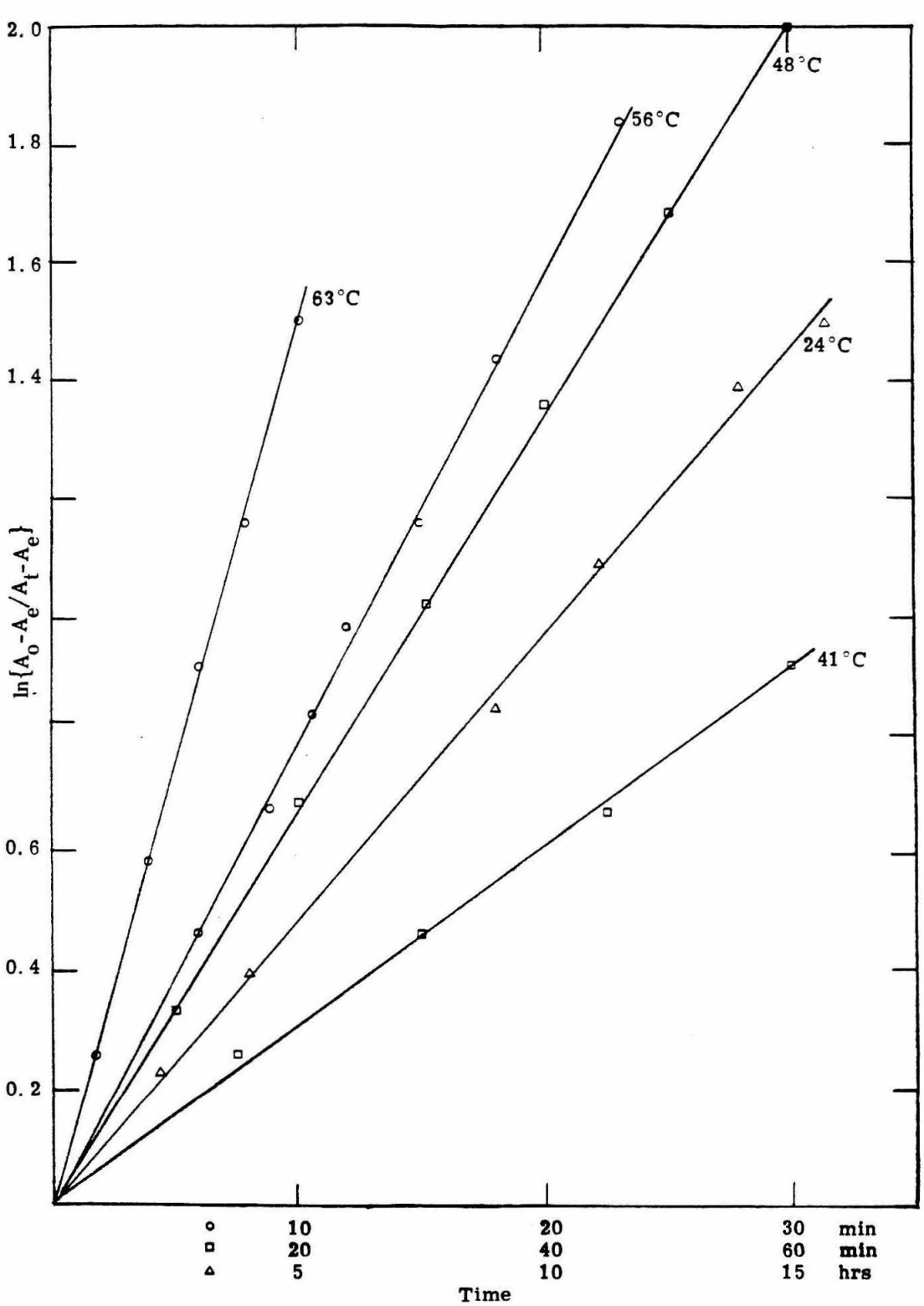

FIGURE 3.8. Plot of Equilibrium Rate Expression vs. Time for the (O-ℓ)-$Cp^*_2Zr(COCHPMe_3)H$ (15) ⇌ (O-c)-$Cp^*_2Zr(COCHPMe_3)H$ (16) Isomerization.[a]

[a] A_o = [A] at t = 0, A_t = [A] at time t, A_e = [A] at equilibrium.

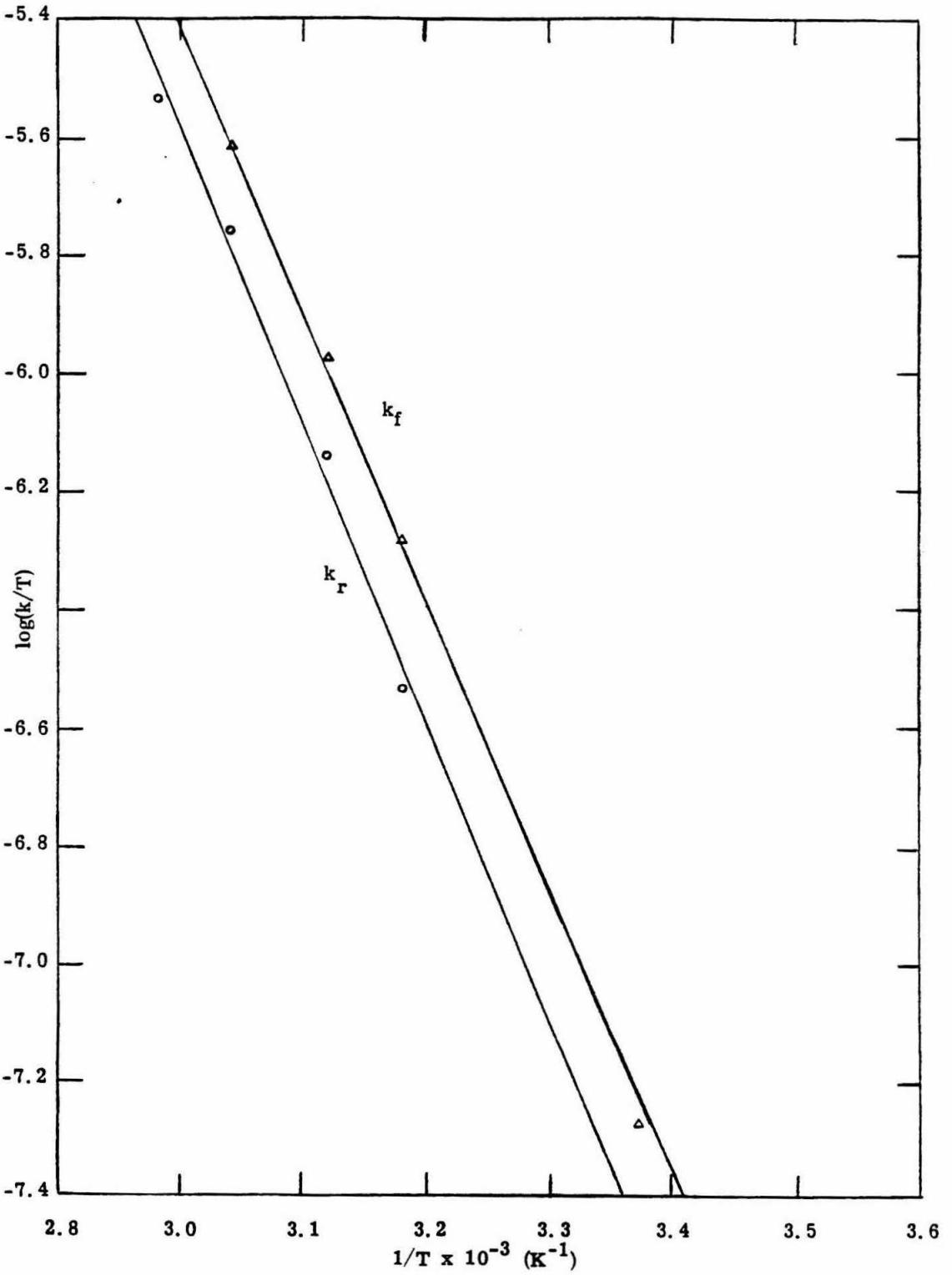

FIGURE 3.9. Arrhenius Plots for the (O-ℓ)-$Cp^*_2Zr(COCHPMe_3)H$ (15) ⇌ (O-c)-$Cp^*_2Zr(COCHPMe_3)H$ (16) Isomerization.

at five temperatures (Figure 3.9) gives an estimate for the activation parameters for k_f as $\Delta H^{\ddagger} = 22.4 \pm 1.8$ kcal/mol and $\Delta S^{\ddagger} = -4.1 \pm 2.5$ eu and for k_r as $\Delta H^{\ddagger} = 23.2 \pm 1.9$ kcal/mol and $\Delta S^{\ddagger} = -2.8 \pm 1.7$ eu. $\Delta S^{\ddagger}$ is not sufficiently negative to question the intramolecularity of this isomerization. The $\Delta H^{\ddagger}$ values give an upper limit to the Zr-O bond strengths in each of the two η^2-acyl isomers, neglecting other factors such as solvation energies and steric effects. Resonance stabilization may contribute in part to the relatively high activation enthalpy (22.4 kcal/mol) of the acyl isomerization (15 → 16). As evident from the resonance forms A, B, and C (Figure 3.7), the Zr-O bond strengths in 15 and 16 are intermediate between that of an η^2-acyl O → Zr dative bond and that of a full Zr-O covalent bond, as in $Cp^*_2Zr(H)OCH_3$. Steric effects may also contribute to the 15 → 16 activation enthalpy; whereas only a single isomer is observed for the η^2-acyl compounds $Cp^*_2Zr(COCH_3)Br$[5b] and $Cp^*_2Zr(COCH_2CH_3)$,[44] $Cp^*_2Zr(COCH_2CMe_3)Cl$[44] exists in two forms, presumably the kinetic (oxygen lateral) and thermodynamic (oxygen central) η^2-acyl isomers.

3.3 Conclusion

The results of this chapter demonstrate that methylenetrimethylphosphorane is an effective methylene transfer reagent in the preparation of methyl-hydride complexes of permethylzirconocene and permethylhafnocene from dihydride precursors. The formation of the metallated-ylide complex, $Cp^*_2\overline{Zr(H)CH_2PMe_2CH_2}$ (11), is interesting, since the mechanism responsible for its formation differs from that of the regular Cp ring analogue, $Cp_2\overline{Zr(H)CH_2PMe_2CH_2}$. Reaction

of 11 with CO affords isolable kinetic and thermodynamic acyl isomers. The crystal structures of these complexes indicate that the oxygen atom occupies a lateral equatorial coordination position in the kinetic isomer while in the thermodynamic isomer, the oxygen atom occupies the central position. The formation of the kinetic acyl isomer followed by its equilibrium-isomerization to the thermodynamic isomer establishes a mechanism for CO insertion into metal-carbon bonds of the early transition metals. The kinetics of the approach to the acyl equilibrium provides an upper limit to the Zr-O bond strength of ca. 22-23 kcal/mol.

3.4 Experimental Section

3.4.1 General Methods

All manipulations were carried-out using either high-vacuum line or inert atmosphere glove box techniques. Argon, hydrogen, and deuterium were passed through MnO on vermiculite and 4 Å molecular sieves.

3.4.2 Physical and Spectroscopic Methods

^{1}H NMR spectra were recorded with a Varian EM390, JEOL FX90Q, or Bruker WM500 spectrometer. Chemical shifts are reported in ppm(δ) relative to Me_4Si (δ 0.0). Carbon magnetic resonance spectra were recorded on a JFOL FX90Q spectrometer chemical shifts are reported in ppm (δ) relative to Me_4Si (δ 0.0). Phosphorous magnetic resonance spectra were recorded on a JEOL FX90Q spectrometer. Chemical shifts are reported in ppm (δ) relative to external H_3PO_4 (δ 0.0). Infrared spectra were recorded using

NaCl plates on a Beckman 4240 spectrometer.

Elemental analyses were performed by the Alfred Bernhardt Analytical Laboratories. Molecular weight analyses were determined by isothermal distillation using the Signer method.[45]

3.4.3 Solvents and Reagents

Solvents were purified by vacuum transfer first from $LiAlH_4$ and then from "titanocene."[46] Benzene-d_6 (Stohler, Inc.) was also purified by vacuum transfer from titanocene. THF-d_8 (Stohler, Inc.) was distilled from sodium benzophenone ketyl. Methyl iodide was distilled from CaH_2. Carbon monoxide (Matheson) was used directly from the cylinder.

The following compounds were prepared by the reported procedures: $Cp^*_2HfH_2$,[47] $Cp^*_2ZrH_2$,[48] $[\eta^5\text{-}C_5(CD_3)_5]_2ZrD_2$,[49] $Cp^*_2Zr(H)Cl$,[50] CH_2PMe_3.[51]

3.4.4 $Cp^*_2Hf(H)Me$ (4)

$Cp^*_2HfH_2$(1) (300 mg, 0.67 mmol) was dissolved in toluene (12 mL) at room temperature. CH_2PMe_3 (70 μL, 0.78 mmol) was added to the solution via syringe and the mixture stirred at 80°C for 1.5 hours. The yellow solution was cooled to room temperature and the solvent removed in vacuo. The yellow-white residue was dissolved in pet. ether (5 mL) and the solution cooled to -78°C for 10 minutes. A white solid precipitated which was isolated by filtration at -78°C. The product 4 was obtained as a fine white powder (90 mg, 30%). Anal. Calcd for $C_{21}H_{34}Hf$: C, 54.20; H, 7.37; Hf, 38.38. Found: C, 54.07; H, 7.26; Hf, 38.21. ^1H NMR (benzene-d_6): δ 116.6 (s,

$\underline{C}_5(CH_3)_5$); 50.99 (q, $^1J_{CH}$ = 86 Hz, Hf-CH_3); 11.74 (q, $^1J_{CH}$ = 126 Hz, $C_5(\underline{C}H_3)_5$). IR (nujol) ν(Hf-H) 1600 cm^{-1}.

3.4.5 $Cp^*_2Hf(I)Me$ (5)

$Cp^*_2Hf(H)Me$ (4) (30 mg, 0.064 mmol) was dissolved in toluene (5 mL) and the solution frozen at -196°C. CH_3I (0.18 mmol) was added by vacuum transfer and the mixture warmed to room temperature and stirred for 12 hours. Toepler pump analysis of the gas product indicated 0.059 mmol CH_4 (0.93 mol CH_4/mol 4). Removal of solvent in vacuo afforded 5 as an off-white solid.

3.4.6 Reaction of $Cp^*_2ZrH_2$ (6) with CH_2PMe_3 to give $Cp^*_2Zr(H)Me$ (7) and $Cp^*_2\overline{Zr(H)CH_2PMe_2CH_2}$ (11)

$Cp^*_2ZrH_2$ (6) (30 mg, 0.082 mmol) was dissolved in C_6D_6 (0.4 mL) in an NMR tube. The solution was degassed on a vacuum line and frozen at -78°C. Under argon counterflow via syringe was added CH_2PMe_3 (20 μL, 0.22 mmol) and likewise frozen. The tube was evacuated, sealed with a torch, and then allowed to warm to room temperature and the solution sloshed for 12 hours. The color of the solution turned from blue to yellow upon warming. The ^1H NMR spectrum of this solution indicates 11 (29%, 0.024 mmol) and 7 (71%, 0.058 mmol) identified by comparison with the ^1H NMR spectra of authentic samples (vide infra). The tube was broken open and Toepler pump analysis of the gas product indicated 0.023 mmol CH_4 (0.28 mol CH_4/mol 6 or 0.97 mol CH_4/mol 11).

3.4.7 Reaction of $Cp^*_2ZrH_2$ (6) with PMe_4Cl

$Cp^*_2ZrH_2$ (6) (25 mg, 0.68 mmol) and PMe_4Cl (8 mg, 0.7 mmol) were placed in an NMR tube. C_6D_6 (0.4 mL) was added to the tube at -78° C by vacuum transfer and the tube then sealed under vacuum with a torch. The mixture was allowed to warm to room temperature and sloshed for 12 hours. The ^1H NMR spectrum of this solution indicates $Cp^*_2\overline{Zr(H)CH_2PMe_2CH_2}$ (11) (36%) and $Cp^*_2Zr(H)Cl$ (8) (64%) as the only zirconium containing products and PMe_3, identified by comparison with the ^1H NMR spectra of authentic samples (vide supra). The tube was broken open and Toepler pump analysis of the noncondensible gases (-196° C) indicated H_2 (38%) and CH_4 (62%).

3.4.8 Reaction of $[\eta^5\text{-}C_5(CD_3)_5]_2ZrD_2$ with CH_2PMe_3

The procedure described in Section 3.4.4 was followed using 20 mg (0.055 mmol) $[\eta^5\text{-}C_5(CD_3)_5]_2ZrD_2$ and 10 μL (0.11 mmol) CH_2PMe_3. After 12 hours at room temperature, the tube was broken open and the gas product transferred via Toepler pump into another NMR tube containing 0.4 mL C_6D_6. The ^1H NMR spectrum (500 MHz) of this solution indicates CH_4, CH_3D, and CH_2D_2 in approximately equal concentrations.

3.4.9 $Cp^*_2Zr(H)Me$ (7)

$Cp^*_2ZrH_2$ (300 mg, 0.82 mmol) was dissolved in toluene (12 ml) and the solution heated to 80° C. CH_2PMe_3 (180 μL, 2.0 mmol) was added to the solution via syringe and the mixture stirred for 30 minutes at this temperature. The color of the solution turned from blue to yellow upon addition of the ylide. The solvent was removed in vacuo to give a white-yellow waxy solid which was redissolved in pet. *ether* (5 mL). The solution was cooled to -78° C and a white solid

precipitated which was isolated by filtration at -78° C to afford 7 as a white powder (95 mg, 31%). Anal. Calcd for $C_{21}H_{33}Zr$: C, 66.78; H, 9.07; Zr, 24.15. Found: C, 66.57; H, 8.90; Zr, 24.22. ^1H NMR (benzene-d_6): δ6.15 (s, 1H, ZrH); 1.86 (s, 30H, $C_5(CH_3)_5$); -0.43 (s, 3H, $ZrCH_3$). $^{13}C\{^1H\}$ NMR (benzene-d_6): δ 117.4 (s, $\underline{C}_5(CH_3)_5$); 44.90 (s, $ZrCH_3$); 11.83 (s, $C_5(\underline{C}H_3)_5$). IR (nujol): ν(Zr-H) 1550 cm^{-1}.

3.4.10 $Cp^*_2Zr(I)Me$ (14)

The procedure described in Section 3.4.5 was followed using 30 mg (0.079 mmol) $Cp^*_2Zr(H)Me$ (7) and 0.16 mmol CH_3I in 6 mL toluene. Toepler pump analysis of the gas product indicated 0.068 mmol CH_4 (0.9 mol CH_4/mol 7). Removal of solvent in vacuo afforded 14 as a yellow solid. ^1H NMR (benzene-d_6): δ 1.83 (s, 30H, $C_5(CH_3)_5$); -0.40 (s, 3H, $ZrCH_3$).

3.4.11 Reaction of $Cp^*_2Zr(H)Me$ (7) with CH_2PMe_3 to give $Cp^*_2ZrMe_2$ (13).

$Cp^*_2Zr(H)Me$ (7) (20 mg, 0.051 mmol), CH_2PMe_3 (11 μL, 0.12 mmol), and C_6D_6 (0.4 mL) were placed in an NMR tube. The solution was frozen at -196° C, the tube evacuated, and then sealed with a torch. The tube was warmed to room temperature and heated at 80°C for 2 days. The ^1H NMR spectrum of the solution indicates 13 (80%), identified by comparison of this spectrum with that of an authentic sample.

3.4.12 $Cp^*_2\overline{Zr(H)CH_2PMe_2CH_2}$ (11)

$Cp^*_2Zr(H)Cl$ (0.50 g, 1.25 mmol) was dissolved in toluene

(20 mL) and CH_2PMe_3 (330 μL, 3.8 mmol) added to the solution via syringe. The color of the solution turned from yellow to deep amber upon addition of the ylide and a fine white solid (PMe_4Cl) precipitated. The mixture was allowed to stir for 12 hours at room temperature. The suspension was then filtered (to remove the PMe_4Cl) and the solvent removed in vacuo to give a yellow-orange residue. The solid was triturated with pet. ether (8 mL), the mixture cooled to -78° C and then filtered at this temperature to afford 11 as an orange crystalline solid (417 mg, 73%). Anal. Calcd for $C_{24}H_{41}PZr$: C, 63.81; H, 9.15; P, 6.86; MW, 452. Found: C, 63.52; H, 8.89; P, 6.54; MW, 498. ^1H NMR (benzene-d_6); δ 4.40 (d, $^3J_{PH}$ = 46 Hz, 1H, ZrH); 1.93 (s, 30H, $C_5(CH_3)_5$); 1.03 (d, $^2J_{PH}$ = 12 Hz, 6H, $P(CH_3)_2$); -0.68 (dd, $^2J_{PH}$ = 5.1 Hz, $^3J_{HH}$ = 2.6 Hz, 2H, $ZrCH_2$); -0.90 (d, $^2J_{PH}$ = 12 Hz, 2H, $ZrCH_2$). $^{13}C\{^1H\}$ NMR (benzene-d_6): δ 111.9 (s, $\underline{C}_5(CH_3)_5$); 21.90 (d, $^1J_{PC}$ = 27 Hz, $P(CH_3)_2$); 12.70 (s, $C_5(C\underline{H}_3)_5$); -4.17 (d, $^1J_{PC}$ = 40 Hz, $ZrCH_2$); -5.70 (d, $^1J_{PC}$ = 41 Hz, $ZrCH_2$). $^{31}P\{^1H\}$ NMR (benzene-d_6): δ 29.82 (s, P).

3.4.13 Crystal structure of $Cp^*_2\overline{Zr(H)CH_2PMe_2CH_2}$ (11)

Orange crystals of $Cp^*_2\overline{Zr(H)CH_2PMe_2CH_2}$ (11) grown from toluene were mounted in glass capillaries under a nitrogen atmosphere. A series of oscillation and Weissenberg photographs established the crystals as monoclinic, and the systematic absences (OkO for k odd, hOℓ for ℓ odd) indicated the space group $P2_1/c$. Crystal data are summarized in Table 3.1. Lattice constants were obtained from the least-squares refinement[52] of fifteen 2θ values

($25 < 2\theta < 40°$); each reflection was centered at four diffractometer settings, ($\pm 2\theta$, $\pm\omega$, ϕ, χ) and ($\pm 2\theta$, $\pm \omega$, $\phi+\pi$, $-\chi$), and the 2θ values averaged.

A total of 12020 reflections were collected on a locally-modified Syntex $P2_1$ diffractometer and included blocks of four check reflections measured after each 96 reflections. No decomposition was observed and the data were reduced to F_o^2. Observational variances, $\sigma^2(F_o^2)$, were based on counting statistics with the additional term $(0.02 \times \text{scan counts})^2$.

The zirconium atom coordinates were derived from the Patterson map and the subsequent Fourier maps revealed the remaining atoms. Several cycles of full-matrix least-squares refinement[53] resulted in a structure with anomalously large U's for the ring carbon atoms. A difference Fourier map indicated disorder and attempts to model this disorder resulted in the 60:40 ratio of electron density for rings A and B using isotropic Gaussian amplitudes. Hydrogen atoms were introduced at idealized positions with the aid of ΔF maps. The coordinates and Gaussian amplitudes of all hydrogen atoms were fixed, except for the hydride atom H and those on the methylene carbon atoms. The final difference map indicated no peaks greater than $0.7\,e^-\,Å^{-3}$. Details concerning the data collection and the final cycle of refinement are given in Table 3.5. Atom coordinates and U_{ij}'s are given in Table 3.6. Final hydrogen atom coordinates and B's are given in Table 3.7. Bond distances and bond angles are given in Tables 3.8 and 3.9, respectively. Least-squares planes of the

TABLE 3.5. Data Collection and Refinement Conditions for $Cp^*_2\overline{Zr(H)CH_2PMe_2CH_2}$ (11).

λ	0.71069 Å (MoK_α, graphite monochromator)
Scan Method	θ-2θ
Scan Range	1.0° below K_{α_1}
	1.0° above K_{α_2}
2θ Scan Rate	2.02°/min
2θ Limits	4-55°
Scan Time/Bkgrd Time	0.5
Number of Reflections[a]	5540, 4990, 3456
R[b] ($F_o^2 > 0$)	0.077
R[b] ($F_o^2 > 3\sigma_{F_o^2}$)	0.052
Goodness-of-Fit[c]	2.20

[a]Total number of unique reflections, all reflections with $F_o^2 > 0$, all reflections with $F_o^2 > 3\sigma_{F_o^2}$.

[b]$R = \sum ||F_o| - |F_c|| / \sum |F_o|$.

[c]Goodness-of-fit = $\{\sum \omega [F_o^2 - (F_c/k)^2]^2/(n_{ref} - n_{par})\}^{\frac{1}{2}}$.

TABLE 3.6. Final Nonhydrogen Parameters for 11 (coordinates x 10^5, U_{ij} ($Å^2$) x 10^4, B ($Å^2$)).

	x	*y*	*z*	*B or* U_{11}	U_{22}	U_{33}	U_{12}	U_{13}	U_{23}
Zr	24448(3)	1964(3)	25064(3)	418(3)	411(3)	332(2)	−5(3)	−13(2)	27(3)
P	15154(10)	9229(11)	7223(7)	703(13)	698(12)	425(10)	6(10)	−73(9)	118(9)
C(1)	25503(39)	15164(48)	12453(29)	628(53)	685(53)	498(44)	−119(40)	−41(38)	104(37)
C(2)	11055(43)	−1063(63)	14307(33)	755(50)	692(64)	552(43)	−213(44)	−245(35)	165(40)
C(*M*1)	6357(49)	20593(56)	3946(48)	1189(88)	1183(82)	1769(113)	79(67)	−716(81)	321(74)
C(*M*2)	17317(54)	2428(74)	−2625(37)	1358(94)	2348(127)	844(72)	−507(91)	187(67)	−626(78)
C(11*A*)	2019(6)	785(6)	4022(4)	3.23(11)					
C(12*A*)	1205(5)	1156(6)	3501(4)	3.09(11)					
C(13*A*)	1510(5)	2125(7)	3004(4)	3.36(11)					
C(14*A*)	2511(7)	2348(6)	3197(5)	3.85(13)					
C(15*A*)	2825(5)	1539(8)	3845(5)	3.61(13)					
C(21*A*)	1951(6)	−127(8)	4732(5)	6.65(19)					
C(22*A*)	172(6)	734(7)	3544(5)	6.18(18)					
C(23*A*)	843(7)	2968(8)	2476(6)	6.73(20)					
C(24*A*)	3141(7)	3392(8)	2919(6)	6.75(20)					
C(25*A*)	3740(7)	1664(8)	4418(6)	7.29(22)					
C(11*B*)	1554(9)	651(10)	3784(7)	3.96(19)					
C(12*B*)	1184(9)	1502(11)	3187(7)	4.07(19)					
C(13*B*)	1925(10)	2328(9)	2991(7)	3.56(18)					
C(14*B*)	2754(7)	2019(10)	3479(7)	3.18(17)					
C(15*B*)	2541(9)	994(10)	3990(6)	3.21(17)					
C(21*B*)	1015(12)	−293(14)	4268(10)	9.17(40)					
C(22*B*)	104(12)	1508(14)	2921(10)	8.68(39)					
C(23*B*)	1723(11)	3478(12)	2517(9)	7.79(34)					
C(24*B*)	3694(13)	2704(14)	3553(10)	8.96(40)					
C(25*B*)	3129(11)	585(12)	4778(9)	7.60(34)					

TABLE 3. 6 (continued)

	x	*y*	*z*	*B*
C(31*A*)	3843(6)	−1094(7)	3259(4)	3.43(11)
C(32*A*)	4228(5)	−352(7)	2477(5)	4.00(12)
C(33*A*)	3807(6)	−801(7)	1697(5)	4.15(13)
C(34*A*)	3134(6)	−1749(7)	1873(5)	3.96(13)
C(35*A*)	3165(5)	−1911(6)	2760(5)	3.77(12)
C(41*A*)	4311(7)	−1203(8)	4002(6)	6.94(21)
C(42*A*)	5004(7)	559(8)	2572(6)	7.23(21)
C(43*A*)	4159(7)	−521(8)	844(6)	7.12(21)
C(44*A*)	2592(7)	−2620(8)	1278(6)	6.64(20)
C(45*A*)	2690(7)	−2927(7)	3244(6)	6.48(19)
C(31*B*)	4187(7)	−682(9)	2914(7)	3.25(16)
C(32*B*)	4198(8)	−365(10)	2051(7)	3.69(17)
C(33*B*)	3574(8)	−1214(9)	1623(7)	3.27(17)
C(34*B*)	3160(8)	−1976(9)	2200(7)	3.54(18)
C(35*B*)	3538(8)	−1634(10)	3002(7)	3.50(17)
C(41*B*)	4954(12)	−255(14)	3578(10)	8.99(39)
C(42*B*)	4897(11)	535(13)	1758(10)	8.23(37)
C(43*B*)	3559(11)	−1358(13)	682(9)	7.88(35)
C(44*B*)	2552(11)	−3048(13)	1958(10)	7.70(34)
C(45*B*)	3364(12)	−2362(13)	3765(10)	8.20(37)

TABLE 3. 7. Final Hydrogen Parameters for 11 (coordinates x 10^4, B ($Å^2$)).

	x	*y*	*z*	*B*
H	1564(29)	−1052(33)	2759(23)	6.25(99)
H(11)	2500(33)	2334(39)	1387(23)	3.96(95)
H(12)	3135(33)	1336(39)	986(27)	6.44(129)
H(21)	959(40)	−804(47)	1271(32)	7.99(171)
H(22)	594(48)	109(57)	1624(41)	11.35(246)
H(*M*11)	493	2501	804	900
H(*M*12)	116	1676	137	900
H(*M*13)	921	2541	−23	900
H(*M*21)	2004	−495	−176	900
H(*M*22)	2135	739	−545	900
H(*M*23)	1144	160	−570	900

TABLE 3.8. Bond Distances for 11 (Å).

	Ring A	Ring B		Ring A	Ring B
Zr-R(1)[a]	2.317	2.230	C(33)-C(34)	1.429(11)	1.388(15)
Zr-R(2)[b]	2.243	2.345	C(34)-C(35)	1.422(11)	1.403(16)
Zr-C(1)	2.486(5)		C(31)-C(35)	1.395(10)	1.384(15)
Zr-C(2)	2.467(6)		C(11)-C(21)	1.515(11)	1.511(20)
Zr-H	1.88(4)		C(12)-C(22)	1.502(11)	1.524(20)
Zr-C(11)	2.602(7)	2.489(12)	C(13)-C(23)	1.520(11)	1.485(18)
Zr-C(12)	2.617(7)	2.539(12)	C(14)-C(24)	1.515(12)	1.494(19)
Zr-C(13)	2.617(7)	2.570(11)	C(15)-C(25)	1.520(12)	1.523(18)
Zr-C(14)	2.596(8)	2.544(11)	C(31)-C(41)	1.510(11)	1.524(19)
Zr-C(15)	2.618(8)	2.517(11)	C(32)-C(42)	1.462(12)	1.472(18)
Zr-C(31)	2.540(7)	2.631(11)	C(33)-C(43)	1.503(12)	1.508(18)
Zr-C(32)	2.532(8)	2.635(11)	C(34)-C(44)	1.511(12)	1.478(18)
Zr-C(33)	2.581(8)	2.653(10)	C(35)-C(45)	1.522(11)	1.485(19)
Zr-C(34)	2.560(8)	2.628(11)	C(1)-P	1.735(5)	
Zr-C(35)	2.531(7)	2.599(11)	C(2)-P	1.713(6)	
C(11)-C(12)	1.416(10)	1.404(17)	M(1)-P	1.792(7)	
C(12)-C(13)	1.403(10)	1.411(16)	M(2)-P	1.778(7)	
C(13)-C(14)	1.417(11)	1.386(16)	C(1)-H(11)	0.93(4)	
C(14)-C(15)	1.409(11)	1.426(15)	C(1)-H(12)	0.95(4)	
C(11)-C(15)	1.424(10)	1.429(16)	C(2)-H(21)	0.83(5)	
C(31)-C(32)	1.440(11)	1.420(15)	C(2)-H(22)	0.82(7)	
C(32)-C(33)	1.428(11)	1.412(15)			

[a] R(1) = C(11)-C(15) ring centroid.

[b] R(2) = C(31)-C(35) ring centroid.

TABLE 3.9. Bond Angles for 11 (°).

	Ring A	Ring B
R(1)[a]-Zr-R(2)[b]	136	145
R(1)-Zr-H	98	107
R(2)-Zr-H	91	86
C(1)-Zr-C(2)	65.9(2)	
C(1)-Zr-H	131(1)	
C(2)-Zr-H	66(1)	
C(1)-Zr-R(1)	102	94
C(1)-Zr-R(2)	104	100
C(2)-Zr-R(1)	111	113
C(2)-Zr-R(2)	112	102
C(11)-C(12)-C(13)	107.2(6)	109.6(10)
C(12)-C(13)-C(14)	109.1(6)	107.6(10)
C(13)-C(14)-C(15)	107.7(7)	108.8(10)
C(14)-C(15)-C(11)	107.5(7)	107.4(9)
C(15)-C(11)-C(12)	108.5(6)	106.5(10)
C(21)-C(11)-C(12)	123.0(6)	129.0(11)
C(11)-C(12)-C(22)	127.3(6)	120.1(11)
C(22)-C(12)-C(13)	125.1(6)	129.9(11)
C(12)-C(13)-C(23)	125.4(7)	122.6(11)
C(23)-C(13)-C(14)	124.4(7)	128.0(11)
C(13)-C(14)-C(24)	129.3(7)	127.1(11)
C(24)-C(14)-C(15)	122.1(7)	123.8(11)
C(14)-C(15)-C(25)	126.4(7)	125.8(10)

TABLE 3.9 (continued)

C(25)-C(15)-C(11)	124.2(7)	124.5(10)
C(15)-C(11)-C(21)	127.8(7)	123.4(11)
C(31)-C(32)-C(32)	106 5(7)	105.5(9)
C(32)-C(33)-C(34)	108.3(7)	109.6(9)
C(33)-C(34)-C(35)	107.7(7)	107.4(10)
C(34)-C(35)-C(31)	108.4(6)	108.4(10)
C(35)-C(31)-C(32)	109.1(6)	109.0(9)
C(41)-C(31)-C(32)	123.7(7)	123.5(10)
C(31)-C(32)-C(42)	127.4(7)	121.0(10)
C(42)-C(32)-C(33)	125.6(7)	132.6(11)
C(32)-C(33)-C(43)	125.6(7)	125.5(10)
C(43)-C(33)-C(34)	124.9(7)	127.9(10)
C(33)-C(34)-C(44)	129.5(7)	123.4(11)
C(44)-C(34)-C(35)	122.0(7)	128.6(11)
C(34)-C(35)-C(45)	127.3(7)	122.3(11)
C(45)-C(35)-C(31)	123.5(7)	128.4(11)
C(35)-C(31)-C(41)	125.1(7)	125.9(11)
C(1)-P-C(2)	102.8(3)	
M(1)-P-M(2)	100.2(3)	
C(1)-P-M(1)	113.8(3)	
C(1)-P-M(2)	113.9(3)	
C(2)-P-M(1)	113.8(3)	
C(2)-P-M(2)	112.7(3)	
Zr-C(1)-P	95.0(2)	

TABLE 3.9 (continued)

Zr-C(2)-P	96.2(3)
H(11)-C(1)-H(12)	113(4)
H(21)-C(2)-H(22)	100(6)

[a]R(1) = C(11)-C(15) ring centroid.

[b]R(2) = C(31)-C(35) ring centroid.

TABLE 3.10. Least-Squares Planes of Pentamethylcyclopentadienyl Rings for 11.

Atom	Deviation from Plane (Å)[a]	
	Ring A	Ring B
	Cp*(1) Ring	
C(11)	-0.006	0.001
C(12)	-0.002	0.015
C(13)	0.010	-0.023
C(14)	-0.013	-0.028
C(15)	0.012	0.012
C(21)	0.17	0.21
C(22)	0.16	0.20
C(23)	0.29	0.26
C(24)	0.17	0.02
C(25)	0.38	0.41
	Cp*(2) Ring	
C(31)	0.018	0.027
C(32)	-0.021	-0.016
C(33)	0.016	0.002
C(34)	-0.005	-0.016
C(35)	-0.009	-0.011
C(41)	0.42	0.41
C(42)	0.08	0.15
C(43)	0.32	0.27

TABLE 3.10 (continued)

C(44)	0.19	0.01
C(45)	0.17	0.17

[a]A negative deviation is a deviation toward the metal atom.

pentamethylcyclopentadienyl rings are given in Table 3.10.

3.4.14 $Cp^*_2Zr(Me)CH_2PMe_2$ (12)

$Cp^*_2\overline{Zr(H)CH_2PMe_2CH_2}$ (11) (100 mg, 0.22 mmol) was dissolved in toluene (10 mL) and the solution heated at 80°C for 4 hours. The solvent was removed in vacuo to afford 12 as an amber oil (purity by ^1H NMR was 90%). ^1H NMR (benzene-d_6): δ 1.80 (s, 30H, $C_5(CH_3)_5$); 0.95 (d, $^2J_{PH}$ = 5 Hz, 6H, $P(CH_3)_2$); 0.0 (d, $^2J_{PH}$ = 6 Hz, 2H, $ZrCH_2$); -0.42 (d, $^4J_{PH}$ = 3 Hz, 3H, $ZrCH_3$). $^{13}C\{^1H\}$ NMR (benzene-d_6): δ 117.9 (s, $\underline{C}_5(CH_3)_5$); 52.60 (d, $^1J_{PC}$ = 50 Hz, $ZrCH_2$); 42.67 (s, $ZrCH_3$); 20.70 (d, $^1J_{PC}$ = 20 Hz, $P(CH_3)_2$); 11.68 (d, $^4J_{PC}$ = 3 Hz, $C_5(\underline{C}H_3)_5$). $^{31}P\{^1H\}$ NMR (benzene-d_6): δ -41.46 (s, P).

3.4.15 (O-ℓ)-$Cp^*_2Zr(COCHPMe_3)H$ (15)

$Cp^*_2\overline{Zr(H)CH_2PMe_2CH_2}$ (11) (140 mg, 0.31 mmol) was dissolved in toluene (20 mL) and the solution stirred under 1 atm CO at 0°C for 12 hours. The color of the solution turned from amber to light purple during this time. The solution was then filtered and the solved removed in vacuo at 0°C to give a light purple-white residue. The solid was triterated with pet. ether (8 mL), the suspension cooled to -78°C and then filtered at this temperature to afford 15 as a purple-white powder (90 mg, 61%). Anal. Calcd for $C_{25}H_{41}OPZr$: C, 62.58; H, 8.61; P, 6.45; Zr, 19.01. Found: C, 62.30; H, 8.43; P, 6.22; Zr, 19.25. ^1H NMR (benzene-d_6); δ 3.90 (d, $^2J_{PH}$ = 43 Hz, 1H, CH); 3.50 (s, 1H, ZrH); 2.07 (s, 30H, $C_5(CH_3)_5$); 0.78 (d, $^2J_{PH}$ = 13 Hz, 9H, $P(CH_3)_3$). $^{13}C\{^1H\}$ NMR (THF-d_8): δ 250.3 (d, $^2J_{PC}$ = 17 Hz, O$\underline{C}$CH); 111.8 (s, $\underline{C}_5(CH_3)_5$); 58.39 (d, $^1J_{PC}$ = 64 Hz, OC$\underline{C}$H); 12.73 (d, $^1J_{PC}$ = 56 Hz, $P(CH_3)_3$); 11.92 (s, $C_5(\underline{C}H_3)_5$). $^{31}P\{^1H\}$ NMR (THF-d_8): δ -6.34

(s, P). IR (benzene): ν(CO) 1427 cm^{-1}; ν(Zr-H) 1490.

3.4.16 (O-ℓ)-$Cp^*_2Zr(^{13}COCHPMe_3)H$

The procedure described in section 3.4.14 was followed using 150 mg (0.033 mmol) $Cp^*_2Zr(H)CH_2PMe_2CH_2$ (11) in 8 mL toluene and stirring the solution under 1 atm ^{13}CO (99.9%) at 0°C for 12 hours. The solution was filtered and the solvent removed in vacuo. The residue was triturated with pet. ether (6 mL), the suspension cooled to -78°C and then filtered at this temperature to afford the product as a purple-white powder (93 mg, 59%). IR (benzene): ν(CO) 1390 cm^{-1}.

3.4.17 Crystal Structure of (O-ℓ)-$Cp^*_2Zr(COCHPMe_3)H \cdot \frac{1}{2}C_7H_8$ (15)

Blue-white crystals of (O-ℓ)-$Cp^*_2Zr(COCHPMe_3)H \cdot \frac{1}{2}C_7H_8$ (15) grown from toluene were mounted in glass capillaries under a nitrogen atmosphere. A series of oscillation and Weissenberg photographs established the crystals as monoclinic, and the systematic absences (OkO for k odd, hOℓ for $h+\ell$ odd) indicated the space group $P2_1/n$. The initial batch of crystals deteriorated within days under X-ray exposure. From a subsequent batch of crystals, an individual was mounted approximately along the b-axis. The oscillation and Weissenberg photographs agreed with the earlier photographic information. Crystal data are summarized in Table 3.2. Lattice constants were obtained from the least-squares refinement[52] of fifteen 2θ values ($20 < 2\theta < 25°$), where each 2θ value was an average of two settings at $\pm 2\theta$.

A total of 2838 reflections were collected on a locally modified Syntex $P2_1$ diffractometer and included blocks of three check reflections measured after each 97 reflections. The shell of redundant data ($+h, \pm k, \pm \ell$), $3 < 2\theta < 25°$), was measured at a rapid rate, 5.86°/min,

to ensure collection of the entire hemisphere (about 40 hours exposure time). The three check reflections indicated only minor deterioration (about 5%), but the intensities were substantially reduced in the next shell of data; consequently, only data from the first shell were used. The data were reduced and the structure solved and refined as described in Section 3.4.13. A difference map indicated that a toluene molecule was disordered around a center of inversion; subsequent work from ΔF maps led to a set of coordinates which adequately model the disorder. The final difference map indicated no peak greater than 1 $e^- Å^{-3}$. Details concerning the data collection and the final cycle of refinement are given in Table 3.11. Atom coordinates and U_{ij}'s are given in Table 3.12. Bond distances and bond angles are given in Tables 3.13 and 3.14, respectively. Least-squares planes of the pentamethylcyclopentadienyl rings and the ZrCOCP group are given in Tables 3.15 and 3.16, respectively.

3.4.18 (O-c)-$Cp^*_2Zr(COCHPMe_3)H$ (16)

(O-ℓ)-$Cp^*_2Zr(COCHPMe_3)H$ (15) (25 mg, 0.052 mmol) was dissolved in toluene (5 mL) and the solution heated at 80°C for 24 hours. Removal of solvent in vacuo afforded 16 as a yellow-tan solid. ^1H NMR (benzene-d_6): δ 4.28 (s, 1H, ZrH); 3.75 (d, $^2J_{PH}$ = 43 Hz, 1H, CH); 2.07 (s, 30H, $C_5(CH_3)_5$); 0.86 (d, $^2J_{PH}$ = 13 Hz, 9H, $P(CH_3)_3$). $^{13}C\{^1H\}$ NMR (benzene-d_6); δ 247.1 (d, $^2J_{PH}$ = 14 Hz, O$\underline{C}$ CH); 112.2 (s, $\underline{C}_5(CH_3)_5$); 57.08 (d, $^1J_{PC}$ = 68 Hz, OC$\underline{C}$H); 13.00 (d, $^1J_{PC}$ = 60 Hz, $P(CH_3)_3$); 12.14 (s, $C_5(\underline{C}H_3)_5$). $^{31}P\{^1H\}$ NMR (benzene-d_6); δ -5.06 (s,

TABLE 3.11. Data Collection and Refinement Conditions for (O-ℓ)-$Cp^*_2Zr(COCHPMe_3)H \cdot \frac{1}{2} C_7H_8$ (15).

λ	0.71069 Å (MoK_α, graphite monochromator)
Scan Method	θ-2θ
Scan Range	1.2° above K_{α_2}
	1.2° below K_{α_1}
2θ Scan Rate	5.86°/min
2θ Limits	3-30°
Scan Time/Bkgrd Time	1.00
Number of Reflections[a]	1192, 1108, 847
$R(F_o^2 > 0)$[b]	0.109
$R(F_o^2 > 3\sigma_{F_o^2})$[b]	0.86
Goodness-of-Fit[c]	4.25

[a]Total number of unique reflections, all reflections with $F_o^2 > 0$, all reflections with $F_o^2 > 3\sigma_{F_o^2}$.

[b]$R = \Sigma || F_o| - |F_c|| / \Sigma |F_o|$.

[c]Goodness-of-fit = $\{\Sigma \omega [F_o^2 - (F_c/k)^2]^2/(n_{ref} - n_{par})\}^{\frac{1}{2}}$.

TABLE 3.12. Final Nonhydrogen Parameters for 15 (coordinates x 10^4, U_{ij} ($Å^2$) x 10^3).

	x	y	z	U or U_{11}	U_{22}	U_{33}	U_{12}	U_{13}	U_{23}
Zr	2712(2)	−475(3)	6883(2)	61(2)	37(2)	43(2)	−2(3)	−1(2)	−4(3)
P	3744(8)	1858(12)	4735(6)	143(12)	88(11)	66(9)	37(9)	25(9)	46(9)
O	2627(16)	927(18)	5991(9)	95(29)	67(20)	20(17)	−11(16)	−23(14)	7(12)
C(1)	3440(24)	407(33)	5913(21)	25(27)	56(29)	109(36)	64(26)	−40(26)	−51(28)
C(2)	3972(26)	797(38)	5368(19)	123(38)	123(41)	46(26)	−11(31)	40(25)	42(30)
C(3)	4593(31)	2004(46)	4106(24)	304(60)	336(66)	248(50)	243(52)	249(51)	281(50)
C(4)	3585(43)	3315(44)	5031(24)	554(105)	79(43)	176(49)	83(53)	−99(54)	56(37)
C(5)	2739(41)	1583(46)	4233(27)	327(71)	236(59)	226(56)	−75(55)	−152(57)	153(47)
C(11)	3853(21)	743(29)	7674(14)	57(10)					
C(12)	3470(20)	−176(29)	8146(15)	55(10)					
C(13)	2550(18)	96(25)	8252(15)	50(10)					
C(14)	2354(21)	1236(28)	7819(13)	52(10)					
C(15)	3200(20)	1634(29)	7485(15)	50(9)					
C(21)	4811(16)	808(38)	7465(17)	−5(21)	261(50)	130(28)	−58(27)	43(19)	−82(32)
C(22)	4001(26)	−1214(33)	8526(17)	202(43)	130(37)	95(30)	109(33)	−116(30)	−14(26)
C(23)	1932(20)	−549(31)	8835(14)	156(32)	79(26)	50(21)	−76(29)	13(22)	32(23)
C(24)	1458(23)	1902(39)	7765(20)	78(31)	230(50)	172(41)	137(34)	−84(28)	−116(35)
C(25)	3313(30)	2820(26)	7038(15)	415(67)	−3(23)	42(25)	−65(30)	−9(30)	25(20)
C(31)	1256(22)	−1213(32)	6305(19)	80(11)					
C(32)	1941(21)	−1767(30)	5885(20)	72(11)					
C(33)	2353(22)	−2659(34)	6383(18)	75(11)					
C(34)	1924(23)	−2586(36)	7048(20)	87(10)					
C(35)	1262(24)	−1662(33)	7016(20)	85(10)					
C(41)	626(25)	−119(35)	6008(25)	150(39)	72(40)	392(67)	20(29)	−178(45)	13(36)
C(42)	2087(29)	−1534(36)	5080(17)	285(58)	160(41)	41(29)	−144(41)	33(29)	−27(27)
C(43)	3088(25)	−3561(35)	6056(28)	111(38)	92(35)	381(70)	44(30)	−40(40)	−166(43)
C(44)	2125(40)	−3477(39)	7679(24)	499(100)	114(39)	180(48)	−178(52)	−183(56)	111(39)
C(45)	541(27)	−1478(50)	7624(23)	150(41)	374(78)	200(46)	−193(48)	121(40)	−220(51)
C(T1)	511	1079	461	101					
C(T2)	120	1751	−32	101					
C(T3)	−381	1232	−534	101					
C(T4)	−481	−4	−529	101					
C(T5)	−100	−633	−51	101					
C(T6)	421	−154	477	101					
C(TM)	902	−660	1054	101					

TABLE 3.13. Bond Distances for 15 (Å).

Zr-R(1)[a]	2.28	C(32)-C(33)	1.46(5)
Zr-R(2)[b]	2.26	C(33)-C(34)	1.38(5)
Zr-O	2.21(2)	C(34)-C(35)	1.40(5)
Zr-C(1)	2.29(4)	C(31)-C(35)	1.39(5)
Zr-C(11)	2.60(3)	C(11)-C(21)	1.50(4)
Zr-C(12)	2.60(3)	C(12)-C(22)	1.53(5)
Zr-C(13)	2.59(3)	C(13)-C(23)	1.58(4)
Zr-C(14)	2.56(3)	C(14)-C(24)	1.53(5)
Zr-C(15)	2.61(3)	C(15)-C(25)	1.52(4)
Zr-C(31)	2.56(3)	C(31)-C(41)	1.60(5)
Zr-C(32)	2.56(3)	C(32)-C(42)	1.51(5)
Zr-C(33)	2.56(3)	C(33)-C(43)	1.59(6)
Zr-C(34)	2.56(4)	C(34)-C(44)	1.52(6)
Zr-C(35)	2.54(4)	C(35)-C(45)	1.57(6)
C(11)-C(12)	1.43(4)	C(1)-O	1.36(4)
C(12)-C(13)	1.44(4)	C(1)-C(2)	1.35(5)
C(13)-C(14)	1.48(4)	C(2)-P	1.65(4)
C(14)-C(15)	1.48(4)	C(3)-P	1.73(5)
C(11)-C(15)	1.41(4)	C(4)-P	1.66(5)
C(31)-C(32)	1.42(5)	C(5)-P	1.80(6)

[a]R(1) = C(11)-C(15) ring centroid.

[b]R(2) = C(31)-C(35) ring centroid.

TABLE 3.14. Bond Angles for 15 (°).

R(1)[a]-Zr-R(2)[b]	141	C(22)-C(12)-C(13)	126(3)
R(1)-Zr-O	103	C(12)-C(13)-C(23)	126(2)
R(1)-Zr-C(1)	106	C(23)-C(13)-C(14)	127(2)
R(2)-Zr-O	103	C(13)-C(14)-C(24)	126(3)
R(2)-Zr-C(1)	112	C(24)-C(14)-C(15)	127(3)
C(1)-Zr-O	35(1)	C(14)-C(15)-C(25)	124(3)
C(2)-P-C(3)	112(2)	C(25)-C(15)-C(11)	128(3)
C(2)-P-C(4)	116(2)	C(15)-C(11)-C(21)	126(3)
C(2)-P-C(5)	115(2)	C(31)-C(32)-C(33)	111(3)
C(3)-P-C(4)	104(2)	C(32)-C(33)-C(34)	104(3)
C(3)-P-C(5)	108(2)	C(33)-C(34)-C(35)	108(3)
C(4)-P-C(5)	101(2)	C(34)-C(35)-C(31)	110(3)
C(1)-O-Zr	76(2)	C(35)-C(31)-C(32)	106(3)
O-C(1)-Zr	69(2)	C(41)-C(31)-C(32)	124(3)
C(2)-C(1)-Zr	171(3)	C(31)-C(32)-C(42)	125(3)
C(2)-C(1)-O	120(3)	C(42)-C(32)-C(33)	131(3)
C(1)-C(2)-P	127(3)	C(32)-C(33)-C(43)	117(3)
C(11)-C(12)-C(13)	110(2)	C(43)-C(33)-C(34)	134(3)
C(12)-C(13)-C(14)	107(2)	C(33)-C(34)-C(44)	123(3)
C(13)-C(14)-C(15)	106(2)	C(44)-C(34)-C(35)	127(3)
C(14)-C(15)-C(11)	108(2)	C(34)-C(35)-C(45)	124(3)
C(15)-C(11)-C(12)	109(3)	C(45)-C(35)-C(31)	128(3)
C(21)-C(11)-C(12)	125(3)	C(35)-C(31)-C(41)	125(3)
C(11)-C(12)-C(22)	124(3)		

[a]R(1) = C(11)-C(15) ring centroid.

[b]R(2) = C(31)-C(35) ring centroid.

TABLE 3.15. Least-Squares Planes of Pentamethylcyclopentadienyl Rings for 15.

Atom	Deviation from Plane (Å)[a]
Cp*(1) Ring	
C(11)	-0.013
C(12)	0.003
C(13)	0.008
C(14)	-0.016
C(15)	0.018
C(21)	0.04
C(22)	0.12
C(23)	0.27
C(24)	0.00
C(25)	0.11
Cp*(2) Ring	
C(31)	0.020
C(32)	-0.011
C(33)	-0.011
C(34)	0.013
C(35)	-0.020
C(41)	-0.03
C(42)	0.09
C(43)	0.13
C(44)	0.16
C(45)	0.23

[a]A negative deviation in a deviation toward the metal atom.

TABLE 3.16. Least-Squares Plane of the ZrC(1)OC(2)P Group for 15.

Atom	Deviation from Plane (Å)[a]
Zr	0.014
C(1)	-0.007
O	-0.014
C(2)	-0.011
P	0.016

[a]A negative deviation is a deviation toward the Cp*(1) ring.

P). IR (benzene): ν(CO) 1417 cm^{-1}, ν(Zr-H) 1490.

3.4.19 (O-c)-$Cp^*_2Zr(^{13}COCHPMe_3)H$

The procedure described in Section 3.4.16 was followed using ca. 10 mg (O-ℓ)-$Cp^*_2Zr(^{13}COCHPMe_3)H$ in 5 mL toluene. Removal of solvent afforded the product as a yellow-tan residue. IR (benzene): ν(CO) 1380 cm^{-1}.

3.4.20 Crystal Structure of (O-c)-$Cp^*_2Zr(COCHPMe_3)H$ (16)

Colorless crystals of (O-c)-$Cp^*_2Zr(COCHPMe_3)H$ (16) grown from toluene were mounted in glass capillaries under a nitrogen atmosphere. For photographic work, the glass capillary of a suitable crystal was remounted at an angle of approximately 30° with respect to the rotation axis of the mounting pin. A series of oscillation and Weissenberg photographs established the crystals as monoclinic, and the systematic absences (OkO for k odd, hOℓ for ℓ odd) indicated the space group $P2_1/c$. Crystal data are summarized in Table 3.3. Lattice constants were obtained from the least-squares refinement[52] of fiteen 2θ values ($25 < 2\theta < 40°$) where each 2θ value was an average of two settings at $\pm 2\theta$.

A total of 10174 reflections were collected on a locally modified Syntex $P2_1$ diffractometer and included blocks of three check reflections. No decomposition was observed. The data were reduced and the structure solved and refined as described in Section 3.4.13. In this case, the position and B's of all hydrogen atoms were refined. The matrix was blocked into three groups: the first including all non-hydrogen atom coordinates and the coordinates of H and H(2); the

second group including the scale factor and Gaussian amplitudes for all atoms in block 1 (anisotropic except for the H atoms); and the third group including atom coordinates and isotropic B's of the remaining hydrogen atoms. At this point, the profile of each reflection was examined and those with unusual backgrounds (35) were weighted zero in the final cycles. The final difference map indicated no peaks greater than 0.40 e^{-} $Å^{-3}$. The $C{=}C(H)PMe_3$ group appears to behave as a rigid-body and correction of bond lengths and angles for vibrational motion was carried out by use of the Trueblood program THMB-3.[54] Details concerning the data collection and the final cycle of refinement are given in Table 3.17. Atom coordinates and U_{ij}'s are given in Table 3.18. Final hydrogen atom coordinates and B's are given in Table 3.19. Bond distances and bond angles are given in Tables 3.20 and 3.21, respectively. Least-squares planes of the pentamethylcyclopentadienyl rings and Zr(H)COCHP group are given in Tables 3.22 and 3.23.

TABLE 3.17. Data Collection and Refinement Conditions for (O-c)-$Cp^*_2Zr(COCHPMe_3)H$ (16).

λ	0.71069 Å (MoK_α, graphite monochromator)
Scan Method	θ-2θ
Scan Range	0.9° below K_{α_1}
	1.0° above K_{α_2}
2θ Scan Rate	2.02°/min
2θ Limits	3-51°
Scan Time/Bkgrd Time	1.0
Number of Reflections[a]	4800, 4413, 3486
R[b] ($F_o^2 > 0$)	0.042
R[b] ($F_o^2 > 3\sigma_{F_o^2}$)	0.028
Goodness-of-Fit[c]	1.52

[a]Total number of unique reflections, all reflections with $F_o^2 > 0$, all reflections with $F_o^2 > 3\sigma_{F_o^2}$.

[b]$R = \Sigma||F_o|-|F_c||/\Sigma|F_o|$.

[c]Goodness-of-fit = $\{\Sigma\, \omega[F_o^2 - (F_c/k)^2]^2/(n_{ref} - n_{par})\}^{\frac{1}{2}}$.

TABLE 3.18. Final Nonhydrogen Atom Parameters for 16 (coordinates x 10^5, U_{ij} ($Å^2$) x 10^4).

	x	y	z	U_{11}	U_{22}	U_{33}	U_{12}	U_{13}	U_{23}
Zr	21779(2)	23647(2)	12409(1)	352(1)	339(1)	333(1)	−6(1)	59(1)	−16(1)
P	−12805(8)	54373(7)	17243(3)	558(5)	468(4)	523(5)	70(3)	184(4)	−37(4)
$C(1)$	6164(25)	38991(24)	13281(10)	402(15)	420(14)	408(16)	−43(11)	46(12)	−66(12)
$C(2)$	−3200(29)	49039(28)	12459(11)	540(18)	516(16)	449(18)	96(14)	101(14)	−11(14)
O	8154(17)	32395(16)	17627(7)	458(11)	452(10)	405(11)	7(8)	113(8)	−11(8)
$C(M1)$	−22305(34)	41633(34)	19933(15)	719(23)	793(23)	1004(30)	−163(19)	377(21)	−98(21)
$C(M2)$	−24570(45)	66661(43)	14568(17)	1311(36)	1212(33)	937(30)	747(29)	491(27)	159(26)
$C(M3)$	−3041(38)	61595(36)	22685(14)	1049(30)	934(26)	715(25)	−307(22)	386(21)	−329(21)
$C(21)$	1386(26)	9606(25)	9165(11)	407(16)	471(15)	576(19)	−93(12)	67(14)	−184(14)
$C(22)$	4180(28)	17474(27)	4924(11)	570(19)	507(16)	479(18)	29(14)	−90(15)	−121(13)
$C(23)$	16573(31)	13182(29)	3419(11)	678(21)	631(19)	396(17)	−126(15)	93(15)	−158(14)
$C(24)$	21527(28)	2736(26)	6754(12)	516(18)	482(16)	628(20)	18(13)	94(15)	−235(14)
$C(25)$	12024(28)	505(24)	10291(11)	592(18)	354(14)	559(19)	−71(13)	47(14)	−111(13)
$C(31)$	47276(22)	24009(26)	14850(10)	332(12)	450(14)	503(15)	−18(12)	43(11)	84(13)
$C(32)$	45428(25)	29423(26)	9784(10)	421(15)	562(17)	466(16)	−60(12)	138(12)	57(13)
$C(33)$	38333(27)	41576(27)	10050(12)	448(17)	507(16)	636(20)	−63(13)	38(15)	213(14)
$C(34)$	36440(26)	43944(25)	15297(12)	380(15)	379(14)	735(21)	−72(12)	66(14)	−50(14)
$C(35)$	41733(25)	33035(26)	18218(10)	371(15)	526(16)	427(16)	−93(12)	26(12)	−5(13)
$C(21M)$	−11210(31)	10437(33)	11924(15)	529(20)	801(23)	968(28)	−180(17)	213(18)	−261(20)
$C(22M)$	−5178(35)	27223(36)	1884(13)	965(26)	876(25)	683(22)	124(21)	−339(20)	−106(20)
$C(23M)$	21784(40)	17244(41)	−1617(13)	1161(32)	1240(32)	460(21)	−274(26)	175(21)	−140(21)
$C(24M)$	33554(34)	−6261(34)	6185(17)	700(24)	721(23)	1327(36)	85(18)	214(23)	−480(23)
$C(25M)$	12346(38)	−10736(29)	14107(15)	1100(29)	409(17)	896(27)	−118(17)	51(22)	−6(17)
$C(31M)$	54956(29)	11645(29)	16548(13)	496(19)	591(18)	838(24)	102(14)	72(17)	162(17)
$C(32M)$	52385(30)	24641(39)	5242(12)	651(19)	1096(27)	619(19)	−62(21)	306(16)	28(21)
$C(33M)$	34906(38)	51207(36)	5629(16)	971(29)	840(25)	1015(32)	−89(21)	29(23)	532(23)
$C(34M)$	30928(33)	56472(31)	17469(16)	691(23)	520(19)	1337(35)	−53(17)	−28(22)	−307(21)
$C(35M)$	42321(33)	31606(36)	24026(12)	723(23)	1017(26)	468(19)	−191(19)	6(17)	−84(17)

TABLE 3.19. Final Hydrogen Atom Parameters for 16 (coordinates x 10^4, B ($Å^2$)).

	x	y	z	B
H	2437(21)	1218(21)	1820(9)	3.15(50)
H(2)	−462(25)	5322(25)	973(10)	4.68(69)
H(PM11)	−2731(31)	4507(30)	2270(13)	7.73(85)
H(PM12)	−1626(30)	3463(29)	2098(12)	6.78(78)
H(PM13)	−2869(38)	3863(36)	1757(16)	10.23(107)
H(PM21)	−3005(39)	6904(40)	1677(17)	10.91(116)
H(PM22)	−3147(34)	6004(35)	1222(15)	9.69(103)
H(PM23)	−1975(43)	7263(44)	1381(18)	13.56(139)
H(PM31)	−869(36)	6432(34)	2497(14)	9.15(100)
H(PM32)	331(37)	5528(38)	2417(15)	10.41(108)
H(PM33)	162(37)	6893(38)	2179(15)	10.49(108)
H(21M1)	−928(41)	651(43)	1531(18)	12.18(127)
H(21M2)	−1475(37)	1850(40)	1199(16)	10.53(110)
H(21M3)	−1753(33)	501(34)	1079(14)	8.22(91)
H(22M1)	−1312(35)	2928(36)	395(15)	10.01(105)
H(22M2)	−19(36)	3476(35)	92(15)	9.90(103)
H(22M3)	−962(35)	2285(37)	−106(15)	10.09(104)
H(23M1)	2274(31)	2714(35)	−172(14)	8.90(94)
H(23M2)	2955(37)	1184(36)	−196(14)	10.01(106)
H(23M3)	1486(34)	1468(33)	−458(13)	8.51(94)

	x	y	z	B
H(24M1)	3885(39)	−723(40)	918(18)	11.46(119)
H(24M2)	3122(34)	−1373(35)	487(15)	9.01(98)
H(24M3)	3892(38)	−175(40)	389(16)	10.92(115)
H(25M1)	703(34)	−880(34)	1698(14)	9.14(96)
H(25M2)	2170(30)	−1243(28)	1568(11)	6.35(75)
H(25M3)	904(32)	−1850(32)	1267(13)	7.86(86)
H(31M1)	6335(31)	1336(30)	1828(13)	7.47(85)
H(31M2)	4982(33)	596(30)	1832(13)	7.64(84)
H(31M3)	5673(32)	644(32)	1383(14)	7.94(88)
H(32M1)	5389(35)	1581(38)	504(15)	10.41(109)
H(32M2)	6069(30)	2907(30)	543(12)	7.15(81)
H(32M3)	4709(29)	2834(30)	207(12)	6.88(78)
H(33M1)	2732(41)	5629(38)	629(16)	10.77(113)
H(33M2)	4107(39)	5781(36)	581(15)	10.25(111)
H(33M3)	3313(40)	4717(41)	252(16)	11.86(121)
H(34M1)	2641(40)	5503(40)	2043(17)	12.14(122)
H(34M2)	3711(32)	6317(30)	1799(13)	7.09(81)
H(34M3)	2483(34)	6012(33)	1478(14)	8.53(93)
H(35M1)	4942(33)	3555(31)	2557(13)	7.91(87)
H(35M2)	3415(33)	3632(32)	2504(13)	8.36(93)
H(35M3)	4260(32)	2261(35)	2494(13)	8.87(93)

TABLE 3.20. Bond Distances for 16 (Å).

Zr-R(1)[a]	2.251	C(31)-C(31M)	1.496(4)
Zr-R(2)[b]	2.258	C(32)-C(32M)	1.508(4)
Zr-H	1.89(2)	C(33)-C(33M)	1.509(5)
Zr-O	2.199(2)	C(34)-C(34M)	1.504(4)
Zr-C(1)	2.214(2)	C(35)-C(35M)	1.508(4)
Zr-C(21)	2.534(3)	C(1)-O	1.303(3)
Zr-C(22)	2.543(3)	C(1)-C(2)	1.372(4)
Zr-C(23)	2.558(3)	C(2)-H(2)	0.82(3)
Zr-C(24)	2.556(3)	C(2)-P	1.731(3)
Zr-C(25)	2.550(3)	C(PM1)-P	1.775(4)
Zr-C(31)	2.543(2)	C(PM2)-P	1.785(4)
Zr-C(32)	2.583(3)	C(PM3)-P	1.777(4)
Zr-C(33)	2.555(3)	C(PM1)-(PM11)	0.98(3)
Zr-C(34)	2.566(3)	C(PM1)-(PM12)	0.94(3)
Zr-C(35)	2.536(3)	C(PM1)-(PM13)	0.88(4)
C(21)-C(22)	1.405(4)	C(PM2)-C(PM21)	0.86(4)
C(22)-C(23)	1.400(4)	C(PM2)-C(PM22)	1.09(4)
C(23)-C(24)	1.412(5)	C(PM2)-C(PM23)	0.80(4)
C(24)-C(25)	1.404(4)	C(PM3)-C(PM31)	0.90(4)
C(21)-C(25)	1.402(4)	C(PM3)-C(PM32)	0.94(4)
C(31)-C(32)	1.415(4)	C(PM3)-C(PM33)	0.91(4)
C(32)-C(33)	1.413(4)		
C(33)-C(34)	1.414(4)		
C(34)-C(35)	1.400(4)		

TABLE 3.20 (continued)

C(31)-C(35)	1.411(3)
C(21)-C(21M)	1.511(4)
C(22)-C(22M)	1.510(4)
C(23)-C(23M)	1.512(5)
C(24)-C(24M)	1.517(5)
C(25)-C(25M)	1.498(4)

[a]R(1) = C(21)-C(25) ring centroid.

[b]R(2) = C(31)-C(35) ring centroid.

TABLE 3.21. Bond Angles for 16 (°).

R(1)[a]-Zr-R(2)[b]	138.9	C(22)-C(23)-C(23M)	123.6(3)
R(1)-Zr-O	112.2	C(23M)-C(23)-C(24)	126.8(3)
R(1)-Zr-C(1)	104.0	C(23)-C(24)-C(24M)	127.3(3)
R(1)-Zr-H	96.5	C(24M)-C(24)-C(25)	124.2(3)
R(2)-Zr-O	108.4	C(24)-C(25)-C(25M)	125.7(2)
R(2)-Zr-C(1)	105.8	C(25M)-C(25)-C(21)	126.0(2)
R(2)-Zr-H	97.9	C(25)-C(21)-C(21M)	125.6(2)
O-Zr-H	78.0(6)	C(31)-C(32)-C(33)	107.4(2)
C(1)-Zr-H	112.2(6)	C(32)-C(33)-C(34)	108.1(2)
O-Zr-C(1)	34.35(8)	C(33)-C(34)-C(35)	107.9(2)
C(2)-P-C(PM1)	114.7(1)	C(34)-C(35)-C(31)	108.4(2)
C(2)-P-C(PM2)	108.9(2)	C(35)-C(31)-C(32)	108.0(2)
C(2)-P-C(PM3)	113.6(2)	C(31M)-C(31)-C(32)	126.9(2)
C(PM1)-P-C(PM2)	107.2(2)	C(31)-C(32)-C(32M)	125.4(2)
C(PM1)-P-C(PM3)	104.4(2)	C(32M)-C(32)-C(33)	125.9(2)
C(PM2)-P-C(PM3)	107.7(2)	C(32)-C(33)-C(33M)	125.9(3)
C(1)-O-Zr	73.4(1)	C(33M)-C(33)-C(34)	125.5(3)
O-C(1)-Zr	72.2(1)	C(33)-C(34)-C(34M)	126.3(2)
C(2)-C(1)-Zr	164.8(2)	C(34M)-C(34)-C(35)	125.5(2)
C(2)-C(1)-O	122.9(2)	C(34)-C(35)-C(35M)	125.9(2)
P-C(2)-H(2)	113(2)	C(35M)-C(35)-C(31)	125.6(2)
C(1)-C(2)-H(2)	124(2)	C(35)-C(31)-C(31M)	124.8(2)
C(1)-C(2)-P	122.2(2)	H(PM11)-C(PM1)-H(PM12)	114(3)
C(21)-C(22)-C(23)	107.5(2)	H(PM11)-C(PM1)-H(PM13)	104(3)

TABLE 3.21 (continued)

C(22)-C(23)-C(24)	108.4(2)	H(PM12)-C(PM1)-H(PM13)	109(3)
C(23)-C(24)-C(25)	107.7(2)	H(PM21)-C(PM2)-H(PM22)	98(3)
C(24)-C(25)-C(21)	107.8(2)	H(PM21)-C(PM2)-H(PM23)	113(4)
C(25)-C(21)-C(22)	108.6(2)	H(PM22)-C(PM2)-H(PM23)	131(4)
C(21M)-C(21)-C(22)	125.8(2)	H(PM31)-C(PM3)-H(PM32)	112(3)
C(21)-C(22)-C(22M)	127.5(2)	H(PM31)-C(PM3)-H(PM33)	107(3)
C(22H)-C(22)-C(23)	124.3(2)	H(PM32)-C(PM3)-H(PM33)	108(3)

[a]R(1) = C(21-25) ring centroid.

[b]R(2) = C(31-35) ring centroid.

TABLE 3.22. Least-Squares Planes of Pentamethylcyclopentadienyl Rings for 16.

Atom	Deviation from Plane (Å)[a]
Cp*(1)	
C(11)	-0.000
C(12)	-0.000
C(13)	0.004
C(14)	-0.004
C(15)	0.002
C(21)	0.04
C(22)	0.19
C(23)	0.28
C(24)	0.19
C(25)	0.17
Cp*(2)	
C(31)	-0.006
C(32)	0.014
C(33)	-0.017
C(34)	0.013
C(35)	-0.004
C(41)	0.10
C(42)	0.32
C(43)	0.08
C(44)	0.17
C(45)	0.07

[a]A negative deviation is a deviation toward the metal atom.

TABLE 3.23. Least-Squares Plane of the Zr(H)C(1)OC(2)H(2)P Group for 16.

Atom	Deviation from Plane (Å)[a]
Zr	0.056
H	-0.082
C(1)	0.033
O	0.061
C(2)	-0.024
H(2)	-0.049
P	0.006

[a]A negative deviation is a deviation toward the $Cp^*(1)$ ring.

3.5 References and Notes

1. For a review of phosphorous ylide chemistry see A. W. Johnson, "Ylide Chemistry," in Organic Chemistry, A Series of Monographs, Vol. 7, A. T. Blomquist, Ed., Academic Press, New York, 1966.

2. a) H. Schmidbaur, Accounts Chem. Res., 8, 62 (1975);
b) F. R. Kreissl and P. Friedrich, Angew. Chem. Int. Ed. Engl., 16, 542 (1977);
c) F. R. Kreissl, W. Vedelhoven, and A. Ruhs, J. Organomet. Chem., 113, C55 (1976);
d) F. R. Kreissl, ibid., 99, 305 (1975).

3. R. R. Schrock and P. R. Sharp, J. Amer. Chem. Soc., 100, 2389 (1978).

4. L. W. Messerle, P. Jennische, R. R. Schrock, and G. Stucky, ibid., 102, 6744 (1980).

5. a) L. Messerle, Ph.D. Dissertation, Massachusetts Institute of Technology, Cambridge, MA, 1979.
b) E. J. Moore, D. A. Straus, J. Armantrout, B. D. Santarsiero, R. H. Grubbs, and J. E. Bercaw, J. Amer. Chem. Soc., 105, 2068 (1983);
c) See also ref. 44.

6. P. R. Sharp and R. R. Schrock, J. Organomet. Chem., 171, 43 (1979).

7. J. Schwartz and K. Gell, ibid., 184, C1 (1980).

8. J. M. Manriquez, D. R. McAlister, R. D. Sanner, and J. E. Bercaw, J. Amer. Chem. Soc., 98, 6733 (1976).

9. a) E. O. Fischer, W. Hafner, and H. O. Stahl, Z. Anorg. Allg. Chem., 282, 47 (1955);

b) T. S. Piper and G. Wilkinson, J. Inorg. Nucl. Chem., 3, 104 (1956);

c) W. Hieber and G. Wagner, Liebigs. Ann. Chem., 618, 24 (1958).

10. CH_2PPh_3 may be substituted for CH_2PMe_3 without reduction in yield. However, it was not possible to separate the products PPh_3 and $Cp^*_2Hf(H)Me$.

11. Protons bound to an α-carbon adjacent to hafnium generally resonate upfield of TMS in the ^1H NMR spectrum. D. M. Roddick, M. D. Fryzuk, P. F. Seidler, and J. E. Bercaw, manuscript in preparation.

12. The hydride ligands in $Cp^*_2HfH_2$ and $Cp^*_2ZrH_2$ are hydridic in contrast to $HCo(CO)_4$ in which the hydride ligand is protonic: J. E. Bercaw, Adv. Chem. Ser., 167, 136 (1978).

13. Although the molecular weight of 4 has not been determined, the high solubility of 4 in such nonpolar solvents as petroleum ether suggests it is monomeric.

14. P. C. Wailes and H. Wiegold, J. Organomet. Chem., 24, 405 (1970).

15. J. R. Norton, Accounts Chem. Res., 12, 139 (1979).

16. For reports of other methyl hydride complexes see:

a) J. Chatt and R. G. Hayter, J. Chem. Soc., 6017 (1964);

b) K. Jonas and G. Wilke, Angew. Chem. Int. Ed., Engl., 8, 519 (1969);

c) D. Strope and D. F. Schriver, J. Amer. Chem. Soc., 95, 8197 (1973);

d) J. Evans, S. J. Okrasinski, A. J. Pribula, and J. R. Norton, ibid., 98, 4000 (1976);

e) D.J. Cole-Hamilton and G. Wilkinson, J. Chem. Soc., Dalton Trans., 797 (1977);

f) M. Berry, S. G. Davies, and M. L. H. Green, J. Chem. Soc., Chem. Commun., 99 (1978).

17. K. J. Gell and J. Schwartz, Inorg. Chem., 19, 3207 (1980).

18. N. J. Cooper and M. L. H. Green, J. Chem. Soc., 761 (1974).

19. P. T. Barger, J. Armantrout, B. D. Santarsiero, and J. E. Bercaw, manuscript in preparation.

20. Attempts to prepare $Cp^*_2Zr(H)Me$ by other routes have not been successful. Treatment of $Cp^*_2Zr(H)Cl$ with MeLi affords $Cp^*_2ZrMe_2$ (50%) and $Cp^*_2Zr(H)Cl$ (50%). D. R. McAlister, personal communication.

21. Based on Toepler pump experiments.

22. R. A. Schunn, "Systematics of Transition Metal Hydride Chemistry," in Transition Metal Hydrides, E. L. Muetterties, Ed., Marcel Dekker, Inc., New York, 1971.

23. J. M. Manriquez, D. R. McAlister, R. D. Sanner, and J. E. Bercaw, J. Amer. Chem. Soc., 100, 2716 (1978).

24. D. M. Roddick, personal communication.

25. G. Rice, G. B. Ansell, M. A. Modrick, and S. Zentz, Organometallics, 2, 154 (1982).

26. J. Jeffery, M. F. Lappert, N. T. Luong-Thi, M. Webb, J. L. Atwood, and W. E. Hunter, J. Chem. Soc., Dalton Trans. 1593 (1981).

27. G. Facinetti, C. Floriani, F. Marchetti, and S. Merlino, J. Chem. Soc., Chem. Commun., 522 (1976).

28. J. L. Atwood, G. K. Barker, J. Holton, W. E. Hunter, M. F. Lappert, and R. Pearce, J. Amer. Chem. Soc., 99, 6645 (1977).

29. J. D. Dunitz, "X-Ray Analysis and the Structure of Organic Molecules," Cornell University Press, New York, 1979.

30. S B. Jones and J. L. Petersen, Inorg. Chem., 20, 2889 (1981).

31. M. B. Fischer, E. J. James, T. J. McNeese, S. C. Nyburg, B. Posin, W. Wong-NG, and S. S. Wreford, J. Amer. Chem. Soc., 102, 4941 (1980). The coordinates of the H atom were taken from a Fourier difference map and not refined.

32. D. M. Roddick, B. D. Santarsiero, and J. E. Bercaw, manuscript in preparation.

33. M. E. Silver, O. Eisenstein, and R. C. Fay, Inorg. Chem., 22, 759 (1983).

34. N. E. Schore and H. Hope, J. Amer. Chem. Soc., 102, 4251 (1980).

35. The electrochemical reduction of tetraalkylphosphonium salts does afford trialkylphosphines and alkyl radicals, C. K. White and R. D. Rieke, J. Org. Chem., 43, 4638 (1978).

36. Based on ^{1}H NMR spectroscopy.

37. The relative concentrations of CH_4, CH_3D_2 and CH_2D_2 were

measured by 500 MHz ^{1}H NMR spectroscopy.

38. a) M. F. Lappert, N. T. Luong-Thi, and C. R. C. Milne, J. Organomet. Chem., 174, C35 (1979);
b) G. Fachinetti and C. Floriani, ibid., 71, C5 (1974);
c) G. Erker and F. Rosenfeldt, Angew. Chem. Int. Ed. Engl., 17, 605 (1978);
d) G. Fachinetti, G. Fochi, and C. Floriani, J. Chem. Soc., Dalton Trans., 1946 (1977);
e) J. C. Baldwin, N. L. Keder, C. E. Strouse, and W. C. Kaska, Z. Naturforsch., 35b, 1289 (1980).

39. (O-ℓ)-$Cp^*_2Zr(COCHPMe_3)H$ refers to the kinetic η^2-acyl isomer in which the oxygen atom occupies a lateral coordination site. (O-c)-$Cp^*_2Zr(COCHPMe_3)H$ refers to the thermodynamic η^2-acyl isomer in which the oxygen atom occupies the central coordination site.

40. a) P. J. Fagan, J. M. Manriquez, T. J. Marks, V. W. Day, S. H. Vollmer, and C. S. Day, J. Amer. Chem. Soc., 102, 2297 (1980);
b) T. J. Marks, J. M. Manriquez, P. J. Fagan, V. W. Day, C. S. Day, and S. H. Vollmer, "Lanthanide and Actinide Chemistry and Spectroscopy," N. H. Edelstein, Ed., (ACS Symposium Series 131), American Chemical Society, Washington, D. C., 1980, pp. 3-29.

41. G. Erker and F. Rosenfeldt, J. Organomet. Chem., 188, C1 (1980).

42. a) R. E. Cramer, R. B. Maynard, J. C. Paw, and J. W. Gilje, Organometallics, 1, 869 (1982);
b) $Cp_2Zr(COCHPPh_3)Cl$ has also been reported but has not been structurally characterized.

43. J. W. Moore and R. G. Pearson, "Kinetics and Mechanism," John Wiley and Sons, New York, 1981, p. 304.

44. See Chapter 2 of this thesis.

45. a) R. Signer, Justus Liebigs Ann. Chem., 478, 246 (1930);
b) E. P. Clark, Ind. Eng. Chem. Anal. Ed., 13, 820 (1941).

46. R. H. Marvick and H. H. Brintzinger, J. Amer. Chem. Soc., 93, 2046 (1971).

47. D. M. Roddick, M. D. Fryzuk, P. F. Seidler, and J. E. Bercaw, manuscript in preparation.

48. J. E. Bercaw, Adv. Chem. Ser., No. 167, 136 (1978).

49. J. Manriquez, Ph.D. Dissertation, California Institute of Technology, Pasadena, CA, 1976.

50. R. Threlkel, Ph.D. Dissertation, California Institute of Technology, Pasadena, CA, 1980.

51. R. Köster, D. Simič, and M. A. Grassberger, Liebigs Ann. Chem., 739, 211 (1970).

52. The program LATCON, taken from the XRAY-76 system of crystallographic programs, was used; XRAY-76: J. M. Stewart, Ed., Technical Report TR-446 of the Computer Science Center, University of Maryland, College Park, MD.

53. The CRYM package of crystallographic programs was used. In least-squares the quantity minimized is $\sum\omega[F_o^2 - (F_c/k)^2]^2$ with

$\omega = \sigma^{-2}(F_o^2)$. Scattering factors for Zr were taken from the International Tables for X-ray Crystallography, Kynoch Press, Birmingham, England, Vol. IV, 1974, pp. 71-98; for P, O, and C from ibid., Vol. III, 1962, pp. 202-205; and for H from R. F. Stewart, E. R. Davidson, and W. T. Simpson, J. Chem. Phys., 42, 3175 (1965). The Zr scattering factors were corrected for anomalous dispersion, International Tables, Vol. IV, 1974, pp. 148-150.

54. K. N. Trueblood, Acta Cryst., A34, 950 (1978).

CHAPTER 4

The Reaction of Permethylzirconocene and Permethylhafnocene Alkyls and Hydrides with Diazoalkanes and Their Derivatives

4.1 Introduction

4.1.1 General Introduction

Diazoalkanes ($R_2C{=}N{=}N$) have been used extensively as carbene ($R_2C{:}$) transfer reagents in organic synthesis. Numerous reports indicate that Group VI-VIII transition metal complexes also react with diazoalkanes. In some cases, loss of molecular nitrogen leads to the production of free or coordinated carbene reaction products.[1] In other cases, the diazoalkane molecule remains intact and diazoalkane-metal complexes are isolated.[2] At the time this project was begun, no report of the reaction of an early transition metal complex (Groups III-V) with a diazoalkane had appeared in the literature.

We sought to investigate the reactivity of diazoalkanes with permethylzirconocene and permethylhafnocene hydride and alkyl compounds in hope of observing or isolating metal-carbene or carbene-insertion products. As discussed in Chapter 3, reaction of permethylzirconocene or permethylhafnocene dihydride with CH_2PMe_3 leads to products in which methylene inserts into a metal-hydride bond. No intermediates are observed in these reactions, however. Hopefully, a zirconium- or hafnium-diazoalkane intermediate could be observed which would decompose by loss of N_2 to afford carbene reaction products. This chapter describes the reaction of permethylhafnocene and permethylzirconocene alkyl and hydride complexes with $R_1R_2C{=}N{=}N$ (R_1 = H, R_2 = Tol; R_1 = Tol, R = Tol) to give products in which the diazoalkane molecule inserts into a metal-carbon or metal-hydride bond. The spectral and crystal structure data indicate that these complexes are best formulated as permethylmetallocene-hydrazonido

species in which the hydrozonido ligand is η^2-N, N′-bonded to the metal center.

4.1.2. Reaction of Zirconocene Hydride and Alkyl Complexes with Diphenyldiazomethane

During the course of this study, Floriani reported the reaction of diphenyldiazomethane with $[Cp_2Zr(H)Cl]_x$ and Cp_2ZrMe_2 to afford the η^2-N, N′-hydrazonido complexes 1 and 2 (equations 1 and 2).[3] No

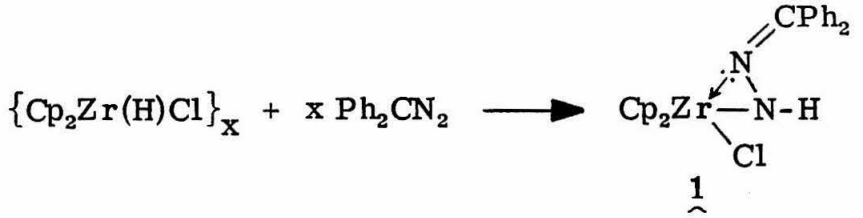

$$\{Cp_2Zr(H)Cl\}_x + x\,Ph_2CN_2 \longrightarrow Cp_2Zr(Cl)(N(CPh_2)-N-H) \quad (1)$$

1

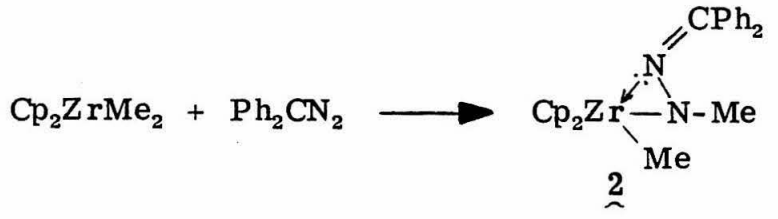

$$Cp_2ZrMe_2 + Ph_2CN_2 \longrightarrow Cp_2Zr(Me)(N(CPh_2)-N-Me) \quad (2)$$

2

products attributable to carbene insertion into the zirconium-hydride or zirconium-methyl bond were observed. The crystal structure of the methyl complex 2 indicates that the diazoalkane molecule has inserted into a zirconium-methyl bond to afford an η^2-N, N′-hydrazonido complex in which the terminal nitrogen atom of the hydrazonido ligand (N(2)) occupies the central equatorial coordination position. The formation of 1 and 2 is unusual in that reaction of diazoalkanes with metal-hydrido or metal-alkyl complexes normally affords 1, 4-addition products, not 1, 2-addition products as observed by Floriani. These compounds were found to be unreactive toward carbon monoxide and

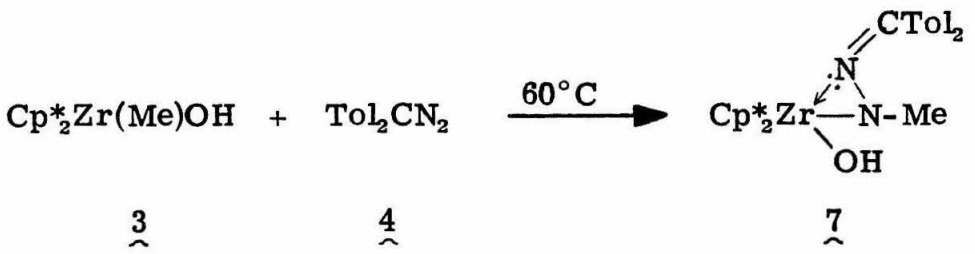

(3)

3 4 7

were stable toward loss of N_2 at moderate temperatures.

4.2 Results and Discussion

4.2.1 Reaction of Permethylzirconocene Methyl-Hydroxide with Bis(p-tolyl)diazomethane

Treatment of the monoalkyl complex $Cp^*_2Zr(Me)OH$ (3) with one equivalent of bis(p-tolyl)diazomethane (4) at 60°C affords the η^2-N, N'-hydrazonido-hydroxide complex (7) quantitatively by ^1H NMR spectroscopy (eq. 3). Compound 7 can be isolated as a lemon-colored solid in 47% yield by recrystallization from petroleum ether. The ^1H NMR spectrum of 7 displays a single resonance at δ 1.90 for the η^5-$C_5(CH_3)_5$ protons, a resonance at δ 2.86 assigned to the NCH_3 protons, and resonances characteristic of two inequivalent tolyl ligands. The presence of the hydroxyl ligand is confirmed by an OH proton resonance at δ 2.60[4] and an O-H stretch at 3695 cm^{-1} in the IR spectrum.

4.2.2 Crystal Structure of $Cp^*_2Zr(NMeNCTol_2)OH$ (7)

The structure of $Cp^*_2Zr(NMeNCTol_2)OH$ (7) was confirmed by X-ray diffraction methods. Yellow crystals of 7 grown from benzene are monoclinic, crystallizing in the space group $P2_1/n$ with four molecules per unit cell. The pertinent crystal data are summarized in Table 4.1. 6116 independent data were collected with $3.5° < 2\theta < 44°$ ($\pm h, k, \ell$). Using anisotropic Gaussian amplitudes for all nonhydrogen atoms, least-squares refinement gave R = 0.051 (3798 $F_o^2 > 3\sigma_{F^2}$) and a goodness-of-fit of 1.94.

The molecular structure of $Cp^*_2Zr(NMeNCTol_2)OH$ (7) is presented in Figure 4.1 and a skeletal view of the immediate ligation about

TABLE 4.1. Crystal Data for $Cp^*_2Zr(NMeNCTol_2)OH$ (7).

Formula	$C_{36}H_{48}N_2OZr$
Formula Weight	616.02
Space Group	$P2_1/n$
a	10.935(3) Å
b	20.557(6) Å
c	14.777(3) Å
β	90.09(2) Å
v	3321.7(15) $Å^3$
z	4
ρ_{calcd}	1.23 g/cm^3
Crystal Size	0.30× 0.35× 0.70 mm

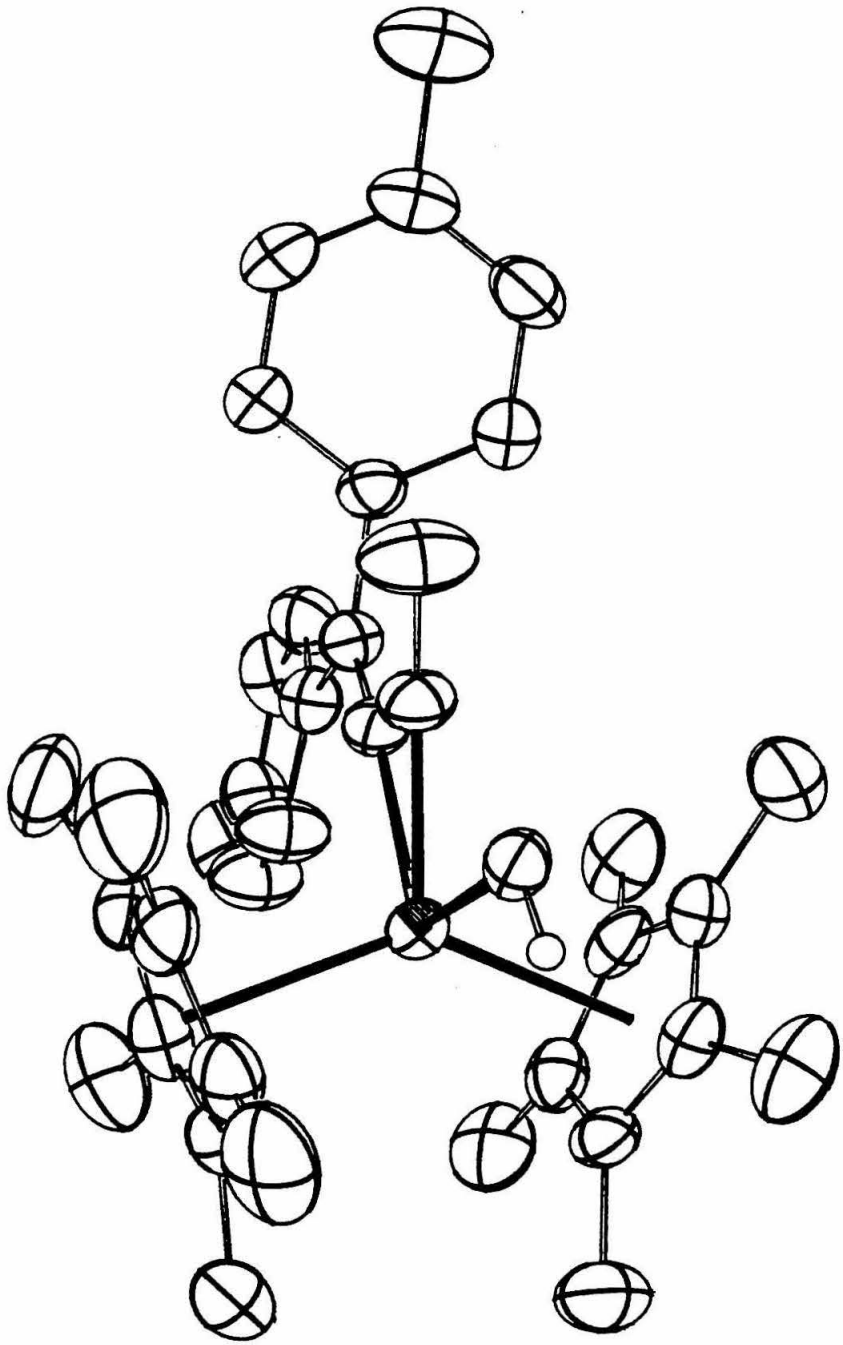

FIGURE 4.1. Molecular Configuration of $Cp^*_2Zr(NMeNCTol_2)OH$ (7).

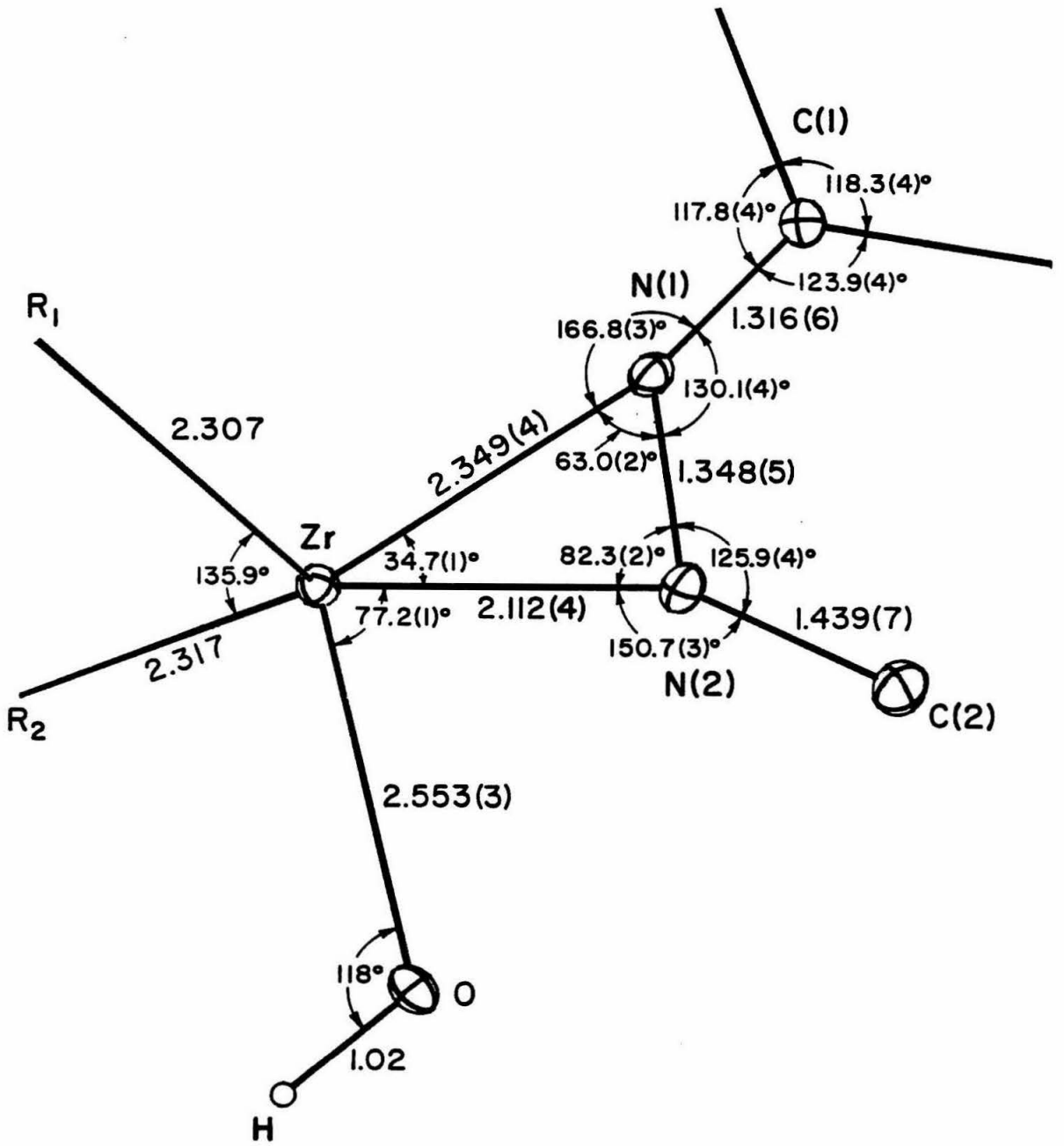

FIGURE 4. 2. Skeletal View of $Cp^*_2Zr(NMeNCTol_2)OH$ (7). [a]

[a]Bond distances are in Å.

zirconium with relevant bond distances and bond angles is given in Figure 4.2. The hydrazonido ligand is coordinated to the zirconium in an η^2-(N, N′) fashion with the N(2) atom occupying the central equatorial position.[6] The O-H hydrogen atom, although not refined, was located from the ΔF map and extends into the equatorial "wedge" formed by the pentamethylcyclopentadienyl ligands.

The structure of 7 is quite similar to that of $Cp_2Zr(NMeNCPh_2)Me$ (2) reported by Floriani.[3] The Zr-N(1) (2.349(4) Å) and Zr-N(2) (2.112(4) Å) bond distances compare with those observed for 2 (Zr-N(1), 2.283(3); Zr-N(2), 2.103(3)). In both cases, the Zr-N(central) bond distance is shorter than the Zr-N(lateral) bond distance, implying a greater interaction between the zirconium and nitrogen (central) atoms. The Zr-N(2) bond distance in 7 would be expected to be shorter than the Zr-N(1) distance, since the former bond results from a sigma interaction whereas the latter results from a dative interaction. A purely dative Zr-N interaction has been observed in the zirconium-ketene compound $Cp^*_2Zr(OCCH_2)pyr$, which exhibits a Zr-N bond distance of 2.403(1) Å.[7] The N(1)-C(1) bond distance of 1.316(6) Å in 7 is characteristic of a N=C double bond,[8] but the N(1)-N(2) distance of 1.348(5) Å is intermediate between an N-N single (1.45 Å)[8] and N=N double (1.25 Å) bond,[8,9] implying some electronic delocalization over the C-N-N unit. The Zr, O, H, N(1), N(2), and C(1) atoms are approximately coplanar with the greatest deviation from planarity observed for the N(2) (0.091 Å) and H (0.087 Å) atoms. A review of the crystallographic literature establishes that the Zr-O bond distance of 2.553(3) Å in 24 is the longest Zr-O distance yet reported.[10]

Typical Zr-O bond distances for complexes which exhibit a Zr-O sigma interaction are 2.1-2.3 Å.[11] Apparently, electron donation from the two nitrogen atoms to the zirconium results in a rather substantial charge accumulation at the metal center and a formally closed shell configuration, resulting in a decrease in the zirconium-oxygen π interaction. It is also interesting that the O-H hydrogen atom extends toward the equatorial "wedge" formed by the pentamethylcyclopentadienyl ligands. Steric interactions between the H atom and the N-Me and Cp^* groups and the very weak (perhaps nonexistent) Zr-O π interaction must dictate this preferred geometry over those in which the H atom extends toward the N(2) atom or toward one of the two Cp^* rings. A substantial electron donation from N(2) to zirconium resulting in a slight positive charge on N(2) may also explain why no N(2)-H hydrogen bonding is observed in this complex.

4.2.3 Mechanism for the Formation of $Cp^*_2Zr(NMeNCTol_2)Me$ (7)

A mechanism proposed for the formation of 7 from 3 and 4 is depicted in Scheme 4.1. The mechanism involves initial nucleophilic attack of the nitrogen lone pair of the more basic terminal nitrogen (N(2)) on the highly electrophilic zirconium (IV) center to afford intermediate 5. Intermediate 5 is drawn so that the incoming diazoalkane molecule interacts with the LUMO in the lateral equatorial coordination position. Migration of the methyl ligand to N(2) via a 1,2-methyl shift affords the η'-N-bonded intermediate 6. Dative coordination of the N(1) nitrogen atom to the zirconium affords the η^2-N,N'-hydrazonido product 7. Rotation about the Zr-N(2) bond must be restricted since

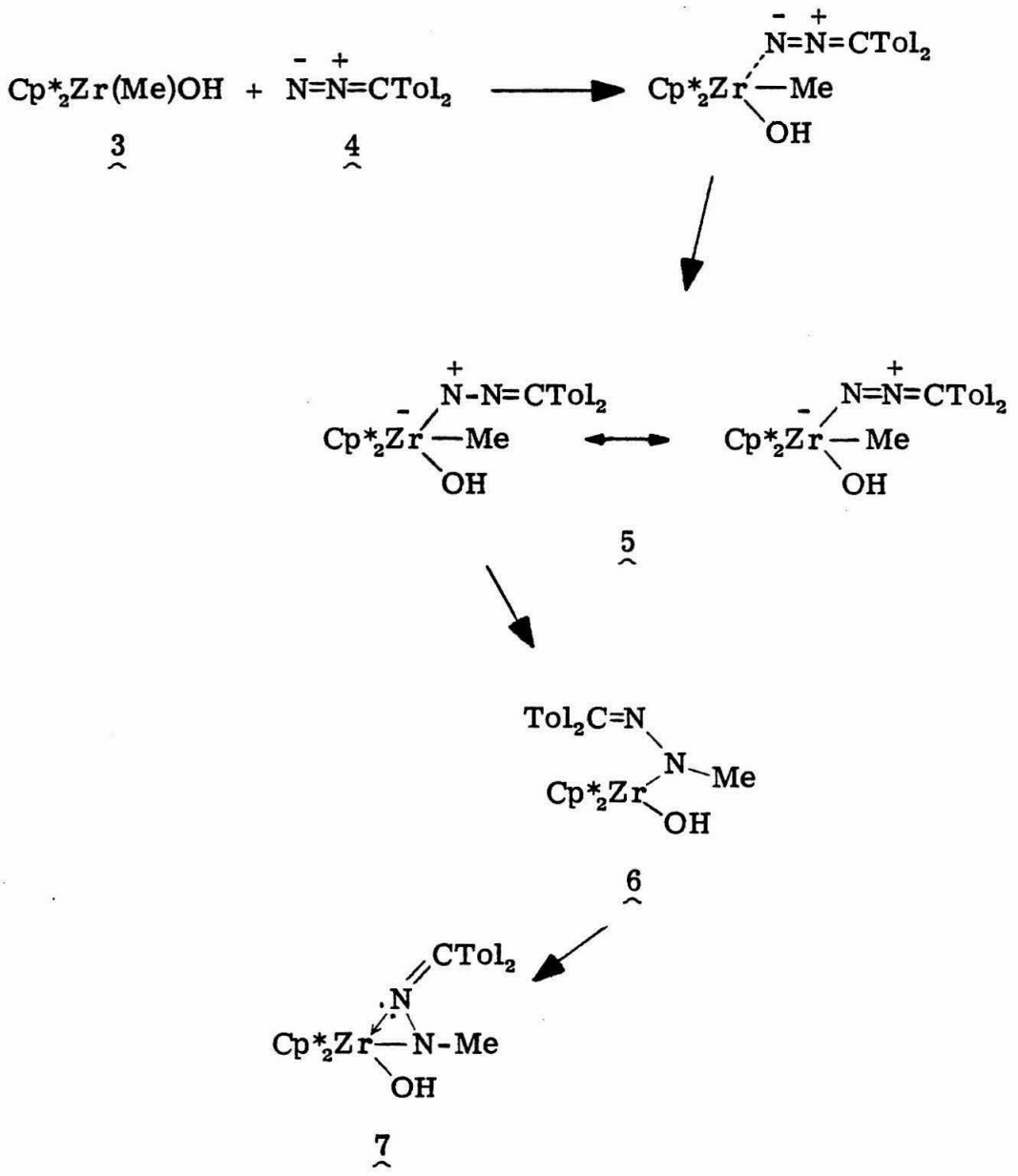

SCHEME 4.1. Mechanism for the Formation of $Cp^*_2Zr(NMeNCTol_2)Me$ (7).

only the N(2)-central isomer is observed as the product. Coordination of the diazoalkane molecule to the lateral bonding position should be favored over coordination to the central bonding position due to in creased overlap between the lateral LUMO's on zirconium and the nitrogen lone pair. Steric constraints imposed by the methyl and hydroxyl ligands may also inhibit nucleophilic attack of the diazoalkane molecule at the central bonding position.

4.2.4 Reaction of Permethylzirconocene Dimethyl with Bis(p-tolyl)diazomethane

$Cp^*_2ZrMe_2$ (8) also reacts with one equivalent of Tol_2CN_2 (4) at 60°C to afford the η^2-N,N'-hydrazonido-methyl complex 9 (eq. 4).

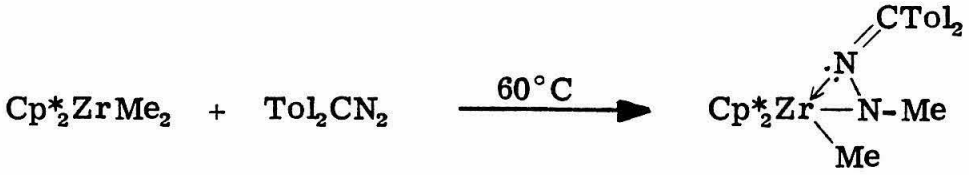

(4)

8 4 9

Complex 9 can be isolated as a yellow-white solid in 56% yield by recrystallization from petroleum ether. A similar compound (2, eq. 2) was prepared by Floriani in the reaction of Cp_2ZrMe_2 with diphenyldiazomethane.[3] The ^1H NMR spectrum of 9 displays a single resonance at δ 2.56 assigned to the NCH_3 protons, and a high field singlet at δ 0.0 consistent with a methyl ligand coordinated to zirconium.[12] Complex 9 does not react with an additional equivalent of Tol_2CN_2 (4) even at 80°C when decomposition of the diazoalkane is rapid. Similar to the reactivity observed for 2,[3] 9 also does not react with H_2 or donor

molecules such as CO. Although the insertion of carbon monoxide into metal-nitrogen bonds is rare,[13] the insertion of CO into metal-carbon bonds of the early transition metals is generally a facile process.[14] Floriani has attributed the nonreactivity of complexes such as 2 and 9 with CO as a consequence of the η^2-N,N′ coordination of the hydrazonido ligand which effectively coordinatively saturates the metal center.[3] Apparently, the electrophilic Zr(IV) center (6, Scheme 4.1) prefers the nucleophilic lone pair on N(1) to carbon monoxide coordination. Considering that N(1) would be expected to be a better σ-donor than CO and remembering that the η^2-N,N′-hydrazonido ligand has the additional stabilization of the chelate effect,[15] it is not surprising that complexes such as 2 and 9 are unreactive toward donor molecules such as CO.

4.2.5 Reaction of Permethylzirconocene Haloalkyl and Haloaryl Complexes with Bis(p-tolyl)diazomethane

The relatively slow rate of reaction between the zirconium methyl complexes $Cp^*_2Zr(Me)OH$ (3) and $Cp^*_2ZrMe_2$ (7) with Tol_2CN_2 (4) (60° C, 12 hours) prompted an investigation of the relative reaction rates between various monosubstituted permethylzirconocene halide complexes and Tol_2CN_2. A series of monoalkyl(aryl) permethylzirconocene bromide complexes were prepared by treating the dibromide, $Cp^*_2ZrBr_2$, with the appropriate Grignard reagent. In this manner, the methyl, ethyl, benzyl, and phenyl complexes were prepared (eq. 5). $Cp^*_2Zr(H)Br$ was prepared by a disproportionation reaction between

$$Cp^*_2ZrBr_2 + RMgX \rightarrow Cp^*_2Zr(R)Br + MgBr(X) \qquad (5)$$

R = Me, Et, Ph; X = Br

R = Ph; X = Cl

$$Cp^*_2ZrBr_2 + Cp^*_2ZrH_2 \xrightarrow[2\ \text{weeks}]{120^\circ C} 2\,Cp^*Zr(H)Br \qquad (6)$$

$Cp^*_2ZrBr_2$ and $Cp^*_2ZrH_2$ (eq. 6), analogous to the procedure used in the synthesis of $Cp^*_2Zr(H)Cl$.[16]

Treatment of the $Cp^*_2Zr(R)Br$ (R = H, Me, Et, CH_2Ph, Ph) derivatives with Tol_2CN_2 affords the respective η^2-N,N'-hydrazonido complexes quantitatively by ^1H NMR spectroscopy (eq. 7). These compounds can be isolated as light-colored solids and their formulation is confirmed by elemental analysis and ^1H NMR and IR spectroscopy

$$Cp^*_2Zr(R)Br + Tol_2CN_2 \longrightarrow Cp^*_2Zr\begin{matrix} \diagup \\ \diagdown \end{matrix}\!\!\begin{matrix} N{=}CTol_2 \\ N\text{-}R \\ Br \end{matrix} \qquad (7)$$

R=H, Me, Et, CH_2Ph, Ph

The rates of these reactions were obtained by ^1H NMR spectroscopy at 25°C and are reported as $t_{\frac{1}{2}}$ measurements (Table 4.2). The rate of reaction of the hydride complex with Tol_2CN_2 is extremely fast ($t_{\frac{1}{2}} < 5$ sec); the reaction is complete by the time the reaction solution can be examined by ^1H NMR spectroscopy. The rate of reaction of the phenyl complex with Tol_2CN_2 is extremely slow; complete reaction is obtained only after days at room temperature. Examination of the $t_{\frac{1}{2}}$

TABLE 4.2. $t_{\frac{1}{2}}$ Values for the Reaction of $Cp^*_2Zr(R)Br$ (R = H, Me, Et, CH_2Ph, Ph) with Tol_2CN_2 (4) to Afford $Cp^*_2Zr(NRNCTol_2)Br$.

Compound	$t_{\frac{1}{2}}$ 23°C (min)
$Cp^*_2Zr(H)Br$	$< 8.0 \times 10^{-2}$
$Cp^*_2Zr(Me)Br$	1.4×10^{2}
$Cp^*_2Zr(Et)Br$	2.1×10^{1}
$Cp^*_2Zr(CH_2Ph)Br$	1.0×10^{1}
$Cp^*_2Zr(Ph)Br$	$> 7.2 \times 10^{2}$

[a]Reactions were performed in C_6D_6 and were monitored by ^1H NMR spectroscopy. Solutions were 8.7 M in zirconium complex and 8.7 M in Tol_2CN_2 (4).

values indicates that the relative rates of reaction between monosubstituted permethylzirconocene bromide complexes and Tol_2CN_2 is hydride $\gg$ benzyl $>$ ethyl $>$ methyl $\gg$ phenyl.

The rates of the migratory insertion reactions observed in this system are best viewed as controlled by the migratory aptitude of the transfering groups and by the initial rate (or preequilibrium) of coordination of the diazoalkane molecule to the metal center. As evident from intermediate $\underset{\sim}{6}$ in Scheme 4.1, if the migrating group transfers with its electron pair, electron donating groups should migrate more readily than electronegative groups. Since hydride and alkyl groups are less electronegative than aryl groups,[17] hydride and methyl should migrate faster than phenyl. Several reports indicate this to be the case. Methyl has been found to migrate faster than phenyl in the formation of zirconocene acyl complexes from dialkyl precursors and CO.[18] The migratory insertion of various groups into a niobocene-carbene bond follows the order H $>$ Me $>$ CH_2Ph,[19] precisely what is predicted on the basis of increasing electronegativity within this series.[17] Thus, it is not surprising that in the hydrazonido system, the hydride complex reacts much more rapidly than the phenyl complex. On the basis of electronegativities, the methyl and ethyl complexes should react more rapidly than the benzyl complex; the opposite order of reactivity is observed. This may be due to the rate (or position of the preequilibrium) of coordination of the diazoalkane molecule to the metal center. Since this process is believed to occur by nucleophilic attack of a nitrogen (N(2)) lone pair on the electrophilic zirconium(IV) center, electron donating ligands on zirconium

would inhibit this coordination. Although both methyl and ethyl would be expected to migrate faster than benzyl, the alkyl ligands must substantially reduce the electrophilicity of the zirconium so that initial diazoalkane coordination is inhibited. Apparently, the migratory aptitude of phenyl is so low, that even with the reactivity inhibition imposed by the zirconium alkyl ligands, the reaction of the phenyl complex is slower still. Steric effects may also play some role in this process.

4.2.6 Reaction of Permethylhafnocene and Permethylzirconocene Dihydride with Bis(p-tolyl)diazomethane and its Hydrazone

In an effort to observe whether a diazoalkane would insert into two ligands coordinated to a group (IV) metal, the reaction of Tol_2CN_2 with permethylhafnocene and permethylzirconocene dihydride ($Cp^*_2HfH_2$ (10) and $Cp^*_2ZrH_2$ (17)) was investigated. Treatment of $Cp^*_2HfH_2$ (10) with one equivalent of Tol_2CN_2 (4) at room temperature in toluene solution affords the η^2-N,N'-hydrazonido-hydride complex (12) (eq. 8) quantitatively by ^1H NMR spectroscopy. Complex 12 can be isolated as a yellow solid in 50% yield by recrystallization from petroleum ether. The ^1H NMR spectrum of 12 consists of a single resonance at δ 1.93 for the η^5-$C_5(CH_3)_5$ protons and a broad resonance at δ 5.95 assigned to the NH proton. A broad low field singlet observed at δ 9.62 is characteristic of hafnium hydride ligand resonances.[20] Resonances indicative of two inequivalent tolyl groups are also observed. The IR spectrum of 12 confirms the presence of the NH and HfH protons with a N-H stretch at 3292 cm^{-1} and a Hf-H stretch at

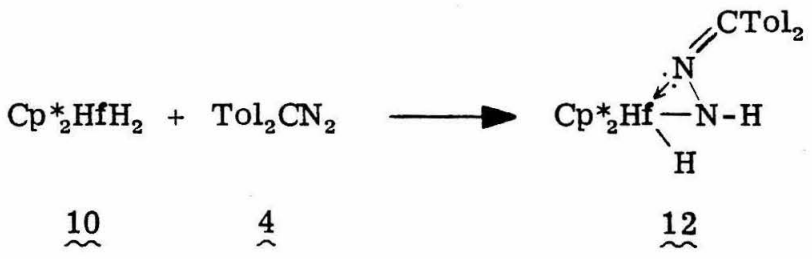

(8)

10 4 12

1620 cm^{-1}. Complex 12 can also be prepared by treating $Cp^*_2HfH_2$ (10) with one equivalent of the hydrazone derivative of 4, Tol_2CNNH_2 (11) (eq. 9). One equivalent of H_2 is liberated in this reaction as evidenced

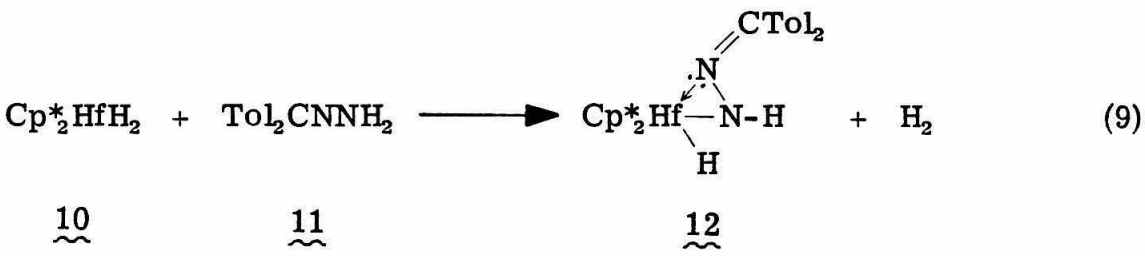

(9)

by Toepler pump analysis of the gas product. This reaction is similar to that used to prepare hafnium amido-hydride complexes, by the reaction of $Cp^*_2HfH_2$ with primary amines,[20b] and hafnium hydroxy-hydride complexes, by the reaction of $Cp^*_2HfH_2$ with water.[5] As with many hydride complexes of hafnium and zirconium, 12 reacts with CH_3I to afford the iodo derivative of 12 (13) and CH_4 (1.0 mol CH_4/mol 12)[21] (eq. 10). The spectral data of 13 are similar to those observed for 12

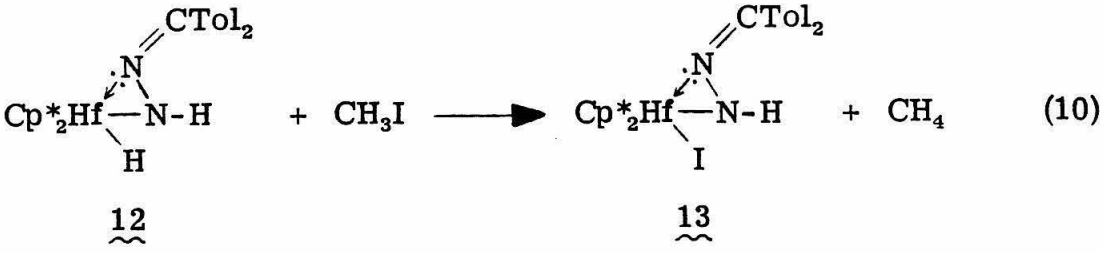

(10)

except for the expected absence of a HfH proton resonance in the ^1H NMR spectrum and a Hf-H stretch in the IR spectrum. Thus, 13 is also formulated as an η^2-N,N′-hydrazonido species.

Although 12 does not react with CO even at elevated temperatures

(80 °C), treatment of 12 with one equivalent of Tol_2CN_2 (4) does afford the bis-hydrazonido complex 16 (eq. 11). Although 16 can only be

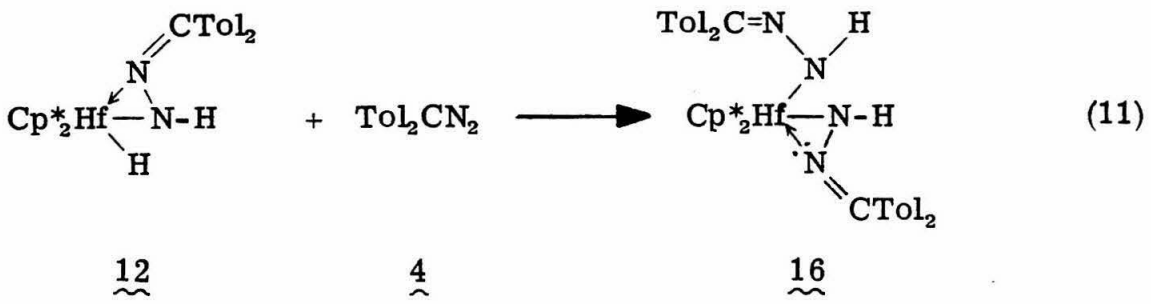

(11)

12 4 16

isolated as an orange oil, elemental analysis of a related zirconium complex (vide infra) suggests a configuration in which two diazoalkane molecules are coordinated to a single metal center. Complex 16 can also be prepared by treating $Cp^*_2HfH_2$ (10) with two equivalents of Tol_2CN_2 (4). The ^1H NMR spectrum of 16 consists of a single resonance at δ 1.88 for the η^5-$C_5(CH_3)_5$ protons and a broad singlet at δ 6.83 assigned to one of the two NH protons. Presumably, the second NH proton resonance is obscured by solvent or tolyl proton resonances. To satisfy the 18-electron rule, 16 is formulated with one hydrazonido ligand coordinated in an η^2-N,N′ fashion and the other in an η'-N fashion. The ^1H NMR spectrum also indicates that 16 is nonfluxional on the NMR time scale at room temperature; no equivalence of the tolyl ligands is observed. The reaction of 12 with 4 contrasts with the stability of the hydrazonido-methyl complex 9 toward a second insertion of diazoalkane.

The insertion of Tol_2CN_2 into the Hf-H bond of 12 probably

requires a vacant coordination site for diazoalkane complexation. The most reasonable method for generating such a site would be to dissociate the N(1) atom of the η^2-N,N'-hydrazonido ligand in an equilibrium step to afford the η^1-N-hydrazonido intermediate 14 (Scheme 4.2). This equilibrium lies to the left, since 12 can be formed with little or no trace of 16 when solutions of $Cp^*_2HfH_2$ are treated with one equivalent of Tol_2CN_2 at room temperature and since no proton resonances attributable to a species such as 14 are present in the ^1H NMR spectrum of 16. The coordinatively unsaturated intermediate 14 then reacts with Tol_2CN_2 to give the diazoalkane adduct 15 in which the N(2) atom of the entering diazoalkane molecule interacts with the LUMO in the lateral equatorial coordination position. Coordination to the lateral position is preferred over coordination to the central position again because of better orbital overlap and because of steric restrictions induced by the hydride and hydrazonido ligands. A 1,2-hydrogen shift followed by dative coordination of the N(1) nitrogen atom as per Scheme 4.1 affords the η^1-N-hydrazonido-η^2-N,N'-hydrazonido product 16. It is noteworthy that although 12 reacts with Tol_2CN_2, no reaction is observed with CO. Since the N(1) atom would be expected to be a better σ-donor than CO, coordination of carbon monoxide may be inhibited. The reaction of 12 with Tol_2CN_2 is probably a consequence of the greater nucleophilicity of the N(2) atom of the entering diazoalkane as compared with that of the N(1) atom of the coordinated hydrazonido ligand.

The reactivity of Tol_2CN_2 with permethylzirconocene dihydride was also investigated. Treatment of $Cp^*_2ZrH_2$ (17) with one equivalent of Tol_2CN_2 (4) affords a mixture of products identified by ^1H NMR

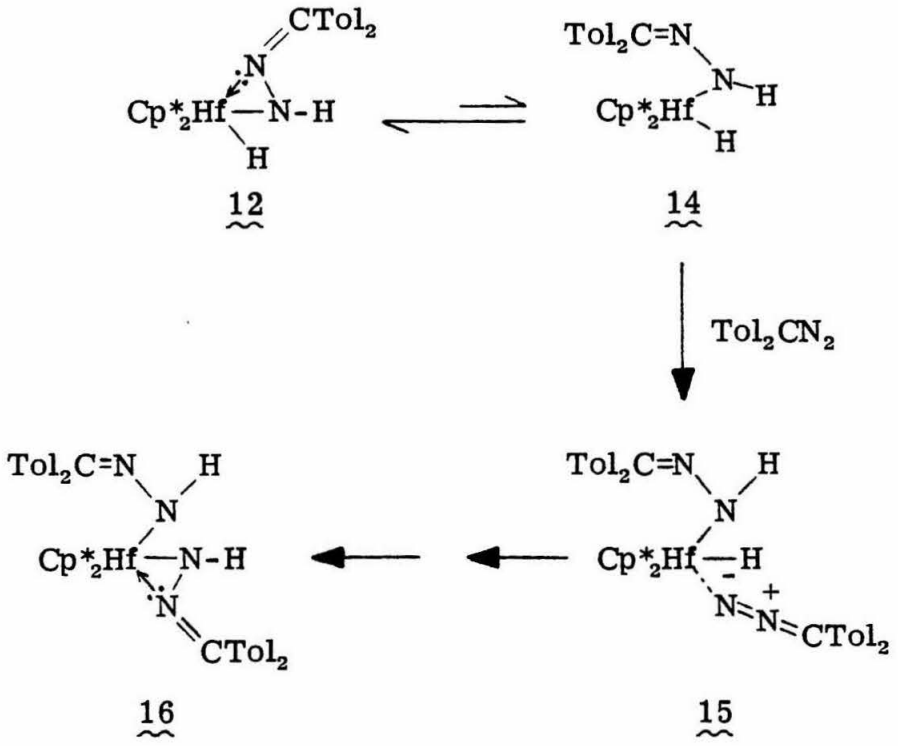

SCHEME 4. 2. Mechanism for the Formation of $Cp^*_2Hf(NHNCTol_2)_2$ (16).

spectroscopy as mono- and bishydrazonido complexes. Even when this reaction is performed at -78°C, the monohydrazonido complex cannot be isolated cleanly. Treatment of 17 with two equivalents of 4 does afford the bishydrazonido complex 18 as an orange oil, quantitatively by ^{1}H NMR spectroscopy (eq. 12). The ^{1}H NMR spectrum of 18

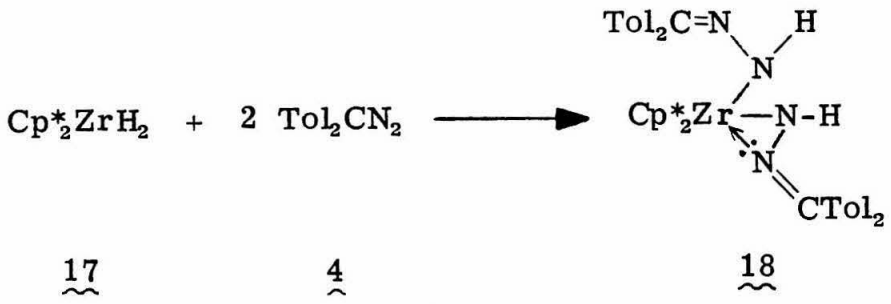

(12)

17 4 18

is similar to that of 16 and, by analogy, 18 is formulated as the η^1-N-hydrazonido-η^2-N,N'-hydrazonido complex. It is not surprising that the monohydrazonido complex cannot be isolated cleanly in the zirconium system. Typically, the hydride complexes of zirconium are found to be more reactive than those of hafnium.[22]

4.2.7 Reaction of Permethylhafnocene and Permethylzirconocene Dihydride with (p-Tolyl)diazomethane and its Hydrazone

In an effort to observe the effects of steric interactions in these insertion reactions, the reaction of $Cp^*_2HfH_2$ with a less bulky diazoalkane was investigated. para-Tolyldiazomethane (TolCHN$_2$ (19)) was chosen for this study because it is one of the least sterically hindered diazoalkanes which is moderately stable at room temperature.

Treatment of $Cp^*_2HfH_2$ (10) with one equivalent of $TolCHN_2$ (19) in toluene solution affords a yellow oil consisting of two products formed in a 70:30 ratio (^1H NMR). The ^1H NMR spectrum of this mixture suggests that these products may be the N(2)-central (22) and N(2)-lateral (23) η^2-N,N'-hydrazonido-hydrides (eq. 13). Resonances

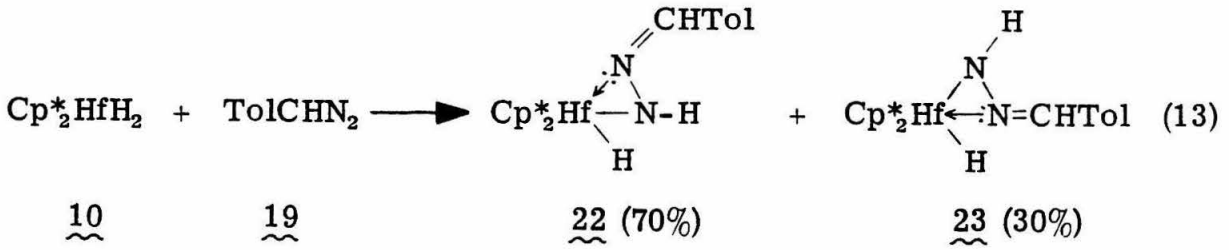

assigned to the N(2)-central configuration (22) include a singlet δ 1.94 (Cp^*), a broad singlet at δ 6.57 (NH), a low field singlet at δ 9.33 characteristic of a hafnium-hydride ligand resonance,[20] and a resonance at δ 7.28 assigned to the CH proton. Typical tolyl resonances are also observed. Resonances assigned to the N(2)-lateral configuration (23) are similar: δ 1.93 (Cp^*), δ 5.50 (NH), δ 8.58 (HfH), δ 7.07 (CH). Although 22 and 23 could be formulated as having the same metal-hydrazonido coordination but different geometries about the nitrogen-carbon double bond, this appears less likely. The ^1H NMR spectra of 22 and 23 are significantly different that a simple rotation about the nitrogen-carbon bond would not account for these differences. Also, because the reaction of diazoalkanes with zirconium and hafnium complexes normally affords N(2)-central coordinated hydrazonido species, 22 (the major product in the 22-23 mixture) is

also formulated as N(2)-central coordinated. The hydrazonido complexes 22 and 23 are similar in configuration to the η^2-C,O-acyl compounds $Cp^*_2Zr(COCHPMe_3)H$ (oxygen-central) and $Cp^*_2Zr(COCHPMe_3)H$ (oxygen-lateral).[11b] Unlike the η^2-acyl compounds, 22 and 23 do not interconvert; the 22:23 ratio of 70:30 (formed upon mixing 10 and 19) does not change when solutions of the 22-23 mixture are heated at 80° C. Also, complex 23 can be isolated cleanly by another route (vide infra) and does not isomerize to the N(2)-central species 22 when heated.

The 22-23 mixture does react with CH_3I to afford a yellow powder 24 and methane (eq. 14). The ^1H NMR spectrum of 24 indicates

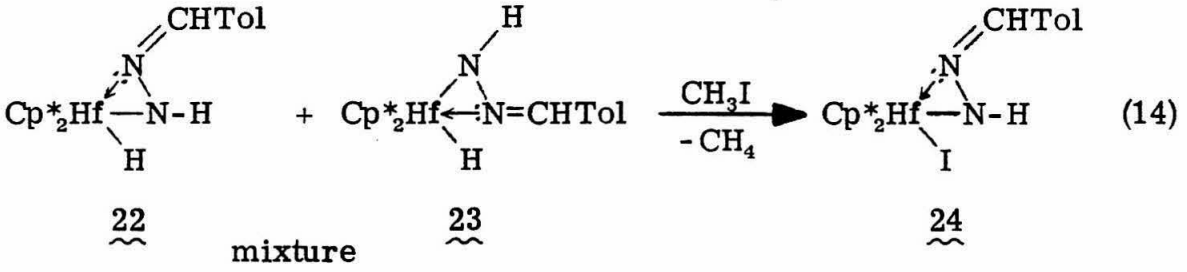

(14)

only a single species in solution. Because of the similarity between the ^1H NMR spectrum of 22 and 24, complex 24 is formulated as the N(2)-central isomer.

In an attempt to prepare the N(2)-central η^2-N,N'-hydrazonido complex 22 cleanly, the hydrazone derivative of 19 ($TolCHNNH_2$ (20)) was employed. A reaction similar to that observed for $Cp^*_2HfH_2$ and Tol_2CNNH_2 (equation 9) was expected. Unlike $TolCHN_2$ (19) (which is a metastable liquid at room temperature),[23] the hydrazone 20 is a stable

white solid. Treatment of $Cp^*_2HfH_2$ (10) with one equivalent of 20, however, affords the N(2)-lateral complex 23 and H_2 (eq. 15). The ^1H NMR spectrum of this reaction mixture indicates no resonances

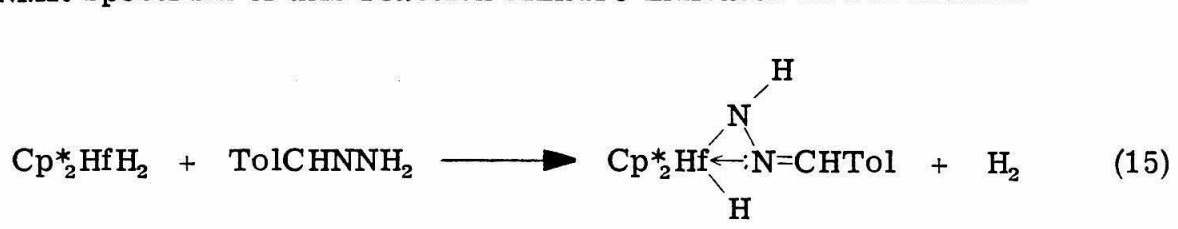

10 20 23 (15)

attributable to the N(2)-central isomer 22. Treatment of 23 with CH_3I affords an intractable mixture of products, explaining why no iodo derivative of 23 is formed when the 22-23 mixture is similarly treated. Steric interactions between the N(2)CHTol moiety and iodide ligand may account for the instability of the iodide derivative of 23.

As previously mentioned, the η^2-N,N′-hydrazonido isomers 22 and 23 do not interconvert. Resonance structures such as those depicted in Figure 4.3 may be responsible for the strength of the Hf-N(2) bonds in these complexes and the inability of 22 and 23 to isomerize from one isomer to another. It is reasonable, then, to suppose that different mechanisms are operative in the formation of each isomer. A likely mechanism for the formation of the N(2)-central isomer 22 would follow the reasoning used in Scheme 4.1 for the formation of 7. In this mechanism, the diazoalkane molecule initially coordinates to a lateral equatorial bonding position. The mechanism proposed for the formation of the N(2)-lateral isomer 23 is depicted in

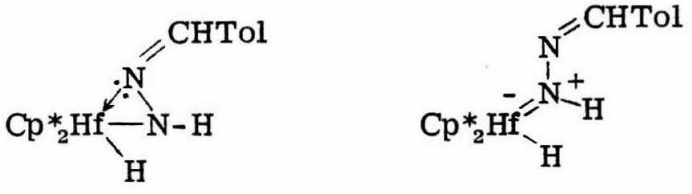

FIGURE 4. 3. $Cp^*_2Hf(NHNCHTol)H$ (22) Resonance Structures.

Scheme 4.3. This mechanism is similar to that of Scheme 4.1, except that the diazoalkane now initially coordinates to the central equatorial bonding position (intermediate 21). A 1,2-hydrogen shift followed by dative coordination of the N(1) atom affords the N(2)-lateral isomer 23. Apparently, $TolCHN_2$ is sufficiently small so that some initial coordination to the central position on hafnium is possible. Tol_2CN_2 (4), however, must be too sterically hindered for favorable coordination to the central position (cf. eq. 8). The reaction of $Cp^*_2HfH_2$ (10) with $TolCHNNH_2$ (20) to afford 23 is unusual in that only a single isomer (N(2)-lateral) is observed. It is not clear whether this process involves prior coordination of the diazoalkane molecule or simply a concerted loss of H_2.

Treatment of the 22-23 mixture with a second equivalent of $TolCHN_2$ (19) affords the bishydrazonido complex 25 (Scheme 4.4). Complex 25 is conveniently prepared by treating $Cp^*_2HfH_2$ (10) with two equivalents of $TolCHN_2$ (19) in toluene solution and is isolated as a yellow solid in 51% yield by recrystallization from petroleum ether. Elemental analysis suggests a formulation in which two diazoalkane molecules are coordinated to one hafnium center. The ^1H NMR spectrum of 25 consists of an η^5-$C_5(CH_3)_5$ proton resonance at δ 1.83, two NH proton resonances at δ 7.10 and δ 6.29, two methyne proton resonances at δ 7.42 and δ 7.10, and resonances characteristics of two inequivalent tolyl groups. Thus, the bishydrazonido complex is probably nonfluxional on the NMR time scale. Two N-H stretches are also observed in the IR spectrum at 3300 cm^{-1} and 3180 cm^{-1}. It is interesting that both N(2)-central (22) and N(2)-lateral (23) hydrazonido

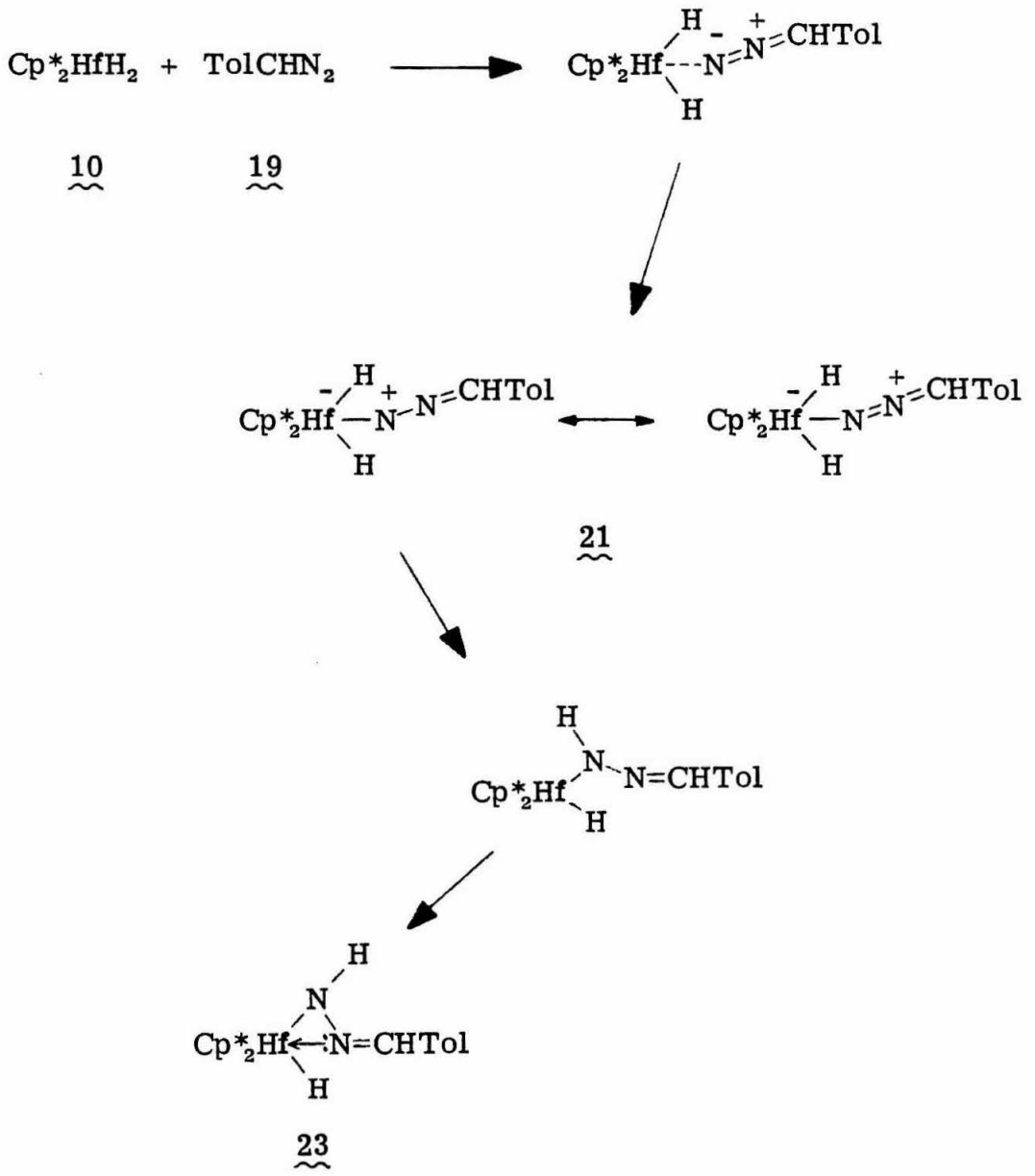

SCHEME 4. 3. Mechanism for the Formation of $Cp^*_2Hf(NHNCHTol)H$ (23).

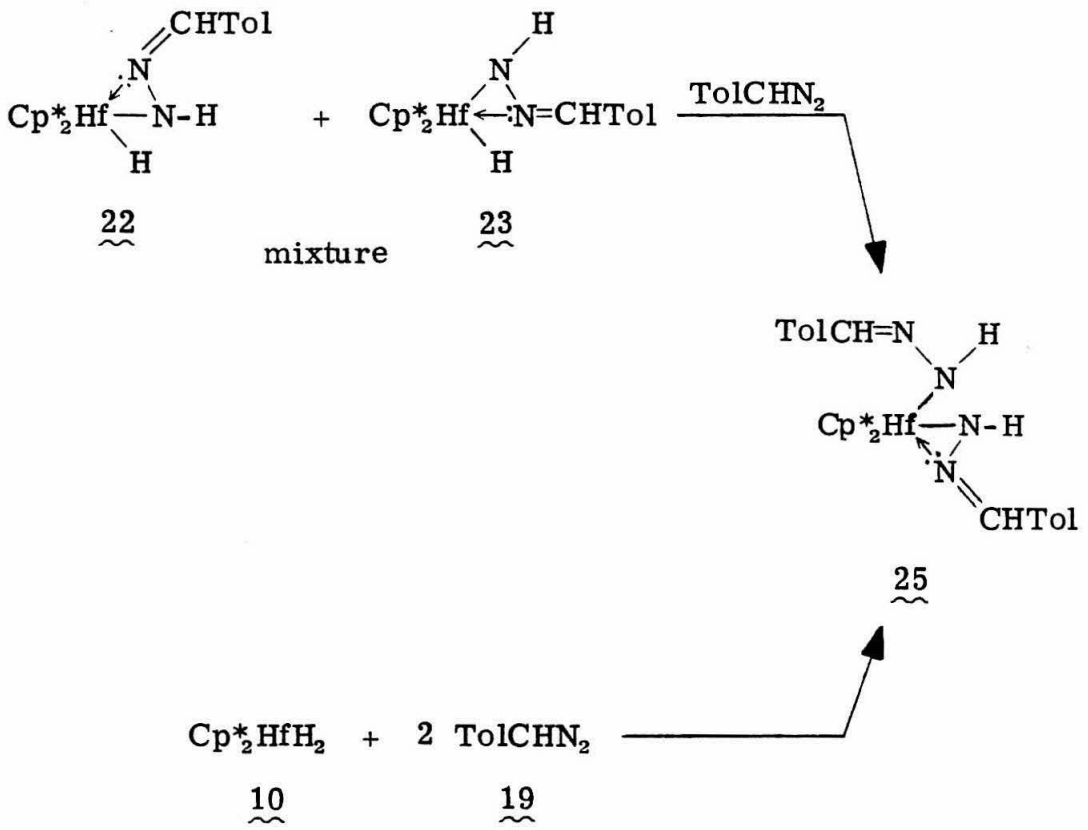

SCHEME 4.4. Synthesis of $Cp^*_2Hf(NHNCHTol)_2$ (25).

complexes afford the same bishydrazonido species. Apparently, once initial coordination of the second diazoalkane molecule is achieved, rotation about the Hf-N bond of the previously coordinated diazoalkane is a facile process. Steric interactions in the hafnium coordination group probably affect this rotation.

4.3 Conclusion

The results of this chapter indicate that permethylhafnocene and permethylzirconocene complexes react with diazoalkanes and their derivatives to afford η^2-N,N'-hydrazonido species. These reactions formally represent the insertion of a diazoalkane molecule into hafnium and zirconium hydride and carbon bonds. No carbene-insertion products are observed in these reactions. The hydrazonido complexes are extremely stable to substrates such as H_2 and CO, but the hydride complexes readily react with a second equivalent of diazoalkane to afford bishydrazonido compounds. Rate studies for the reaction of permethylzirconocene haloalkyl and haloaryl complexes with bis(p-tolyl)diazomethane suggest that these insertion reactions are governed by the migratory aptitude of the transferring group and by the rate (or preequilibrium) of initial complexation of the diazoalkane to the metal center.

4.4 Experimental Section

4.4.1 General Methods

All manipulations involving air sensitive compounds were performed in an inert atmosphere using high vacuum line or glove box techniques. Argon was passed through MnO on vermiculite and 4 Å molecular sieves.

4.4.2 Physical and Spectroscopic Methods

Proton magnetic resonance spectra were recorded using a Varian EM390 spectrometer. Chemical shifts are reported in ppm (δ) relative to Me_4Si (δ 0.0). Infrared spectra were recorded using NaCl plates on a Beckman 4240 spectrometer.

Molecular weight determinations (by osmometry) and elemental analyses were performed by the Alfred Bernhardt or Dornis and Kolbe Analytical Laboratories.

4.4.3 Solvents and Reagents

Solvents used with air-sensitive compounds were distilled first from $LiAlH_4$ and then from "titanocene".[24] Benzene-d_6 was also distilled from titanocene. Methyl iodide was vacuum transferred from CaH_2.

The following compounds were prepared by the literature procedures: $Cp^*_2ZrMe_2$,[12a] $Cp^*_2ZrBr_2$,[7] $Cp^*_2Zr(Me)Br$,[7] $Cp^*_2HfH_2$,[25] $Cp^*_2ZrH_2$,[26] $TolCHN_2$,[26] $TolCHNNH_2$.[26]

4.4.4 $Tol_2C{=}N{-}NH_2$ (11)

The method of preparation was a modification of that for benzophenone hydrazone.[27] 4,4'-Dimethylbenzophenone (5.0 g, 24 mmol) was suspended in 40 mL absolute ethanol. Via pipette, hydrazine (5.0 g, 0.15 mol) was added slowly to the stirred benzophenone mixture and when addition was complete, the solution was brought to reflux and maintained at this temperature for 12 hours. Upon heating, the solid dissolved and the solution became cloudy and orange in color. The solution was then cooled at 0° C for 12 hours. White crystals of 11 precipitated which were isolated by filtration and washed with cold absolute ethanol (3.6 g, 67%) ^{1}H NMR (benzene-d_6): δ 7.72 (d, $^3J_{HH}$ = 9.9 Hz, 2H, Tol); 7.10-6.85 (m, 6H, Tol); 5.01 (s, 2H, NH_2); 2.05 (s, 6H, Tol).

4.4.5 $Tol_2C{=}N{=}N$ (4)

The method of preparation was a modification of that for diphenyldiazomethane.[27] $Tol_2C{=}N{-}NH_2$ (11) (3.6 g, 16 mmol) and HgO (4.5 g, 21 mmol) were suspended in 25 mL pet. ether and the mixture stirred under an argon atmosphere for 9 hours. The reaction solution was filtered through Celite, quickly dried over $MgSO_4$, and again filtered to remove the drying agent. The solvent was removed with a rotary evaporator to afford 4 as a purple crystalline solid (2.0 g, 56%). ^{1}H NMR (benzene-d_6): δ 7.07-6.85 (m, 8H, Tol); 2.07 (s, 6H, Tol).

4.4.6 $Cp^*_2Zr(Me)OH$ (3)

$Cp^*_2ZrMe_2$ (8) (300 mg, 0.77 mmol) was dissolved in THF (25 mL) and the solution cooled to -78°C. With rapid stirring,

770 μL of a solution of H_2O in THF (1.0 M, 0.78 mmol) was added to the zirconium solution via syringe and the mixture allowed to warm slowly to room temperature and stir for 12 hours. The solvent was reduced to 10 mL, the solution filtered, and the toluene removed in vacuo. The residue was triterated with pet. ether (4 mL), the suspension cooled to -78°C and then filtered at this temperature to afford 8 as a white crystalline solid (250 mg, 83%). Anal. Calcd for $C_{21}H_{34}OZr$: C, 64.06; H, 8.70; Zr, 23.17. Found: C, 63.84; H, 8.72; Zr, 22.91. ^{1}H NMR (benzene-d_6): δ 4.20 (s, 1H, OH); 1.80 (s, 30H, $C_5(CH_3)_5$); -0.2 (s, 3H, $ZrCH_3$).

4.4.7 $Cp^*_2Zr(NMeNCTol_2)OH$ (7)

$Cp^*_2Zr(Me)OH$ (3) (230 mg, 0.58 mmol) and Tol_2CN_2 (4) (137 mg, 0.62 mmol) were suspended in toluene (15 mL) at -78° C. The mixture was warmed to room temperature and then heated at 50°C for 2 days, after which time the toluene was removed from the light orange-colored solution in vacuo to give an orange oil. The oil was triturated with pet. ether (5 mL) which effected precipitation of a lemon-colored solid. Filtration of the mixture at room temperature afforded 7 as a light-yellow powder (170 mg, 47%). Anal. Calcd for $C_{36}H_{48}N_2OZr$: C, 70.19; H, 7.85; N, 4.55; Zr, 14.81. Found: C, 70.31; H, 7.90; N, 4.61; Zr, 14.87. ^{1}H NMR (benzene-d_6): δ 7.68 (d, $^3J_{HH}$ = 9.2 Hz, 2H, Tol); 7.35 (d, $^3J_{HH}$ = 9.2 Hz, 2H, Tol); 7.02 (d, $^3J_{HH}$ = 9.2 Hz, 2H, Tol); 2.86 (s, 3H, NCH_3); 2.60 (s, 1H, OH); 2.20 (s, 6H, Tol); 2.14 (s, 6H, Tol); 1.90 (s, 30H, $C_5(CH_3)_5$).[13] The remaining aromatic tolyl resonances were obscured by solvent. IR (nujol): ν(OH) 3695 cm^{-1}.

4.4.8 Crystal Structure of $Cp^*_2Zr(NMeNCTol_2)OH$ (7)

Yellow crystals of $Cp^*_2Zr(NMeNCTol_2)OH$ (7) grown from benzene were mounted in glass capillaries under a nitrogen atmosphere. A series of oscillation and Weissenberg photographs established the crystals as monoclinic, and the systematic absences (OkO for k odd, hOℓ for k+ℓ odd) indicated the space group $P2_1/n$. Crystal data are summarized in Table 4.1. Lattice constants were obtained from the least-squares refinement of twenty-nine 2θ values ($20 < 2\theta < 36°$).[28]

A total of 6116 reflections were collected on a locally modified Syntex $P2_1$ diffractometer and included blocks of three check reflections measured after each 97 reflections. No decomposition was observed and the data were corrected for Lorentz and polarization effects. Observational variances, $\sigma^2(F_{\sigma 2})$, were based on counting statistics with the additional term $(0.02 \times \text{scan counts})^2$.

The zirconium atom coordinates were derived from the Patterson map and the subsequent Fourier maps revealed the remaining atoms. Hydrogen atoms were introduced at idealized positions with the aid of ΔF maps and the coordinates and Gaussian amplitudes were fixed. The O-H hydrogen atom was located on the ΔF maps.

The final difference map indicated no peaks greater than 0.7 $e^- Å^{-3}$. Details concerning the data collection and the final cycle of refinement[29] are given in Table 4.3. Fractional atomic coordinates and U_{ij}'s are given in Table 4.4. Final hydrogen atom coordinates and B's are given in Table 4.5. Bond distances and bond angles are given in Tables 4.6 and 4.7, respectively. Least-squares planes of the pentamethylcyclopentadienyl and tolyl rings are given in Table 4.8 and

TABLE 4.3. Data Collection and Refinement Conditions for $Cp^*_2Zr(NMeNCTol_2)OH$ (7).

λ	0.71069 Å (MoK_α, graphite monochromator)
Scan Method	θ-2θ
Scan Range	1.1° below K_{α_1}
	1.1° above K_{α_2}
2θ Scan Rate	3.91°/min
2θ Limits	3.5-44°
Scan Time/Bkgrd Time	0.2
Number of Reflections[a]	6116, 5546, 3798
R[b] ($F_o^2 > 0$)	0.080
R[b] ($F_o^2 > 3\sigma_{F_o^2}$	0.051
Goodness-of-Fit[c]	1.94

[a]Total number of unique reflections, all reflections with $F_o^2 > 0$, all reflections with $F_o^2 > 3\sigma_{F_o^2}$.

[b]$R = \Sigma||_o|-|F_c||/\Sigma|F_o|$.

[c]Goodness-of-fit = $\{\Sigma w[F_o^2 - (F_c/k)^2]^2/(n_{ref} - n_{par})\}^{\frac{1}{2}}$.

TABLE 4.4. Final Nonhydrogen Atom Parameters for 7 (coordinates x 10^6, U_{ij} ($Å^2$) x 10^4).

	x	y	z	U_{11}	U_{22}	U_{33}	U_{12}	U_{13}	U_{23}
Zr	94078(4)	22302(2)	4650(3)	341(2)	325(2)	301(2)	16(3)	16(2)	−1(2)
O	109820(28)	16315(13)	14335(19)	440(20)	265(18)	476(19)	13(16)	127(16)	−33(14)
N(1)	90733(34)	32952(18)	9841(22)	352(22)	465(26)	288(21)	10(21)	−50(17)	−8(18)
N(2)	98436(36)	29217(18)	14726(23)	463(25)	522(29)	322(21)	22(22)	−86(19)	−52(19)
C(1)	87447(43)	39053(22)	11000(28)	385(27)	379(30)	358(26)	−13(24)	10(22)	−21(22)
C(2)	103461(61)	30827(26)	23449(35)	961(50)	607(37)	535(35)	185(37)	−306(35)	−48(28)
C(11)	113189(44)	26546(23)	−3944(30)	402(28)	518(36)	417(27)	−68(27)	97(22)	2(25)
C(12)	112559(47)	19786(22)	−5936(32)	428(30)	435(32)	471(30)	114(26)	129(25)	24(24)
C(13)	102225(47)	18648(23)	−11121(29)	526(33)	394(30)	324(26)	−41(27)	97(24)	−41(22)
C(14)	96073(45)	24651(24)	−12398(30)	373(28)	604(34)	326(26)	21(25)	31(22)	59(22)
C(15)	103191(48)	29431(22)	−8223(30)	573(34)	371(32)	404(27)	25(26)	235(25)	26(22)
C(21)	123305(54)	29924(28)	1011(38)	574(38)	862(46)	701(38)	−231(35)	60(32)	−63(32)
C(22)	122865(57)	15059(30)	−4468(38)	650(41)	865(45)	716(40)	282(38)	154(34)	42(34)
C(23)	100127(59)	12382(27)	−16388(37)	839(47)	596(38)	658(37)	−104(37)	65(35)	−200(30)
C(24)	85876(56)	25881(29)	−18908(33)	692(41)	1017(49)	404(31)	66(38)	−25(29)	100(29)
C(25)	101667(61)	36757(27)	−9395(39)	896(49)	508(37)	803(40)	−39(36)	324(37)	144(31)
C(31)	73112(46)	21043(24)	12863(33)	468(31)	531(37)	537(31)	−88(28)	206(25)	−63(27)
C(32)	80555(48)	16025(26)	16012(31)	521(34)	652(38)	390(29)	−103(31)	101(26)	137(27)
C(33)	82688(49)	11730(24)	8780(36)	484(33)	406(32)	706(37)	−50(28)	97(29)	73(28)
C(34)	76285(50)	13991(26)	1309(34)	497(34)	631(38)	553(33)	−253(31)	97(28)	−94(29)
C(35)	70561(47)	19905(25)	3595(36)	378(30)	581(37)	659(36)	−84(27)	67(27)	62(28)
C(41)	67625(59)	26302(30)	18466(44)	775(45)	800(48)	1058(50)	−35(39)	533(40)	−176(39)
C(42)	83838(62)	15032(36)	25715(38)	782(49)	1453(66)	588(39)	−183(49)	47(36)	340(40)
C(43)	88799(66)	5206(29)	9253(51)	799(49)	453(38)	1616(67)	−69(38)	286(49)	176(41)
C(44)	73106(64)	10067(34)	−7162(43)	852(51)	1196(58)	853(45)	−533(47)	230(40)	−411(42)
C(45)	60542(56)	22918(33)	−1941(43)	550(37)	989(50)	1008(48)	−100(42)	−97(35)	224(42)
C(51)	78620(44)	41828(22)	4575(30)	397(28)	402(31)	417(28)	13(25)	21(23)	28(23)
C(52)	72709(55)	38285(25)	−1928(35)	717(41)	474(34)	617(36)	107(33)	−192(32)	−77(28)
C(53)	65052(57)	41665(28)	−8169(37)	745(44)	667(42)	635(37)	121(36)	−228(34)	−113(31)
C(54)	62829(51)	47708(27)	−8231(36)	473(34)	664(41)	604(36)	16(31)	−33(29)	120(30)
C(55)	68321(53)	51268(24)	−1747(39)	572(37)	403(34)	834(42)	45(30)	11(33)	169(30)
C(56)	76139(51)	48519(24)	4638(35)	531(35)	455(35)	618(35)	−39(29)	9(29)	−28(28)
C(57)	54849(63)	50930(30)	−15353(43)	812(49)	835(47)	892(47)	41(43)	−155(41)	306(39)
C(61)	92685(45)	43376(21)	18048(30)	444(29)	332(28)	401(27)	1(25)	10(23)	−46(21)
C(62)	104221(49)	46000(26)	17105(34)	443(32)	723(40)	491(32)	−74(31)	79(26)	−77(28)
C(63)	108941(50)	50314(27)	23400(36)	488(35)	652(39)	623(36)	−213(33)	−62(29)	−31(30)
C(64)	102277(55)	52195(24)	30758(35)	653(40)	439(34)	556(34)	−42(30)	−144(31)	−66(27)
C(65)	90834(57)	49611(31)	31685(38)	637(41)	964(49)	611(38)	−40(40)	152(33)	−409(34)
C(66)	85933(51)	45350(28)	25428(35)	486(34)	808(43)	561(34)	−136(33)	140(28)	−242(31)
C(67)	107189(70)	57016(30)	37596(44)	1128(63)	698(45)	953(50)	−167(45)	−222(47)	−268(38)

TABLE 4. 5. Final Hydrogen Atom Parameters for 7
(coordinates x 10^5, B ($Å^2$).

	x	y	z	B
H	11219	1171	1256	5.00
$H(1C2)$	10930	3433	2280	5.00
$H(2C2)$	9717	3205	2756	5.00
$H(3C2)$	10760	2701	2610	5.00
$H(121)$	12600	3386	−231	5.00
$H(221)$	12080	3125	697	5.00
$H(321)$	13020	2698	177	5.00
$H(122)$	12850	1509	−940	5.00
$H(222)$	12720	1601	99	5.00
$H(322)$	11970	1070	−369	5.00
$H(123)$	9190	1264	−1917	5.00
$H(223)$	10610	1175	−2805	5.00
$H(323)$	10010	871	−1225	5.00
$H(124)$	8544	3032	−2053	5.00
$H(224)$	8700	2324	−2430	5.00
$H(324)$	7819	2432	−1638	5.00
$H(125)$	10440	3900	−414	5.00
$H(225)$	10610	3821	−1477	5.00
$H(325)$	9292	3772	−1062	5.00
$H(141)$	7390	2860	2180	5.00
$H(241)$	6300	2980	1390	5.00
$H(341)$	6200	2470	2250	5.00
$H(142)$	8669	1891	2834	5.00
$H(242)$	7702	1334	2898	5.00
$H(342)$	9048	1157	2612	5.00
$H(143)$	9489	472	474	5.00
$H(243)$	9316	479	1538	5.00
$H(343)$	8234	169	886	5.00
$H(144)$	6484	992	−830	5.00
$H(244)$	7737	1191	−1249	5.00
$H(344)$	7646	557	−654	5.00
$H(145)$	5768	2687	151	5.00
$H(245)$	6338	2441	−756	5.00
$H(345)$	5390	2010	−265	5.00
$H(157)$	5624	5521	−1580	5.00
$H(257)$	5723	4859	−2196	5.00
$H(357)$	4574	4895	−1457	5.00
$H(167)$	11290	5981	3488	5.00
$H(267)$	10040	5963	4006	5.00
$H(367)$	11110	5474	4260	5.00
$H(52)$	7440	3338	−237	5.00
$H(53)$	6082	3826	−1296	5.00
$H(55)$	6659	5616	−154	5.00
$H(56)$	8006	5145	955	5.00
$H(62)$	10948	4469	1158	5.00
$H(63)$	11754	5223	2249	5.00
$H(65)$	8580	5098	3722	5.00
$H(66)$	7733	4355	2629	5.00

TABLE 4.6. Bond Distances for 7 (Å).

Zr-R(1)[a]	2.307	C(31)-C(4)	1.489(8)
Zr-R(2)[b]	2.317	C(32)-C(42)	1.491(8)
Zr-N(1)	2.349(4)	C(33)-C(43)	1.500(9)
Zr-N(2)	2.112(4)	C(34)-C(44)	1.529(9)
Zr-O	2.553(3)	C(35)-C(45)	1.500(8)
Zr-C(11)	2.598(5)	O-H	1.016(3)
Zr-C(12)	2.610(5)	N(2)-C(2)	1.439(7)
Zr-C(13)	2.607(5)	N(2)-N(1)	1.348(5)
Zr-C(14)	2.575(5)	N(1)-C(1)	1.316(6)
Zr-C(15)	2.601(5)	C(1)-C(51)	1.468(6)
Zr-C(31)	2.609(5)	C(1)-C(61)	1.484(6)
Zr-C(32)	2.584(5)	C(51)-C(52)	1.367(7)
Zr-C(33)	2.579(5)	C(52)-C(53)	1.370(8)
Zr-C(34)	2.635(5)	C(53)-C(54)	1.387(8)
Zr-C(35)	2.623(5)	C(54)-C(55)	1.346(8)
C(11)-C(12)	1.422(7)	C(54)-C(57)	1.518(9)
C(12)-C(13)	1.384(7)	C(55)-C(56)	1.392(8)
C(13)-C(14)	1.418(7)	C(51)-C(56)	1.402(7)
C(14)-C(15)	1.396(7)	C(61)-C(62)	1.379(7)
C(11)-C(15)	1.394(7)	C(62)-C(63)	1.384(7)
C(31)-C(32)	1.394(7)	C(63)-C(64)	1.366(8)
C(32)-C(33)	1.406(7)	C(64)-C(65)	1.367(8)
C(33)-C(34)	1.387(7)	C(64)-C(67)	1.513(9)
C(34)-C(35)	1.408(7)	C(65)-C(66)	1.381(8)
C(31)-C(35)	1.417(7)	C(61)-C(66)	1.379(7)

TABLE 4.6 (continued)

C(11)-C(21)	1.497(7)
C(12)-C(22)	1.504(8)
C(13)-C(23)	1.522(7)
C(14)-C(24)	1.493(7)
C(15)-C(25)	1.525(8)

[a]R(1) = C(11)-C(15) ring centroid.

[b]R(2) = C(31)-C(35) ring centroid.

TABLE 4.7. Bond Angles for 7 (°).

R(1)[a]-Zr-R(2)[b]	135.9	C(33)-C(34)-C(35)	108.8(5)
R(1)-Zr-N(1)	103.3	C(34)-C(35)-C(31)	106.7(4)
R(1)-Zr-N(2)	112.0	C(35)-C(31)-C(32)	108.4(4)
R(1)-Zr-O	99.6	C(21)-C(32)-C(42)	124.2(5)
R(2)-Zr-N(1)	105.5	C(42)-C(32)-C(33)	127.2(5)
R(2)-Zr-N(2)	100.8	C(32)-C(33)-C(43)	126.9(5)
R(2)-Zr-O	99.8	C(43)-C(33)-C(34)	124.2(5)
H-O-Zr	118.4	C(33)-C(34)-C(44)	126.0(5)
C(1)-N(1)-N(2)	130.1(4)	C(44)-C(34)-C(35)	123.5(5)
C(1)-N(1)-Zr	166.8(3)	C(34)-C(35)-C(45)	123.3(5)
C(2)-N(2)-N(1)	125.9(4)	C(45)-C(35)-C(31)	127.0(5)
C(2)-N(2)-Zr	150.7(3)	C(35)-C(31)-C(41)	125.3(5)
N(1)-C(1)-C(51)	117.8(4)	C(51)-C(52)-C(53)	122.6(5)
N(1)-C(1)-C(61)	123.9(4)	C(52)-C(53)-C(54)	121.5(5)
C(11)-C(12)-C(13)	108.6(4)	C(53)-C(54)-C(55)	116.9(5)
C(12)-C(13)-C(14)	108.3(4)	C(53)-C(54)-C(57)	122.3(5)
C(13)-C(14)-C(15)	106.9(4)	C(57)-C(54)-C(55)	120.8(5)
C(14)-C(15)-C(11)	109.7(4)	C(55)-C(56)-C(51)	120.8(5)
C(15)-C(11)-C(12)	106.5(4)	C(56)-C(51)-C(52)	115.9(4)
C(21)-C(11)-C(12)	126.2(4)	C(61)-C(62)-C(63)	121.5(5)
C(11)-C(12)-C(22)	124.4(4)	C(62)-C(63)-C(64)	121.2(5)
C(22)-C(12)-C(13)	125.6(4)	C(63)-C(64)-C(65)	117.4(5)
C(12)-C(13)-C(23)	123.2(4)	C(63)-C(64)-C(67)	121.9(5)
C(23)-C(13)-C(14)	126.7(4)	C(67)-C(64)-C(65)	120.8(5)

TABLE 4.7 (continued)

C(13)-C(14)-C(24)	125.9(4)	C(65)-C(66)-C(61)	120.6(5)
C(24)-C(14)-C(15)	125.5(4)	C(66)-C(61)-C(62)	117.1(4)
C(14)-C(15)-C(25)	125.7(4)		
C(25)-C(15)-C(11)	123.8(4)		
C(15)-C(11)-C(21)	127.1(4)		
C(31)-C(32)-C(33)	108.0(4)		
C(32)-C(33)-C(34)	108.1(4)		

[a]R(1) = C(11)-C(15) ring centroid.

[b]R(2) = C(31)-C(35) ring centroid.

TABLE 4.8. Least-Squares Planes of Pentamethylcyclopentadienyl Rings for 7.

Atom	Deviation from Plane (Å)[a]
Cp*(1) Ring	
C(11)	-0.013
C(12)	0.002
C(13)	0.009
C(14)	-0.017
C(15)	0.019
C(21)	0.060
C(22)	0.283
C(23)	0.357
C(24)	0.231
C(25)	0.286
Cp*(2) Ring	
C(31)	-0.006
C(32)	-0.005
C(33)	0.014
C(34)	-0.017
C(35)	0.014
C(41)	0.155
C(42)	0.204
C(43)	0.158
C(41)	0.382
C(45)	0.335

[a]A negative deviation is a deviation toward the metal atom.

TABLE 4.9. Least-squares Planes of Tolyl Rings for 7.

Atom	Deviation from Plane (Å)
Tol(1)	
C(51)	0.011
C(52)	-0.006
C(53)	-0.005
C(54)	0.011
C(55)	-0.006
C(56)	-0.005
C(57)	0.078
Tol(2)	
C(61)	-0.008
C(62)	0.003
C(63)	0.000
C(64)	0.001
C(65)	-0.006
C(66)	0.009
C(67)	0.028

TABLE 4.10. Least-Squares Plane of ZrON(1)N(2)C(1)C(2)H Group for 7 (Å).

Atom	Deviation from Plane (Å)[a]
Zr	-0.034
O	-0.030
N(1)	0.025
N(2)	0.091
C(1)	0.003
C(2)	0.378
H	-0.087

[a]A negative deviation is a deviation toward the Cp*(1) ring.

4.9 and the least-squares plane of the ZrOHN(1)N(2)C(1)C(2) group is given in Table 4.10.

4.4.9 $Cp^*_2Zr(NMeNCTol_2)Me$ (9)

The procedure described in section 4.4.7 was followed using 200 mg (0.51 mmol) $Cp^*_2ZrMe_2$ (8), 120 mg (0.54 mmol) Tol_2CN_2(4), and 5 mL toluene. Removal of toluene in vacuo afforded an orange oil which solidified upon standing. The solid was triturated with pet. ether (4 mL), the suspension cooled to -78° C and then filtered at this temperature to afford 9 as a yellow-white powder (175 mg, 56%). Anal. Calcd for $C_{38}H_{50}N_2Zr$: C, 72.37; H, 8.21; N, 4.56. Found: C, 71.98; H, 8.15; 4.63. ^1H NMR (benzene-d_6): δ 7.52 (d, $^3J_{HH}$ = 9.2 Hz, 2H, Tol); 6.88 (d, $^3J_{HH}$ = 9.2 Hz, 2H, Tol); 2.56 (s, 3H, NCH_3); 2.13 (s, 6H, Tol); 2.07 (s, 6H, Tol); 1.79 (s, 30H, $C_5(CH_3)_5$; -0.14 (s, 3H, $ZrCH_3$). The remaining aromatic tolyl resonances were obscured by solvent.

4.4.10 $Cp^*_2Zr(H)Br$

A 50 mL glass bomb fitted with a teflon needle-valve and stir bar was charged with 280 mg (0.77 mmol) $Cp^*_2ZrH_2$ (17), 358 mg (0.83 mmol) $Cp^*_2ZrBr_2$, and 25 mL toluene. The bomb was filled with 1 atm H_2 and heated at 120° C for 14 days. The solution was then cooled to room temperature, reduced in volume to 20 mL in vacuo, and filtered. The toluene was removed in vacuo and the green residue triturated with pet ether (5 mL). The suspension was then filtered to afford the product as a yellow-white crystalline solid (170 mg, 50%). Anal. Calcd for $C_{20}H_{31}BrZr$: C, 54.28; H, 7.06. Found: C, 54.16;

H, 7.29. ^{1}H NMR (benzene-d_6): δ 7.34 (s, 1H, ZrH); 1.99 (s, 30H, $C_5(CH_3)_5$). IR (nujol): ν(ZrH) 1619 cm^{-1}.

4.4.11 $Cp^*_2Zr(Et)Br$

$Cp^*_2ZrBr_2$ (250 mg, 0.48 mmol) was suspended in toluene (8 mL) and the mixture cooled to -78° C with rapid stirring. 180 μL of a solution of EtMgBr in Et_2O (2.8 M, 0.50 mmol) was added to the zirconium mixture via syringe and the suspension allowed to warm to room temperature and stir for 12 hours. A white solid precipitated ($MgBr_2$) and the solution became light yellow in color after a few hours of reaction. The solvent was removed in vacuo and the resulting yellow-white solid triturated with pet. ether (10 mL) and the suspension filtered to remove the $HgBr_2$. The volume of solvent was reduced to 2 mL and cooled to -78°C. Yellow crystals precipitated which were isolated by filtration at -78°C (170 mg, 75%). Anal. Calcd for $C_{22}H_{35}BrZr$: C, 56.14; H, 7.50; Br, 16.98. Found: C, 56.29; H, 7.45; Br, 17.20. ^{1}H NMR (benzene-d_6): δ 1.87 (s, 30H, $C_5(CH_3)_5$); 1.38 (t, $^3J_{HH}$ = 8.3 Hz, 3H, $CH_2C\underline{H}_3$); 0.57 (q, $^3J_{HH}$ = 8.3 Hz, 2H, $ZrCH_2$).

4.4.12 $Cp^*_2Zr(CH_2Ph)Br$

The procedure described in section 4.4.11 was followed using 255 mg (0.49 mmol) $Cp^*_2ZrBr_2$ in 12 mL toluene and adding 260μL of a solution of $PhCH_2MgCl$ in THF (2 M, 0.52 mmol). The solvent was removed in vacuo, the residue triturated with toluene (6 mL), and the suspension filtered to remove the white MgBrCl. The salt was washed once with toluene (2 mL) and then the solvent removed in vacuo. The residue was triterated with pet. ether (4 mL) and the suspension

cooled to -78° C and filtered at this temperature to afford the product as an orange crystalline solid (220 mg, 84%). Anal. Calcd for $C_{27}H_{37}BrZr$: C, 60.88; H, 7.00; Br, 15.00. Found: C, 60.73; H, 7.03; Br, 15.19. ^{1}H NMR (benzene-d_6): δ 7.30-7.16 (m, 5H, Ph); 1.80 (s, 30H, $C_5(CH_3)_5$); 1.63 (s, 2H, $ZrCH_2$).

4.4.13 $Cp^*_2Zr(Ph)Br$

The procedure described in section 4.4.11 was followed using 324 mg (0.62 mmol) $Cp^*_2ZrBr_2$ in 12 mL toluene and adding 220 μL of a solution of PhMgBr in Et_2O (3 M, 0.66 mmol). The residue obtained by the removal of solvent from the filtrate was triturated with pet. ether (4 mL), the suspension cooled to -78° C, and then filtered at this temperature to afford the product as an off-white colored powder (210 mg, 65%). Anal. Calcd for $C_{26}H_{35}BrZr$: C, 60.19; H, 6.80. Found: C, 60.22; H, 6.78. ^{1}H NMR (benzene-d_6): δ 1.77 (s, 30H, $C_5(CH_3)_5$); 7.23-7.10 (m, 5H, Ph).

4.4.14 $Cp^*_2Zr(NHNCTol_2)Br$

$Cp^*_2Zr(H)Br$ (78 mg, 0.022 mmol) and Tol_2CN_2 (4) (44 mg, 0.020 mmol) were suspended in toluene (5 mL) at -78° C. The solution turned yellow in color upon addition of the solvent at -78° C. The mixture was warmed to room temperature and stirred for 1 hour. Removal of solvent in vacuo afforded the product as a yellow-orange oil. ^{1}H NMR (benzene-d_6): δ 8.43 (s, 1H, NH); 7.82 (d, $^3J_{HH}$ = 9.2 Hz, 2H, Tol); 2.10 (s, 6H, Tol); 2.06 (s, 6H, Tol); 1.85 (s, 30H, $C_5(CH_3)_5$). The remaining aromatic tolyl resonances were obscured by solvent.

4.4.15 $Cp^*_2Zr(NMeNCTol_2)Br$

$Cp^*_2Zr(Me)Br$ (100 mg, 0.22 mmol) and Tol_2CN_2 (4) 53 mg, 0.24 mmol) were dissolved in toluene (6 mL) and the solution stirred at 50° C for 12 hours. The solvent was removed from the light red-colored solution in vacuo and the residue triturated with pet. ether (8 mL). The suspension was cooled to -78°C and then filtered at this temperature to afford the product as a yellow powder (110 mg, 75%). Anal. Calcd for $C_{36}H_{47}BrN_2Zr$: C, 63.04; H, 7.10; N, 4.20; Br, 11.98. Found: C, 63.14; H, 7.16; N, 4.30; Br, 11.88. ^1H NMR (benzene-d_6): δ 7.52 (d, $^3J_{HH}$ = 9.2 Hz, 2H, Tol); 6.95 (d, $^3J_{HH}$ = 9.2 Hz, 2H, Tol); 3.07 (s, 3H, NCH_3); 2.20 (s, 6H, Tol); 2.07 (s, 6H, Tol); 1.97 (s, 30H, $C_5(CH_3)_5$). The remaining aromatic tolyl resonances were obscured by solvent.

4.4.16 $Cp^*_2Zr(NEtNCTol_2)Br$

The procedure described in section 4.4.15 was followed using 100 mg (0.21 mmol) $Cp^*_2Zr(Et)Br$, 50 mg (0.22 mmol) Tol_2CN_2 (4), and 6 mL toluene. After removal of toluene in vacuo, the residue was triturated with pet. ether (8 mL), the suspension cooled to -78° C and then filtered at this temperature to afford the product as an off-white colored powder (100 mg, 71%). Anal. Calcd for $C_{37}H_{49}BrN_2Zr$: C, 62.85; H, 7.38; N, 4.19; Br, 11.94. Found: C, 62.91; H, 7.46; N, 4.25; Br, 12.00. ^1H NMR (benzene-d_6): δ 7.47 (d, $^3J_{HH}$ = 9.2 Hz, 2H, Tol); 7.23-6.90 (m, 4H, Tol); 3.63 (q, $^3J_{HH}$ = 7.6 Hz, 2H, NCH_2); 2.13 (s, 6H, Tol); 2.09 (s, 6H, Tol); 1.91 (s, 30H, $C_5(CH_3)_5$); 0.72 (t, $^3J_{HH}$ = 7.6 Hz, 3H, $CH_2C\underline{H}_3$). The remaining aromatic tolyl resonances were obscured by solvent.

4.4.17 $Cp^*_2Zr(NCH_2PhNCTol_2)Br$

The procedure described in section 4.4.15 was followed using 100 mg (0.19 mmol) $Cp^*_2Zr(CH_2Ph)Br$, 44 mg (0.19 mmol) Tol_2CN_2 (4), and 5 mL toluene. After removal of toluene in vacuo, the residue was triturated with pet. ether (5 mL), the suspension cooled to -78° C and then filtered at this temperature to afford the product as a light-yellow crystalline solid (92 mg, 64%). Anal. Calcd for $C_{42}H_{51}BrN_2Zr$: C, 66.82; H, 6.81; N, 3.71; Br, 10.58. Found: C, 66.74; H, 6.76; N, 3.61; Br, 10.75. ^1H NMR (benzene-d_6): δ 7.46-6.57 (m, 10H, Tol); 4.93 (s, 2H, NCH_2); 2.20 (s, 6H, Tol); 2.10 (s, 6H, Tol); 2.03 (s, 30H, $C_5(CH_3)_5$).

4.4.18 $Cp^*_2Zr(NPhNCTol_2)Br$

The procedure described in section 4.4.15 was followed using 140 mg (0.27 mmol) $Cp^*_2Zr(Ph)Br$, 66 mg (0.30 mmol) Tol_2CN_2 (4), and 10 mL toluene. After removal of solvent in vacuo, the residue was triturated with pet. ether (5 mL), the suspension cooled to -78° C and then filtered at this temperature to afford the product as a light yellow-orange powder (75 mg, 59%). A satisfactory analysis of this material could not be obtained. ^1H NMR (benzene-d_6): δ 7.8-6.8 (m, 13H, Ph and Tol); 2.05 (s, 3H, Tol); 2.0 (s, 3H, Tol); 1.73 (s, 30H, $C_5(CH_3)_5$).

4.4.19 $Cp^*_2Hf(NHNCTol_2)H$ (12)

$Cp^*_2HfH_2$ (10) (250 mg, 0.55 mmol) and Tol_2CN_2 (4) (123 mg, 0.55 mmol) were suspended in toluene (15 mL) at -78° C. The mixture was warmed to room temperature with stirring during which time the solution turned from purple to yellow in color. The toluene was

removed from the solution in vacuo to give a yellow waxy solid. The solid was triturated with pet. ether (6 mL) at -78° C and then filtered at this temperature to afford 12 as a yellow powder (185 mg, 50%). Anal. Calcd for $C_{35}H_{46}N_2Hf$: C, 62.44; H, 6.89; N, 4.16. Found: C, 62.50; H, 6.88; N, 4.16. ^{1}H NMR (benzene-d_6): δ 9.62 (s, 1H, HfH); 8.20 (d, $^3J_{HH}$ = 9.2 Hz, 2H, Tol); 5.95 (s, 1H, NH); 2.13 (s, 3H, Tol); 2.09 (s, 3H, Tol), 1.93 (s, 30H, $C_5(CH_3)_5$). The remaining tolyl resonance was obscured by solvent. IR (nujol): ν(NH) 3292 cm^{-1}; ν(HfH) 1620.

4.4.20 Reaction of $Cp^*_2HfH_2$ (10) with Tol_2CNNH_2 (20) to give $Cp^*_2Hf(NHNCTol_2)H$ (12)

$Cp^*_2HfH_2$ (10) (20 mg, 0.044 mmol) and Tol_2CNNH_2 (20) (10 mg, 0.045 mmol) were placed in an NMR tube. Benzene-d_6 (0.4 mL) was added and the tube stoppered with a rubber septum. Upon addition of the solvent, the solution bubbled violently as H_2 was formed. The ^{1}H NMR spectrum of this solution indicates 12 had formed in greater than 99% yield.

4.4.21 $Cp^*_2Hf(NHNCTol_2)I$ (13)

$Cp^*_2Hf(NHNCTol_2)H$ (12) (30 mg, 0.046 mmol) was dissolved in toluene (5 mL) and the solution frozen at -196° C. CH_3I (0.091 mmol) was distilled onto the frozen solution and the mixture warmed to room temperature and stirred for 12 hours. Toepler pump analysis of the gas product indicated 0.046 mmol CH_4 (1.0 mol CH_4/mol 12). Removal of solvent in vacuo afforded 13 as a yellow solid. ^{1}H NMR (benzene-d_6): δ 8.50 (s, 1H, NH); 7.79 (d, $^3J_{HH}$ = 9.2 Hz, 2H, Tol); 210 (s, 6H, Tol);

1.97 (s, 30H, $C_5(CH_3)_5$). The remaining aromatic tolyl resonances were obscured by solvent. IR (nujol): ν(NH) 3275 cm^{-1}.

4.4.22 Reaction of $Cp^*_2HfH_2$ (10) with Tol_2CN_2 (4) to give $Cp^*_2Hf(NHNCTol_2)_2$ (16)

The procedure described in section 4.4.16 was followed using 50 mg (0.14 mmol) $Cp^*_2HfH_2$ (10) and 61 mg (0.27 mmol) Tol_2CN_2 (4) in 6 mL toluene. Removal of solvent in vacuo afforded an orange-yellow oil. ^1H NMR (benzene-d_6): δ 7.80 (d, $^3J_{HH}$ = 9.24 Hz, 2H, Tol); 6.83 (s, 1H, NH); 2.20 (s, 6H, Tol); 2.15 (s, 6H, Tol); 1.88 (s, 30H, $C_5(CH_3)_5$). The remaining NH and tolyl aromatic resonances were obscured by solvent.

4.4.23 Reaction of $Cp^*_2ZrH_2$ with Tol_2CN_2 (4) to give $Cp^*_2Zr(NHNCTol_2)_2$ (18)

The procedure described in section 4.4.14 was followed using 50 mg (0.14 mmol) $Cp^*_2ZrH_2$ (17) and 61 mg (0.27 mmol) Tol_2CN_2 (4) in 6 mL toluene. Removal of solvent in vacuo afforded an orange-yellow oil. ^1H NMR (benzene-d_6): δ 7.80 (d, J_{HH} = 9.24 Hz, 2H, Tol); 6.83 (s, 1H, NH); 2.20 (s, 6H, Tol); 2.15 (s, 6H, Tol); 1.88 (s, 30H, $C_5(CH_3)_5$). The remaining NH and tolyl aromatic resonances were obscured by solvent.

4.4.24 Reaction of $Cp^*_2HfH_2$ (10) with $TolCHN_2$ (19) to give (N(2)-c)-$Cp^*_2Hf(NHNCHTol)H^{30}$ (22) and (N(2)-ℓ)-$Cp^*_2Hf(NHNCHTol)H^{30}$ (23)

$Cp^*_2HfH_2$ (10) (0.30 g, 0.67 mmol) was dissolved in toluene

(20 mL) and the solution cooled to -78° C. With rapid stirring, 550 μL of a solution of TolCHN$_2$ (19) in benzene (1.21 M, 0.67 mmol) was added to the hafnium solution via syringe and the mixture warmed slowly to room temperature. Upon addition of the diazoalkane, the hafnium solution turned from clear to light yellow in color. After warming to room temperature, the solvent was removed from the solution in vacuo to afford a yellow oil which, by ^{1}H NMR, contained both 22 (70%) and 23 (30%).

22. ^{1}H NMR (benzene-d$_6$): δ 9.33 (s, 1H, HfH); 7.33 (d, $^3J_{HH}$ = 9.2 Hz, 2H, Tol); 7.28 (s, 1H, CH); 6.94 (d, $^3J_{HH}$ = 9.2 Hz, 2H, Tol); 6.57 (s, 1H, NH); 2.10 (s (3H, Tol); 1.94 (s, 30H, $C_5(CH_3)_5$).

4.4.25 (N(2)-c)-Cp$^*_2$Hf(NHNCHTol)I[30] (24)

The yellow oil obtained from procedure 4.4.24 was dissolved in toluene (20 mL), the solution cooled to -78° C, and CH_3I (1.3 mmol) added with rapid stirring. The mixture was warmed to room temperature and stirred for 12 hours. The toluene was reduced in volume to ca. 2 mL and pet. ether (6 mL) distilled onto the solution at -78° C. A yellow solid precipitated which was isolated by filtration at -78°C to afford 24 as a light yellow-white powder (170 mg, 38%). Anal. Calcd for $C_{28}H_{38}IN_2Hf$: C, 47.43; H, 5.54; N, 3.95; MW, 709. Found: C, 47.61; H, 5.41; N, 4.00; MW, 684. ^{1}H NMR (benzene-d$_6$): δ 7.32 (d, J_{HH} = 9.2 Hz, 2H, Tol); 7.28 (s, 1H, CH); 6.94 (d, $^3J_{HH}$ = 9.2 Hz, 2H, Tol); 6.57 (s, 1H, NH); 2.10 (s, 3H, Tol). 1.94 (s, 30H, $C_5(CH_3)_5$). IR (nujol mull) ν (NH) 3300 cm^{-1}.

4.4.26 (N(2)-ℓ)$Cp^*_2Hf(NHNCHTol)H$[30] (23)

$Cp^*_2HfH_2$ (10) (300 mg, 0.67 mmol) was dissolved in toluene (12 mL) and the solution cooled to -78° C. With rapid stirring, $TolCHNNH_2$ (20) (89 mg, 0.67 mmol) was added to the hafnium solution via a side-arm addition tube and the mixture then warmed to room temperature. Immediate gas evolution accompanied the addition and the solution turned light yellow in color. Toepler pump analysis of the gas product indicated H_2 (0.061 mmol, 0.91 mol H_2/mol 10). The yellow-white residue remaining from the Toepler experiment was redissolved in toluene (1 mL) and pet. ether (8 mL) distilled onto the solution at -78°C. After 3 hours of cooling, a yellow solid had precipitated which was isolated by filtration at -78°C to afford 23 as a yellow powder (240 mg, 62%). Anal. Calcd for $C_{28}H_{40}N_2Hf$: C, 57.65; H, 6.92; N, 4.81, MW, 582; Found: C, 57.67; H, 6.89; N, 4.99, MW, 563. ^{1}H NMR (benzene-d_6): δ 8.58 (s, 1H, HfH); 7.91 (d, $^3J_{HH}$ = 9.2 Hz, 2H, Tol); 7.07 (s, 1H, CH); 7.03 (d, $^3J_{HH}$ = 9.2 Hz, 2H, Tol); 5.50 (s, 1H, NH); 2.10 (s, 3H, Tol); 1.93 (s, 30H, $C_5(CH_3)_5$). IR (nujol): ν(NH) 3260 cm^{-1}; ν(HfH) 1613.

4.4.27 $Cp^*_2Hf(NHNCHTol)_2$ (25)

The procedure described in section 4.4.24 was followed using 300 mg (0.67 mmol) $Cp^*_2HfH_2$ (10) and 110 μL of a solution of $TolCHN_2$ (19) in benzene (1.21 M, 0.67 mmol). The solution turned red in color upon the addition of the diazoalkane at -78°C and then slowly turned orange-yellow upon warming to room temperature. The toluene was removed in vacuo to afford a yellow oil which solidified upon standing.

The solid was triturated with pet. ether (12 mL), the suspension cooled to -78°C, and then filtered at this temperature to afford 25 as a yellow crystalline solid (240 mg, 51%). Anal. Calcd for $C_{36}H_{48}N_4Hf$: C, 60.43; H, 6.77; N, 7.84. Found: C, 60.21; H, 6.61; N, 7.82. ^1H NMR (benzene-d_6): δ 7.67 (d, $^3J_{HH}$ = 9.2 Hz, 2H, Tol); 7.42 (s, 1H, CH); 7.36 (d, $^3J_{HH}$ = 9.2 Hz, 2H, Tol); 7.10 (s, 1H, CH); 7.10 (s, 1H, NH); 7.02 (d, $^3J_{HH}$ = 5.0 Hz, 2H, Tol); 6.87 (d, $^3J_{HH}$ = 5.0 Hz, 2H, Tol); 6.29 (s, 1H, NH); 2.15 (s, 3H, Tol); 2.02 (s, 3H, Tol); 1.83 (s, 30H, $C_5(CH_3)_5$). IR (nujol): ν(NH) 3300 cm^{-1}; ν(NH) 3180.

4.5 References and Notes

1. W. A. Herrmann, Angew. Chem., Int. Ed. Engl., 17, 800 (1978) and references therein.
2. a) W. A. Herrmann and H. Biersack, Chem. Ber., 110, 896 (1977);

   b) M. F. Lappert and J. S. Poland, J. Chem. Soc., Chem. Commun., 1061 (1969);

   c) G. L. Hillhouse and B. L. Haymore, J. Amer. Chem. Soc.,
3. S. Gambrotta, M. Basso-Bert, C. Floriani, and C. Guastini, J. Chem. Soc., Chem. Commun., 374 (1982).
4. For example, the ^{1}H NMR OH resonance for $Cp^*_2Zr(OH)_2$ is observed at δ 3.47 and that for $Cp^*_2Zr(Cl)OH$ is observed at δ 4.38. See ref. 5.
5. G. L. Hillhouse and J. E. Bercaw, manuscript in preparation.
6. The N(2) atom is taken to be the terminal nitrogen atom of the original diazoalkane.
7. E. J. Moore, D. A. Straus, J. Armantrout, B. D. Santarsiero, R. H. Grubbs, and J. E. Bercaw, J. Amer. Chem. Soc., 105, 2068 (1983).
8. J. D. Dunitz, "X-Ray Analysis and the Structure of Organic Molecules," Cornell University Press, Ithaca, NY, 1979.
9. a) The N-N bond distance in HN=NH is 1.238(7) Å. A. Trombetti, Can. J. Phys., 46, 1005 (1978);

   b) The N-N bond distance in MeN=NMe is 1.254(3) Å. C. H. Chang, R. E. Porter, and S. H. Bauer, J. Amer. Chem. Soc., 92, 5313 (1970);

c) The N-N bond distance in PhN=NPh is 1.244 Å. C. J. Brown, Acta Crystallogr., 21, 153 (1966).

10. The longest Zr-O distance yet reported is 2.446 Å for the compound $(COT)_2Zr \cdot THF$. D. J. Brauer and C. Kruger, J. Organomet. Chem., 42, 129 (1972).

11. a) G. Fachinetti, C. Floriani, F. Marchetti, and S. Merlino, J. Chem. Soc., Chem. Commun., 522 (1976);
b) See Chapter 3 of this thesis.

12. For example, the ^1H NMR $Zr-CH_3$ resonance for $Cp^*_2ZrMe_2$ is observed at δ -0.62,[a] that for $Cp^*_2Zr(H)Me$ is observed at δ -0.43,[11b] and that for $Cp^*_2Zr(Me)OH$ is observed at δ -0.20.[b]
a) J. M. Manriquez, D. R. McAlister, R. D. Sanner, and J. E. Bercaw, J. Amer. Chem. Soc., 100, 2716 (1978);
b) See experimental section.

13. P. J. Fagan, J. M. Manriquez, S. H. Vollmer, C. S. Day, V. W. Day, and T. J. Marks, J. Amer. Chem. Soc., 103, 2206 (1981).

14. Carbon monoxide readily inserts into zirconium-alkyl bonds at or below room temperature. See Ref. 11b and references therein.

15. F. A. Cotton and G. Wilkinson, "Advanced Inorganic Chemistry," 3rd. ed., Interscience, New York, 1972, p. 650.

16. R. S. Threlkel, Ph.D. Dissertation, California Institute of Technology, Pasadena, CA, 1980.

17. J. E. Huheey, "Inorganic Chemistry: Principles of Structure and Reactivity," Harper and Row, New York, 1972, p. 167.

18. G. Erker and F. Rosenfeldt, J. Organomet. Chem., 188, C1 (1980).

19. R. S. Threlkel and J. E. Bercaw, J. Amer. Chem. Soc., 103, 2650 (1981).

20. Hafnium hydride ligand resonance are typically observed in the δ 9.9-15.6 ^{1}H NMR spectral region and appear as broad singlets.
a) D. M. Roddick, M. D. Fryzuk, P. F. Seidler, and J. E. Bercaw, manuscript in preparation;
b) G. L. Hillhouse and J. E. Bercaw, Organometallics, 1, 1025
c) See ref. 5.

21. Based on Toepler pump analysis.

22. D. M. Roddick, personal communication.

23. Neat TolCHN$_2$ (19) decomposes rapidly at room temperature to the corresponding azine (TolCH=N-N=CHTol) and so is stored and used as a benzene or toluene solution at -78°C. G. L. Hillhouse, Ph.D. Dissertation, Indiana University, Bloomington IN, 1980.

24. R. H. Marvick and H. H. Brintzinger, J. Amer. Chem. Soc., 93, 2046 (1971).

25. D. M. Roddick, M. D. Fryzuk, P. F. Seidler, and J. E. Bercaw, manuscript in preparation.

26. J. E. Bercaw, Adv. Chem. Ser. No. 167, 136 (1978).

27. L. I. Smith and K. L. Howard, in "Organic Syntheses," Collective Volume 3, E. C. Horning Ed., John Wiley and Sons, Inc., New York, p. 351.

28. The program LATCON, taken from the XRAY-76 system of crystallographic programs, was used. XRAY-76: J. M. Stewart, Ed., Technical Report TR-446 of the computer Science Center, University of Maryland, College Park, MD.

29. The CRYM package of crystallographic programs were used. In least-squares, the quantity minimized is $\sum w[F_o^2 - (F_c/k)^2]^2$ with $w = \sigma^{-2}(F_o^2)$. Scattering factors for Zr were taken from the International Tables for X-ray Crystallography, Kynoch Press, Birmingham, England, 1974, Vol. IV, pp. 71-98; for O, C, and N from ibid., Vol. III, 1962, 202-205; and for H from R. F. Stewart, E. R. Davidson, and W. T. Simpson, J. Chem. Phys., 42, 3175 (1965). The Zr scattering factors were corrected for anomalous dispersion, International Tables, Vol. IV, pp. 148-150, 1974.

30. N(2)-c refers to coordination of the N(2) atom of the η^2-N,N'-hydrazonido ligand to the central zirconium bonding position. N(2)-ℓ refers to coordination of the N(2) atom to the lateral bonding position.

CHAPTER 5

The Synthesis of (2-methyl-5-t-butyl)phenyltetramethylcyclopentadiene and its Use as a Ligand in the Preparation of Coordinatively Unsaturated Tantalum Hydride Complexes

5.1 Introduction

The search for homogeneous organometallic complexes which affect the catalytic reduction of carbon monoxide is an area of intense interest. Work in our laboratories has focussed on coordinatively unsaturated d^0 metal hydride compounds containing one or more pentamethylcyclopentadienyl ligands.[1] Of these hydride complexes, bis(pentamethylcyclopentadienyl) zirconium dihydride, $Cp^*_2ZrH_2$ ($Cp^* \equiv \eta^5\text{-}C_5Me_5$), has been the most thoroughly studied.[1] Although the reaction of $Cp^*_2ZrH_2$ with carbon monoxide under hydrogen is complicated, one product obtained is the methoxy-hydride species $Cp^*_2Zr(H)OCH_3$. Addition of HCl to this methoxy-hydride complex affords methanol stoichiometrically, but not catalytically. The exceptional reactivity of $Cp^*_2ZrH_2$ is a consequence of several factors. First, the hydride ligands are hydridic in contrast to compounds such as $HCo(CO)_4$ in which the hydride ligand is protonic.[2] Casey, Gladysz, and others have shown that hydridic alkali metal hydride complexes are capable of reducing coordinated CO to formyl, hydroxymethyl, and methyl groups.[3] Thus, carbon monoxide reduction seems to be favored by highly hydridic hydride ligands. Second, $Cp^*_2ZrH_2$ is a 16-electron coordinatively unsaturated species. Ligand dissociation is therefore not required for initial CO coordination. Third, the bulky pentamethylcyclopentadienyl ligands inhibit oligomerization which might effectively "saturate" the metal center, preventing CO coordination. Finally, the strength of the zirconcium-oxygen bond[4] provides a thermodynamic "sink" in the formation of the methoxy-hydride complex, a major factor why zirconium activation of CO is a

stoichiometric and not a catalytic process.

The search for later transition metal hydride complexes which would catalytically reduce carbon monoxide was undertaken by James Mayer of the Bercaw research group. A series of pentamethylcyclopentadienyl tantalum phosphino hydride complexes were synthesized and their reactivity with CO explored.[5] Tantalum was chosen because of the availability of starting materials and because tantalum(V)-oxygen bonds are expected to be weaker than zirconium(IV)-oxygen bonds.[4] Although several tantalum hydride complexes were prepared (eqs. 1, 2), all are coordinatively saturated 18-electron species and

$$Cp^*TaMe_4 + 2L \xrightarrow[800\ psi]{H_2} Cp^*TaH_4L_2 + 4\ CH_4 \qquad (1)$$

$L = PMe_3,\ PMe_2Ph,\ P(OMe)_3$
$L_2 = dmpe$

$$Cp^*TaMe_3Cl + 2L \xrightarrow[800\ psi]{H_2} Cp^*TaH_3ClL_2 + 3\ CH_4 \qquad (2)$$

$L = PMe_3$

are ineffective in reducing carbon monoxide; the reductive elimination of hydrogen to form carbonyl complexes (eqs. 3, 4) appears to be more

$$Cp^*TaH_4(PMe_3)_2 \xrightarrow{CO} Cp^*TaH_2(CO)(PMe_3)_2 + \underline{cis}\text{-}Cp^*Ta(CO)_2(PMe_3)_2 \qquad (3)$$

$$Cp^*TaH_3Cl(PMe_3)_2 \xrightarrow{CO} Cp^*TaHCl(CO)(PMe_3)_2 + Cp^*TaHCl(CO)_2(PMe_3) \qquad (4)$$

favorable than hydride reduction of coordinated CO. The use of bulky phosphines as an attempt to generate a coordinatively unsaturated complex was also unsuccessful; tri-t-butylphosphine and tricyclohexylphosphine failed to give a clean product.

A second approach to making coordinatively unsaturated tantalum hydride complexes is to increase the steric demands of the cyclopentadienyl ligand. A simple synthetic approach is to replace one of the methyl groups of Cp^* with a bulkier group. A disubstituted phenyl group (Figure 5.1) was chosen because the phenyltetramethylcyclo-

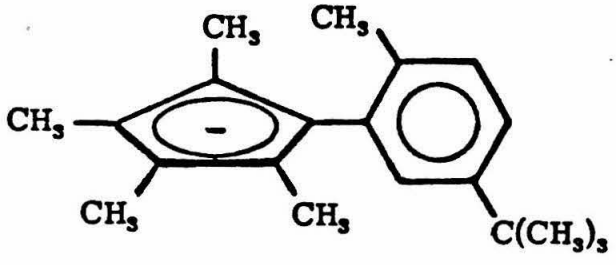

FIGURE 5.1. Diagram of (2-methyl-5-t-butyl)phenyltetramethylcyclopentadienyl anion (Cp^{EJ}).

pentadienyl anion had previously been prepared.[6] The phenyl group by itself would not be expected to inhibit bisphosphine formation; phosphine-phenyl steric interactions would be minimized because the tetramethylcyclopentadienyl ligand and phenyl substituent could conceivably attain a coplanar configuration. To circumvent this problem, a phenyl group consisting of a methyl substituent at the C(2) position[7]

and a t-butyl substituent at the C(5) position was chosen. A CPK model[8] of the (2-methyl)-5-t-butyl)phenyltetramethylcyclopentadienyl anion (Cp^{EJ}) indicates that free rotation about the Cp-phenyl bond is restricted because of the methyl substituent. Furthermore, the methyl substituent is forced into the π system of the cyclopentadienyl ligand, thereby directing metal coordination to the opposite face of the Cp ligand. The t-butyl substituent is then forced into the metal coordination sites occupied by the hydride and phosphine ligands (Figure 5.2).

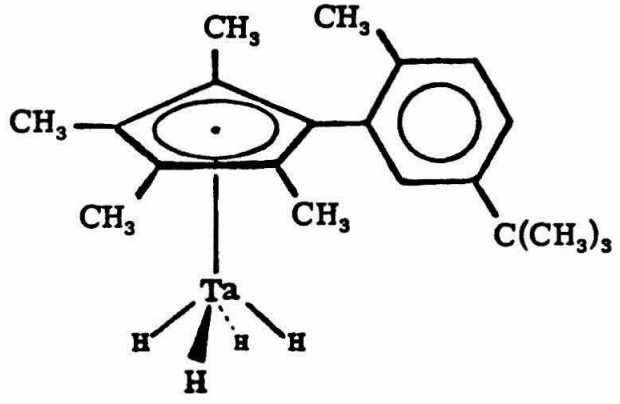

FIGURE 5.2. Diagram of a Cp^{EJ} Complex of Tantalum.

Phosphine-t-butyl steric interactions should inhibit the formation of a bis-phosphine product, thereby generating a vacant coordination site. This chapter describes the synthesis of (2-methyl-5-t-butyl)phenyl-tetramethylcyclopentadiene and its use as a ligand in the preparation of coordinatively saturated and unsaturated polyhydride compounds of tantalum. The reactivity of these complexes with CO is also discussed.

5.2 Results and Discussion

5.2.1 Synthetic Strategy

The synthetic strategy employed in this work for making a disubstituted phenyltetramethylcyclopentadiene ligand is a modification of the general procedure used by Bercaw and Threlkel.[6] In this method, two equivalents of 2-lithio-2-butene are condensed with the appropriate R-substituted alkyl ester to obtain the acyclic carbinol 1 (eq. 5). Protonation with acid affords the cyclopentadiene 2 (eq. 6). For the

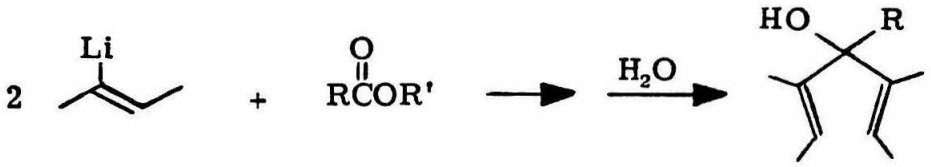

(5)

1

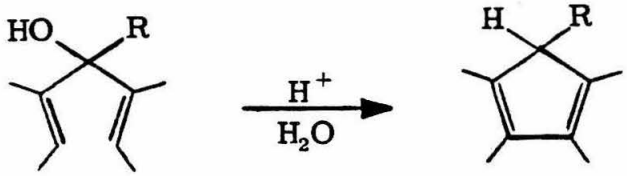

(6)

1 2

preparation of $Cp^{EJ}H$, the initial target molecule was the 2,5-disubstituted benzoate ester 5 (Scheme 5.1). Since 2-bromo-4-t-butyltoluene (3) can be obtained by bromination of readily available t-butyltoluene,[9] it was hoped that treatment of the bromide with magnesium would afford the Grignard reagent which could then be carboxylated with CO_2 to give the benzoic acid 4. Esterification of 4 with methanol to give 5 should proceed straightforwardly.

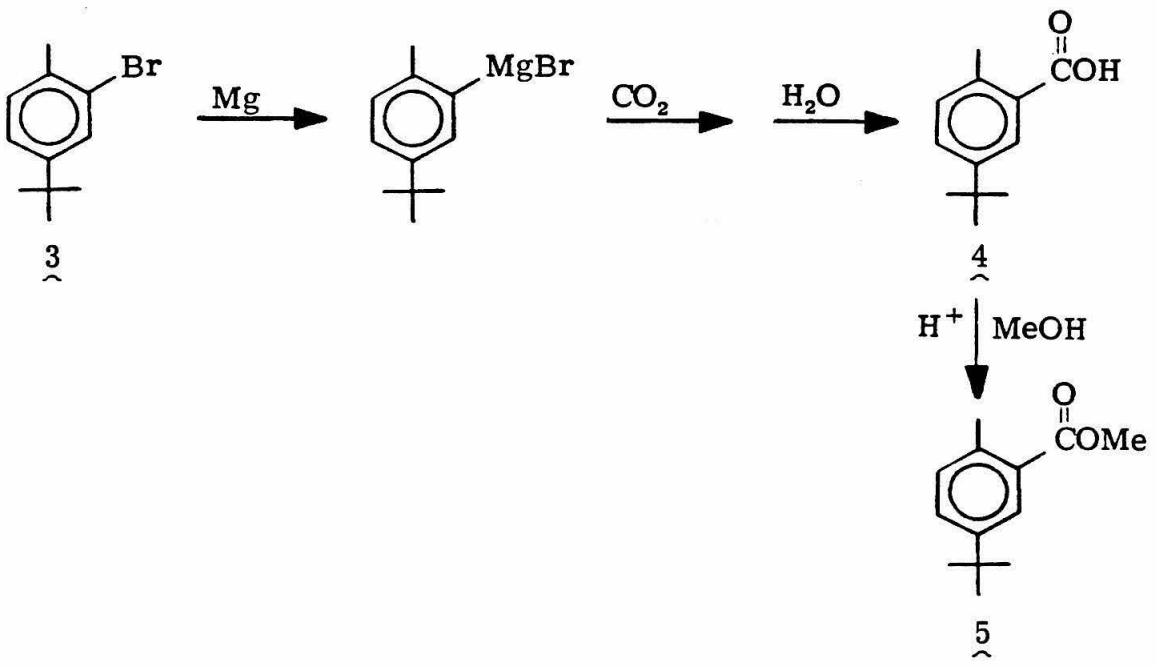

SCHEME 5.1. Synthesis of Methyl-2-methyl-5-t-butylbenzoate (5).

5.2.2 Synthesis of Methyl-2-methyl-5-t-butylbenzoate (5)

2-Bromo-4-t-butyltoluene (3) is easily prepared in mole quantities by treating 4-t-butyltoluene with bromine in the presence of an iron catalyst (iron powder) (eq. 7). Under mild conditions, only the

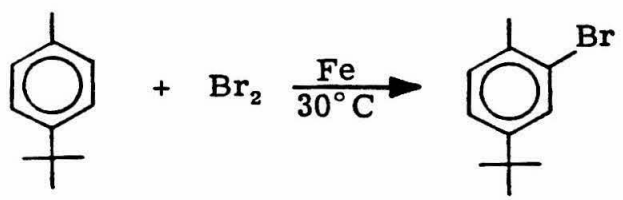

(7)

3

ortho-substituted toluene is obtained.[9] Treatment of the bromide with magnesium turnings in dry THF, followed by quenching with solid carbon dioxide and hydrolysis affords the carboxylic acid 4 as a white crystalline solid in 87% yield (eq. 8). Although rigorously anhydrous

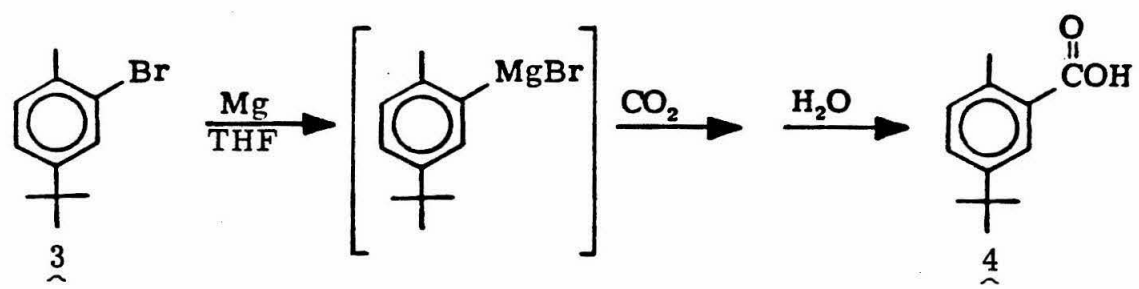

(8)

3 4

conditions were employed, significant amounts (10%) of 4-t-butyltoluene were also obtained using this procedure. Substitution of "bone dry" CO_2 gas for solid CO_2 had little effect in the elimination of the presumed hydrolysis product. Use of dry diethyl ether as solvent reduced the yield of 4 even further. Proton transfer processes from the solvent rather than hydrolysis by small amounts of water are probably responsible for the formation of 4-t-butyltoluene. Although this compound could not be eliminated as a byproduct in the

carbonylation reaction, 4 could be obtained in pure form by standard acid-base extraction techniques. The methyl-benzoate 5 was prepared by esterification of the carboxylic acid in methanol using p-toluene-sulfonic acid (TsOH) as the catalyst and 2,2-dimethoxypropane (DMP) as the dehydrating agent (eq. 9). The ester was isolated as a high

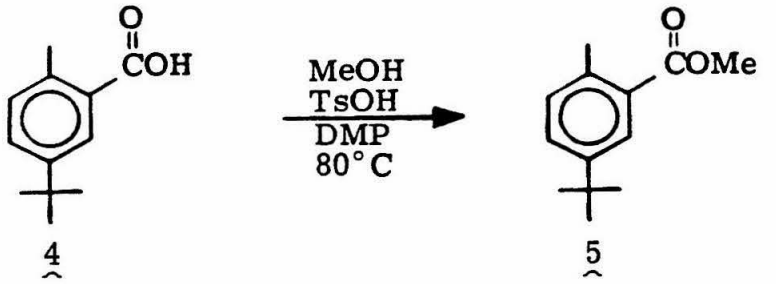

4 5 (9)

boiling liquid (bp 74°C (0.2 mm)) in 96% yield.

5.2.3 Synthesis of $LiCp^{EJ}$

With the synthesis of the initial target molecule realized, standard procedures could be employed for the preparation of the cyclopentadiene, $Cp^{EJ}H$.[6] Condensation of the methyl-benzoate 5 with two equivalents of 2-lithio-2-butene (prepared from cis/trans-2-bromo-2-butene and Li) afforded the carbinol 6 (eq. 10). However,

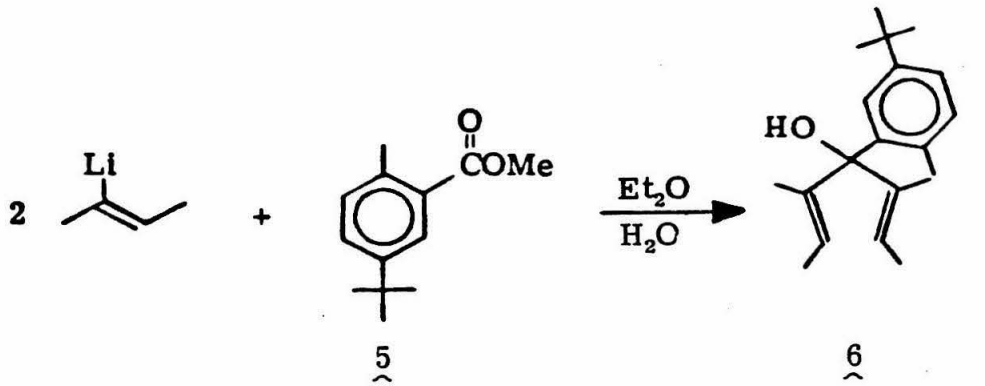

5 6 (10)

treatment of 6 with p-toluenesulfonic acid in diethyl ether failed to

give the desired ring-closed product. The acyclic triene $\underset{\sim}{7}$[10] was the only product isolated by distillation of the product mixture (eq. 11).

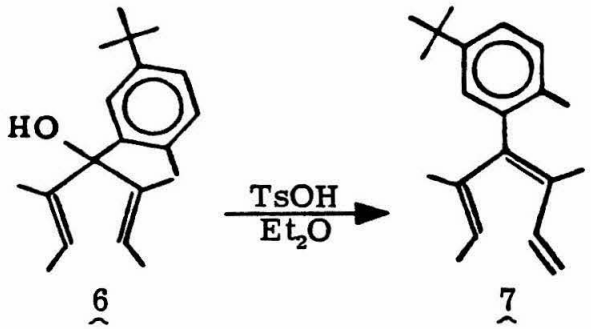

$\underset{\sim}{6}$ $\underset{\sim}{7}$ (11)

Following the procedure used in the preparation of phenyltetramethylcyclopentadiene,[6] $\underset{\sim}{6}$ was slowly added to ice-cold concentrated sulfuric acid. Again, no ring-closed products were observed after work-up of the reaction mixture. To further stabilize the resulting carbocation formed by protonation of the carbanol, a polar solvent was used in hope that electrocyclic ring closure would predominate over elimination reactions. Thus, treatment of $\underset{\sim}{6}$ with p-toluenesulfonic acid in refluxing chloroform for 12 hours afforded $Cp^{EJ}H$ as a dark amber oil in 87% yield. If the reaction time is reduced to 1 hour, however, the acyclic triene $\underset{\sim}{7}$ is the only product observed. Further reaction of $\underset{\sim}{7}$ with TsOH in refluxing chloroform does afford $Cp^{EJ}H$ after several hours (eq. 12). Thus, protonation of the carbanol proceeds first

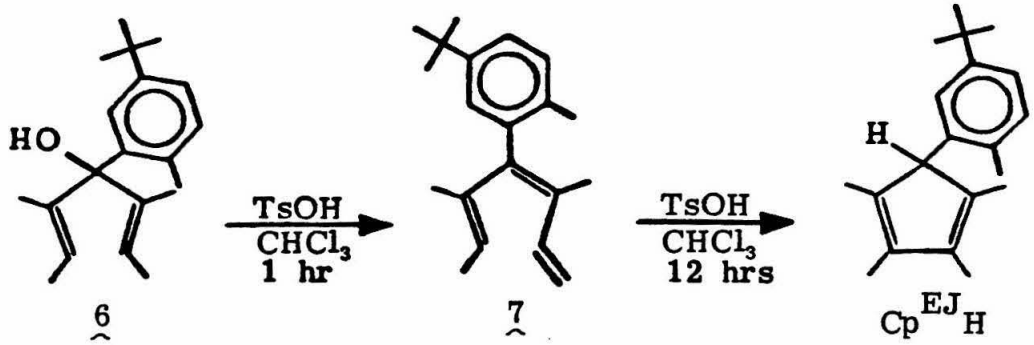

$\underset{\sim}{6}$ $\underset{\sim}{7}$ $Cp^{EJ}H$ (12)

through an isolable kinetic product, the acyclic triene 7, which then tautomerizes in chloroform to the more stable product, the cyclopentadiene $Cp^{EJ}H$. This tautomerization could not be effected using diethylether or neat sulfuric acid as solvents. The ^1H NMR spectrum of $Cp^{EJ}H$ indicates the presence of one major isomer in solution and mass spectral analysis confirms the molecular weight with a parent ion peak at 268.

Conversion of $Cp^{EJ}H$ to the lithium cyclopentadienide, $LiCp^{EJ}$, was accomplished by treatment with n-butyllithium in refluxing petroleum ether for 48 hours (eq. 13). $LiCp^{EJ}$ can be isolated as a

$$Cp^{EJ}H + \text{n-BuLi} \xrightarrow[\substack{\text{reflux}\\ 48\text{ hrs}}]{\text{pet. ether}} LiCp^{EJ} + \text{butane} \qquad (13)$$

white solid in 49% yield. The ^1H NMR spectrum of $LiCp^{EJ}$ (Figure 5.3) consists of two resonances for the two pairs of inequivalent methyl groups (δ 2.03, 1.83) and single resonances for the tolyl-methyl (δ 2.07) and t-butyl groups (δ 1.30). The use of other reaction solvents such as toluene or THF resulted in viscous oils which did not crystallize. Also, attempts to deprotonate more than one gram of $Cp^{EJ}H$ failed to give an isolable solid. Apparently, efficient stirring of the reaction mixture is not achieved when this reaction is scaled-up.

5.2.4 Synthesis of Tantalum-Methyl Complexes

The synthesis of Cp^{EJ} compounds of tantalum was accomplished by following the procedure used by Schrock for the preparation of Cp^*TaMe_3Cl.[11] Thus, treatment of $TaMe_3Cl_2$ with one equivalent of

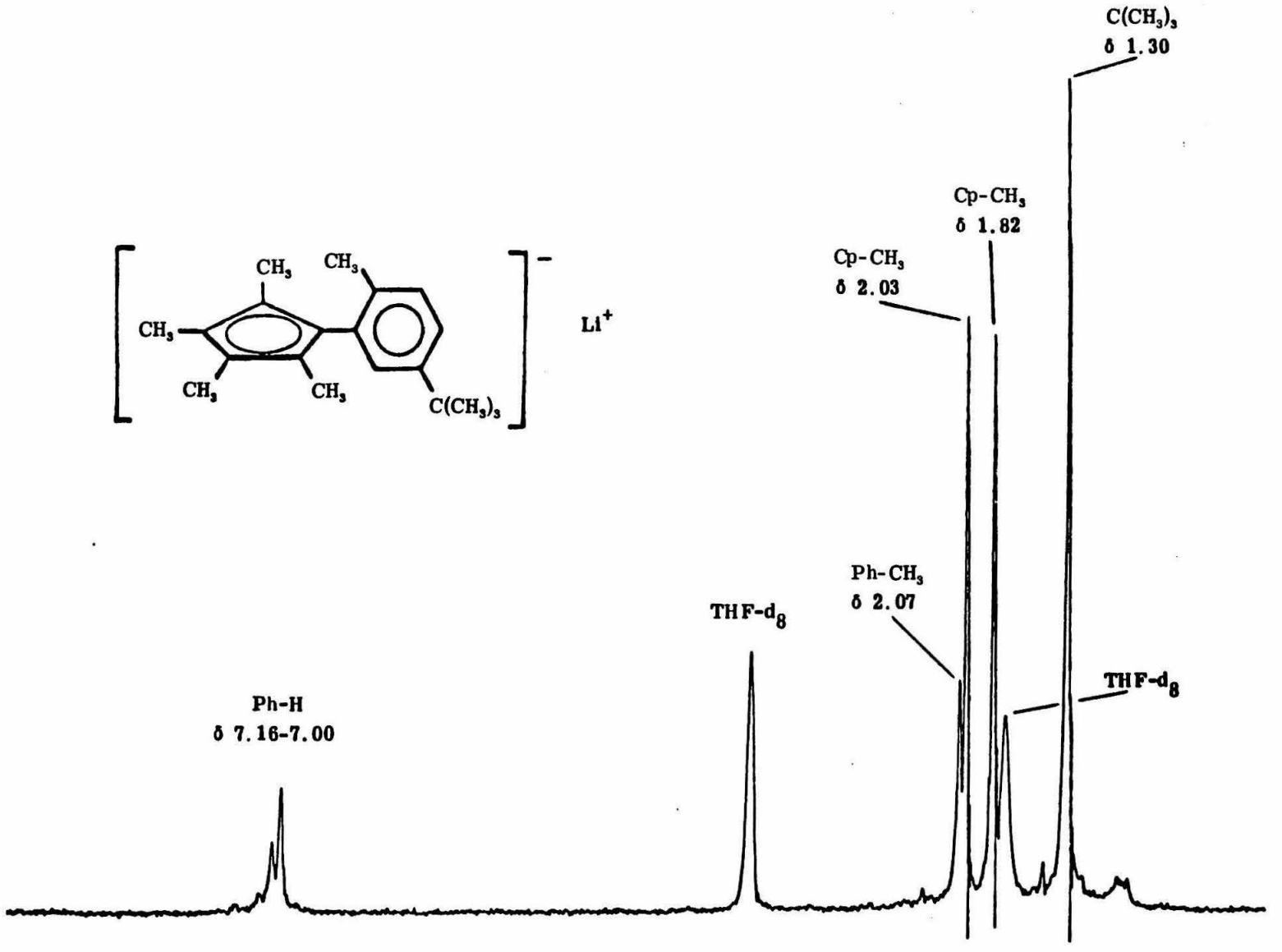

FIGURE 5.3. ^{1}H NMR Spectrum of $LiCp^{EJ}$.

$LiCp^{EJ}$ in diethyl ether affords $Cp^{EJ}TaMe_3Cl$ (8) as a yellow crystalline solid in 44% yield (eq. 14). The ^1H NMR spectrum of 8 (Figure 5.4)

$$TaMe_3Cl_2 + LiCp^{EJ} \xrightarrow{Et_2O} \underset{8}{Cp^{EJ}TaMe_3Cl} + LiCl \qquad (14)$$

indicates the presence of only one isomer in solution. As in the spectrum of $LiCp^{EJ}$, two resonances are observed for the two pairs of inequivalent Cp-methyl groups (δ 1.77, 1.73). The tantalum-methyl groups are equivalent, however, with a single resonance at δ 1.13. Treatment of 8 with one equivalent of MeLi in diethyl ether affords the tetramethyl complex, $Cp^{EJ}TaMe_4$ (9), in 63% yield (eq. 15). The ^1H

$$\underset{8}{Cp^{EJ}TaMe_3Cl} + MeLi \xrightarrow{Et_2O} \underset{9}{Cp^{EJ}TaMe_4} + LiCl \qquad (15)$$

NMR spectrum of 9 (Figure 5.5) is similar to that of 8 except that only a single resonance is observed for the Cp-methyl protons at δ 1.73. Use of high field ^1H NMR (500 MHz) does resolve the singlet observed in the 90 MHz spectrum into two distinct resonances, however. The question arises as to which isomer of 9 (and also of 8) is present in solution, since the metal could coordinate on the t-butyl side of the cyclopentadienyl ligand or on the tolyl-methyl side. As mentioned earlier, a CPK model of Cp^{EJ} indicates that the tolyl-methyl group is forced into the π system of the Cp ligand. Thus, metal coordination should occur on the t-butyl side of the ring, forcing the t-butyl group into close proximity with the tantalum methyl ligands. This effect was

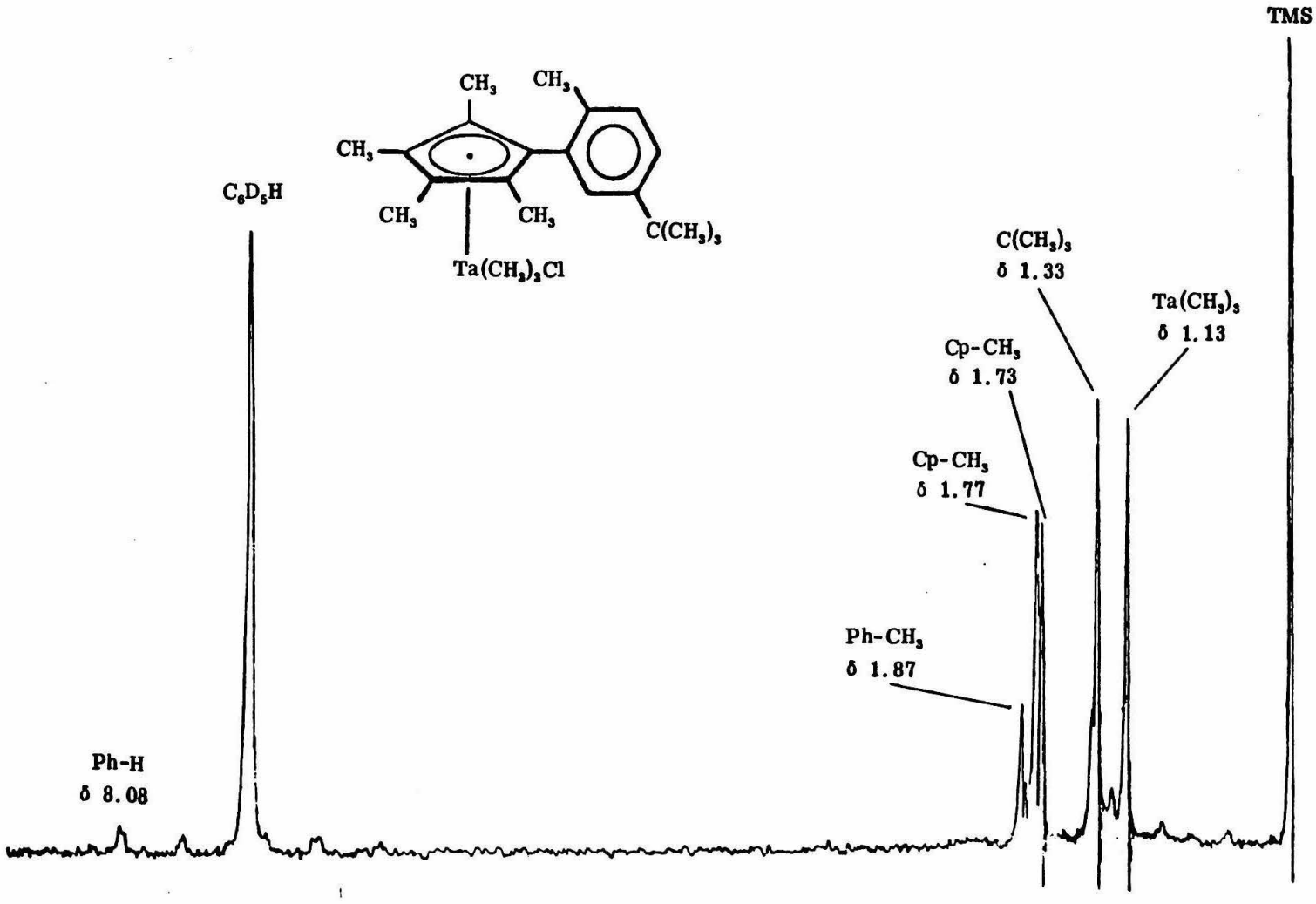

FIGURE 5.4. ^{1}H NMR Spectrum of $Cp^{EJ}Ta(CH_3)_3Cl$ (8).

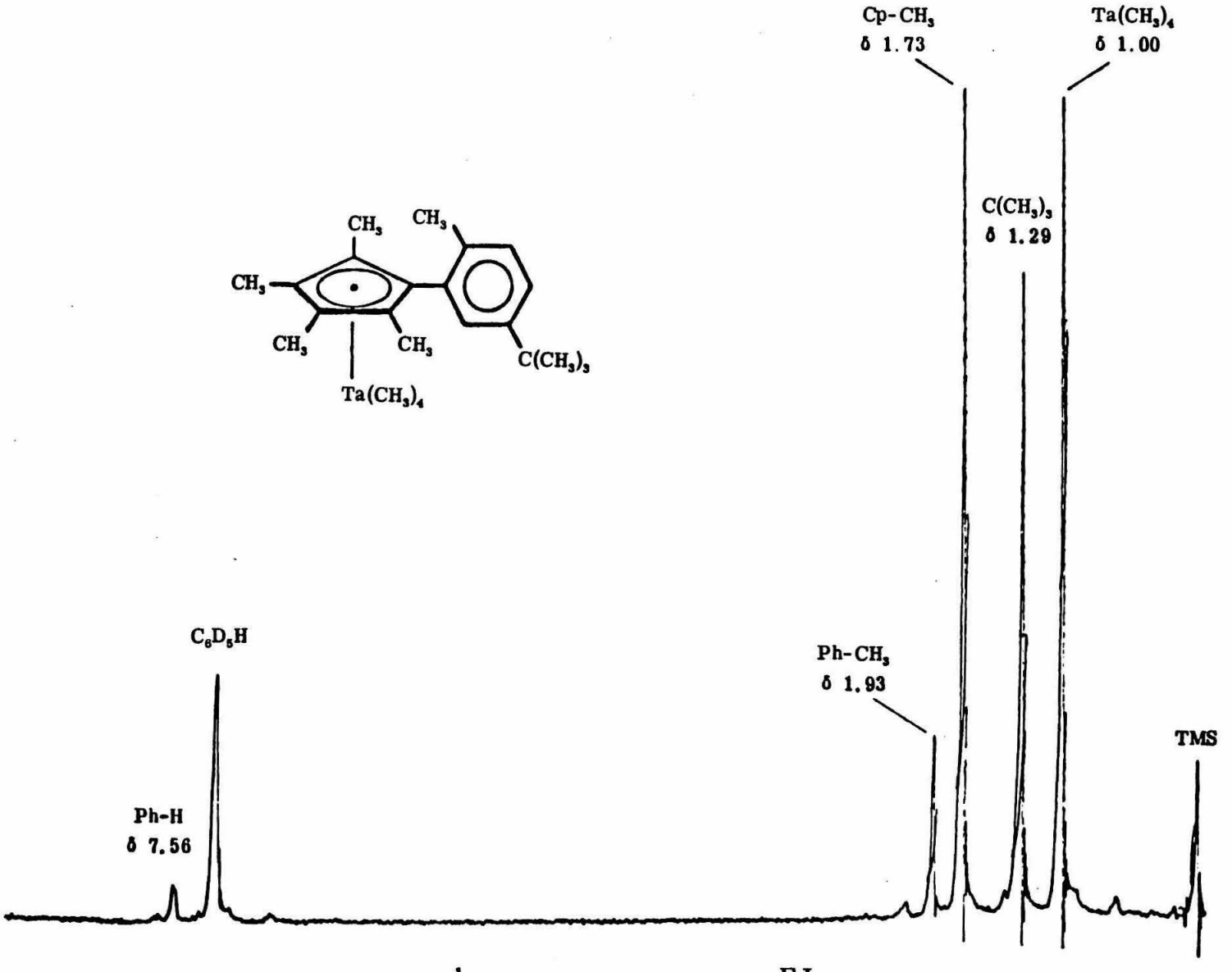

FIGURE 5.5. ^{1}H NMR Spectrum of $Cp^{EJ}Ta(CH_3)_4$ (9).

demonstrated by means of a 500 MHz ^{1}H NMR nuclear Overhauser enhancement (NOE) experiment (Figure 5.6). Selective irradiation of the tantalum-methyl resonance resulted in enhancement of the t-butyl resonance. Irradiation of the t-butyl resonance had a similar effect on the tantalum-methyl resonance. In both instances, the tolyl-methyl resonance remained unaffected. Because NOE is a through-space phenomenon dependent upon distance,[12] the results of this experiment indicate that the tantalum methyl groups are much closer to the t-butyl than to the tolyl-methyl group. Thus, both the tantalum and the t-butyl group reside on the same side of the cyclopentadienyl ligand, verifying the steric and coordination arguments made earlier.

5.2.5 Synthesis of Tantalum Hydride Complexes

Following the procedure used by Mayer[5] for the preparation of $Cp^*TaH_4(PMe_3)_2$, $Cp^{EJ}TaMe_4$ (9) was hydrogenated at 1800 psi in the presence of two equivalents of PMe_3 to give $Cp^{EJ}TaH_4(PMe_3)_2$ (10) as a white-brown solid in 48% yield (eq. 16). The ^{1}H NMR spectrum of 10

$$\underset{9}{Cp^{EJ}TaMe_4} + 2PMe_3 \xrightarrow[1800\ psi]{H_2} \underset{10}{Cp^{EJ}TaH_4(PMe_3)_2} + CH_4 \qquad (16)$$

clearly indicates the presence of two phosphine ligands with a triplet for the hydride ligand resonance at δ 1.12 ($^2J_{PH}$ = 59 Hz). Hydrogenation using one equivalent of PMe_3 does not afford a mono-phosphine complex, but rather results in incomplete reaction. Thus, the Cp^{EJ} ligand does not appear to be sufficiently bulky to permit isolation of a tetrahydrido-mono-phosphine complex.

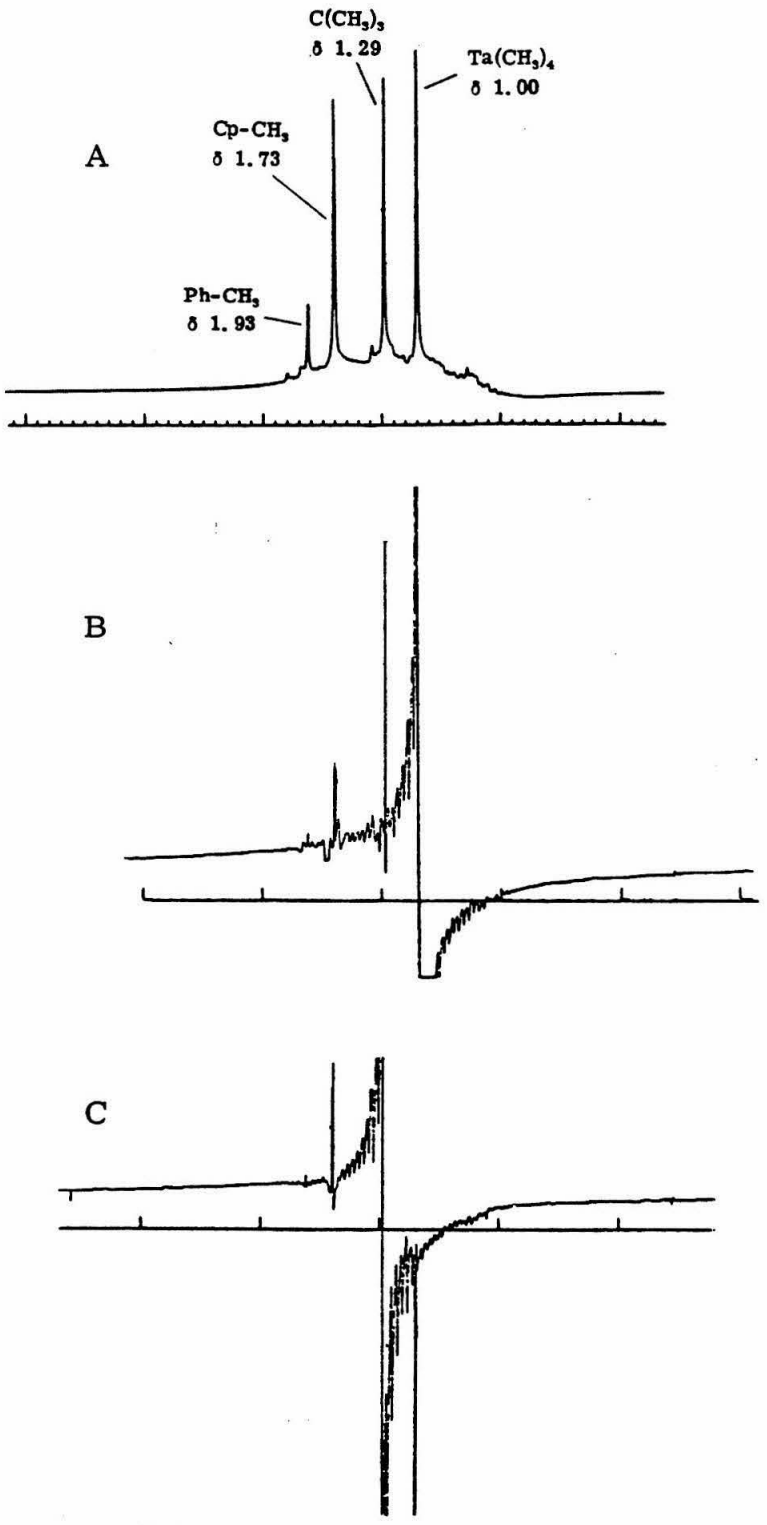

FIGURE 5.6. $Cp^{EJ}TaMe_4$ (9) ^1H NMR NOE Experiment: (A) Normal Spectrum; (B) Irradiation at δ 1.00; (C) Irradiation at δ 1.29.

To increase the steric demands of the tantalum ligands, the synthesis of trihydridochloro tantalum complexes was attempted. Hydrogenation of $Cp^{EJ}TaMe_3Cl$ (8) at 1800 psi in the presence of two equivalents of PMe_3 afforded the 16-electron, coordinatively unsaturated compound $Cp^{EJ}TaH_2Cl_2(PMe_3)$ (11) in 9% yield (eq. 17). The ^1H

$$Cp^{EJ}TaMe_3Cl \xrightarrow[H_2,\ 1800\ psi]{2PMe_3} Cp^{EJ}TaH_2Cl_2(PMe_3) \qquad (17)$$

8

NMR spectrum of 11 displays a low field doublet ($^2J_{PH}$ = 56 Hz) at δ 12.23 for the tantalum hydride resonance, confirming a monophosphine adduct, and the ^{31}P NMR spectrum consists of a triplet, confirming the presence of two hydride ligands. The mechanism by which 11 is formed is not known, but it undoubtedly involves chloride exchange reactions. It should be noted that the isolated yield of 11 is extremely low (9%). This reaction contrasts with the hydrogenation of Cp^*TaMe_3Cl which, in the presence of two equivalents of PMe_3, affords the 18-electron, coordinatively saturated compound $Cp^*TaH_3Cl(PMe_3)_2$.[5] Thus, with the added steric bulk of the chloride ligand, the Cp^{EJ} complex can be isolated as a coordinatively unsaturated species.

Hydrogenation of $Cp^{EJ}TaMe_3Cl$ (8) at 1800 psi in the presence of one equivalent of PMe_3 affords two products, the dihydrido-dichloride complex 11, and the trihydrido-chloride, $Cp^{EJ}TaH_3Cl(PMe_3)$ (12) (eq. 18). The ^1H NMR spectrum of 12 displays a single doublet ($^2J_{PH}$ = 13 Hz) for the phosphine methyl resonance at δ 1.33 with a

$$Cp^{EJ}TaMe_3Cl \xrightarrow[H_2,\ 1800\ psi]{1\,PMe_3} Cp^{EJ}TaH_2Cl_2(PMe_3) + Cp^{EJ}TaH_3Cl(PMe_3) \quad (18)$$

8 → 11 + 12

relative integration of 9 protons confirming a mono-phosphine adduct. The hydride ligand resonances are observed as a broad multiplet (δ 5.54-5.20) with a relative integration of 3 protons.[13] The two hydride complexes 11 and 12 were obtained as an inseparable mixture in a 1/1 ratio. Upon standing at room temperature, 12 decomposes over a period of weeks.

5.2.6 Reactions with Carbon Monoxide

The reaction of $Cp^{EJ}TaH_2Cl_2(PMe_3)$ (11) with one atmosphere of carbon monoxide results in loss of hydrogen and formation of $Cp^{EJ}Ta(CO)_2Cl_2(PMe_3)$ (13). No CO reduction products were observed. Similarly, the 11,12 mixture affords 13, $Cp^{EJ}TaHCl(CO)(PMe_3)$, and $Cp^{EJ}TaHCl(CO)_2(PMe_3)$ when treated with CO.[14] In all cases, CO induces the reductive elimination of hydrogen from the hydride complexes to give a series of lower valent carbonyl complexes. Apparently, generation of an open site for CO coordination does not facilitate hydride reduction of the coordinated CO. It appears to be more favorable for the tantalum complexes to reductively eliminate H_2 and form metal-carbonyl bonds than to reduce coordinated CO, initially forming metal-oxygen bonds. Zirconium hydride complexes are effective reducing agents primarily because the strength of the zirconium-oxygen bond provides a thermodynamic "sink" in the formation of the reduction products. Whether the *inability* of these

tantalum hydride complexes to reduce CO is a consequence of kinetic loss of H_2 or the stability of tantalum carbonyl complexes, has not been determined.

5.3 Experimental Section

5.3.1 General Methods

All manipulations involving air sensitive compounds were performed using high vacuum line or inert atmosphere glove box techniques. Argon and nitrogen were passed through MnO on vermiculite and 4 Å molecular sieves.

5.3.2 Physical and Spectroscopic Methods

Proton magnetic resonance spectra were recorded using a Varian EM 390 spectrometer. Chemical shifts are reported in ppm (δ) relative to Me_4Si (δ 0.0). NOE experiments were performed with a Bruker WM 500 spectrometer. Phosphorous magnetic resonance spectra were recorded using a JEOL FX90Q spectrometer. Chemical shifts are reported in ppm (δ) relative to external H_3PO_4 (δ 0.0). Infrared spectra were recorded using NaCl plates on a Beckman 4240 spectrometer.

Elemental Analyses were performed by the Caltech Microanalytical Laboratory.

5.3.3 Solvents and Reagents

Solvents used with air sensitive compounds (except THF) were purified by vacuum transfer first from $LiAlH_4$ and then from "titanocene."[15] THF and THF-d_8 were distilled from sodium benzophenone ketyl. Benzene-d_6 (Stohler, Inc.) was purified by vacuum transfer

from "titanocene". 2-Bromo-2-butene (cis-trans mixture, Columbia Organic) was distilled prior to use and stored over activated 4 Å molecular sieves. Lithium wire (0.8% Na) was purchased from Aldrich. Reactions at high pressures of hydrogen were performed using hydrogen (Matheson) of minimum purity 99.999%. Carbon monoxide was used directly from the cylinder.

$TaMe_3Cl_2$ was prepared by the reported procedure.[11]

5.3.2 2-Bromo-4-t-butyltoluene (3).

The method of preparation was a modification of that used by Meidar.[9] A 1-L three-necked round-bottomed flask equipped with a magnetic stir bar and 500 mL addition funnel was charged with 100 mL CCl_4, 0.5 g iron powder, and 174 mL (148 g, 1.00 mole) 4-t-butyltoluene. The entire apparatus was flushed with argon and the dropping funnel then charged with a solution of Br_2 (50 mL, 160 g, 1.0 mol) in CCl_4 (100 mL). The bromine solution was slowly added to the stirred t-butyltoluene solution over a period of 12 hours, maintaining the temperature below 30° C. The dark red solution was extracted twice with 1 N KOH (2×100 mL), the CCl_4 layer dried over $MgSO_4$, and filtered. The solvent was removed with a rotary evaporator and the resulting liquid distilled under reduced pressure at 75° C (1.5 mm) (lit. 88° C (2.55 mm)) to afford 3 as a colorless liquid (183 g, 81%). ^1H NMR (neat): δ 7.43 (d, $^5J_{HH}$ = 2.5 Hz, 1H, C(3)H); 7.00 (dd, $^3J_{HH}$ = 8.3 Hz, $^5J_{HH}$ = 2.5 Hz, 1H, C(6)H; 6.85 (d, $^3J_{HH}$ = 8.3 Hz, 1H, C(5)H); 2.15 (s, 3H, Ph · CH_3); 1.12 (s, 9H, $C(CH_3)_3$).

5.3.3 3-t-butyl-6-methylbenzoic acid (4)

A 2-L three-necked round-bottomed flask equipped with a magnetic stir bar, 500 mL addition funnel, and reflux condenser was charged with 20 g (0.84 moles) magnesium turnings and the apparatus flushed with argon. THF (15 mL) was added to the flask followed by 8 mL 2-bromo-4-t-butyltoluene and 1 mL dibromoethane. Reaction started immediately. The reaction mixture was diluted with THF (600 mL) and the addition funnel charged with a solution of 2-bromo-4-t-butyltoluene (183 g total used, 0.81 mol) in THF (200 mL). With constant stirring, the bromide solution was added to the magnesium suspension at a rate sufficient to maintain a gentle reflux. After addition, the mixture was brought to reflux for an additional 40 min by means of an oil bath. The mixture was allowed to cool to room temperature and then quickly poured over 1000 mL of crushed dry ice. When all unreacted CO_2 had evaporated (ca. 3 hours), 6 N HCl was added to the gelatinous mass until no further reaction was observed (ca. 200 mL). The THF was removed with a rotary evaporator to give a two-layered product. The lower (aqueous) layer was washed three times with Et_2O (3×100 mL) and the combined ether washings together with the upper (organic) layer were washed three times with 5% NaOH solution (3×100 mL). The aqueous fractions were combined and acidified with concentrated HCl until a white layer separated. The mixture was extracted three times with Et_2O (3×150 mL), the ether fractions dried over $MgSO_4$, and filtered. Removal of solvent using a rotary evaporator afforded 4 as a white crystalline solid (136 g, 87%): mp 74-76° C. ^1H NMR (CCl_4): δ 12.73 (s, 1H, *COOH*); *8.08 (d,*

$^5J_{HH}$ = 2.5 Hz, 1H, C(2)H); 7.45 (dd, $^3J_{HH}$ = 8.3 Hz, $^5J_{HH}$ = 2.5 Hz, 1H, C(5)H); 7.10 (d, $^3J_{HH}$ = 8.3 Hz, 1H, C(4)H); 2.60 (s, 3H, CH_3); 1.32 (s, 9H, $C(CH_3)_3$). IR (KBr): ν (C=O) 1685 cm^{-1}.

5.3.4 Methyl-2-methyl-5-t-butylbenzoate (5)

A 1-L one-necked round-bottomed flask equipped with a magnetic stir bar and reflux condenser was charged with 136 g (0.71 mol) 3-t-butyl-6-methylbenzoic acid, 10 g (0.53 mmol) p-toluenesulfonic acid, 173 mL (148 g, 1.4 mol) 2,2-dimethoxypropane and 600 mL CH_3OH. The mixture was brought to reflux and allowed to stir at this temperature for 12 hours. The solution was cooled to room temperature and the solvent removed with a rotary evaporator. The dark-red liquid was dissolved in Et_2O (300 mL) and washed three times with 10% $NaHCO_3$ solution (3×300 mL), dried over $MgSO_4$, and filtered. Removal of solvent using a rotary evaporator afforded 5 as a yellow liquid (141 g, 96%): bp 74° C (0.2 mm). Anal. Calcd for $C_{13}H_{18}O_2$: C, 75.69; H, 8.79. Found: C, 75.13; H, 8.66. ^1H NMR (CCl_4): δ 7.90 (d, $^5J_{HH}$ = 2.5 Hz, 1H, C(2)H); 7.36 (dd, $^3J_{HH}$ = 10 Hz, $^5J_{HH}$ = 2.5 Hz, 1H, C(5)H); 7.08 (d, $^3J_{HH}$ = 10 Hz, 1H, C(4)H; 3.82 (s, 3H, OCH_3); 2.50 (s, 3H, Ph-CH_3); 1.31 (s, 9H, $C(CH_3)_3$). IR (neat): ν (C=O) 1730 cm^{-1}.

5.3.5 4-4[(2-methyl-5-t-butyl)phenyl]-3,5-dimethyl-2,5-heptadienol (6).

The method of preparation was a modification of that for 4-4-phenyl-3,5-dimethyl-2,5-heptadienol used by Threlkel and Bercaw.[6] A 3-L three-necked round-bottomed flask equipped with a

mechanical stirrer, condenser, and 500 mL addition funnel was charged with 1500 mL Et_2O and 20.5 g (3.0 mol) lithium wire (cut into small pieces) and the entire apparatus flushed with argon. The dropping funnel was charged with 145 mL (192 g, 1.4 mol) 2-bromo-2-butene, 10 mL of which was then added to the Li suspension with stirring. Reaction started immediately as evidenced by the turbidity of the diethyl ether and the remainder of the bromide was then added at a rate sufficient to maintain a gentle reflux. After addition, the cloudy green solution was stirred for an additional hour at room temperature. The addition funnel was then charged with a solution of methyl-2-methyl-5-t-butylbenzoate (141 g, 0.68 mol) in Et_2O (150 mL) and this solution then added to the lithio reagent at a rate sufficient to maintain a gentle reflux. After addition, the yellow-green solution was filtered through glass wool (to remove unreacted Li wire) into 1 L of a saturated NH_4Cl solution. The ether layer was separated and the aqueous layer washed three times with Et_2O (3×150 mL). The ether fractions were combined, dried over $MgSO_4$, and filtered. Removal of solvent using a rotary evaporator afforded 6 as an orange liquid (182 g, 93%). ^1H NMR (CCl_4): δ 7.33 (d, $^3J_{HH}$ = 1.5 Hz, 1H, Ph-C(6)H); 7.13-7.00 (m, 2H, Ph); 5.64-5.40 (m, 2H, CH): 2.38 (s, 3H, Ph-CH_3); 1.73 (br-s, 6H, C(3,5)-CH_3); 1.33 (m, 6H, CH(CH_3)); 1.27 (s, 9H, $C(CH_3)_3$). IR (neat): ν (OH) 3500 cm^{-1}; ν (C=C) 1682.

5.3.6 (2-methyl-5-t-butyl)phenyltetramethylcyclopentadiene ($Cp^{EJ}H$)

The method of preparation was a modification of that for phenyltetramethylcyclopentadiene used by Threlkel and Bercaw.[6] A 2-L

round-bottomed flask equipped with a magnetic stir bar and reflux condenser was charged with 182 g (0.63 mol) 6, 18 g (0.09 mol) TsOH, and 1.5 L $CHCl_3$. The mixture was brought to reflux and stirred at this temperature for 12 hours. The black solution was cooled to room temperature and poured into a solution of 8 g Na_2CO_3 in saturated $NaHCO_3$ (1 L). The organic layer was separated and the aqueous layer washed twice with $CHCl_3$ (2×100 mL). The organic fractions were combined, dried over $MgSO_4$, and filtered. The solvent was removed using a rotary evaporator and the resulting liquid distilled at 130° C (0.01 mm) using a Kugelruhr apparatus to give $Cp^{EJ}H$ as a dark amber liquid (160 g, 87%): m/e = 268. ^1H NMR (benzene-d_6): δ 7.20-7.00 (m, 3H, Ph); 3.08 (m, 1H, C(1)H); 2.10 (s, 3H, Ph-CH_3); 1.76 (s, 6H, Cp-CH_3); 1.63 (s, 6H, Cp-CH_3); 1.23 (s, 9H, $C(CH_3)_3$).

5.3.7 Reaction of $Cp^{EJ}H$ with TsOH to give 4-[(2-methyl-5-t-butyl)phenyl]-1,3,5-trimethyl-3,5,6-heptatriene (7)

A 25-mL round-bottomed flask equipped with a magnetic stir bar and reflux condenser was charged with 7 mL $CHCl_3$, 0.5 g (0.3 mmol) 6, and 50 mg (0.03 mmol) TsOH. The solvent was brought to reflux and stirred at this temperature for 1 hour. The dark black-purple solution was cooled to room temperature and washed three times (3×10 mL) with a solution of 8 g Na_2CO_3 in saturated $NaHCO_3$ (1 L). The organic layer was dried over $HgSO_4$, filtered, and the solvent removed on a rotary evaporator. The resulting amber liquid was distilled at 80°C (0.01 mm) using a Kugelruhr apparatus to give 7 of a yellow liquid. ^1H NMR (benzene-d_6): δ 6.48 (dd, $^3J_{HH}$ = 20 Hz,

$^3J_{HH}$ = 11 Hz, 1H, C(2)-H); 5.30 (m, 1H, C(6)-H); 5.20 (dd, $^3J_{HH}$ = 20 Hz, $^2J_{HH}$ = 2 Hz, 1H, C(1)-trans-H); 4.90 (dd, $^3J_{HH}$ = 11 Hz, $^2J_{HH}$ = 2 Hz, 1H, C(1)-cis-H); 2.20 (s, 3H, Ph-CH_3); 1.86 (s, 3H, C(3)-CH_3); 1.63 (s, 3H, C(5)-CH_3); 1.40 (d, $^3J_{HH}$ = 6 Hz, 3H, C(6)-CH_3); 1.24 (s, 9H, $C(CH_3)_3$). The phenyl proton resonances were obscured by solvent.

5.3.8 Reaction of 7 with TsOH to give $Cp^{EJ}H$

A 10 mL round-bottomed flask equipped with a magnetic stir bar and reflux condenser was charged with the triene 7 obtained from procedure 5.4.7, 30 mg (0.02 mmol) TsOH, and 5 mL $CHCl_3$. The solution was brought to reflux and stirred at this temperature for 12 hours. The dark purple solution was cooled to room temperature and washed two times (2×5 mL) with a solution of 8 g Na_2CO_3 in saturated $NaHCO_3$ (1 L). The organic layer was dried over $MgSO_4$, filtered, and the solvent removed on a rotary evaporator. The resulting liquid was distilled at 100° C (0.01 mm) using a Kugelruhr apparatus to give a yellow liquid. The ^1H NMR spectrum of this liquid was identical to that of $Cp^{EJ}H$.

5.3.9 (2-Methyl-5-t-butyl)phenyltetramethylcyclopentadienyl lithium ($LiCp^{EJ}$)

A 50 mL round-bottomed flask equipped with a magnetic stir bar and reflux condenser was charged with 1.0 g (3.7 mmol) $Cp^{EJ}H$ and the apparatus attached to a vacuum line. The liquid was degassed by evacuation at room temperature and then 25 mL pet. ether distilled into the flask at -78° C. With an argon counter flow, 2.5 mL (1.55 M,

3.9 mmol) n-BuLi in pet. ether were added to the cold solution via syringe. The mixture was warmed to room temperature and then brought to reflux with stirring and maintained at this temperature for 48 hours. After several hours, a white solid began to precipitate from the orange solution. The mixture was cooled to room temperature and the apparatus brought into an inert atmosphere glovebox. The solid was isolated by filtration and washed well with pet. ether. Drying in vacuo afforded $LiCp^{EJ}$ as a light orange-white powder (500 mg, 49%). Attempts to scale-up this procedure were unsuccessful; only orange oils could be obtained. ^1H NMR (THF-d_8): δ 7.16-7.00 (m, 3H, Ph); 2.07 (s, 3H, Ph-CH_3); 2.03 (s, 6H, Cp-CH_3); 1.82 (s, 6H, Cp-CH_3); 1.30 (s, 9H, $C(CH_3)_3$).

5.3.10 $Cp^{EJ}TaMe_3Cl$ (8)

The method of preparation was a modification of that for Cp^*TaMe_3Cl used by Schrock.[11] $TaMe_3Cl_2$ (300 mg, 1.1 mmol) and $LiCp^{EJ}$ (325 mg, 1.1 mmol) were suspended in Et_2O (8 mL) at -78° C and stirred for 2 hours. The mixture was then warmed to room temperature and allowed to stir for an additional 90 min. The solvent was removed from the yellow-green solution in vacuo, the residue triterated with pet. ether (8 mL), and the suspension filtered. The green-black solid isolated on the frit was washed five times with pet. ether until the washings were colorless. The volume of the filtrate was reduced to 2 mL and the solution cooled to -78°C. A yellow solid precipitated which was isolated by filtration at -78° C to afford 8 as dark yellow crystals (254 mg, 44%). ^1H NMR (benzene-d_6): δ 8.08 (m,

1H, C(6)-H); 1.87 (s, 3H, Ph-CH_3); 1.77 (s, 6H, Cp-CH_3); 1.73 (s, 6H, Cp-CH_3); 1.33 (s, 9H, $C(CH_3)_3$); 1.13 (s, 9H, TaCH_3). The remaining phenyl resonances were obscured by solvent.

5.3.11 $Cp^{EJ}TaMe_4$ (9)

The method of preparation was a modification of that for Cp^*TaMe_4 used by Schrock,[11] $Cp^{EJ}TaMe_3Cl$ (250 mg, 0.47 mmol) was dissolved in Et_2O (8 mL) and the solution cooled to -78° C. MeLi (4 mL, 0.5 mmol, 1.25 M in pet. ether) was added to the stirred tantalum solution via syringe and the mixture allowed to warm to room temperature. Upon warming, the solution became cloudy and a white solid (LiCl) precipitated. The solvent was removed in vacuo and the green residue triterated with pet. ether. The suspension was filtered and the salt washed twice with pet. ether. The solvent was removed in vacuo to afford 9 as a yellow crystalline solid (151 mg, 63%). ^1H NMR (benzene-d_6): δ 7.56 (m, 1H, C(6)-H); 1.93 (s, 3H, Ph-CH_3); 1.73 (s, 12H, Cp-CH_3); 1.29 (s, 9H, $C(CH_3)_3$); 1.00 (s, 12H, TaCH_3).

5.3.12 $Cp^{EJ}TaH_4(PMe_3)_2$ (10)

The method of preparation was a modification of that for $Cp^*TaH_4(PMe_3)_2$ used by Mayer.[5] $Cp^{EJ}TaMe_4$ (150 mg, 0.29 mmol) and 50 mL of a solution of PMe_3 (0.6 mmol) in pet. ether were placed in a high pressure reactor and stirred for 2 days under 1800 psi of hydrogen. Removal of solvent in vacuo afforded 10 as a white-brown solid (85 mg, 48%) ^1H NMR (benzene-d_6): δ 8.67 (m, 1H, C(6)-H); 2.23 (s, 6H, Cp-CH_3); 1.93 (s, 3H, Ph-CH_3); 1.86 (s, 6H, Cp-CH_3); 1.40 (s, 9H, $C(CH_3)_3$); 1.12 (t, $^2J_{PH}$ = 59 Hz, 4H, TaH). The phosphine

methyl resonances were not located. The remaining phenyl resonances were obscured by solvent.

5.3.13 $Cp^{EJ}TaH_2Cl_2(PMe_3)$ (11)

The procedure described in section 5.3.12 was followed using 150 mg (0.30 mmol) $Cp^{EJ}TaMe_3Cl$ and 50 mL of a solution of PMe_3 (0.60 mmol) in pet. ether. The solvent was removed from the solution in vacuo and the residue triturated with 1.5 mL pet. ether. The suspension was cooled to -78° C and then filtered at this temperature to afford 11 as a white solid (15 mg, 9%). ^1H NMR (benzene-d_6): δ 12.23 (d, $^2J_{PH}$ = 56 Hz, 2H, TaH); 7.94 (m, 1H, C(6)-H); 2.08 (s, 6H, Cp-CH_3); 2.09 (s, 6H, Cp-CH_3); 2.00 (s, 3H, Ph-CH_3); 1.60 (d, $^2J_{PH}$ = 14 Hz, 9H, $P(CH_3)_3$); 1.40 (s, 9H, $C(CH_3)_3$). The ^{31}P NMR spectrum ($P(CH_3)_3$) is a triplet.

5.3.14 High Pressure Hydrogenation of $Cp^{EJ}TaMe_3Cl$ in the Presence of One Equivalent of PMe_3

The procedure described in section 5.3.12 was followed using 0.4 g (0.69 mmol) $Cp^{EJ}TaMe_3Cl$ and 50 mL of a solution of PMe_3 (0.70 mmol) in pet. ether. The solvent was removed from the solution in vacuo and the residue triturated with 2 mL pet. ether. The suspension was cooled to -78° C and then filtered at this temperature to afford 131 mg of an off-white solid. The ^1H NMR spectrum of this solid indicated two products in equal concentrations, $Cp^{EJ}TaH_2Cl(PMe_3)$ (11) and $Cp^{EJ}TaH_3Cl(PMe_3)$ (12). $Cp^{EJ}TaH_3Cl(PMe_3)$ ^1H NMR (benzene-d_6). δ 8.53 (m, 1H, C(6)-H); 5.54-5.20 (br, 3H, TaH); 2.14 (s, 6H, Cp-CH_3); 2.04 (s, 3H, Ph-CH_3); 1.87 (s, 6H, Cp-CH_3); 1.43 (s, 9H, $C(CH_3)_3$);

1.33 (d, $^2J_{PH}$ = 13 Hz, 9H, $P(CH_3)_3$). The remaining phenyl resonances were obscured by solvent.

5.3.15 Reaction of $Cp^{EJ}TaH_2Cl_2(PMe_3)$ with CO to give $Cp^{EJ}TaCl_2(CO)_2(PMe_3)$ (13)

$Cp^{EJ}TaH_2Cl_2(PMe_3)$ (5 mg) and C_6D_6 (0.4 mL) were placed in an NMR tube and the solution frozen at -78° C. The tube was evacuated on a vacuum line and backfilled with 700 torr CO. The tube was sealed with a torch and the solution allowed to warm to room temperature, the color of the solution turning from colorless to purple upon warming. The ^1H NMR spectrum of this solution indicates 13 had formed quantitatively. ^1H NMR (benzene-d_6): δ 8.19 (m, 1H, C(6)-H); 1.93 (s, 6H, Cp-CH_3); 1.87 (s, 3H, Ph-CH_3); 1.77 (s, 6H, Cp-CH_3); 1.47 (s, 9H, $C(CH_3)_3$); 1.43 (d, $^2J_{PH}$ = 13 Hz, 9H, $P(CH_3)_3$). The remaining phenyl resonances were obscured by solvent.

5.3.16 Reaction of the $Cp^{EJ}TaH_2Cl_2(PMe_3)$ - $Cp^{EJ}TaH_3Cl(PMe_3)$ Mixture with CO

The procedure described in section 5.3.15 was followed using 20 mg of the $Cp^{EJ}TaH_2Cl_2(PMe_3)$-$Cp^{EJ}TaH_3Cl(PMe_3)$ mixture (procedure 5.3.14) and 0.4 mL C_6D_6. The NMR tube was sealed under 700 torr CO at -78° C and allowed to warm to room temperature, the color of the solution turning from colorless to purple-red upon warming. The ^1H NMR spectrum of this solution indicates three products: 13, $Cp^{EJ}TaHCl(CO)(PMe_3)$, and $Cp^{EJ}TaHCl(CO)_2(PMe_3)$. The latter two compounds were identified by their respective hydride and phosphine resonances: (δ 6.13, d, $^2J_{PH}$ = 40 Hz, 1H, TaH, δ 1.08, d,

$^2J_{PH}$ = 9 Hz, 9H, $P(CH_3)_3$) (δ 6.10, t, $^2J_{PH}$ = 50 Hz, 1H, TaH; δ 1.33, m, $^2J_{PH}$ = 5 Hz, 9H, $P(CH_3)_3$).

5.4 References and Notes

1. a) J. E. Bercaw, Adv. Chem. Ser., 167, 136 (1978);
   b) J. M. Manriquez, D. R. McAlister, R. D. Sanner, and J. E. Bercaw, J. Amer. Chem. Soc., 100, 2716 (1978);
   c) P. T. Wolczanski and J. E. Bercaw, Accounts Chem. Res., 13, 121 (1980).
2. J. P. Collman and L. S. Hegedus, "Principles and Applications of Organotransition Metal Chemistry," University Science Books, Mill Valley, CA, 1980, p. 68.
3. a) C. P. Casey and S. M. Neumann, J. Amer. Chem. Soc., 98, 5395 (1976);
   b) J. A. Gladysz and W. Tam, ibid., 100, 2545 (1978);
   c) W. Tam, W.-K. Wong, and J. A. Gladysz, ibid., 101, 1589 (1979);
   d) C. Masters, C. van der Woude, and J. A. van Dorn, ibid., 101, 1633 (1979);
   e) D. L. Thorn, ibid., 102, 7109 (1980);
   f) D. L. Thorn, Organometallics, 1, 197 (1982);
   g) D. L. Thorn and T. H. Tulip, ibid., 1, 1580 (1982).
4. J. A. Connor, Top. Curr. Chem., 71, 71 (1977).
5. a) J. M. Mayer, Ph.D. Dissertation, California Institute of Technology, Pasadena, CA, 1982;
   b) J. M. Mayer and J. E. Bercaw, J. Amer. Chem. Soc., 104, 2157 (1982).
6. R. S. Threlkel and J. E. Bercaw, J. Organomet. Chem., 136, 1 (1977).

7. The C(1) position is taken to be the point of attachment to the tetramethylcyclopentadienyl ligand.

8. Corey-Pauling-Koltun molecular models.

9. D. Meidar and Y. Halpern, J. Appl. Chem. Biotech., 26, 590 (1976).

10. Identified by ^{1}H NMR spectroscopy. See experimental section.

11. C. D. Wood and R. R. Schrock, J. Amer. Chem. Soc., 101, 5421 (1979).

12. Edwin D. Becker, "High Resolution NMR-Theory and Chemical Applications," Academic Press, New York, 1980, pp. 206-211.

13. The hydride ligand resonances of a similar compound ($Cp^*TaH_3Cl(PMe_3)_2$) are observed in the same general region of the ^{1}H NMR spectrum (δ 4.8, 5.2). See ref. 5.

14. Compounds 14 and 15 were characterized by comparison of their ^{1}H NMR hydride ligand and phosphine methyl resonances with those of $Cp^*TaHCl(CO)(PMe_3)$ and $Cp^*TaHCl(CO)_2(PMe_3)$. See ref. 5.

15. R. H. Marvick and H. H. Brintzinger, J. Amer. Chem. Soc., 93, 2046 (1971).

16. Non-first-order NMR pattern intermediate between a doublet and triplet. See R. K. Harris, Can. J. Chem., 42, 2275 (1964).